CHEMICAL REVIEWS

pubs.acs.org/CR

Review

Self-Assembling Nucleic Acid Nanostructures Functionalized with Aptamers

Abhichart Krissanaprasit, Carson M. Key, Sahil Pontula, and Thomas H. LaBean*

Cite This: https://doi.org/10.1021/acs.chemrev.0c01332

Read Online

ACCESS | Metrics & More | Article Recommendations

ABSTRACT: Researchers have worked for many decades to master the rules of biomolecular design that would allow artificial biopolymer complexes to self-assemble and function similarly to the diverse biochemical constructs displayed in natural biological systems. The rules of nucleic acid assembly (dominated by Watson−Crick base-pairing) have been less difficult to understand and manipulate than the more complicated rules of protein folding. Therefore, nucleic acid nanotechnology has advanced more quickly than *de novo* protein design, and recent years have seen amazing progress in DNA and RNA design. By combining structural motifs with aptamers that act as affinity handles and add powerful molecular recognition capabilities, nucleic acid-based self-assemblies represent a diverse toolbox for use by bioengineers to create molecules with potentially revolutionary biological activities. In this review, we focus on the development of self-assembling nucleic acid nanostructures that are functionalized with nucleic acid aptamers and their great potential in wide ranging application areas.

CONTENTS

Special Issue: Molecular Self-Assembly

Received: December 29, 2020

1. INTRODUCTION

This review seeks to highlight important progress over the past couple of decades in the area of biomolecular engineering concerned with the creation of artificial nucleic acid constructs. Particularly, we will focus on research topics in which the self-assembling capacity of nucleic acids is utilized to create rationally designed nanostructures decorated with aptamers. Aptamers are functional affinity handles that are selected from *in vitro* combinatorial libraries of partially randomized nucleic acid sequences. As such, we will briefly review background literature in aptamer selection, structural DNA nanotechnology, and RNA nanotechnology. These separate topics have already been extensively reviewed, so we will refer readers to these excellent summaries for the deeper details.[1−8] Here we will focus more on the applications of nucleic acid nanostructures that have been rationally designed by combining structural modules from previous design studies (i.e., nanostructures) as well as previous selection experiments (i.e., aptamers). We can think of these two types of components as "designable" and "selectable", respectively; combining both types of components demonstrates and emphasizes the modularity of nucleic acid nanostructure design. Structural or functional modules developed separately can often be combined such that the useful properties of each substructure are maintained. Further rounds of sequence, structure, and functional optimization can be applied to constructs with combined modules. Aptamers have been reviewed here a few times,[9−11] as have DNA and RNA nanotechnology topics;[4,12,13] therefore we will focus primarily on describing self-assembling nucleic acid constructs bearing aptamer functionalization and on their application toward solving practical problems. We will examine specific application areas including therapeutics, biosensors, imaging agents, cell signaling, and response to external stimuli.

2. MOLECULAR SELF-ASSEMBLY OF NUCLEIC ACID NANOSTRUCTURES

While DNA and RNA are both well-known as carriers of encoded genetic information in nature, they can also be thought of as structural materials, since their nucleotide sequences specify particular folded structures on the low nanometer length scale. Biological DNA structure is relatively simple and dominated by the rules of Watson−Crick base-pairing, while RNA displays more diverse and complex structural motifs in its larger biological assemblies such as the ribosome. Over several decades, scientists have studied and discovered geometries of double-stranded DNA and RNA (Figure 1A).[14] Biomolecular engineers have made use of structural knowledge gleaned from nature as well as leveraging nucleic acids' propensity for programmed assembly by hybridization and self-folding to create a wide spectrum of useful artificial molecules and supramolecular assemblies. In this section, we will describe advances in both DNA and RNA structural engineering that have led to the array of functional assemblies described in later sections.

2.1. Self-Assembled DNA Nanostructures

The field of structural DNA nanotechnology was founded by Nadrian Seeman at NYU in the early 1980s when he set out to create three-dimensional (3D) periodic material for use as host lattice for docking multiple identical guest protein molecules to facilitate atomic resolution structure elucidation by X-ray diffraction.[15,16] Seeman reasoned that the slow step of X-ray crystallography, obtaining high quality protein crystals, could be eliminated by reprogramming self-assembling DNA crystals with carefully positioned protein binding sites each time one wished to solve a new protein structure. Early attempts at DNA building blocks made use of topologically branched, multistrand assembles inspired by the biological 3-arm junction of the DNA replication fork and 4-arm Holliday junction of the recombination complex (Figure 1B). These artificial motifs came to be known as multiarm junctions and differed from their biological analogs by the use of designed sequences that made them "immobile" such that they could not migrate up and down the double-helical ladder as they can in the natural homologous recombination complex. Unfortunately, these multiarm junctions proved to be insufficiently stiff to reliably define designed geometric angles, so while junctions formed, they did not readily assemble into desired higher-order structures.

After toiling mostly alone for over a decade, Seeman's group succeeded in creating stable and sufficiently rigid building blocks, known as double crossover (DX) complexes, by bridging two double-helices at two separate, well-spaced 4-way junctions. These DX "tiles" allowed assembly into higher order lattices (i.e., periodic arrays) (Figure 1B).[17,18] This strategy is typically referred to as tile-and-lattice assembly, since first the synthetic oligonucleotides are assembled into small tiles (e.g., DX complexes) and then as thermal annealing continues the tiles assemble into large multitile lattices. The tiles typically contained a few to a dozen oligonucleotides with tile length scales in the low nanometer range, while lattices could contain tens of thousands of tiles and reach tens of micrometers on an edge and some approach the millimeter range. The first wave of diverse structural designs mostly focused on increasing the tile

https://doi.org/10.1021/acs.chemrev.0c01332
Chem. Rev. XXXX, XXX, XXX−XXX

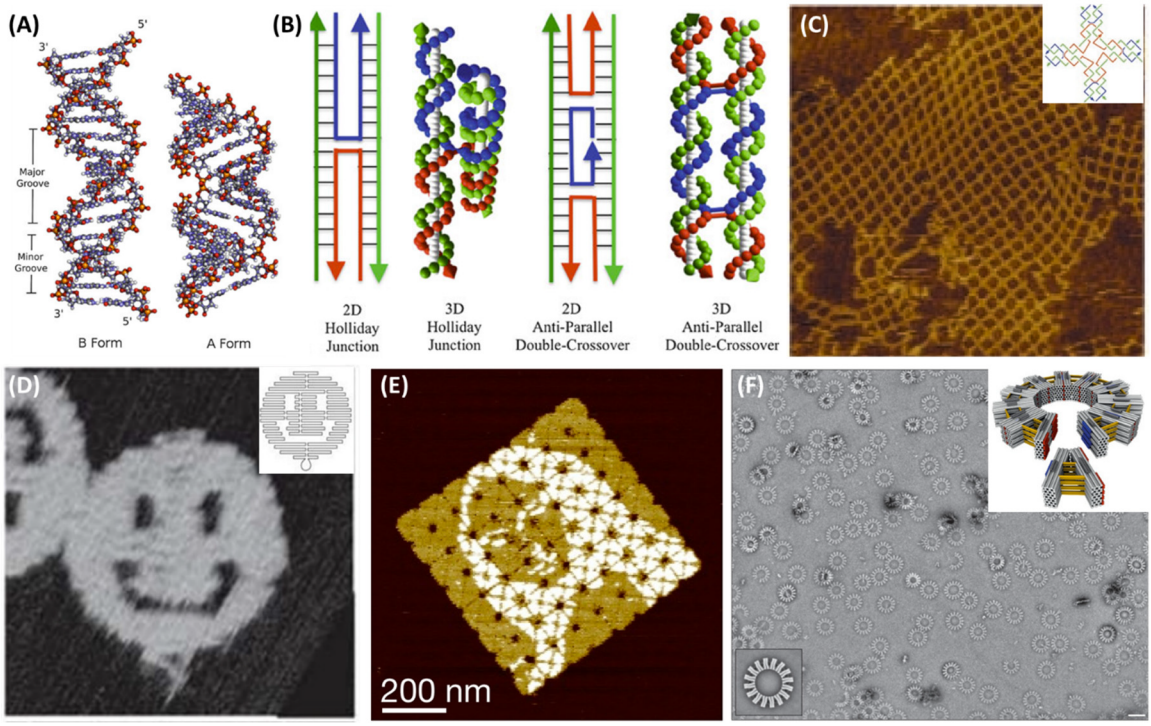

Figure 1. Geometries and architectures of self-assembling structural DNA nanotechnology. (A) Geometry of nucleic acid double helices: (left) B-form helix, normal geometry expected for dsDNA under physiologic-like solution conditions, and (right) A-form helix, normal geometry of dsRNA and special cases of dsDNA. Adapted with permission from ref 14. Copyright 2014 Springer-Verlag Berlin Heidelberg. (B) Four-arm (Holliday) junction schematics in 2D and 3D showing relative rotation of double-helices and double crossover (DX) complex shown in 2D and 3D schematics demonstrating rigid, coplanar ordering of paired double-helices. Adapted with permission from ref 14. Copyright 2014 Springer-Verlag Berlin Heidelberg. (C) Schematic of 4 × 4 DNA tile (inset) and 500 nm × 500 nm AFM image of lattice formed from 4 × 4 tiles. Adapted with permission from ref 19. Copyright 2003 The American Association for the Advancement of Science. (D) Schematic of DNA origami scaffold strand trace (inset) and 165 nm × 165 nm AFM image of assembled DNA origami on mica. Adapted with permission from ref 25. Copyright 2006 Springer Nature. (E) AFM image of assembled, fully addressable, 2D lattice formed from multiple DNA origami tiles. Adapted with permission from ref 29. Copyright 2017 Springer Nature. (F) Schematic of multiple DNA origami assemblies joining to form circular gear-like object (inset) and negative-stained SEM image of fully formed 3D gears (scale bar = 300 nm). Adapted with permission from ref 38. Copyright 2017 Springer Nature.

complexity and expanding the range of tile and lattice geometric options.[19−22] Figure 1C shows an example tile and lattice assembly (i.e., 4 × 4 tile).[19] The development of atomic force microscopy allowed rapid structural characterization of 2D lattices and sped design cycles, thus promoting quick diversification of prototyped nanostructures.[23]

2.1.1. From Tile−Lattice to Origami-like Designs and then to Tile-less Lattice (DNA Legos). An early 3D geometrical object was demonstrated by Shih who described an octahedron in which a long single strand of enzymatically produced DNA was designed to self-fold with the assistance of chemically synthesized "helper strands".[24] Another architecture involving a long strand was introduced in 2006 when Rothemund described the origami strategy in which a set of a couple of hundred synthetic oligonucleotides (staple strands) were used to force a long biological (scaffold) strand into designed geometric shapes (Figure 1D).[25] DNA origami was a major advance and allowed essentially any arbitrary 2D or 3D shape to be formed by simply heating and cooling the scaffold strand with a carefully designed set of staple strands together in buffered solution with the proper level of divalent cations (usually 12.5 mM Mg^{2+}). Further developments pushed the origami size by designing longer scaffold strands and bigger staple sets[26] or by using origami complexes as tiles (i.e., substructures or building blocks) for assembly of larger periodic or fully addressable lattices (Figure 1E).[27−29] Another design strategy eliminated the long scaffold strand as well as the need for tile assembly prior to lattice formation; this method is sometimes called single-strand tiles or tile-less lattice and is also referred to as DNA Legos.[30−32] In this "DNA brick" or "Lego" strategy, individual ssDNA oligonucleotides bind directly to the growing 2D or 3D object without first forming an intermediate complex such as a DX tile or even a multiarm junction.

2.1.2. Three-Dimensional DNA Objects and Crystals. After Shih's early octahedron, other 3D objects followed, including strategies using tiles that formed curved lattices resembling soccer balls and other polyhedrons.[33] DNA origami with 3D lattices including curved and twisted lattices further expanded the DNA toolbox.[34,35] More 3D objects were prototyped including rope-basket-like spheres and "bottles",[36] a controllable DNA box,[37] and finally multiorigami constructs culminating in gigadalton gear-like wheels assembled and isolated in surprising purity (Figure 1F).[38] Most recently, several groups demonstrated a variety of ways to tesselate virtually any desired 3D object using edges defined by DNA helices or multiple helices on complex tessellations of 3D meshes.[39−41] Seeman's group also finally succeeded in creating regular DNA crystals using a logpile local geometry that grew to high micrometer scale and diffracted X-rays on the nanometer scale promising the realization of the original goal for the engineering of DNA as a structural building material.[42]

https://doi.org/10.1021/acs.chemrev.0c01332
Chem. Rev. XXXX, XXX, XXX−XXX

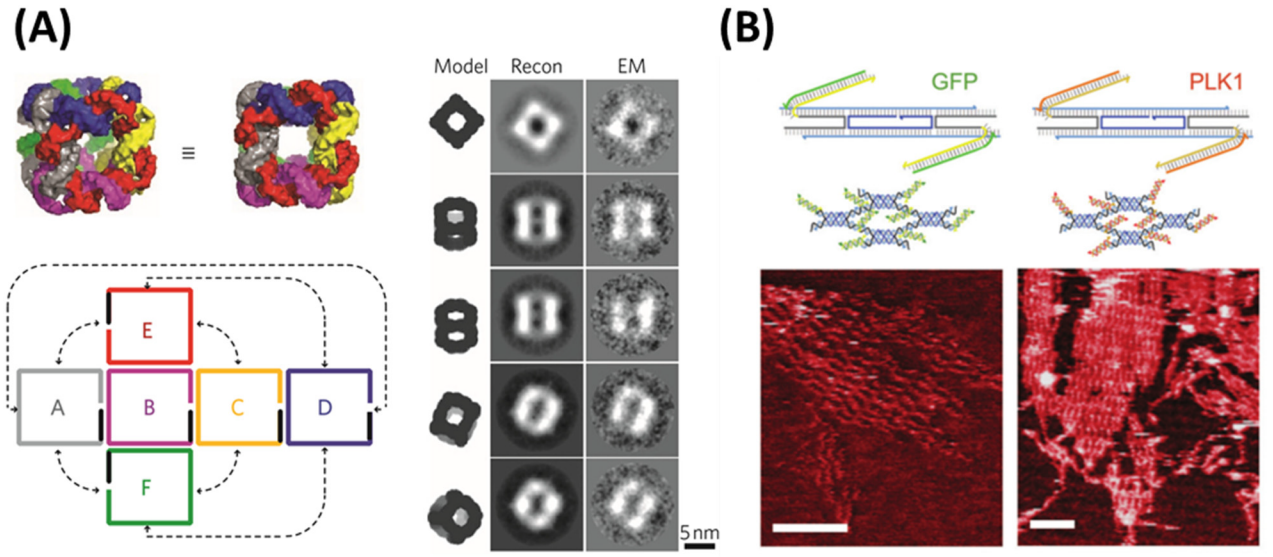

Figure 2. Multistranded RNA nanostructure assemblies. (A) Self-assembly of cubic RNA using multiple strands of ssRNA. Adapted with permission from ref 49. Copyright 2010 Springer Nature. (B) Molecular self-assembly of RNA tiles and formation of RNA tile-based lattices (Scale bar = 50 nm). Reprinted with permission from ref 51. Copyright 2016 Royal Society of Chemistry.

2.2. Self-Assembly of RNA Nanostructures

RNA is a biopolymer that plays essential roles in biology from the origin and evolution of life to the normal function and regulation of cellular machinery. The sugar−phosphate backbone of RNA contains ribose sugar groups rather than the deoxyribose sugar found in DNA (with its hydroxyl exchanged for hydrogen on the 2′-carbon). The set of nitrogenous bases that appear as side chains in the RNA polymer add uracil and lose thymine as compared to DNA bases. The crystallographic structures of dsDNA and dsRNA show that they are well-defined right-handed helical structures in which RNA is known as A-form helix, while DNA double-helix is called B-form; these helices differ in diameter, pitch, and other geometric parameters (Figure 1A). Due to their overall geometric similarities, designer DNA nanostructures have helped to inspire and pave the way for RNA nanoarchitectures. Although DNA nanotechnology has helped advance the creation of RNA nanostructures, the multiple secondary and tertiary structures of RNA found in nature (especially in the rRNAs) are not found in biological DNA. Structural biologists have employed advanced techniques to reveal, study, and understand diverse, sophisticated substructures in naturally occurring RNA, such as riboswitches, tRNA, rRNA, and ribozymes. The immense structural diversity and capacity for molecular self-assembly of RNA makes it a great building material for the construction of programmable nanostructures. In the past three decades, self-assembly of artificial RNA-based nanostructures has been extensively developed. In this review, we classify the development of RNA nanostructures into five different groups: (1) multistranded assembly of RNA nanostructures, (2) multistranded assembly of RNA/DNA hybrid nanostructures, (3) RNA motif-based RNA nanostructures (RNA architectonics), (4) RNA origami, and (5) rolling-circle transcription (RCT)-based RNA nanoparticles.

2.2.1. Multistranded Assembly of RNA Nanostructures. In DNA nanotechnology, multistranded DNA-based nanoassemblies using sets of cleverly designed synthetic oligonucleotides have been extensively developed to construct two- and three-dimensional (2D and 3D) DNA nanostructures.[18,43−48] This molecular self-assembly technique was then also applied to the development of multistranded RNA-based nano-objects using chemically synthesized strands.[49−52] In 2010, Jaeger constructed small RNA nanocubes with six or ten synthetic RNA strands (Figure 2A) and individual double-helices on each edge of the object.[49] The RNA cubes were assembled using one-pot annealing processes. By employing multistranded RNA-based assembly, Guo further developed RNA 3D nanoprisms that contained two planar equilateral RNA triangles.[50] Each RNA triangle was assembled with four RNA stands and used as a building block to form a nanoprism. To build RNA prisms, two planar RNA triangles were connected by canonical base-pairing of sticky-ends. The prismatic RNA was successfully constructed and visualized by AFM and cryo-EM.

In addition to finite RNA nanostructures, infinite RNA nanostructures based on multistranded RNA nanoassembly have also been developed.[51,52] Franco demonstrated the construction of RNA tiles by connecting two RNA helices with two double crossover motifs (DX).[51] The individual RNA tiles were assembled and connected to neighboring tiles to form micrometer-scale RNA lattices based on a canonical base pairing of sticky-ends as shown in Figure 2B. Furthermore, they extended the design of 2D tile-based RNA lattices to fabricate 3D RNA nanotubes.[52] Five RNA strands were assembled to create a DX RNA tile that served as a monomer unit. To construct micrometer-length RNA nanotubes, RNA tiles were connected by complementary sequences of sticky-end domains that are present in each tile. The authors found that the formation of RNA nanotubes depends on the distance of intertile connections. They successfully fabricated micrometer-length RNA nanotubes and characterized them with AFM.

2.2.2. Multistranded Assembly of RNA/DNA Hybrid Nanostructures. Current technology for chemical synthesis of DNA enables inexpensive production of long strand ssDNAs (up to 200 nt) with high fidelity and the ability to functionalize the DNA products with diverse chemical modifications that offer significant advantages in broad ranges of applications. However, the chemical synthesis of long ssRNA strands (more than 120 nt) remains a challenge. The combination of synthetic DNA

https://doi.org/10.1021/acs.chemrev.0c01332
Chem. Rev. XXXX, XXX, XXX−XXX

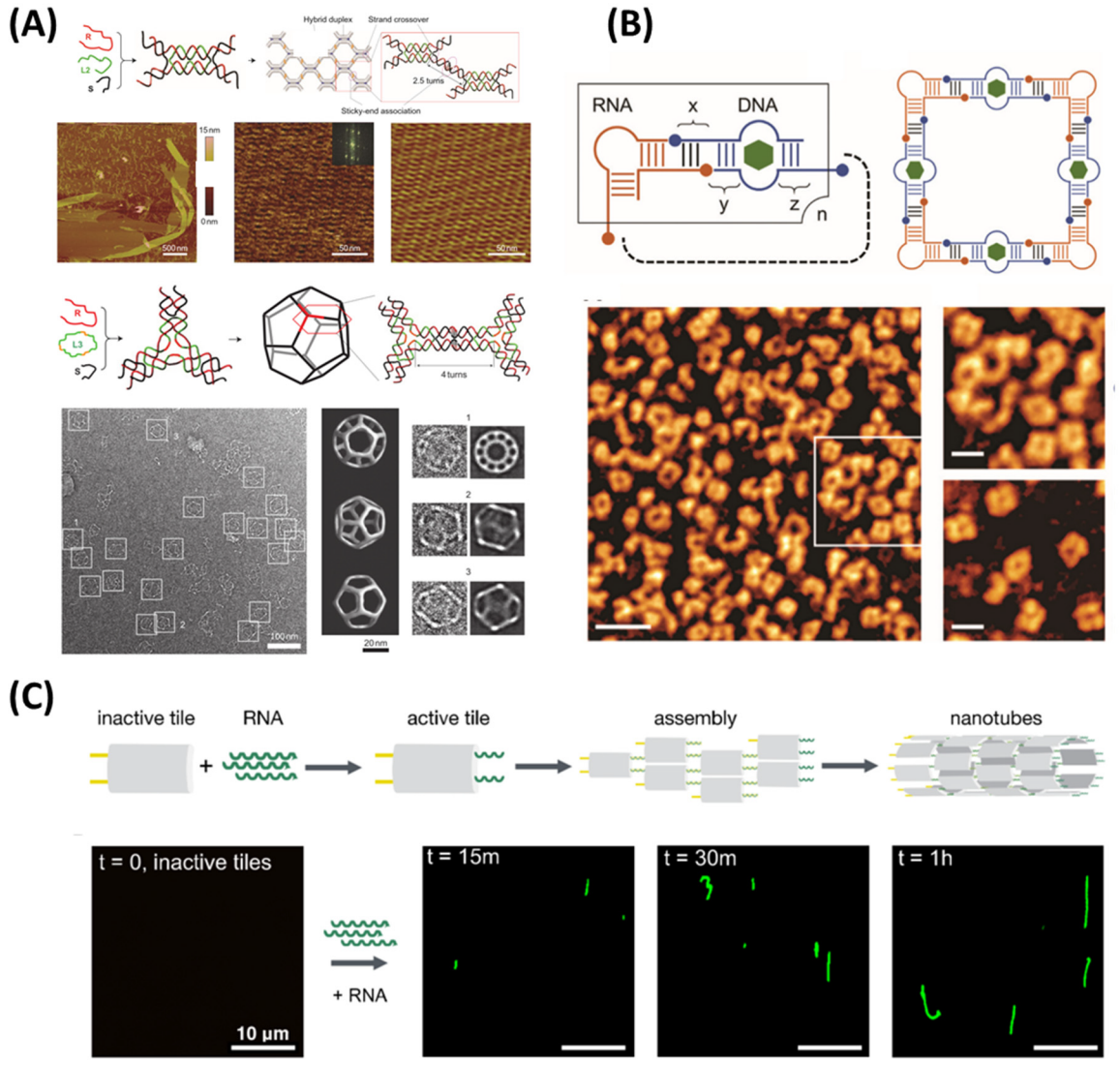

Figure 3. Self-assembly of multistranded nucleic acid nanostructures based on RNA/DNA hybrids. (A) DNA/RNA hybrid-based tiles, lattices, and dodecahedrons. Adapted with permission from ref 56. Copyright 2010 Springer Nature. (B) Ligand-dependent DNA/RNA hybrid nanosquares (Scale bar = 50 nm). Adapted with permission from ref 55. Copyright 2020 Royal Society of Chemistry. (C) Dynamic formation of DNA/RNA nanotubes fueled by ssRNA. Reprinted from ref 58. Copyright 2019 American Chemical Society.

production and naturally occurring RNA structures provides opportunities to create and construct DNA/RNA hybrid nanostructures including DNA/RNA heteroduplexes that form via Watson−Crick base pairing. Note that a homoduplex of dsDNA forms B-form helix, while a homoduplex of dsRNA and the heteroduplex of DNA/RNA both prefer the geometrically distinct A-form helix. The predictable, well-defined structure of DNA/RNA heterohybrids has been used to develop hybrid nanostructures.

In the past decade, multistranded DNA/RNA hybrid nanostructure assemblies have been developed and designed in various 2D and 3D shapes, such as triangles,[53,54] squares,[54,55] cubes,[49] dodecahedrons,[56] and nanotubes.[57] In 2010, Mao and colleagues reported DNA/RNA hybrid branched motifs that form 1D nanofibers, 2D nanoarrays, and also 3D dodecahedral nanospheres (Figure 3A).[56] They designed and constructed DNA/RNA hybrid-based DX tiles that consist of three DNA strands and two RNA strands. The hybrid tiles have single-stranded domains that allow adjacent tiles to connect and form highly ordered nanostructures. With three- and four-arm junction hybrid motifs, hexagonal and square lattices were built and characterized by AFM. Additionally, they demonstrated construction of DNA/RNA hybrid dodecahedrons based on self-assembly of three-way junction motifs (Figure 3A).

With the natural structural diversity of RNA and well-defined architecture of DNA, Herman further extended the multistranded RNA/DNA hybrid strategy to assemble polygonal nanoshapes by the combination of an RNA motif with dsDNA structure.[54,55] To fold hybrid nanoarchitectures, they harnessed a bending RNA motif from an internal loop of RNA from the hepatitis C virus that served as a corner point and connected bending RNA motifs with dsDNA. With this tool, polygonal DNA/RNA hybrid nanoshapes, including triangles, squares, pentagons, and hexagons, were created and visualized by AFM. Furthermore, they developed a technique for the formation of ligand-dependent DNA/RNA hybrid nanostructure.[55] In this work, an adenosine monophosphate (AMP)-binding DNA aptamer was utilized as a connector module to link bending RNA motifs to form nanoshapes. When the AMP ligand is bound by its specific DNA aptamer, the AMP-DNA stabilizes

https://doi.org/10.1021/acs.chemrev.0c01332
Chem. Rev. XXXX, XXX, XXX−XXX

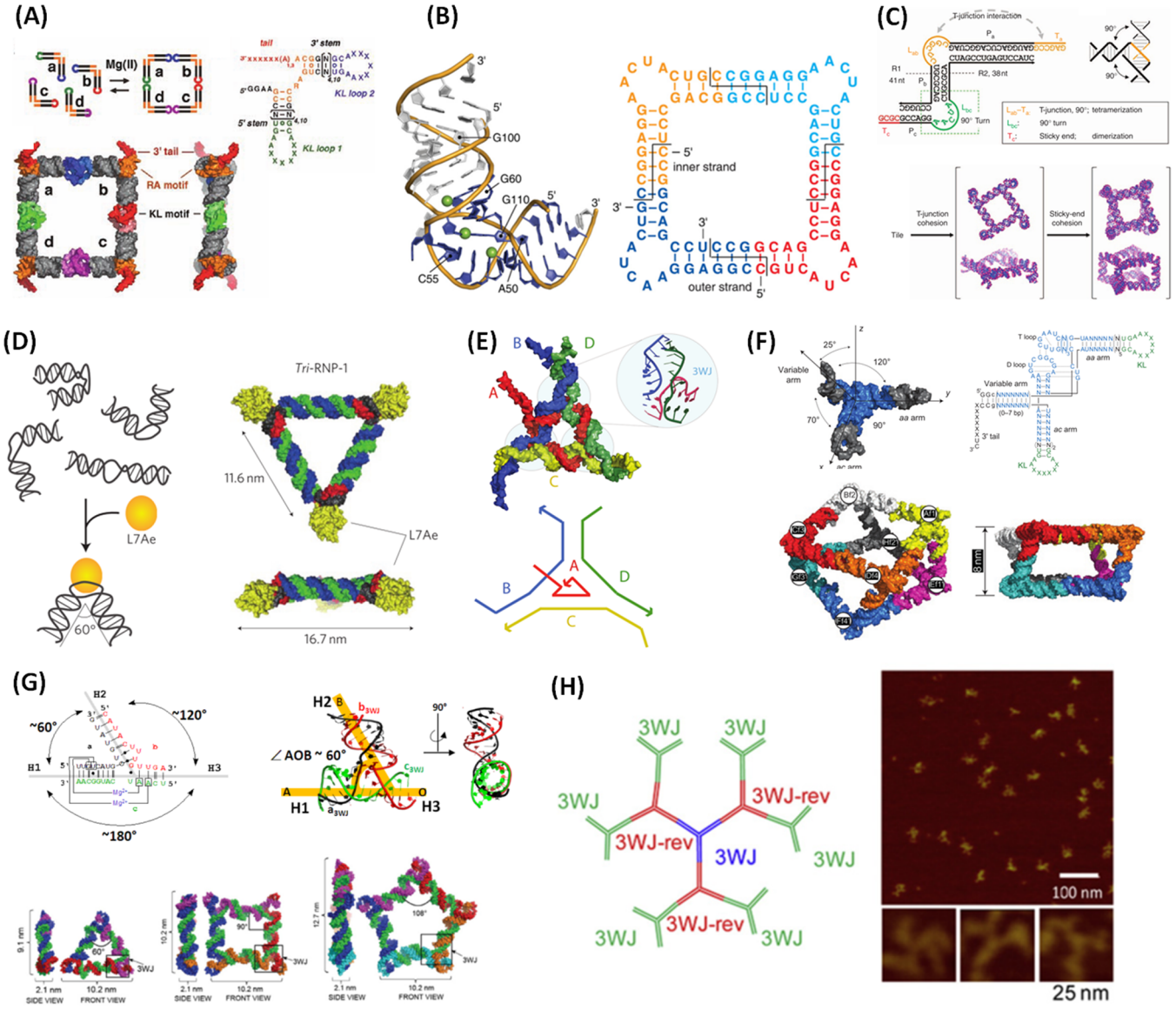

Figure 4. Self-assembly of RNA nanoarchitectures using naturally occurring RNA structures. (A) Self-assembled RNA nanosquare with tectoRNAs containing an RA motif. Adapted with permission from ref 62. Copyright 2004 The American Association for the Advancement of Science. (B) Three-dimensional structure of domain IIa of HCV IRES and square-like RNA nanostructures. Adapted with permission from ref 69. Copyright 2011 National Academy of Sciences. (C) Construction of an RNA nanoprism using HCV IRES motifs. Adapted with permission from ref 65. Copyright 2015 Springer Nature. (D) Programmable construction of equilateral triangle RNA using the K-turn/L7Ar complex, an RNA−protein complex. Adapted with permission from ref 70. Copyright 2011 Springer Nature. (E) Self-assembled RNA triangle with bending 3WJ derived from 16s rRNA motif of *Thermus thermophilus*. Adapted from ref 72. Copyright 2011 American Chemical Society. (F) Polygonal RNA nanostructure made of tRNA motifs. Adapted with permission from ref 75. Copyright 2010 Springer Nature. (G) Construction of triangular, square, and pentagonal RNA nanoobjects using pRNA-3WJ from the bacteriophage phi29 DNA packaging motor. Adapted from ref 79. Published 2014 Oxford University Press. Licensed under the creative commons agreement (https://creativecommons.org/licenses/by/4.0/). (H) Formation of dendrimeric RNA with pRNA-3WJ. Adapted with permission from ref 85. Copyright 2016 Elsevier.

the DNA/RNA complex. In the absence of AMP, DNA/RNA hybrid is not formed due to a much lower stability under those conditions. This ligand-dependent DNA/RNA hybrid formation provides modularity of structure design and offers possibilities to further develop and apply this technology in various applications such as biosensing and target-responsive materials.

Besides static designs and constructions of DNA/RNA hybrids, the dynamic control of formation and dissolution of RNA/DNA hybrid systems has been further developed. Franco's group has developed transcriptional control of the assembly and disassembly of DNA nanotubes.[57,58] DX DNA tiles were used as building blocks, and a ssRNA linker was introduced to direct and trigger DNA/RNA hybrid formation (Figure 3C).[58] Additionally, ssRNA triggers can be produced by *in vitro* transcription using a DNA template and RNA polymerase. RNase H, an enzyme that degrades RNA in DNA/RNA heteroduplex, was introduced to disassemble the DNA/RNA hybrid nanotubes. To understand the dynamic assembly/disassembly of hybrid nanotubes, fluorescently labeled nanotubes were observed by epifluorescence microscopy. By fine-tuning parameters for both the transcription reaction and RNase H activity, they controlled the rates of assembly/disassembly of DNA/RNA hybrid nanotubes. Fur-

https://doi.org/10.1021/acs.chemrev.0c01332
Chem. Rev. XXXX, XXX, XXX−XXX

thermore, they demonstrated the disassembly of the DNA nanotubes by introducing transcribed ssRNA invader strands. The DX tile-based DNA nanotubes contained a ssDNA overhang that allowed ssRNA to hybridize and deform the nanotubes based on strand displacement interactions.[57] The disassembly of the nanotubes was reversed, and the nucleic acid nanotubes were reformed by the addition of RNase H. This autonomous, controllable assembly/disassembly of DNA/RNA hybrid nanotubes demonstrated a programmable molecular oscillator that may be useful in a broad range of applications such as smart materials, synthetic biology, and drug delivery.

2.2.3. RNA Motif-Based RNA Nanostructures (RNA Architectonics). Over the past three decades, structural biologists have employed advanced microscopy and spectroscopy (X-ray and NMR) together with biochemical methods to study, understand, and reveal the beauty and complexity of naturally occurring RNA architectures such as ribosomes, tRNAs, ribozymes, and riboswitches. In nature, self-folding RNAs show sophisticated 2D and 3D structures such as bends and junctions.[59−61] In 1996, Jaeger and colleagues implemented an intriguing strategy for designing RNA nanostructures called RNA tectonics in which modular RNA units (TectoRNAs) were used to assemble molecular objects.[59] A large collection of structural and interacting RNA motifs represents a library of nanobricks that enable the engineering of sophisticated, programmable RNA nanoarchitectures. Due to the versatility and modularity of RNA motifs, a limitless number of well-defined RNA nanostructures and supramolecular RNA nanostructures can be produced.

Tectonics-based RNA nanoassembly has been reviewed in multiple journals.[5,6,8] In this review, we classified RNA motifs into two main groups: (1) structural motifs and (2) interaction motifs.

2.2.3.1. Structural Motifs. Here, we categorize structural RNA motifs into two categories: bending and branching motifs. The bending motifs are comprised of two main subgroups, right angle motifs and RNA−protein complex motifs. These motifs have been extensively used as structural components of RNA tectonics to form RNA nanostructures, including squares,[62,63] triangles,[64] and prisms.[65]

2.2.3.1.1. Right-Angle Motifs. A small structural motif found in the ribosome provides a 90° bend between two adjacent helices called the right angle (RA) motif.[66,67] In 2004, Jaeger's group demonstrated the self-assembly of an RNA nanosquare through RNA tectonics.[62] Each of the RNA units comprised two interacting hairpin or kissing loop motifs (KL) connected by RA motifs (Figure 4A). The RNA nanosquare was formed by self-assembly of four RNA units via intermolecular interaction of 180° KL motifs. In 2009, Jaeger and colleagues further developed three different sizes of RNA nanosquares by using three kinds of 90° bending motifs: RA motif, 3-way junction motif, and tRNA motif.[63]

The hepatitis C virus (HCV) genome contains an internal ribosomal entry site (IRES) that binds to the 40S ribosomal subunit of host cells. The three-dimensional structure of IRES has been studied, and cryo-EM results revealed the three-dimensional structure of the domain IIa of IRES that establishes a 90° bend.[68] The domain IIa of HCV IRES is thus another type of right-angle motif used to build RNA nanostructures. In 2011, Hermann's group utilized IRES bending motifs to construct an RNA nanosquare (Figure 4B).[69] Furthermore, they analyzed the three-dimensional structure of a IIa motif from the IRES elements of Seneca Valley virus (SVV), finding that it showed a bending conformation. They employed this motif to build triangular RNA nanostructures.[64] In 2015, Mao's group further developed a sophisticated RNA nanoprism by self-assembly of RNA tiles.[65] The RNA tile was comprised of two strands RNA containing a 90° bending motif derived from HCV IRES. To build the RNA nanoprism, four RNA tiles first formed a tetrameric RNA square through a T-junction, and two RNA squares then formed an octameric RNA nanoprism via sticky-end hybridization (Figure 4C). The self-assembled RNA nanoprisms were characterized by AFM and cryo-EM.

2.2.3.1.2. RNA−Protein Complex Motifs. Many RNAs bind specifically with proteins to form complex supramolecular structures that play essential roles in biology. RNA−protein complexes (RNP), such as ribosomes and spliceosomes, display sophisticated three-dimensional structures. In 2011, Saito's group reported an equilateral triangle RNA nano-object using an RNP complex comprising the C/D box binding with the ribosomal L7Ae protein.[70] The box C/D Kink-turn (K-turn) is relatively flexible, so it is more difficult to use as a building block in creating stable nanostructures, but the flexibility of the K-turn is decreased and the stability increased following binding with L7Ae. The K-turn/L7Ae complex forms a 60° bending angle, and using this RNP motif, triangular RNA nanostructures were formed (Figure 4D). Saito's group further developed square-shaped RNA nanostructures with 90° angle RNP motifs consisting of a ribosomal protein, RPL1, bound with an RNA motif that was derived from 23S rRNA.[71]

2.2.3.1.3. Branching Motifs. Several RNA branching motifs, comparable to the Holliday junction in DNA, have been identified from various types of RNAs, including rRNAs, tRNAs, and packaging RNAs (pRNAs). Branching motifs not only provide multiarm junction points that enable connection between multiple domains but also offer fixed angle bending modules. For example, a three-way junction motif derived from *Thermus thermophilus* 16s rRNA comprises three-branched duplexes linked with a 60° bending angle. Using this three-way junction from 16s rRNA, Shapiro and co-workers built a triangular RNA nanostructure from four strands of RNA (Figure 4E).[72] A couple of years later, Shapiro reported construction of a self-assembled RNA nanosquare using a three-way junction motif identified from the large ribosomal subunit of *Deinococcus radiodurans*.[73] Using a similar strategy, Jaeger's group made square-shaped RNA nanostructures by using the 90° bending angle of a three-way junction motif derived from *Haloarcula marismortui* 23S rRNA.[63]

The crystal structure of tRNA reveals the detailed tertiary structure of tRNA motifs containing four- to five-helix junctions.[74] With the 90° angle bend and multijunctions of tRNA, Jaeger demonstrated the development of a tetrameric RNA containing the tRNA motif located at each vertex of the RNA nanosquare.[63] In 2010, Jaeger further developed self-assembly of polyhedral RNA nano-objects using class II tRNA (Ser) (Figure 4F).[75] The crystallographic structure of tRNA shows that the variable arm is oriented in the *Z*-direction and makes angles of 120°, 70°, and 25° with the *X*, *Y*, and *Z* axes, respectively.[76] The well-defined and stable structure of the tRNA motif can be combined with two kissing loops and one ssRNA tail to serve as a building block to form polyhedral RNA via KL and tail−tail intermolecular interactions (Figure 4F).

The packaging RNA (pRNA) from the bacteriophage phi29 DNA packaging motor has a unique three-way junction (3WJ) with a well-defined bending angle.[7,77] The 3WJ motif identified from pRNA contains three helices (H1, H2, and H3). The angle

https://doi.org/10.1021/acs.chemrev.0c01332
Chem. Rev. XXXX, XXX, XXX−XXX

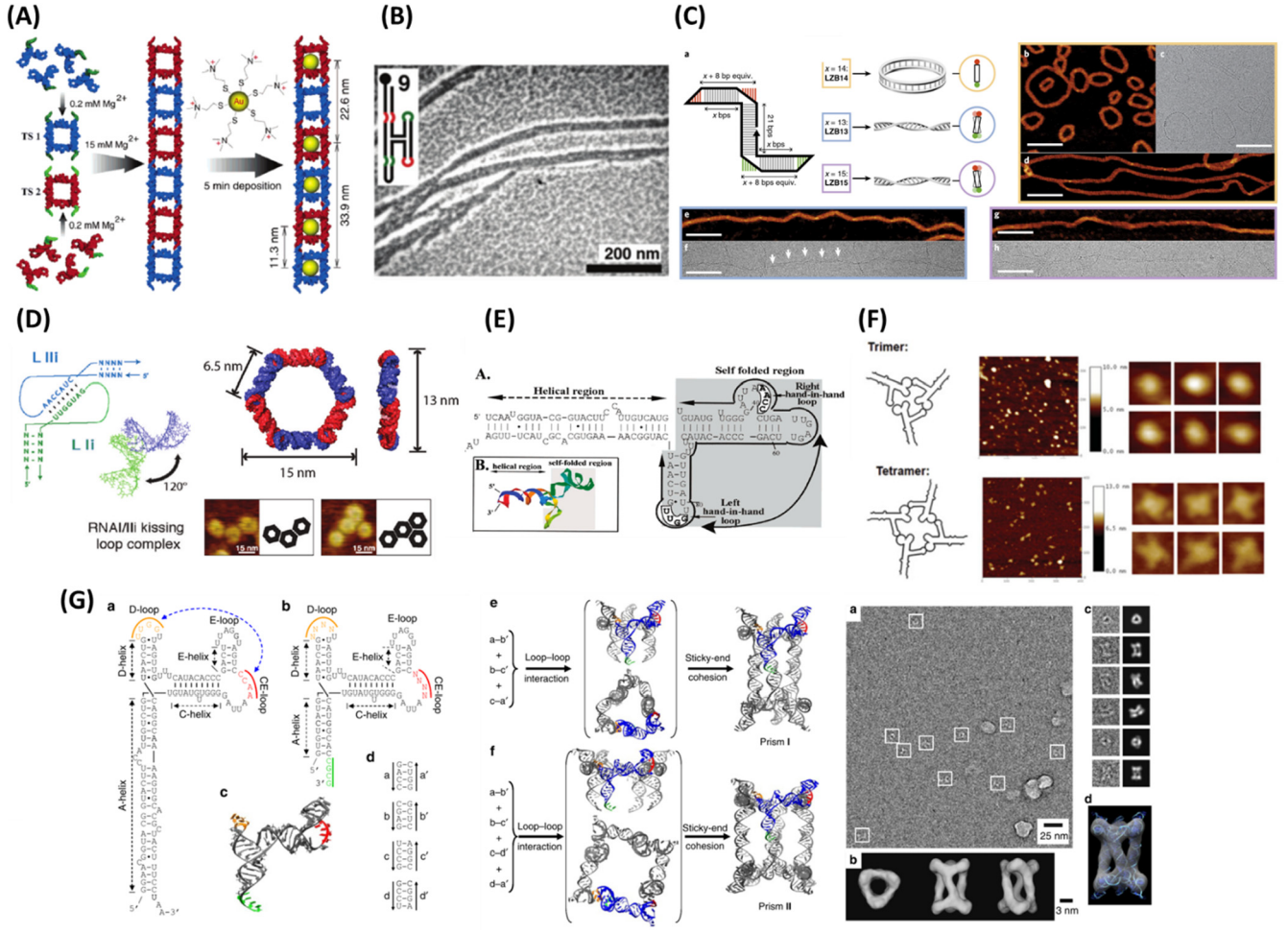

Figure 5. Self-assembly of RNA architectures with interaction motifs. (A) Hierarchical self-assembly of an RNA nanoladder using the tail−tail interaction. Reprinted from ref 86. Copyright 2005 American Chemical Society. (B) Formation of RNA fiber via the LR interaction. Adapted with permission from ref 88. Copyright 2006 Oxford University Press. (C) Construction of RNA nanoring and nanowire using branched kissing-loop motifs (Scale bar = 100 nm). Adapted with permission from ref 91. Copyright 2020 Springer Nature. (D) The 120° KL motifs derived from RNAI/IIi kissing complex and formation of hexagonal RNA nanoring with 120° KL motifs. Adapted from ref 92. Copyright 2011 American Chemical Society. (E) 2D drawing of pRNA-3WJ. Adapted from ref 77. Copyright 2004 American Chemical Society. (F) Multimeric RNA nanoring formed by loop−loop interaction called hand-in-hand interaction. Adapted from ref 96. Published 2013 Cold Spring Harbor Laboratory Press. Licensed under a Creative Commons agreement (https://creativecommons.org/licenses/by/4.0/). (G) Construction of RNA nanocages by re-engineering pRNA-3WJ. Adapted with permission from ref 97. Copyright 2014 Springer Nature.

between H1 and H3 is 180°, while H1 and H2 create a 60° angle (Figure 4G). With this feature of pRNA-3WJ, Guo, a pioneer in development and utilization of pRNA motifs to make RNA nanostructures, built an equilateral RNA nanotriangle.[78] The naturally occurring conformation of pRNA-3WJ is limited to a 60° angle, but Guo introduced 90° and 108° angles into engineered nanostructures. Exploiting the conformations of these angular motifs, Guo demonstrated triangular, square, and pentagonal RNA nanostructures (Figure 4G).[79] Using the 90° angle of pRNA-3WJ, he rationally designed and built multifunctional and tunable RNA squares.[80]

Besides polygonal RNA nano-objects with pRNA-3WJ placed at the vertices of nanostructures, pRNA-3WJ has been used as a central module to create arm-extended 3WJs, thus allowing nanostructures to be decorated with additional functional motifs, such as RNA aptamers and miRNAs.[81−83] Due to the modularity of the pRNA motif, Guo designed and built a 4-arm junction from the native pRNA-3WJ motif by replacing two right-hand loops of pRNA with dsRNA.[84] Using pRNA-3WJ, Guo further developed higher-order RNA dendrimers, as shown in Figure 4H.[85] The structural diversity and bending angle variety of branching motifs provide enormous possibilities to construct 2D and 3D RNA nanostructures.

2.2.3.2. Interaction Motifs. Interaction motifs are essential modules needed to create and build complex nucleic acid nanostructures. In DNA nanotechnology, sticky-end hybridization domains are the predominant interaction motif, and they have been utilized to fabricate many sophisticated synthetic DNA nanostructures and lattices. However, naturally occurring, self-folding RNA provides a broader diversity of structural and functional RNA motifs that have been used as interaction modules and are not limited to sticky-end hybridization. In this review, we classified RNA interaction motifs into two groups: (1) sticky-end hybridizations and (2) loop−loop interactions. Loop−loop interactions are further broken down into three subgroups: loop−receptor (LR) motifs, kissing-loop (KL) motifs, and packaging RNA (pRNA) motifs.

2.2.3.2.1. Sticky-End Hybridization. Sticky-end hybridization, also called tail−tail interaction, has been extensively used to construct complex RNA nanostructures such as

https://doi.org/10.1021/acs.chemrev.0c01332
Chem. Rev. XXXX, XXX, XXX−XXX

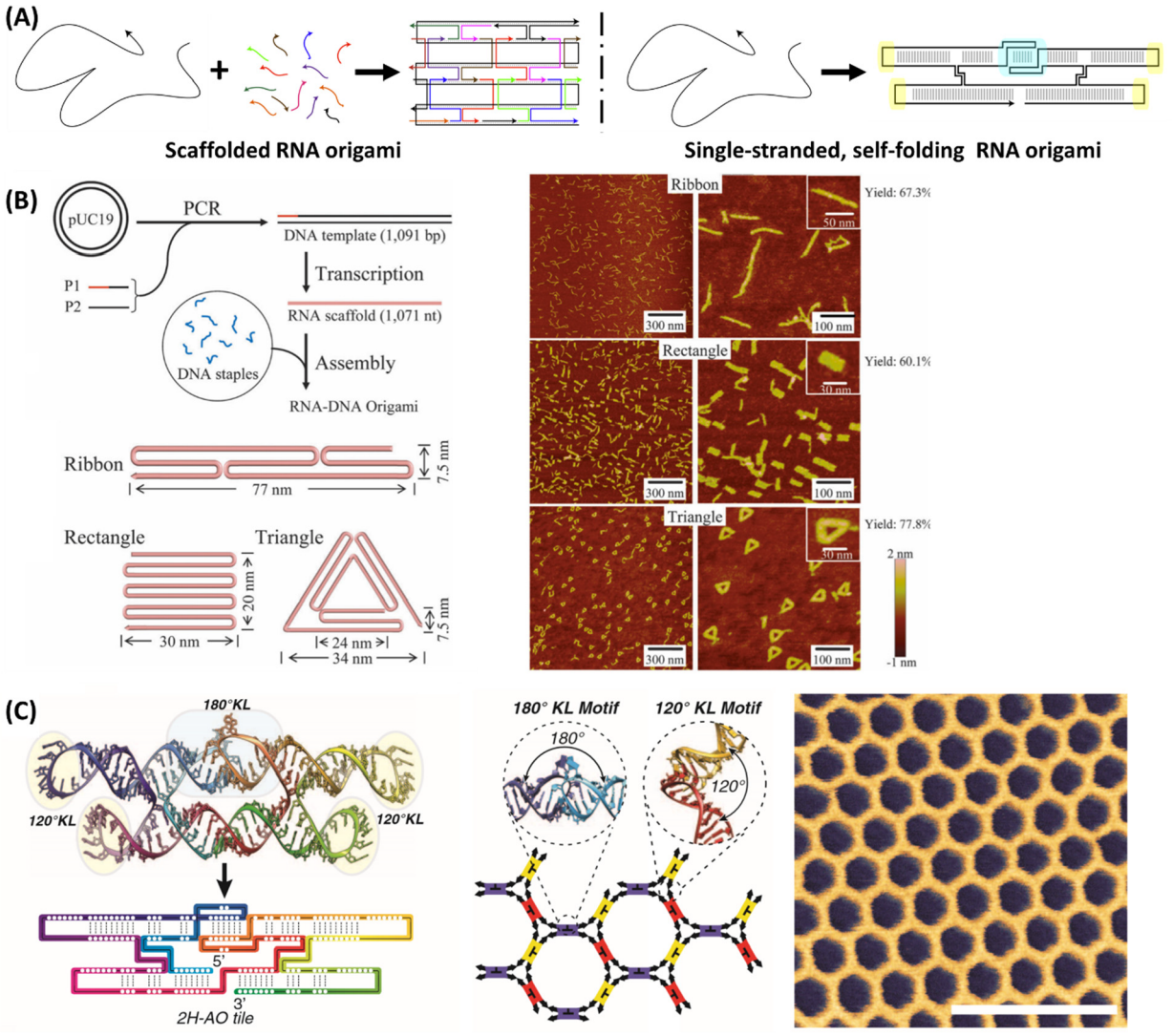

Figure 6. Self-assembly of RNA origami. (A) Scaffolded RNA origami (left) and single-stranded, self-folding RNA origami (right). (B) Molecular self-assembly of RNA origami with RNA scaffold and DNA staples. Adapted with permission from ref 99. Copyright 2013 Royal Society of Chemistry. (C) Single-stranded RNA origami containing 120° and 180° kissing loops (KLs) represented in yellow and blue, respectively, and formation of hexagonal RNA lattice with 2-helix ssRNA origami tiles via intermolecular interaction of 120° KL (Scale bar = 100 nm). Adapted with permission from ref 103. Copyright 2014 The American Association for the Advancement of Science.

triangles,[64] squares,[62,69,86] dendrimers,[85] polyhedrons,[75] and lattices.[62,86] Due to the modularity of RNA architectonics, tectoRNA containing complementary ssRNA motifs have been designed. Jaeger constructed square-like RNA nanostructures bearing ssRNAs that form two-dimensional RNA nanolattices by using sticky-end interactions.[62] With rationally designed RNA nanosquares and tail−tail connectors, Jaeger further developed hierarchical self-assembling RNA nanowires as shown in Figure 5A.[86] The well-defined space within each RNA square enabled the placement of gold nanoparticles inside RNA squares. Using this method, the authors demonstrated well-controlled spacing between gold nanoparticles using RNA nanowires. With the simplicity of tail−tail interactions and three-dimensional tectoRNAs made of tRNA motifs, polygonal RNA nano-objects have been developed (Figure 4F).[75] In 2016, Guo reported RNA dendrimers constructed by connecting pRNA-3WJ motifs through tail−tail interactions (Figure 4H).[85]

2.2.3.2.2. Loop−Receptor (LR) Motifs. Loop−receptor (LR) motifs are one of the loop−loop interactions that have been used to construct RNA nanostructures. Jaeger and Leontis designed a single-stranded, self-folding RNA that formed a stem structure containing hairpin loops and internal loops. The internal loops served as receptors, and the LR interaction occurs via interactions of hairpin loops and their receptor loops.[87] In 2006, they further developed 4WJ H-shaped tectoRNAs bearing LR motifs that formed micrometer-scale RNA filaments via LR interaction (Figure 5B).[88] By employing H-shaped tectoRNAs via intermolecular interactions of LR motifs, Leontis showed the self-assembly of multimeric ring-shaped RNA nano-objects.[89]

2.2.3.2.3. Kissing-Loop (KL) Motifs. The crystallographic structure of the human immunodeficiency virus (HIV) revealed loop−loop interactions, consisting of six complementary bases that interacted via Watson−Crick base pairing. This 180° loop−loop interaction is called a 180° KL motif and can be used as intermolecular connectors to build RNA architectures. Jaeger used 180° KL interactions in combination with other structural motifs such as RA, 3WJ, and tRNA motifs to assemble four tectoRNAs into a square-like RNA structure (Figure 4A).[62,63] Additionally, Jaeger built 2D and 3D RNA nanostructures (RNA nanowires and polyhedral RNA nanostructures) through

https://doi.org/10.1021/acs.chemrev.0c01332
Chem. Rev. XXXX, XXX, XXX−XXX

intermolecular interactions of 180° KL and tail−tail interactions (Figure 4F).[75,86] Similarly, Afonin utilized the HIV kissing-loop motif to create RNA nanofibers,[90] and in 2020, Weizmann developed ssRNA tile-based supramolecular RNA nanostructures based on artificially designed, branched KL motifs inspired by the 180° HIV KL motifs.[91] They designed a Z-shaped ssRNA tile, containing bulged helices and hairpin loops, that served as a monomer unit. The branched KL forms via intermolecular interactions between a bulged helix and a hairpin loop (Figure 4C). Self-assembled RNA nanorings were built by connecting multiple Z-tiles via branched KL interactions. Furthermore, micrometer-long RNA filaments have been constructed by introducing torsion into the structures, as shown in Figure 5C.

The RNAI/RNAII inverse (RNAI/IIi) kissing complex identified from CoLE1 plasmid-encoded transcripts from *Escherichia coli* is another example in the family of KL motifs. NMR and theoretical analysis revealed that the RNAI/IIi complex forms loop−loop interactions via Watson−Crick base pairing and bends at a 120° angle. Using a 120° RNAI/IIi KL motif, Jaeger successfully built hexagonal RNA nanorings (Figure 5D).[92] With this KL motif, Shapiro et al. further developed multifunctional RNA nanoparticles by appending functional motifs (aptamers, siRNAs, proteins, and small molecules) on hexagonal RNA nanorings.[93]

2.2.3.2.4. Packaging RNA (pRNA) Motifs. The RNA portion of the DNA packaging motor of bacteriophage phi29 consists of six copies of pRNA that form a hexameric ring.[94,95] Each of the pRNAs contains a helical region (called the foot) and single-stranded internal loops (called hands) as shown in Figure 5E.[77] The naturally occurring ring-like RNA nanomotor forms due to loop−loop interactions. Using bioinspired RNA nanodesigns, Guo employed an intermolecular interaction of the hand-in-hand formation to assemble multimeric nanorings as well as RNA nanofibers (Figure 5F).[96] Furthermore, Mao re-engineered pRNA motifs by mutating sequences of the loops and incorporating ssRNA tail. With rational designs of the loop and sticky-end sequences, triangular and tetragonal RNA nanoprisms have been constructed based on loop−loop interactions and sticky-end hybridizations (Figure 5G).[97] Loop−loop and foot-to-foot interactions alike have been engineered to build RNA nano-objects.[77]

2.2.4. RNA Origami. In 2006, Rothemund developed an intriguing strategy to construct DNA nanostructures called DNA origami.[25] RNA nanotechnology has drawn inspiration from the success of DNA origami and has developed a similar set of RNA origami-based nanostructures. In this section, we classify RNA origami into two groups: (1) scaffold-based RNA origami (Figure 6A,B) and (2) single-stranded, self-folding RNA origami (Figure 6A,C).

2.2.4.1. Scaffold-Based RNA Origami. Sugiyama's group presented a strategy of RNA-templated DNA origami structures seven years after Rothemund introduced DNA origami.[98] They designed DNA/RNA hybrid origami assembled from a ssRNA scaffold and DNA staple strands. The unmodified and chemically modified ssRNA templates were produced by *in vitro* transcription with T7 RNA polymerase. The seven-helix planar and six-helix bundle DNA/RNA hybrid origami were constructed and characterized by AFM. Importantly, they harnessed the versatility of DNA chemical modifications by functionalizing DNA staple strands with biotin and other chemical moieties. With incorporation of biotin-modified DNA staple stands, the hybrid origami was efficiently purified using streptavidin-coated magnetic beads. A couple of months later, Mao's group reported an isothermal, quick folding DNA/RNA hybrid nanostructure.[99] The DNA/RNA origami were completely folded within 5 min under isothermal assembly. In their work, three designs of two-dimension hybrid nucleic acid nanostructures (ribbons, rectangles, and triangles) were constructed and visualized by AFM, as shown in Figure 6B. This RNA scaffold/DNA staple origami has been developed further. Rolling-circle transcription (RCT) is one of the potential methods to produce long strands of ssRNA by using a circular DNA template and T7 RNA polymerase. A DNA/RNA hybrid nanoribbon has been designed and constructed using a RCT-produced RNA scaffold and chemically produced short DNA staple strands.[100] Furthermore, Sugiyama reported a self-assembled RNA origami architecture consisting of RNA staple strands that facilitated the folding of an RNA scaffold strand. Both the RNA scaffold and staples were produced by *in vitro* transcription. Rectangular and tubular RNA origami have been constructed and characterized by AFM.[101] For the *in vitro* production of RNA scaffolds and RNA staples, chemically modified NTPs (biotinylated and aminoallyl UTP) were incorporated into RNA origami structures, allowing conjugation with other molecules and providing an expanded toolbox with various functionalities to the RNA origami nanostructures. Andersen's group has further developed octahedral RNA origami containing small interfering RNA (siRNA) that silence gene expression.[102]

2.2.4.2. Single-Stranded, Self-Folding RNA Origami. In nature, RNA is a self-folding molecule that displays a variety of structural motifs, including turns, junctions, and intermolecular interaction motifs. With these abundant natural examples of RNA structural motifs and self-folding behaviors, Geary et al. demonstrated single-stranded, cotranscriptional folding of RNA nanostructures (Figure 6C).[103] The ssRNA origami consisted of antiparallel RNA helices connected with multiple strand-exchange junctions. To construct single-stranded RNA origami, hairpin loops (tetraloop motifs) were placed at the ends of the RNA helices and one of the helical domains was replaced with a 180° KL. Due to the modularity and high structural diversity of RNA, tetraloop motifs located at the ends of RNA helices can be replaced by a KL domain, enabling RNA lattices to form by intermolecular interactions. By KL interaction, hexagonal and rectilinear RNA lattices can be programmed to form via 120° and 180° KLs, respectively. Single-stranded RNA origami harnesses the structural diversity of naturally folded RNA motifs and provides modularity and architectural flexibility. With Lego-like assembly, design concepts have been expanded by replacing tetraloops with functional motifs such as fluorescent aptamers and protein-binding RNA aptamers.[104−106] For example, Andersen's group developed an RNA aptamer-based FRET system by using a ssRNA origami bearing two fluorescent RNA aptamers.[104] This RNA origami FRET system has been adapted for detection of ssRNA or the small molecule *S*-adenosylmethionine. In 2019, LaBean's group developed a single-molecule, self-folding RNA origami anticoagulant by incorporating thrombin-binding RNA aptamers on RNA origami.[106] With tremendous structural diversity and functionality, single-stranded RNA origami platforms can be functionalized for use in a wide range of applications, including biosensors and medical applications that will be discussed later in this review.

In 2017, Yan developed novel designs of self-folding single-stranded DNA and RNA origami to form arbitrary shapes including rectangles, rhombi, squares, and heart-like shapes.[107] The key concept for folding ssOrigami is to produce a knot-free

https://doi.org/10.1021/acs.chemrev.0c01332
Chem. Rev. XXXX, XXX, XXX−XXX

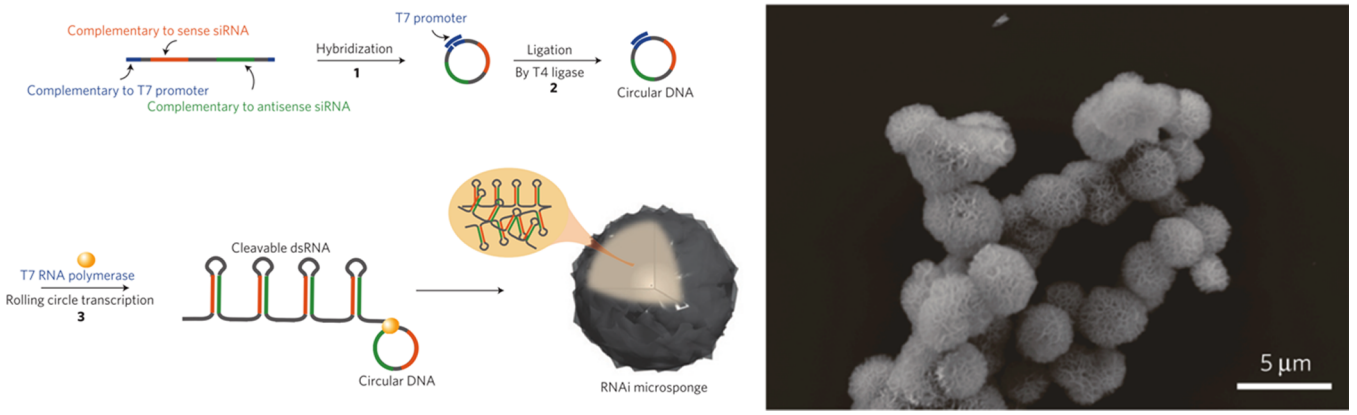

Figure 7. Self-assembled RNA nanoparticles produced by rolling circle transcription and scanning electron micrograph of RNA particles. Adapted with permission from ref 110. Copyright 2012 Springer Nature.

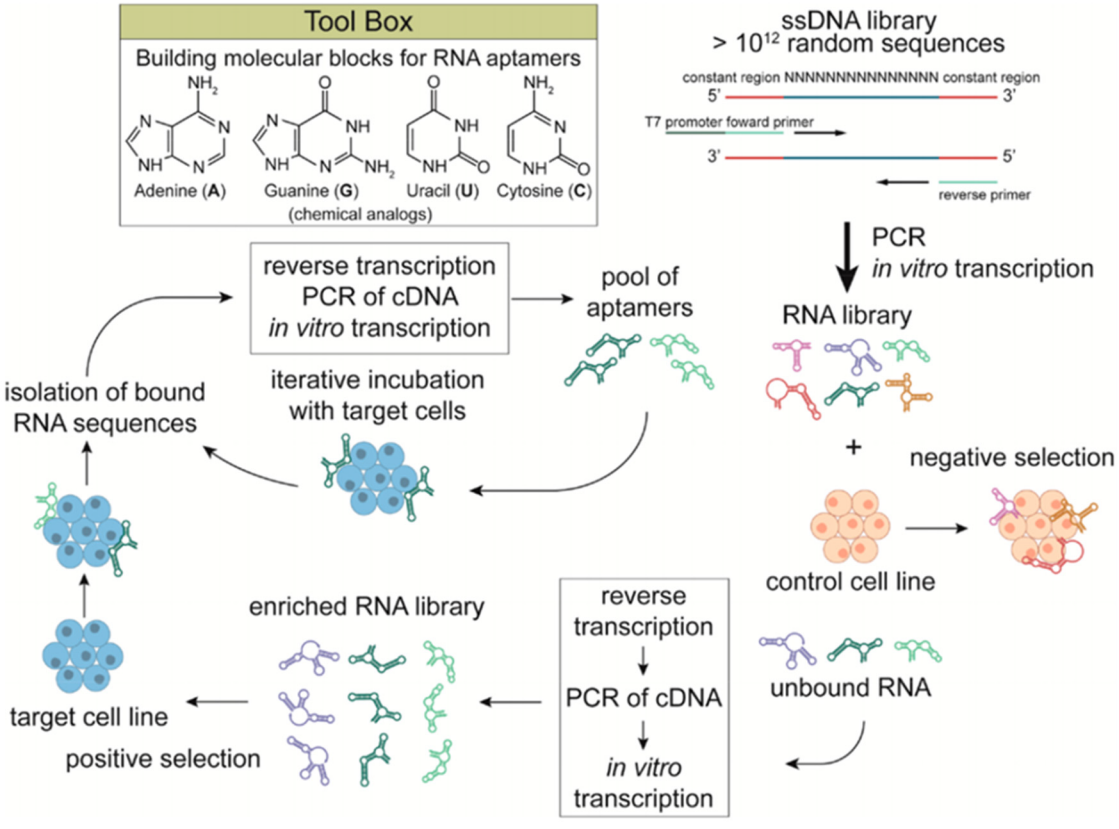

Figure 8. Diagram of whole-cell SELEX. RNA aptamers are selected against a cell population expressing specific target receptors. A large, randomized library of DNA nucleotide sequences is amplified via PCR and transcribed into RNA via in vitro transcription. The RNA is then incubated with control cells that do not express the target receptors, and nonbinding RNA is retained and subsequently amplified via RT-PCR. The process of incubation with the target cells and isolation is repeated to yield a more selective RNA library that has higher binding affinity to the target cells. Reprinted from ref 119. Copyright 2019 American Chemical Society.

structure. To achieve self-folding ssOrigami, ssDNA or ssRNA are designed in partially complementary dsDNA or dsRNA fashion and the helical domains are connected by parallel crossovers to obtain zero-knot structures. With this method, multikilobase ssDNA and ssRNA origami have been constructed. Yan's group successfully produced a 6337-nt ssRNA origami, nearly 10-fold bigger than Geary's 660-nt RNA tile.[103,107] Additionally, Yan employed ssRNA origami to excite an immunostimulatory response that could be utilized for cancer immunotherapy.[108]

2.2.5. Rolling-Circle Transcription (RCT)-Based RNA Nanoparticles. Rolling circle transcription (RCT) involves enzymatic production of long RNA strands using circular DNA template and T7 RNA polymerase. In 1995, Kool and colleagues developed RCT by using synthetic circular DNA templates, obtaining long RNA molecules bearing multimeric repeats.[109] A decade later, Hammond's group employed RCT to construct self-assembled RNA microspheres for siRNA delivery.[110] Multiple tandem copies of RNA transcripts were produced using RCT, and RNA microparticles were formed based on RNA condensation, as shown in Figure 7. Due to the high

https://doi.org/10.1021/acs.chemrev.0c01332
Chem. Rev. XXXX, XXX, XXX−XXX

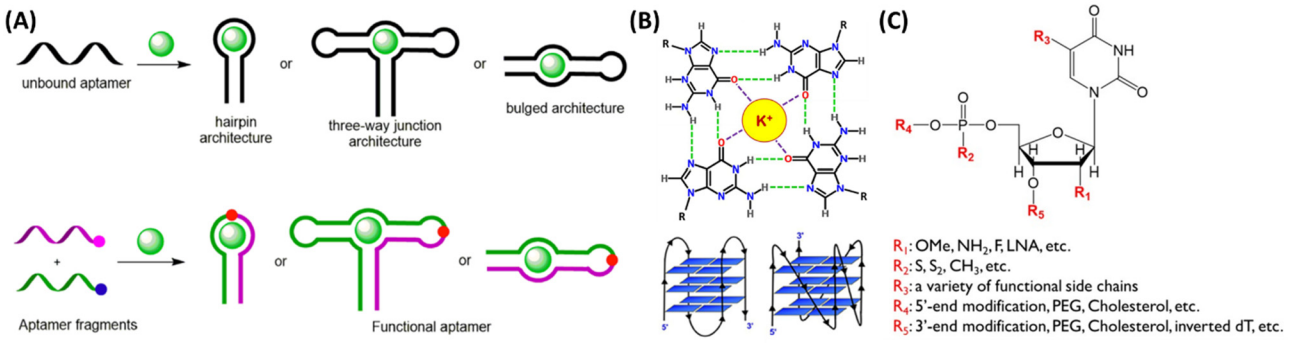

Figure 9. Aptamer architectures and chemical modifications. (A) Folding of a single-strand aptamer in the presence of a target into various architectures (top) and folding of a split aptamer in the presence of a target (bottom). Adapted from ref 123. Published 2020 Oxford University Press. Licensed under a Creative Commons agreement (https://creativecommons.org/licenses/by/4.0/). (B) Details of a G-quartet structure (top) and examples of topological variations of G-quadruplexes including intramolecular antiparallel and parallel structures (bottom). Adapted from ref 124. Published 2016 Frontiers Media SA. Licensed under a Creative Commons agreement (https://creativecommons.org/licenses/by/4.0/). (C) A nucleotide, the building block of nucleic acid aptamers. The ribose sugar, phosphate group, and nitrogenous base all have positions at which chemical modifications can be incorporated for increased nuclease resistance. OMe, *O*-methyl; LNA, locked nucleic acid. Adapted from ref 129. Published 2019 Multidisciplinary Digital Publishing Institute. Licensed under a Creative Commons agreement (http://creativecommons.org/licenses/by/4.0/).

number of sequence repeats within the RNA produced in the RCT process, self-assembled RNA particles are densely packed and provide significant nuclease resistance. With economical production and versatility of sequence designs, RCT-produced RNA nanoparticles carrying functional RNA molecules (e.g., RNA aptamers[111] and siRNA[112]) have been developed and used in a wide range of applications that will be discussed in further detail in section 5.

3. NUCLEIC ACID APTAMERS

Oligonucleotide aptamers are short strands of ssDNA or ssRNA, generally 15−90 nt in length, that act as affinity ligands by specifically binding a certain target molecule or material. In 1990, Tuerk and Gold as well as Ellington and Szostak reported the biochemical selection of RNA aptamers that targeted T4 DNA polymerase as well as several organic dyes.[113,114] Over the past three decades, nucleic acid aptamers have been extensively explored and developed for binding a wide range of targets, from whole cells in the microscale to proteins and small molecules in the nanoscale. The high target specificity and affinity of aptamers renders them similar in function to antibodies. Moreover, a crucial property of aptamers is their ability to self-assemble into complicated tertiary and quaternary structures, which gives rise to their utility in diverse applications, including biosensing, targeted delivery, and therapeutics.[115] In this section, we describe aptamer synthesis, selection, architecture, and stability, and the use of stand-alone aptamers in various applications. Furthermore, we highlight limitations of stand-alone aptamers and provide insight into the improvement of aptamer function by decoration upon more substantial nucleic acid nanostructure platforms.

3.1. Affinity Handle Selection and SELEX

As mentioned above, aptamers are affinity handles or ligands created using diverse libraries of randomized sequences and an integrated selection procedure. In the first two studies describing such artificial processes and their resulting specific binding strands, Ellington and Szostak coined the term "aptamer"[114] and Tuerk and Gold coined the term "SELEX", meaning the process of systematic evolution of ligands by exponential enrichment.[113] Although originally performed with RNA sequence libraries, SELEX has since been applied to produce numerous DNA aptamers as well. *In vitro* selected affinity peptides are also sometimes referred to as peptide aptamers.[116] For nucleic acids, SELEX is the *in vitro* process that involves cycles of amplification, incubation, and isolation of aptamers from a diverse initial library (often up to 10^{12}−10^{15}) of randomized oligonucleotides. The nucleic acids are repeatedly incubated with the target, sorted for binding, and amplified, with subsequent rounds typically resulting in aptamers with higher affinities for the target. In such processes, RNA aptamers require the additional steps of transcription and reverse transcription, including reverse transcription polymerase chain reaction (RT-PCR).[117] The last step of the SELEX process is to isolate those aptamers with the greatest affinity to the target. The general steps of SELEX applied to RNA aptamers are depicted in Figure 8.

Through SELEX, aptamers have been selected to target various types of molecules. Typical targets, from most to least common, are proteins, small molecules, cells, viruses, and other nucleic acids.[118] Given these targets, different types of SELEX have been developed, including protein-based and whole-cell SELEX.[119] An additional type of SELEX, known as toggle SELEX, selects aptamers against more than one target (often orthologs of the same molecule). This works by alternating the target between successive rounds of selection. In 2001, the Sullenger group introduced the concept of toggle SELEX and used it to isolate RNA aptamers with high binding affinity to both human and porcine thrombin.[120] Unlike normal SELEX, which can result in the development of an overly specific aptamer that only works well *in vitro*, toggle SELEX shows more promise for *in vivo* preclinical trials, where it may assist in demonstrating efficacy in animal models. Odeh et al. provide an excellent table summarizing the various types of SELEX.[121]

3.2. Aptamer Architectures

Aptamers are developed to fold into specific architectures and bind with high affinities to target molecules. Their high surface area to volume ratio allows them to interact strongly with their surroundings despite their small size, which ranges from 5 to 30 kDa. In the presence of a target, many aptamers undergo conformational changes to reach their final form, which can consist of various tertiary and quaternary structures. The most common aptamer architecture is the hairpin-like structure, with

https://doi.org/10.1021/acs.chemrev.0c01332
Chem. Rev. XXXX, XXX, XXX−XXX

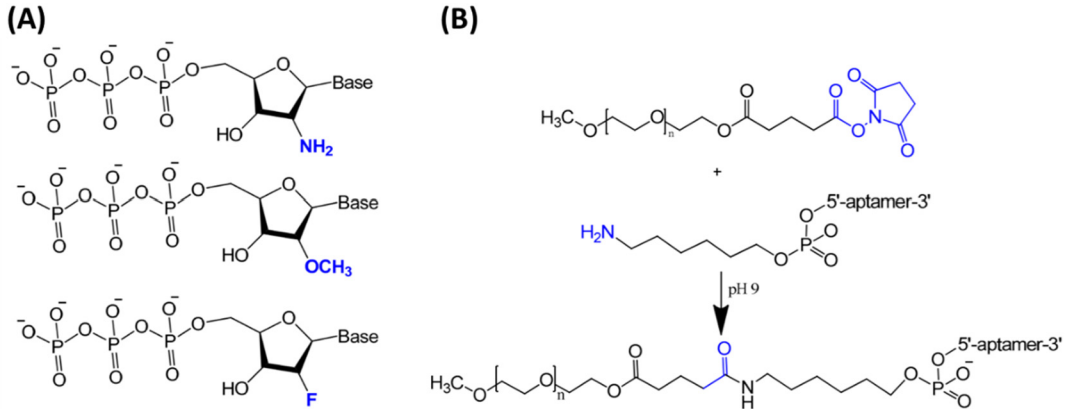

Figure 10. Chemical modifications for nucleic acid aptamers. (A) 2′ substitutions with an amine, methoxy, and fluoride group. (B) Chemical strategy for PEGylation of an aptamer at the 5′ terminus. Adapted from ref 121. Published 2019 Multidisciplinary Digital Publishing Institute. Licensed under a Creative Commons agreement (http://creativecommons.org/licenses/by/4.0/).

a single loop region as the target binding site. Other conformations include three-way junctions, pseudoknots, G-quartet, and bulged architectures (Figure 9A).[122,123] The guanine-quartet is formed via hydrogen bonding of four guanosines in Hoogsteen base-pairing fashion and stabilized by monovalent cations interacting with carbonyl oxygen atoms.[124,125] Two or more G-quartets formed and stacked on top of each other form G-quadruplex motifs that can contribute to the stability of aptamer architectures (Figure 9B).

Aptamers selected as single strands can be split into fragments that assemble in the presence of a ligand to form a tripartite complex. Due to their shorter length, split aptamers have increased binding specificity because they are less likely to form unwanted secondary structures. Split aptamers are commonly utilized in sensing applications and can aid in the intracellular delivery of aptamers. The negative charge of nucleic acids typically limits intracellular delivery; however splitting aptamers reduces the total number of negative charges per strand, allowing for somewhat easier intracellular entry.[123] In 2005, Kolpashchikov reported a split malachite green aptamer (MGA) used for the detection of nucleic acids.[126] The development of many other split aptamers has followed, including the extensively studied spinach[127] and broccoli aptamers.[128]

3.3. Chemical Modifications for Aptamers

Native nucleic acid aptamers are susceptible to nuclease degradation, rapid renal clearance, and other disadvantages that could reduce their favorability for certain uses, particularly in clinical and therapeutic applications. Indeed, the half-lives of unmodified aptamers in the blood serum are typically less than 10 min.[130] Therefore, researchers commonly endow aptamers with chemical modifications to help solve these problems and improve functional efficiency (Figure 9B). The issue of enzymatic degradation generally affects RNA aptamers more due to the presence of the 2′-OH group in the ribose sugar, and for this reason, RNA aptamers are often chemically modified by substituting another functional group for the 2′-OH group, most commonly a fluoride, amine, or *O*-alkyl group. These substitutions are shown in Figure 10A. Other modifications to improve nuclease stability include inverted thymidine capping on the 3′ end of the nucleic acid, use of enantiomeric forms of ribose or deoxyribose known as Spiegelmers,[131] and thiophosphate substitution.[132] Many groups have shown that these chemical substitutions on aptamers offer significant improvement in nuclease resistance, making them crucial for *in vivo* experiments and applications.

Besides enzymatic degradation, aptamers are also quickly cleared by the kidney due to their small size. Studies have shown that small molecules, of weights less than about 30−50 kDa, are quickly removed from blood by the kidney.[133] To avoid this, poly(ethylene glycol) (PEG) moieties are often grafted in a process known as PEGylation to extend the half-life of aptamers in blood circulation, as shown in Figure 10B. Solutions to renal filtration problems can also involve addition of other bulky chemical groups or nanomaterials to increase molecular mass. Aptamers may also be assembled into multivalent 2D and 3D nanostructures to increase their size and improve the target binding interaction by increasing the aptamers' local concentration at the binding site.[133]

Additionally, the introduction of amino acids on nucleic acid aptamers has shown potential for increasing the chemical diversity of nucleic acid libraries in SELEX. For example, in 2014, Rohloff et al. reported that the addition of hydrophobic aromatic side chains can significantly influence the ability to identify slow off-rate modified aptamers (SOMAmers), that is, aptamers with low dissociation constants.[134] The introduction of such side chains makes many more structural motifs possible for aptamers. Furthermore, as the authors found, increased hydrophobicity made it possible for aptamers to effectively target a more diverse range of protein families, including hormones, growth factors, and cytokines.

It is important to note, however, that although many chemical modifications carry added benefit, such as increased binding affinity, most also come with undesirable side effects. For example, addition of lipophilic molecules raises the risk of hepatotoxicity,[135] while PEG has been shown to sometimes trigger severe allergies in clinical studies.[136] As such, the risks and benefits of chemically modified aptamers must be carefully weighed before aptamers are applied in any clinical setting. Additionally, chemical modifications can increase the cost of aptamer production which can make large-scale use more difficult.

3.4. Comparison to Antibodies

Due to their specific folded conformations and reasonable binding abilities, aptamers are considered the nucleic acid equivalents of antibodies. Although antibodies are more broadly used and understood, aptamers have several advantages over antibodies. Unlike antibodies, aptamers are chemically synthe-

https://doi.org/10.1021/acs.chemrev.0c01332
Chem. Rev. XXXX, XXX, XXX−XXX

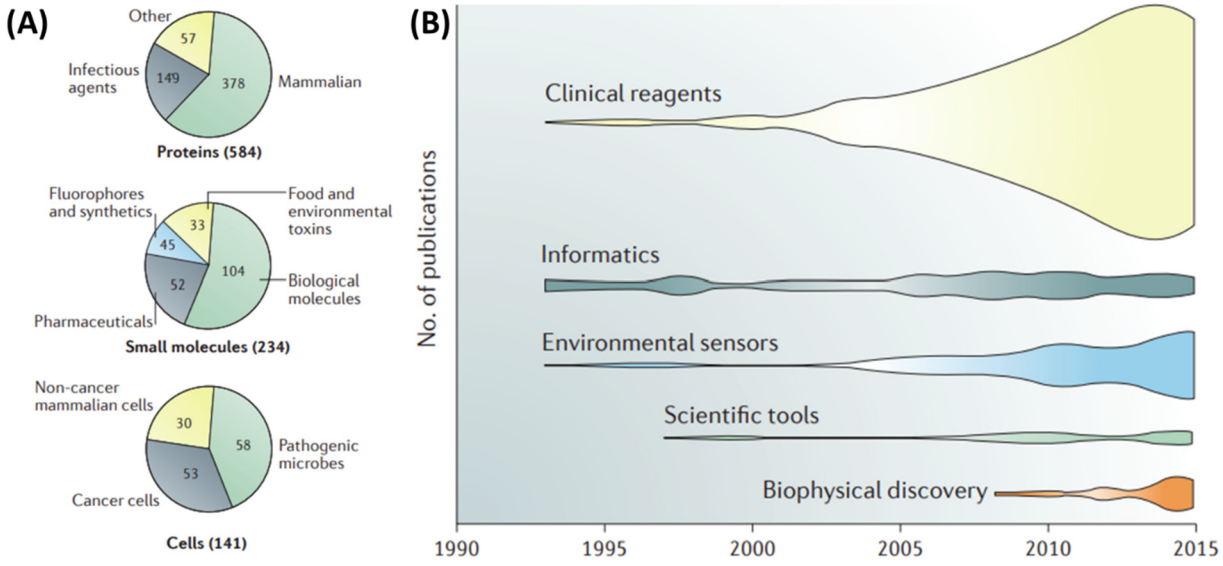

Figure 11. Nucleic acid aptamer targets and applications. (A) Breakdown of 3 most common target categories based on a library of 1003 aptamers selected by SELEX. (B) Number of publications discussing applications of aptamers from 1990 to 2015, organized by five broad application areas. Adapted with permission from ref 118. Copyright 2017 Springer Nature.

sized, which lowers production costs and minimizes batch to batch variation. Being one-tenth the size of antibodies, aptamers can bind with targets that typically escape the immune system and are not limited to targeting immunogenic antigens.[137] Unlike antibodies, aptamers are generally considered non-immunogenic and nontoxic, and aptamer activity can be easily reversed in the presence of an antidote (i.e., a complementary strand).[138] *In vitro* selection of aptamers also requires a relatively shorter production time of 2−14 days, compared with the monoclonal antibody screening time of around three months.[139] Additionally, aptamers can be stored for longer periods of time and have the benefit that they can be easily refolded by denaturing with mild heating and then annealing by cooling in order to regain their activity. A further advantage of aptamers is their ability to be easily chemically modified or conjugated with other nanomaterials. A detailed comparison of aptamer and antibody properties can be found in previous reviews.[133,137,140]

3.5. Aptamer Bonding and Targeting

Aptamers can recognize and bind with their targets through a variety of noncovalent bonds including hydrogen bonds, electrostatics, van der Waals, hydrophobic, and aromatic interactions. The molecular recognition mechanisms also rely on the flexibility of aptamers and vary heavily depending on the characteristics of the target.[141] van der Waals interactions increase with the geometric goodness-of-fit between the molecules and scale with interaction surface area. Hydrogen bonds involve a hydrogen atom in a strongly polar environment and add significant binding energy to aptamer/target binding.[142] Hydrogen bonding is also responsible for the specificity and stability of the G-quadruplex structure adopted by a thrombin-binding DNA aptamer.[143] Other groups have also found that hydrogen bonding contributes significantly to aptamer stability.[144−146]

Aromatic amino acid side chains in SOMAmers have been found to increase hydrophobic character and favor both a stronger binding interaction with the nonpolar regions of a protein target and greater stability of the aptamer structure.[147] Furthermore, Chou and colleagues reported that guanine-rich DNA sequences take on stable G-quadruplex structures that are mediated at least partially by hydrophobic effects.[147] Despite these advantages, Gupta and colleagues have found that the aromatic side chains may also be responsible for higher rates of renal clearance.[148]

In addition to simple aliphatic hydrophobic effects, aromatic rings are involved in another binding interaction utilized by aptamers known as $\pi-\pi$ stacking. In this bonding, the attraction between the aptamer and target is attributed to overlap of stacked π orbitals, and $\pi-\pi$ stacking is commonly cited as the force responsible for the attraction between MGA and the malachite green molecule as well as between the RNA aptamer Toggle-25t and thrombin.[149,150]

Aptamer binding can also be mediated by electrostatic effects. These effects are primarily due to the attraction of the negatively charged phosphate backbone of the aptamer to the positively charged amino acids of the protein target.[151] It has been suggested that electrostatic interaction is the main force responsible for RNA aptamer−protein binding.[152] However, electrostatic attraction is not directionally biased and commonly results in nonspecific binding, suggesting that there are other determinants for the specific binding interactions of aptamers and targets.[153] It is also important to note that electrostatic effects can be heavily influenced by the surrounding medium, where the presence of conductive ions, including H^+, Na^+, and K^+, affects the electrostatic interaction between the aptamer and its target.[154]

The last major type of binding interaction involves van der Waals forces. These forces are weaker than any of the aforementioned interactions and occur via attraction of dipoles and induced dipoles. These dipoles are associated with the aptamer and target atoms and must be very close together for the van der Waals forces to be comparable in strength to the other forces. Like the electrostatic effects, van der Waals forces are noncovalent and nondirectional. Given their weak strength, these forces are often dominated by the stronger hydrogen bonding or electrostatic effects. It is important to note that the extent to which any of the binding forces play a role in aptamer

https://doi.org/10.1021/acs.chemrev.0c01332
Chem. Rev. XXXX, XXX, XXX−XXX

binding can depend sensitively on several factors, including solution conditions and molecular flexibility.[155]

Due to their many binding interactions, aptamers can be selected for many types of targets, such as small molecules, macromolecules, and whole cells (Figure 11A).[118] Small molecule targets include metal ions,[156,157] antibiotics,[158] dye molecules,[126] and more. Aptamers that bind with macromolecules, primarily proteins, have been reported. Not surprisingly, since proteins possess large, convoluted surfaces, aptamers that bind the same protein can have very different conformations. For example, Lin et al. discovered that two popular thrombin aptamers, one a 15-mer and the other a 29-mer, had differing structures. The former was found to bind with a G-quadruplex structure dominated by electrostatic interactions and the latter with a duplex structure dominated by hydrophobic effects.[159] In 1998, Gold's group selected for aptamers that bind to red blood cell membrane targets.[160] Later, in 2006, Tan's group developed the cell-SELEX method and many cell-targeting aptamers followed.[161] An informative review of various available aptamers and their target binding interactions has been previously published by Cai and colleagues.[141]

3.6. Possible Application Areas

The plethora of aptamer targets available has resulted in a broad range of potential applications such as targeted therapy, fluorescence-based sensing, and targeted delivery. Although aptamers have been developed for a variety of purposes, the bulk of recent applications are for clinical reagents, as demonstrated by Figure 11B.[118] Both agonist and antagonist therapeutic aptamers have been developed. The latter have been developed to inhibit targets affiliated with bleeding disorders, autoimmune disease, ocular disorders, and cancer;[133] the former have been developed to stimulate immune co-stimulatory receptors,[162−167] as well as VEGF receptor 2[168] and insulin receptors.[169]

Aptamers have also been developed to aid in the advancement of synthetic biology. For example, RNA aptamers have been applied as riboswitches to regulate gene expression. Due to their high affinity for a specific target, aptamers can selectively bind to key molecules in cellular processes such as transcription and translation. Nudler and Mironov have reviewed the use of riboswitches in regulating bacterial metabolism.[170] In the past decade, RNA aptamer riboswitches have been extensively developed, resulting in the potential for clinically viable aptamer antibiotics and biosensors.[171]

Aptamers have been recognized as strong candidates for biosensing and bioimaging applications due to available chemistry for conjugating them with fluorescent molecules. In 2011, Paige et al. demonstrated the development of an RNA aptamer known as spinach, the RNA analog of GFP, wherein the aptamer binds to a specific fluorophore and significantly enhances its quantum yield.[172] Three years later, Dolgosheina et al. reported the synthesis of RNA Mango, an RNA aptamer that complexes with thiazole orange derivatives, for tracking RNA *in vivo*.[173] Targets for aptamer biomolecule detection range from ATP and cocaine to malaria biomarkers.[174] However, since unmodified aptamers are vulnerable to enzymatic degradation and cannot easily cross the cell membrane, they are usually complexed with other nanostructures for cell delivery. The aptamer binds to the target and undergoes a conformational change that enables a signaling output to occur via electrochemical or optical assays. For this reason, the RNA Mango and spinach aptamers have seen extensive application as receptor molecules in fluorescence-based sensing. Wang et al. summarized the applications of aptamers as fluorescent biosensors.[175]

Logic gates and nanocircuits have also incorporated aptamers. This is generally tied to gene/protein regulation and biomolecule detection applications. In 2018, Goldsworthy et al. reported the creation of AND, OR, NAND, and NOR RNA aptamer logic gates controlled by DNA oligonucleotide inputs. The authors used the outputs of the gates, conformational changes in the aptamer, to regulate the binding affinity of the fluorescent dye to which the aptamer was bound.[176] In 2015, You et al. described the use of DNA aptamers to create AND, OR, and NOT gates capable of detecting cancer cell biomarkers.[177] Aptamer-based logic gates have even been used in nanocarriers and for targeted drug delivery.

3.7. Limitations of Aptamers

Although aptamers are useful in many applications, they are not without limitations. Native aptamers composed of natural nucleotides, particularly RNA aptamers, are readily degraded by nucleases, making them very short-lived and typically ineffective *in vivo*. As mentioned previously, this problem has been circumvented somewhat by engineered chemical modifications. Another challenge with aptamers is unwanted secondary structure that can lower the specificity and efficacy of aptamer structures, especially for aptamers with longer sequences. Unwanted secondary structures can be limited by using shorter sequences, which have fewer available conformations. Additionally, long aptamer sequences can be split into two shorter sequences that join in the presence of a target, as shown in Figure 9A.[123]

Aptamers interact with less surface area of their target molecule due to their smaller size and are thus more susceptible to off target binding and cross-reactivity.[178] One way to increase aptamer specificity is by adding selection cycles during the SELEX process to select against likely off target moieties. Unfortunately, negative selection requires additional PCR cycles, which can amplify undesired biases. There have been aptamer selection methodologies that include selection against target-similar competitor molecules and require no PCR amplification.[179] Additionally, multiple aptamers that bind to various places on the same target can be assembled into one structure using nanostructures.[106,180,181] The activity of aptamers seems to be largely unaffected when incorporated carefully into nanostructures, provided they are placed in a way that does not sterically impede access to their target molecule. Thus, combining multiple targeting aptamers into a single nanostructure could increase its target interaction, increase binding affinity for target molecules, and reduce off target effects.

There are other limitations of free aptamers that can be surmounted by the addition of nonaptamer nucleic acid sequences. Aptamers alone are small and have fast renal clearance times of 5−10 min in mouse models.[182] When longer clearance times are desired, aptamers can be tethered to larger nucleic acid structures to increase their size. If the activity of the aptamer needs to be turned off prior to clearance, complementary antidote sequences can be used to bind to aptamers and unfold them, eliminating their effects. Complementary antidotes to aptamers, such as the coagulation factor IXa aptamer, have been developed and tested *in vivo* and show great promise as a new class of drug molecules.[183−185] Zhou and Rossi provide an excellent review of the challenges and limitations of aptamer therapeutics.[133]

https://doi.org/10.1021/acs.chemrev.0c01332
Chem. Rev. XXXX, XXX, XXX−XXX

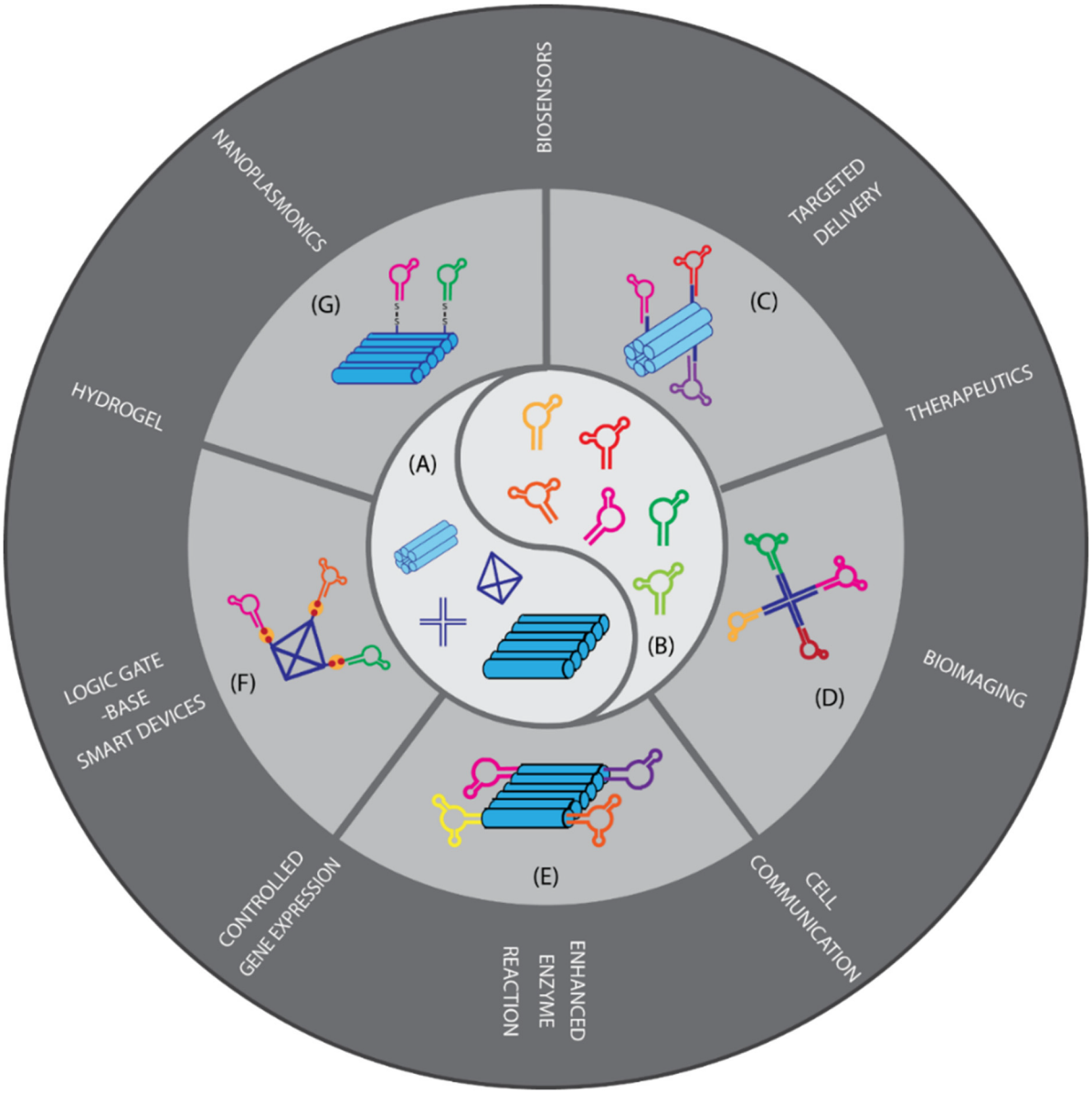

Figure 12. Illustration of multivalent aptamer decoration on nucleic acid nanostructures and its potential applications. Inner circle: (A) self-assembled nucleic acid nanostructures; (B) nucleic acid aptamers. Middle layer, common approaches for decoration of multivalent aptamers on nanostructures: (C) sticky-end hybridization; (D) terminal sequence extension; (E) internal sequence integration; (F) streptavidin−biotin interaction; (G) covalent linkages. Outer circle: potential applications of nucleic acid nanostructures bearing aptamers as functional motifs.

Lastly, free aptamers are limited in their function. Alone, aptamers are typically designed to target one molecule, one binding site on one protein, or one epitope on a cell surface marker. However, using larger nucleic acid nanostructure platforms, multiple aptamers can be combined to create multivalent structures with increased targeting and regulatory power, including dynamic sensors and nanocircuits. Here, we will review work that has been published to advance the development of aptamer-functionalized nucleic acid nanostructures.

4. DECORATION OF APTAMERS ON NUCLEIC ACID NANOSTRUCTURES

Aptamers have been raised for specific binding to a broad range of targets, from small molecules to whole cells. Due to their intriguing properties and straightforward production process, aptamers have been extensively developed and show great potential in a broad range of applications.[133,186] To address the challenging issues of stand-alone aptamers and enhance their abilities, various types of nanomaterials, such as gold nanoparticles, liposomes, quantum dots, magnetic nanoparticles, and carbon-based nanomaterials, have been used as nanocarriers for aptamer functionalization and have been utilized in a wide range of applications, including targeted delivery, bioimaging, and advanced biosensing.[187−190] Self-assembled nucleic acid nanostructures are promising carriers for aptamer decoration and offer great benefits over other nanomaterials due to their programmability, addressability, and direct compatibility with aptamers.[108,191,192] Nucleic acid nanostructures serving as biomolecular platforms allow localization and organization of multivalent aptamers with nanoscale precision, of which other materials are not capable. While this generally does not change aptamer specificity, it increases the local concentration of aptamers near the target, thus decreasing the likelihood of

https://doi.org/10.1021/acs.chemrev.0c01332
Chem. Rev. XXXX, XXX, XXX−XXX

dissociation. The action of the aptamer is not typically hindered except for very large nanostructures, for which steric effects may be important in binding energetics and target accessibility. Several approaches have been employed to achieve display of aptamers on nucleic acid nanostructures (Figure 12C−G). Due to the compatibility between nucleic acid nanostructures and aptamers, methods such as sticky-end hybridization, terminal sequence extension, and modular sequence integration are commonly used for functionalization of aptamers on nucleic acid nanostructures. Displaying aptamers on nucleic acid nanostructures using terminal sequence extension and internal sequence integration may cause misfolding of nucleic acid aptamers with the structural sequences of nucleic acid nanostructures that may result in loss of functionality. Due to the modularity of nucleic acid aptamer decoration on nucleic acid nanostructures, sticky-end hybridization, streptavidin−biotin interaction, and covalent linkage can be employed to avoid this misfolding problem. The thermodynamics of aptamer-integrated nanostructure synthesis has not been extensively studied, but it is generally accompanied by a loss in conformational entropy due to the presence of folded products (particularly in the case of highly ordered DNA/RNA origami).[193,194] However, other effects such as the exothermic nature of hybridization and entropic effects on other degrees of freedom must be considered. These factors are also relevant for aptamer binding, wherein entropic and enthalpic effects alike determine binding affinity. Note also that while appending multiple aptamers onto a nucleic acid nanostructure does not typically change the aptamer's specificity, it can increase the local concentration of aptamers near the target, thus decreasing the likelihood of dissociation. Binding of the aptamer to its target is not typically hindered except by very large nanostructures, for which steric effects may be important in binding energetics and target accessibility. Strategies for chemical modification and conjugation of nucleic acid nanostructures have been reviewed previously.[195] The combination of aptamers and programmable nucleic acid nanostructures offers excellent potential for the utilization of aptamers on nanostructures from basic research to advanced applications that we will discuss in this review (Figure 12).

5. APPLICATIONS OF APTAMERS ON NUCLEIC ACID NANOSTRUCTURES

5.1. Chemosensors and Biosensors

Biosensors and chemosensors are tools to detect biomolecules and chemical compounds, many of which are key components in biological and chemical processes, from small ions to whole cells. For this reason, advanced sensing platforms have been developed and utilized in a wide variety of fields, from food safety and environmental pollution to disease diagnosis.[196−199] Crucial parts of any sensor must include a receptor that specifically binds to the analyte and a reporter that allows transduction of a detectable signal in the presence of the analyte; optionally, sensors can include mechanisms for signal amplification. Many biomolecules, including DNA, RNA, enzymes, and antibodies, have been used as bioreceptors to capture a variety of analytes, such as nucleic acids, small molecules, and pathogenic agents.[200] Aptamers have recently emerged as promising candidates for bioreceptors that specifically bind to a wide range of biochemical analytes, including biomolecules, small molecules, and whole cells, due to their versatility, high target binding affinity, and ease of production.[201] Furthermore, they have also been utilized as fluorescent reporters to show signaling output in optical aptamer-based sensors.[202]

Electrochemical and optical-based aptasensors have been extensively developed for food safety and environmental and clinical diagnostic applications, as reviewed previously.[203,204] They have been conjugated to various nanostructures such as carbon nanomaterials in order to provide a highly sensitive platform by improving target accessibility and reducing steric hindrance of the capture probe.[205] In electrochemical aptasensors, aptamer−analyte binding leads to the catalytic reduction of a redox probe, generating a response current.[206] Simple electrochemical aptasensors have been developed using split aptamers and target-induced strand displacement to detect specific biomolecules and small molecule targets.[207−209] Optical-based aptasensors are broader in operational scope, encompassing Förster resonance energy transfer (FRET), surface plasmon resonance, surface-enhanced Raman scattering, and other techniques.[210] Optical DNA and RNA aptamer-based biosensors have been coupled with FRET pairs, fluorophores, and quantum dots to detect a wide range of analytes, including ATP, thrombin, and intracellular chloride.[211−213] In both optical and electrochemical sensors, aptamer decoration on nanomaterials has shown great potential for improving the performance of aptamer-based sensors.[214−216]

Nucleic acid nanostructures are a promising biomaterial for organizing and assembling aptamer-based sensors, owing to their programmability, well-controlled sizes and shapes, and ability to be functionalized with nucleic acid aptamers. To this end, multivalent aptamer decoration allows for multiplex target detection and logic gate-based sensing. In this section of the review, we will focus on aptamer-functionalized nucleic acid nanostructures for biosensing and chemosensing applications, categorizing them broadly into static and dynamic nucleic acid nanostructure-based sensors. Of course, none of these aptamer−target binding molecular interactions is truly "static" given changes in local polymer chain conformational and hydration, but we will reserve the term "dynamic" for examples in which large, designed switching of the nanostructure from one state to another state represents an important part of the sensors' signal transduction mechanism.

5.1.1. Aptamer-Functionalized Static Nucleic Acid Nanostructures. Aptamer-decorated static nucleic acid nanostructures have been utilized as biomolecular platforms for a multitude of sensing applications. In this section, we group static nucleic acid nanostructure-assisted aptasensors into four categories: (1) tetrahedral DNA nanostructures and DNA nanocages, (2) branching DNA nanostructures, (3) nucleic acid nanotiles, and (4) DNA and RNA origami.

5.1.1.1. Tetrahedral Nanostructures and DNA Nanocages. Tetrahedral DNA nanostructures (TDNs) have been developed and extensively used in sensing applications due to the potential to decorate them with various receptors, including ssDNA, antibodies, and nucleic acid aptamers.[217,218] They also offer improvement in control over target accessibility and binding, resulting in enhanced sensitivity of the sensing platform. For these reasons, electrochemical and optical-based aptamer-conjugated TDNs have been widely used for biosensing and chemosensing applications.

5.1.1.1.1. Electrochemical-Based Aptasensors. The TDN-based electrochemical biosensing platform has been used in the past decade to detect a wide variety of targets. In 2010, Fan's group assembled TDNs on gold electrodes for DNA and protein detection.[219] Three (downfacing) vertices of the tetrahedron

https://doi.org/10.1021/acs.chemrev.0c01332
Chem. Rev. XXXX, XXX, XXX−XXX

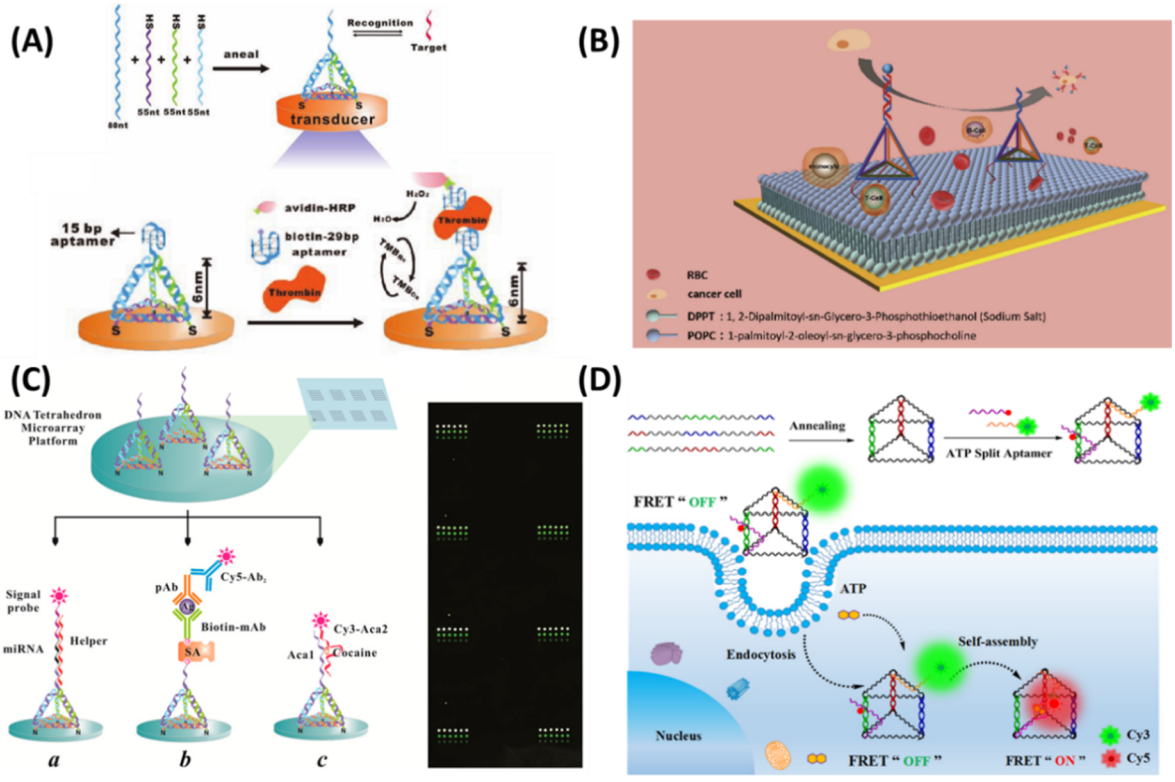

Figure 13. Chemo- and biosensing platform-based tetrahedral DNA nanostructures (TDNs) decorated with aptamers. (A) TDN bearing a thrombin aptamer for electrochemical-based thrombin detection using avidin−HRP. Three thiolated DNA strands were annealed with an 80 nt strand containing the capture probe sequence to form the tetrahedron. Adapted with permission from ref 219. Copyright 2010 John Wiley and Sons. (B) Schematic illustration of the DNA aptasensor constructed on a lipid bilayer membrane. The aptasensor is comprised of a DNA tetrahedron and a functional TLS11a aptamer that targets HepG2 cancer cells. Reprinted with permission from ref 231. Copyright 2020 Elsevier. (C) Universal sensing platform using bioreceptor-conjugated TDN-based microarrays. Reprinted from ref 240. Copyright 2014 American Chemical Society. (D) In vivo detection of ATP using an ATP aptamer-decorated DNA nanoprism. Reprinted from ref 241. Copyright 2017 American Chemical Society.

structure were functionalized with thiol groups, which formed thiol−Au bonds with the gold surface. The fourth (upfacing) vertex was left free to place a capture probe, specifically a ssDNA strand or an aptamer. The authors used a thrombin-binding aptamer appended onto the TDN to detect thrombin (Figure 13A). Together with avidin−horseradish peroxidase (HRP) and a biotinylated aptamer that bound a different exosite on thrombin, the presence of thrombin induced a redox reaction with 3,3′,5,5′-tetramethylbenzidine (TMB), which generated an electrochemical signal. The method was found to exhibit stability, high yield of self-assembled TDNs, and sufficient separation of the signal probe: far enough to allow freedom in target accessibility, while close enough to permit signal transduction. Electrochemical sensing has also been combined with other detection techniques. Three years later, Poturnayová et al. improved TDN-based thrombin detection by functionalizing their nanostructure with two aptamers binding to different exosites of thrombin.[220] Detection of thrombin concentration was achieved using both cyclic voltammetry and the acoustic thickness shear mode (TSM) method. Voltammetry measurements were obtained using $Ru(NH_3)_6^{3+}$ as an electrochemical probe, while TSM involved measurements of changes in series resonant frequency and motional resistance due to DNA−thrombin binding on the surface of a gold-coated quartz crystal. Using an aptamer-bearing TDN, Fan's group further developed an electrochemical-based cocaine sensing platform.[221] TDNs were self-assembled on a gold electrode and functionalized with a split anticocaine aptamer, one of which was appended to the TDN and the other was biotinylated in the surrounding solution. In the presence of cocaine, the split aptamer fused together and brought horseradish peroxidase-conjugated avidin (avidin-HRP) close to the gold electrode, resulting in a detectable electrochemical signal via catalytic reduction of hydrogen peroxide. Expanding on this design, Fan's group also developed a universal, ultrasensitive platform to detect various types of targets.[222] The TDN served as a biomolecular platform that could be decorated with various types of bioreceptors including ssDNA, antibodies, and aptamers. Nucleic acid, protein, and whole cell detection was demonstrated; in particular, detection of MCF-7 breast cancer cells was achieved by using TDNs conjugated with SYL3C aptamers to target the epithelial cell adhesion molecule (EpCAM), which was generally overexpressed in the tumor cells. Recently, Jiang et al. targeted cancerous exosomal proteins via an aptamer-decorated TDN electrochemical biosensor.[223] Using a TDN platform conjugated with AuNPs and HRP, the authors achieved detection of multiple different exosomal proteins from mouse HepG2 liver cancer cells with a detection limit of 10^4 particles/mL. Taken together, these works suggest that electrochemical TDN sensors can be applied to a wide variety of targets, from nucleic acids to whole cells.

Simple and ultrasensitive biosensor platforms that enable detection of targets in human bodily fluids such as whole blood or urine are necessary. 8-Hydroxy-2′-deoxyguanosine (8-OHdG) is a product of oxidative DNA damage that is a key biomarker for many diseases and can be found in urine.

https://doi.org/10.1021/acs.chemrev.0c01332
Chem. Rev. XXXX, XXX, XXX−XXX

Although 8-OHdG could be directly measured by electrochemical methods, ultrasensitive detection methods for this analyte needed to be developed.[224] In 2016, Fan et al. developed a label-free, ultrasensitive detection method for 8-OHdG by using 8-OHdG-binding aptamer-conjugated TDN.[225] In the presence of 8-OHdG, the aptamer formed a hemin/G-quadruplex structure, resulting in deposition of polyaniline (PANI). This method improved sensitivity by around 300-fold compared to previous electrochemical methods. Importantly, this assay enables detection of 8-OHdG in human serum and urine. Recently, a fast, single-step ATP detection method using split anti-ATP aptamer-decorated TDN was developed by Li et al.[226] Methylene blue (MB) labeled aptamers were used as reporting molecules. When ATP was present, the split aptamers came together to form a complex with ATP, bringing MB close to the electrode and resulting in an electrochemical signal that could be detected by square wave voltammetry. This method allows detection of picomolar concentrations with detection times of less than 10 min. These one-step sensors could be used to detect ATP in whole blood samples, benefiting clinical applications.

The TDN-assisted electrochemical biosensors for target identification in biological fluids are valuable for clinical diagnostics and therapeutics. However, a current disadvantage appears to be increased nonspecific target adsorption when working in biological fluids, which reduces the accuracy of detection.[227] Dilution of biological samples has been proposed to resolve this problem, but that will decrease signal intensity in addition to background noise. Other solutions to this problem include the use of surface blocking agents, polymeric separation membranes, and other antifouling layers to prevent the adsorption of nontarget molecules.[228,229] An additional issue with electrochemical biosensors arises from the immobility of probes on the electrode surface, which results in reduced sensing accuracy. For example, in 2018, Liu et al. developed an electrochemical-based TDN biosensor to detect HepG2 cancer cells.[230] The TDNs were immobilized on a gold electrode through Au−S bonds, limiting the freedom of the probes to access the HepG2 cells. Two years later, to overcome this obstacle, the authors developed an aptamer-based electrochemical sensor comprised of a DNA tetrahedron nanostructure and a lipid bilayer assembled on a gold electrode, with an avidin−HRP reporting system (Figure 13B).[231] The authors applied this aptasensor to detect HepG2 tumor cells in whole human blood. Importantly, the fluid phospholipid bilayer allowed freedom in the motion of the aptamer-functionalized DNA biosensor. This permitted a considerable increase in sensing efficiency with just a few cancer cells compared to immobile electrochemical sensors. Signal detection was achieved using cyclic voltammetry and electrochemical impedance spectroscopy. The fluidity of this design allowed improved detection efficiency compared to the prior fixed structure. The use of lipid bilayer membranes as antifouling layers thus has the potential to improve target accessibility for static electrochemical TDN sensors.

Other nanomaterials have been utilized together with aptamer-functionalized TDNs to improve sensing capabilities. In 2019, Chen and colleagues employed an electrochemical TDN biosensor to detect cardiac troponin I (cTnI), an important biomarker in acute myocardial infarction.[232] They immobilized TDNs conjugated with two troponin aptamers, Tro4 and Tro6, on a gold electrode and hybridized the nanostructure with gold and copper nanoparticles functionalized in a magnetic metal−organic framework (MMOF). These nanoparticles were conjugated with ssDNA complementary to the double aptamer. The TDN served to capture the cTnI target, forming a supersandwich structure, while the MMOF aided in electrochemical signal amplification, catalyzing the oxidation of hydroquinone. In the same year, Chen's group reported another TDN complexed with a MMOF, where horseradish peroxidase (HRP) and a G-quadruplex/hemin DNAzyme were additionally used to amplify the electrochemical signal.[233] Furthermore, they developed another TDN immobilized on a gold electrode that targeted the breast cancer protein biomarker human epidermal growth factor receptor 2 (HER2).[234] HRP, Pd/Pt, and Mn_3O_4 nanozymes functioned as electrochemical signal probes by catalyzing hydroquinone oxidation. The hybridization between the HER2 aptamer and complementary ssDNA conjugated to the nanozyme complex allowed formation of a complex, branched nanostructure that further improved signal strength. These works showed that hybrid aptamer-functionalized nanostructures can help improve both the detection sensitivity and target specificity of biosensors.

Besides TDNs, other shapes of immobilized nucleic acid nanostructures have been investigated for target-specific signal transduction. In 2019, Taghdisi and colleagues used a ladder-shaped DNA nanostructure functionalized with an ampicillin aptamer to measure ampicillin concentration in milk samples.[235] This design was proposed after the group had previously tested other shapes, including an M-shape, H-shape, arch-shape, and π-shape. Targets for these nanostructures included tetracyclines,[236] aflatoxin B,[237] cocaine,[238] and streptomycin.[239] As with TDNs, the structures sterically hindered access of the electrochemical indicator (ferric cyanate) to the surface of the gold electrode. In comparison to previously tested aptasensors, the ladder shape more successfully blocked the redox indicator from accessing the electrode, thus improving the change in electrochemical signal strength before and after target binding. Ampicillin−aptamer binding triggered breakdown of the ladder nanostructure, releasing it from the electrode surface and allowing the redox reaction with ferric cyanate to proceed. This work demonstrated how low-cost, sensitive 2D nanostructures could be functionalized as electrochemical chemosensors.

5.1.1.1.2. Optical-Based Sensors. Although most immobilized nucleic acid aptasensors have incorporated electrochemical reporting probes, many groups have also examined surface- and solution-based detection schemes using optical methods. In 2014, Li et al. used an anticocaine aptamer-functionalized TDN immobilized on a glass surface to sense cocaine via microarray fluorescence scanning, as shown in Figure 13C.[240] The fluorophore-conjugated structure was shown to have considerably greater fluorescence intensity when cocaine was present. Because an arbitrary functional module can be appended to the nanostructure, this method shows promise for detecting a wide range of targets. For example, by decorating the TDN with a biotin−streptavidin complex, the authors demonstrated detection of the prostate cancer biomarker prostate specific antigen (PSA). Their results were found to correlate well with results from more arduous conventional chemical luminescent immunoassays.

The use of fluorescent probes, particularly fluorophore−quencher pairs, has emerged as a promising method for selective detection of many targets. In 2020, Kwon and colleagues fabricated a 2D star-shaped DNA nanostructure to target envelope protein domain III (ED3) on the dengue virus surface. ED3-targeting aptamers were placed at each of the construct's

https://doi.org/10.1021/acs.chemrev.0c01332
Chem. Rev. XXXX, XXX, XXX−XXX

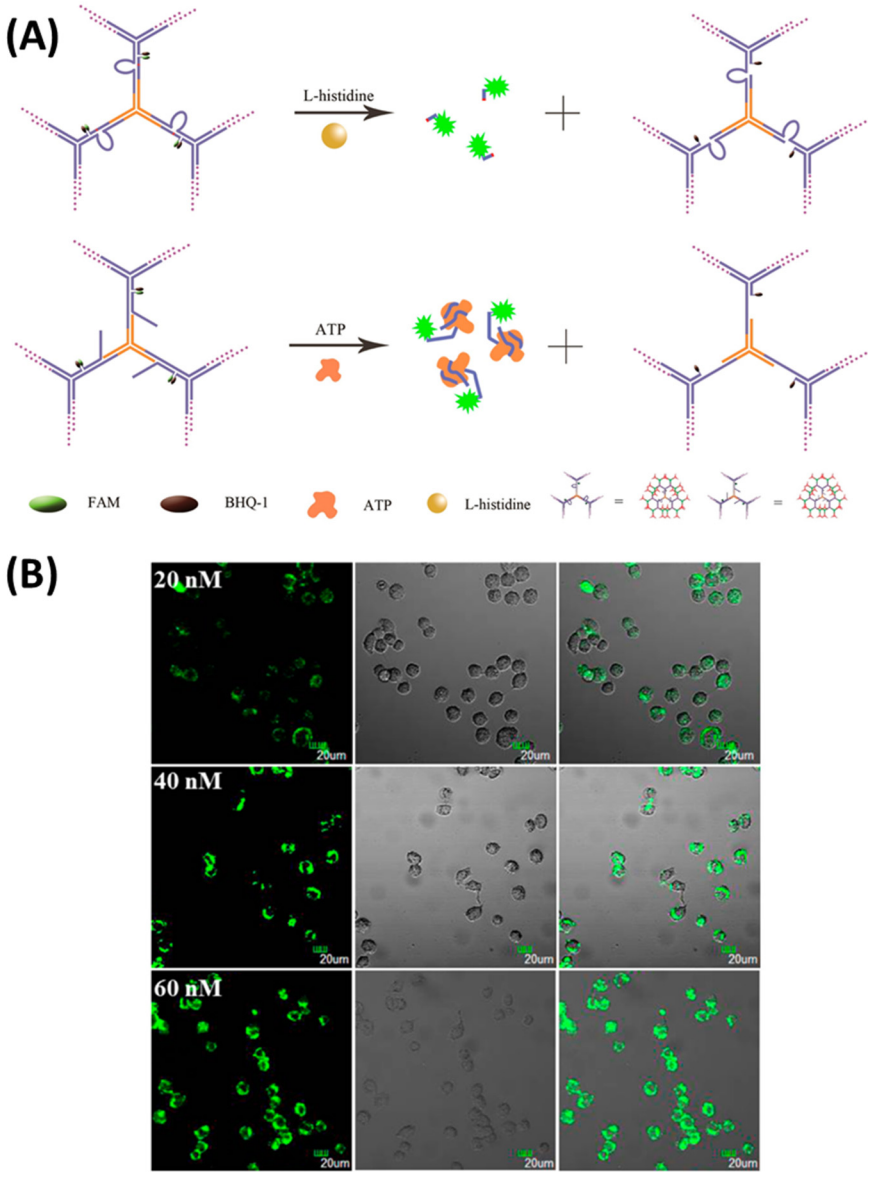

Figure 14. (A) Fluorescent-labeled DNA dendrimer for intracellular histidine and ATP sensing. (B) Confocal microscopy images of MCF-7 cells treated with anti-ATP aptamers decorated on DNA dendrimer nanostructures. Adapted from ref 248. Copyright 2014 American Chemical Society.

ten vertices, helping amplify ED3 sensitivity. By conjugation with a 6-FAM fluorophore and BHQ-1 quencher, a change in fluorescence due to target binding was observed, whereby the fluorophore and quencher separated as a result of hairpin loop disassembly in the nanostructure. This method was demonstrated to show comparable sensitivity to more expensive and laborious strategies, such as RT-qPCR. Additionally, by testing other shapes such as bivalent, linear, hexagonal, and heptagonal structures, the authors confirmed that the pentagonal shape was optimal for matching ED3 sites on the dengue viral surface.[242]

In addition to tetrahedral DNA nanostructures, other aptamer-functionalized 3D polyhedral DNA nanostructures have been used for sensing applications. In 2018, Shiu et al. tested various shapes and sizes of DNA polyhedrons on a streptavidin-coated plate, including differently sized tetrahedrons, square and pentagonal pyramids, and prisms. The polyhedrons were decorated with aptamers targeting *Plasmodium falciparum* lactate dehydrogenase (PfLDH), and the authors found that these 3D nanostructures demonstrated better sensitivity toward PfLDH detection than the aptamers by themselves. This was quantified using Aptamer-Tethered Enzyme Capture (APTEC) assays, a spectrophotometric method that exploits the ability of PfLDH to cause a color change in a nitrotetrazolium-containing solution. The authors found that tetrahedrons were the optimal design, allowing conjugation of signaling probes and maximizing aptamer−target accessibility.[243]

Static optical-based sensors have also been applied for *in vivo* biosensing. In 2017, Zheng et al. fabricated a DNA nanoprism decorated with a split ATP aptamer, whose stem was conjugated with a FRET pair (Figure 13D).[241] When two ATP molecules bound to the triangular prism architecture, the split aptamer self-assembled, reducing the separation among the fluorophores and triggering fluorescent emission. ATP detection was demonstrated *in vitro* and *in vivo*, and the nanoprism showed excellent cellular permeability and sensitivity, avoiding false-positive signals through use of the split aptamer strategy. This method

https://doi.org/10.1021/acs.chemrev.0c01332
Chem. Rev. XXXX, XXX, XXX−XXX

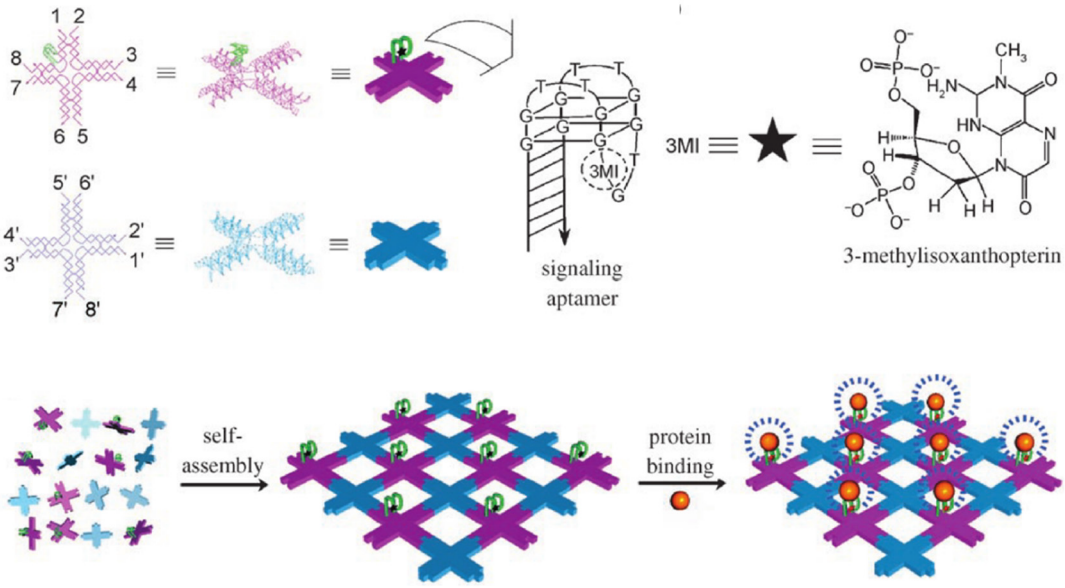

Figure 15. Signaling aptamer-decorated DNA nanoarray for thrombin detection. (top) Schematic illustration of assembling DNA nanoarray using two DNA tiles. The pink tile contains thrombin binding aptamer. The fluorescent nucleotide 3-methylisoxanthopterin is used for signaling the binding of thrombin. (bottom) Self-assembly of DNA nanoarray for thrombin detection. Upon thrombin binding to aptamers on DNA arrays, the fluorescent signal can be detected. Adapted with permission from ref 251. Copyright 2006 John Wiley and Sons.

therefore serves as an effective biosensing platform for intracellular small molecule detection.

5.1.1.1.3. Other. Electrochemiluminescent (ECL) reporting systems have recently been integrated within aptamer-decorated TDN platforms. For example, Bu et al. constructed an ATP biosensor comprised of an anti-ATP aptamer-functionalized tetrahedral DNA nanostructure (TDN) and a functionalized oligonucleotide (FO) complementary to the anti-ATP aptamer.[244] When self-assembled on a gold electrode, aptamer−FO hybridization occurred, inducing ECL emission from $Ru(phen)_3^{2+}$. In the presence of ATP, competitive ATP−aptamer binding released the aptamer−FO−$Ru(phen)_3^{2+}$ complex, resulting in a decrease in ECL emission in proportion to the ATP concentration.

The use of TDNs has also been combined with other sensing techniques besides electrochemical and optical detection. In 2018, Wang et al. used surface plasmon resonance (SPR) to measure tetracycline concentrations in honey samples.[245] The advantages of this method lie in its high specificity and minimal requirement for sample preparation. Prior to this research, attempts at using SPR to detect small molecules suffered from low signal strength and the issue of steric hindrance restricting target sensitivity. To improve sensitivity, nanoparticle labeling has been proposed, but this can be a costly strategy.[246] Instead, the authors appended antitetracycline aptamers (Apt76) to the top and bottom of a TDN nanostructure, moderating the problems of steric hindrance and target accessibility. This demonstrated the first use of an aptamer-functionalized SPR sensor to target small molecules.

5.1.1.2. Branching DNA Nanostructures. Topologically branched, multistrand DNA nanostructures (as described above in section 2) provide multiple connection points to anchor functional motifs such as aptamers and DNAzymes and allow the formation of higher-ordered nanostructures such as DNA dendrimers. With these features, functionalized branching nanostructures offer great benefits for sensing applications, especially signal amplification. As such, ultrasensitive biosensing platforms using aptamer-decorated branching nanostructures have been developed.[247]

In 2014, Meng et al. developed a DNA dendrimer that served as a scaffold to carry an anti-ATP aptamer as well as a DNAzyme whose activity was histidine-dependent (Figure 14).[248] By attaching a quencher (Black Hole Quencher-1, or BHQ-1) and fluorophore (carboxyfluorescein, or FAM) to different parts of the nanostructure, the authors were able to determine the intracellular concentration of L-histidine and ATP. In the presence of each target, separation of FAM from BHQ-1 arose due to structural changes caused by the binding affinity between the aptamer/DNAzyme and the target. This resulted in a detectable fluorescent signal. Four years later, Norouzi and colleagues applied the detection scheme to whole cells, fabricating a branched DNA concatemer decorated via sticky-ends with 3WJ and functionalized with an Sgc8C aptamer that specifically bound to the PTK7 protein, which is overexpressed in T cell acute lymphocytic leukemia cancer cells.[249] The 3WJ consisted of HRP-like DNAzymes, whose catalytic activity was enhanced in the presence of hemin, allowing generation of a colorimetric signal detectable with the naked eye. This assay had a low limit of detection of only 175 cancer cells. Branching nanostructures offer the possibility of decorating sensing platforms with several functional modules, including aptamers and DNAzymes. They can be used to form extensive higher-order structures that amplify transduced signals, thus improving detection sensitivity for a wide variety of targets in both *in vitro* and *in vivo* sensing applications.

5.1.1.3. Nucleic Acid Nanotiles. DNA tiles and nanoarrays have been developed and utilized in a broad range of applications, including nanoelectronics, nanophotonics, and nanosensing.[250] Yan reported the self-assembly of 2D array-based DNA nanotiles functionalized with a signaling aptamer targeting thrombin (Figure 15).[251] The aptamer was formed by changing one nucleotide near the aptamer's thrombin binding sequence to its fluorescent nucleotide analog, which allowed an increase in the fluorescence signal upon binding with thrombin.

https://doi.org/10.1021/acs.chemrev.0c01332
Chem. Rev. XXXX, XXX, XXX−XXX

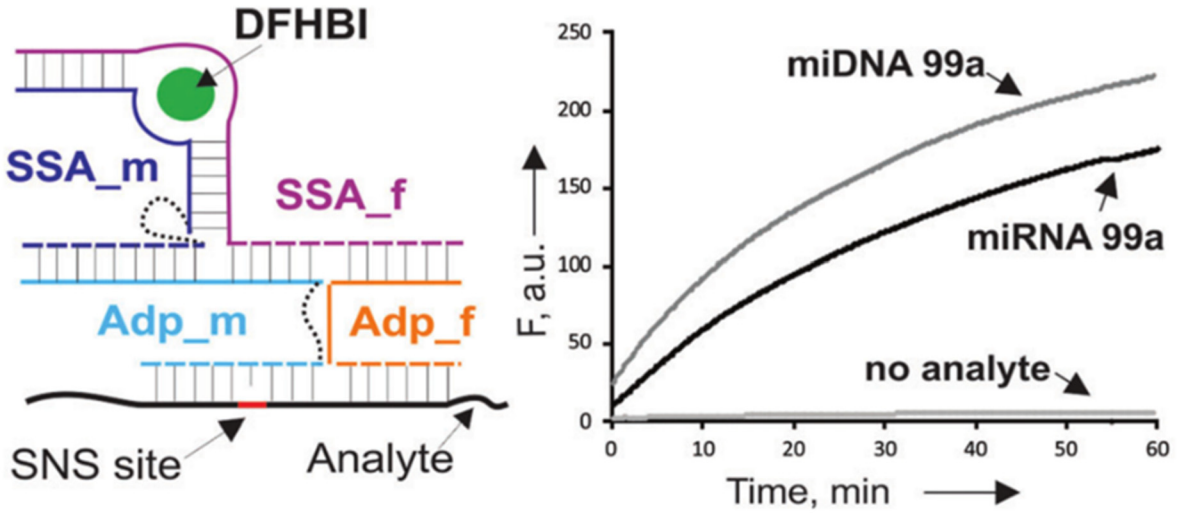

Figure 16. Universal split spinach aptamer (USSA) probe for nucleic acid detection and logic gate formation. DFHBI, fluorophore; SSA, split spinach aptamer; Adp, DNA adaptor strand. Model targets included miRNA 99a and its DNA analog. Fluorescent signal was detected in the presence of target nucleic acids. Reprinted with permission from ref 252. Copyright 2017 Royal Society of Chemistry.

The aptamer-functionalized tiles were assembled in microarrays, and this high-density environment helped amplify the fluorescent signal resulting from aptamer−thrombin binding. This DNA tile-based sensor could detect thrombin at sub-nanomolar concentrations. Furthermore, the assay can be expanded to multiplex target detection by using multiple fluorescent signaling aptamers.

In addition to DNA aptamers, RNA aptamers have found application as bioreceptors and bioreporters in nanosensors. Fluorescent RNA aptamers such as the spinach and mango aptamers can also been used as fluorescent reporters.[202] Many biosensors have made use of fluorescently labeled hybridization probes that bind directly to the target. However, this approach can be expensive and laborious, given that the hybridization probe must be designed, synthesized, purified, and optimized for each new analyte. To overcome this problem, Kikuchi and Kolpashchikov designed a universal split spinach aptamer (USSA) probe to detect nucleic acid targets and construct a NOR logic gate (Figure 16).[252] The label-free split spinach aptamer (SSA) probe consisted of two RNA oligonucleotides that would directly hybridize with the nucleic acid analyte, forming a binding site for the fluorophore (*Z*)-5-(3,5-difluoro-4-hydroxybenzylidene)-2,3-dimethyl-3,5-dihydro-4*H*-imidazol-4-one (DFHBI). Normally, two new RNA strands would need to be optimized for each new target, leading to a cost-inefficient biosensor. In order to bypass this requirement, the authors introduced two inexpensive DNA adaptor strands that underwent complementary base pairing with the nucleic acid target. Thus, the analyte made direct contact with the adaptor strands rather than with the SSA probe. This allowed the SSA probe to remain unchanged, serving as a universal reporter for different nucleic acid targets. As a proof of concept, the authors applied the USSA probe to detection of two miRNA sequences and their DNA analogs, only changing the adaptor strands to accommodate the different targets. A fluorescent signal was detectable within seconds, with a nanomolar detection limit for both DNA and RNA, comparable to traditional hybridization probe reporting systems. Successful detection of the *Mycobacterium tuberculosis rpoB* gene was also demonstrated. This work thus expanded the role of aptamers in nanosensors from target capture probes to cost-efficient, general-purpose signal reporters.

5.1.1.4. DNA and RNA Origami. DNA and RNA origami has been extensively developed for the past two decades to create sophisticated 2D and 3D nucleic acid origami with controllable sizes and shapes. Nucleic acid origami nanostructures are biocompatible, programmable, versatile, and capable of spatially controlled biomolecular and chemical functionalization. For these reasons, the origami technique has been used as a biomolecular platform for nanosensing applications. In 2008, Yan pioneered the use of aptamer-functionalized origami to explore the binding of target thrombin molecules (Figure 17A).[253] Two aptamers, selected against exosites 1 and 2 on thrombin, were placed in different positions at varying distances apart on the rectangular origami structure. The origami allowed precise spatial control over the distance between the aptamers, and thrombin binding was observed using AFM. This work, which for the first time used DNA origami to modulate target reception at the molecular level, inspired the use of DNA origami for biosensor fabrication. Five years later, microchip isotachophoresis (ITP) was used by Yan's group to preconcentrate and electrophoretically separate DNA origami−thrombin complexes within cell lysate for thrombin detection.[254] They found that on-chip ITP permitted separation of the bound thrombin from cell lysate within minutes, with little change in the structure of the complex. AFM and fluorescence measurements were used to confirm thrombin binding. This method showed promise for isolating intracellular thrombin and overcoming the challenge of low analyte concentration in diluted samples. Furthermore, it could be combined with microchip processing techniques to develop a powerful sensing platform. Using a similar approach, Tintoré et al. developed a G-quadruplex DNA nanostructure functionalized with two thrombin binding aptamers (TBA) to sense the repair activity of the human O^6-alkylguanine-DNA alkyltransferase enzyme (hAGT).[255] Using AFM, the authors found a reduction in binding affinity to thrombin when the TBA staple strands contained methylated guanines. Introducing hAGT restored the thrombin binding interaction at the level of unmethylated TBA. In 2016, Godonoga et al. reported the use of a rectangular DNA nanostructures functionalized with 12 aptamers to target the

https://doi.org/10.1021/acs.chemrev.0c01332
Chem. Rev. XXXX, XXX, XXX−XXX

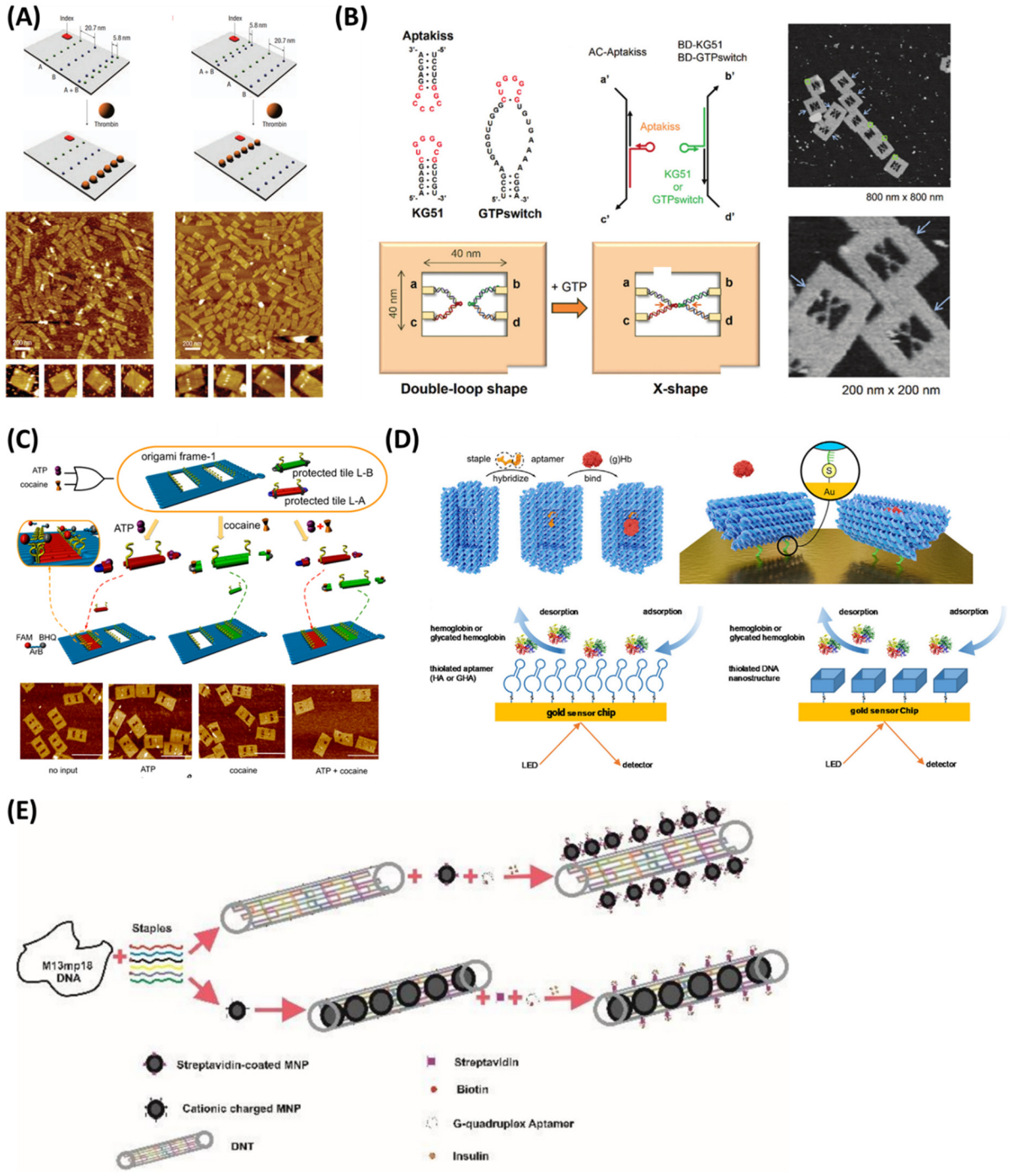

Figure 17. Aptamer-functionalized DNA origami for biosensing applications. (A) Double aptamer-functionalized rectangular DNA origami for thrombin detection (scale bar = 200 nm). Adapted with permission from ref 253. Copyright 2008 Springer Nature. (B) GTPswitch design that undergoes kissing interactions with target RNA kissing loop Aptakiss in the presence of GTP. Adapted from ref 258. Published 2016 Royal Society of Chemistry. Licensed under a Creative Commons agreement (https://creativecommons.org/licenses/by/3.0/). (C) Synthesis of OR, YES, AND DNA origami tile-based logic gates for simultaneous detection of ATP and cocaine (Scale bar = 200 nm). Adapted from ref 259. Copyright 2016 American Chemical Society. (D) Use of surface plasmon resonance for hemoglobin detection using a double aptamer-conjugated DNA nanocage. Adapted with permission from ref 260. Copyright 2020 Elsevier. (E) Colorimetric biosensing of a magnetic DNA nanostructure, comprised of magnetic DNA nanotubes and an insulin-targeting aptamer. Adapted from ref 261. Published 2020 Iranian Society of Nanomedicine. Licensed under a Creative Commons agreement (https://creativecommons.org/licenses/by/4.0/).

malaria biomarker PfLDH in human blood plasma, where target binding was again confirmed using AFM.[256]

Unlike protein−aptamer complexes, small molecule target binding is difficult to observe under AFM. For this reason, other nanostructure platforms have been developed in order to use AFM for signal readout. In 2017, Lu et al. fabricated aptamer-functionalized triangular DNA origami and complementary ssDNA-conjugated gold nanoparticles (AuNPs) to detect aflatoxin B1 (AFB1), a food toxin.[257] In the absence of aflatoxin B1, ssDNA decorated AuNPs could be immobilized at

https://doi.org/10.1021/acs.chemrev.0c01332
Chem. Rev. XXXX, XXX, XXX−XXX

predesigned locations on DNA origami via DNA/DNA hybridization. In contrast, aptamer−AFB1 binding resulted in a folded structure that did not allow immobilization of the AuNPs on the DNA origami; therefore competitive binding of aptamer−AFB1 triggered release of the AuNPs. Thus, measurement of the amount of free AuNPs by AFM allowed direct determination of AFB1 concentration. Takeuchi et al. used an RNA aptamer called "GTPswitch" decorated on DNA origami to detect GTP.[258] GTPswitch possesses two domains to bind to GTP and form a kissing interaction with a specific RNA loop known as "Aptakiss." In the presence of GTP, GTPswitch−Aptakiss binding occurred, forming an X-shaped structure within the DNA origami frame that was detectable using AFM (Figure 17B). Yang et al. developed DNA origami tile-based OR, YES, and AND logic gates, functionalized with aptamers and DNAzymes, to simultaneously detect ATP and cocaine.[259] AFM and fluorescence measurements were used as signal readouts (Figure 17C).

In addition to AFM, which is a somewhat arduous detection method, fluorescent and colorimetric optical readouts have been used for quantitative measurement of biomolecule and small molecule concentrations. In 2020, Duanghathaipornsuk et al. developed dynamic biosensing DNA nanocages conjugated with aptamers that bound hemoglobin and glycated hemoglobin, an important diabetes marker (Figure 17D).[260] The aptamers provided increased specificity and binding affinity, while the origami lent binding stability, resulting in stronger surface plasmon resonance (SPR) response signals. In the same year, Rafati et al. developed nanostructures comprised of magnetic DNA nanotubes (MDNTs) and a bifunctional biotinylated insulin aptamer (Figure 17E).[261] The aptamer both targeted insulin and acted as a peroxidase-mimicking DNAzyme when forming a G-quadruplex structure in the presence of bound insulin. The resulting redox activity could be quantified using spectrophotometry, specifically through the enzyme-linked immunosorbent assay (ELISA). The use of magnetic nanostructures allowed improved insulin capture in blood serum and eliminated nontarget charged particles, thus enabling more accurate measurements of target concentration.

The DNA origami technique has demonstrated viability to improve nanosensing capabilities through both surface immobilization of the sensors and origami-based immobilization of bioreceptor. This is crucial given that bioreceptor-target geometry is key to fabricating more sensitive biosensors. To further develop 3D DNA origami that optimized the binding interaction with thrombin, Rutten et al. immobilized aptamer-functionalized 3D DNA origami on the surface of disc-shaped microparticles in a microfluidic platform.[262] They were able to demonstrate lower steric hindrance and better orientation for target capture, compared to traditional bioassays. This resulted in faster and more efficient binding, improvements in the detection limit and signal-to-noise ratio, and a stronger fluorescent signal for fluorescently labeled thrombin relative to nonorigami methods.

5.1.2. Dynamic Nucleic Acid Nanostructures Functionalized with Aptamers. *5.1.2.1. Nanostructures with Target-Induced Conformational Changes.* Dynamic nucleic acid nanostructures are used to create reconfigurable nanodevices that can be triggered to respond to external stimuli. They have therefore found common use in sensing applications.[263,264] Aptamer-decorated DNA nanostructures that undergo structural changes triggered by target binding have been extensively developed.[192] The resulting structural changes due to the presence of the target can be detected and quantified most commonly using fluorescent or electrochemical outputs.

Dynamic DNA nanostructures have been utilized by multiple groups to detect biomolecules and small molecules *in vitro*. In 2014, Sheng et al. reported a cocaine aptamer-functionalized DNA nanocage capable of sensing cocaine concentration.[265] Cocaine binding induced a conformational change from a "closed" state, a triangular pyramid frustum (TPF), to an "open" state, an equilateral triangle (ET), which in turn caused a detectable drop in Faradaic impedance (Figure 18). The authors

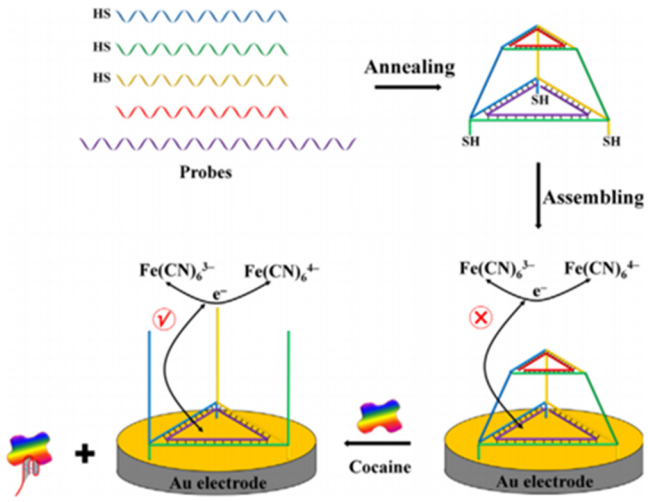

Figure 18. A graphical representation of the electrochemical-based cocaine biosensor using a dynamic DNA nanostructure. DNA probes are folded into the triangular pyramid frustum (TPF) configuration, which is assembled on the surface of the gold electrode. The bulkiness of this nanostructure prevents the redox reaction of the ferric cyanate. Cocaine−aptamer binding triggers a change to the equilateral triangle (ET) structure, which allows the redox reaction to proceed. Reprinted with permission from ref 265. Copyright 2014 Elsevier.

found a linear relation between Faradaic impedance response and cocaine concentration for concentrations between 1.0 nM and 2.0 μM. Inspired by this approach, Xiong's group developed an electrochemical biosensor to detect staphylococcal enterotoxin B (SEB), a leading cause of foodborne illnesses, in milk samples.[266] TPF−ET transformation occurred in the presence of SEB and was made observable by changes in Faradaic impedance.

Signal transduction induced by structural changes in dynamic DNA nanostructures has inspired other groups to develop different structures to accommodate *in vivo* sensing. In 2012, Fan's group pioneered the use of aptamer-functionalized reconfigurable tetrahedral DNA nanostructures (TDNs) for *in vivo* sensing of ATP (Figure 19A).[267] Different functional motifs were incorporated into the edges of the TDN, including an anti-ATP aptamer for ATP detection, an i-motif for pH sensing, and a T-rich mercury-specific oligonucleotide (MSO) for mercury sensing. Aptamer−ATP binding induced a conformational change in the nanostructure, bringing a signaling FRET pair closer together and quenching fluorescent emission. Importantly, the authors were able to incorporate two functional motifs on one TDN structure and perform intracellular ATP sensing using an anti-ATP aptamer and target-mediated logic gates. Five years later, Shiu et al. created a nanocomposite comprised of a split DNA aptamer and G-quadruplex tweezers that closed in the presence of the malaria biomarker protein

https://doi.org/10.1021/acs.chemrev.0c01332
Chem. Rev. XXXX, XXX, XXX−XXX

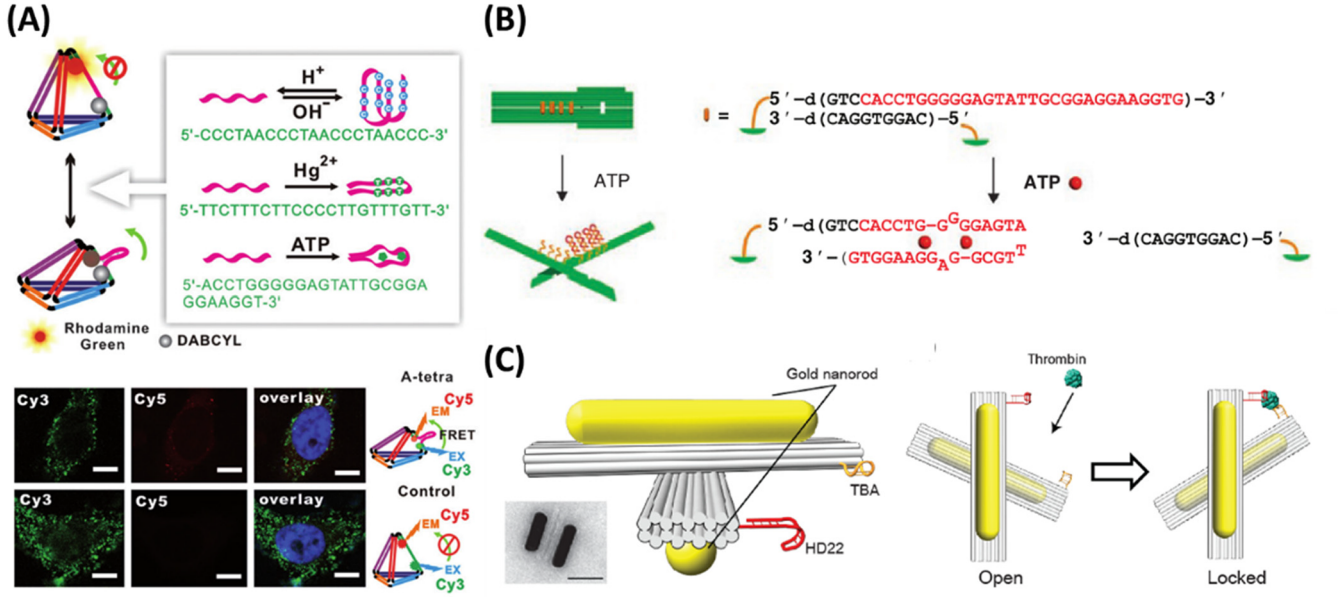

Figure 19. Optical sensing platforms incorporating aptamer-conjugated dynamic nucleic acid nanostructures. (A) Reconfigurable TDN for *in vivo* ATP detection using an anti-ATP aptamer. Other targets were detected using different functional modules (Scale bar = 20 μm). Adapted with permission from ref 267. Copyright 2012 John Wiley and Sons. (B) DNA origami pliers and forceps decorated with ATP-binding aptamers. The nanostructures undergo a conformational change in the presence of ATP. Adapted with permission from ref 270. Published 2011 Springer Nature. Licensed under a Creative Commons agreement (https://creativecommons.org/licenses/by/3.0/). (C) Plasmonic DNA origami metamolecule carrying two gold nanorods and two thrombin-binding aptamers, which transforms into a chirally inverted conformation upon binding to thrombin (scale bar = 50 nm). Adapted from ref 275. Published 2019 Multidisciplinary Digital Publishing Institute. Licensed under a Creative Commons agreement (https://creativecommons.org/licenses/by/4.0/).

(PfLDH).[268] Once aptamer-PfLDH binding occurred, the tweezer transformed from an open state to a closed state, favoring formation of the G-quadruplex and allowing it to catalytically enhance hemin's peroxidase activity. Spectrophotometric quantification of the PfLDH concentration was determined indirectly by ABTS oxidation. This work demonstrated the expansion of G-quadruplex-based tweezers to protein sensing, given that most previous targets for G-quadruplex-based tweezers had been nucleic acid strands, due to the ability of complementary base pairing to modulate the tweezer mechanism via toehold-mediated strand displacement reaction (TMSD).[263,269]

DNA origami has offered the possibility of developing nanosensors that optimize target−bioreceptor interactions.[262] In 2011, Kuzuya et al. introduced the first DNA origami "pliers" and "forceps" for targeting a variety of different targets (Figure 19B).[270] These devices consisted of two DNA "levers" that underwent a conformational change upon binding to their target. ATP detection was achieved using an ATP-binding aptamer, though several other targets were also demonstrated using this method, including IgG, streptavidin, sodium ions, and miRNA, by decorating the nanostructure with other functional motifs. AFM and fluorescence spectroscopy were used as a readout to observe target-induced conformational changes. Inspired by this work, Walter et al. designed two DNA origami levers joined by a split ATP aptamer, each having a fluorescent dye.[271] In the absence of ATP, the levers were separated, and no energy transfer occurred between the fluorophores. However, binding of two ATP molecules to the split aptamer brought the levers together, triggering a fluorescently detectable color change from green to red. This work improved the practical readout method for DNA origami-based sensing through use of FRET.

DNA nanoboxes combined with a FRET reporting system have emerged in the past decade as promising candidates for nanosensing, drug delivery, and molecular computation, mechanized by the "unlocking" action of a target. Their size can be controlled based on the load they carry, and multiple aptamers can be decorated on a single DNA nanobox, allowing logic gate-based sensing to be modulated by multiple targets. Research groups in Denmark have demonstrated the versatility of nanoboxes, including their use as Boolean logic gates. In these designs, the box's lid could be opened and closed by strand displacement interactions using a specific set of DNA "keys," monitored using FRET.[37,272,273] Using DNA nanobox-inspired nanosensors, Tang et al. developed the first nanobox-based biosensor for protein detection.[274] The protein-triggered nanobox was mediated by two DNA strands, a PfLDH aptamer and its complementary strand, that kept the box in a locked state. In the presence of PfLDH, aptamer−PfLDH binding occurred and resulted in unlocking of the nanobox. This was quantitively measured by the reduction in FRET signal intensity, as unlocking caused a larger separation between Cy3−Cy5 FRET pairs.

Plasmonic readouts have also been used for dynamic DNA origami-based sensing, specifically for DNA origami decorated with nanomaterial-based biosensors. In 2019, Funck et al. developed a reconfigurable DNA origami plasmonic metamolecule carrying two immobilized gold nanorods and two thrombin-binding aptamers (Figure 19C).[275] They found that thrombin binding induced an inversion of chirality as the nanostructure transformed from an "open" state to a "locked" state defined by the orientation of the gold nanorods, resulting in a quantitative change in plasmonic circular dichroism (CD) measurements. This allowed detection of thrombin in solution, with detection limits comparable to those achieved by other

https://doi.org/10.1021/acs.chemrev.0c01332
Chem. Rev. XXXX, XXX, XXX−XXX

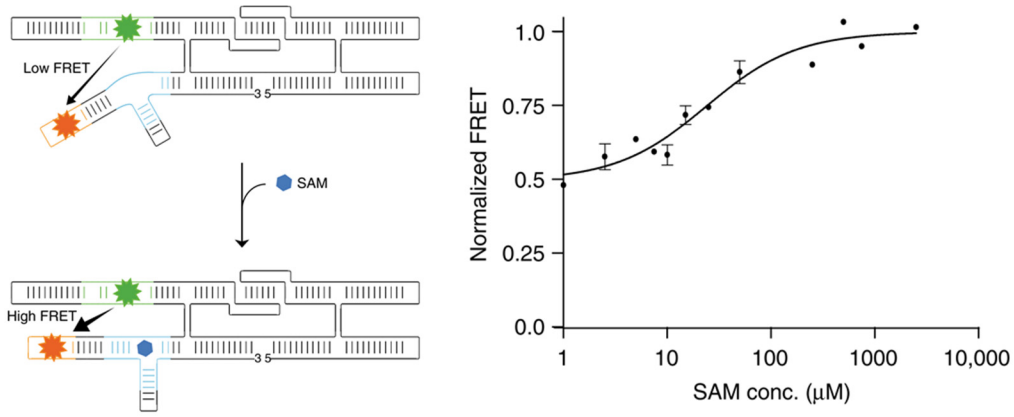

Figure 20. An apta-FRET dynamic RNA origami nanostructure to detect S-adenosylmethionine (SAM). Presence of the target triggers a conformational change that increases FRET emission by bringing the fluorophore pair closer together. FRET emission increases with SAM concentration. Adapted from ref 104. Published 2018 Springer Nature. Licensed under a Creative Commons agreement (https://creativecommons.org/licenses/by/4.0/).

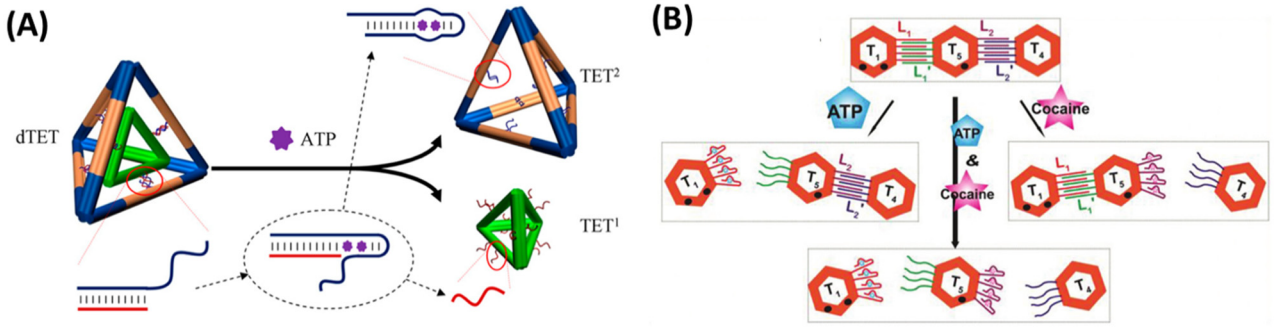

Figure 21. DNA origami disassembly based aptasensors. (A) Multilayered TDN nanocages for ATP detection. ATP−aptamer binding triggers dissociation of the layers. Adapted from ref 278. Copyright 2015 American Chemical Society. (B) Hexagonal DNA origami for simultaneous detection of ATP and cocaine. The presence of either target disassembles the dimer/trimer structure. Adapted with permission from ref 279. Copyright 2016 Royal Society of Chemistry.

methods, such as FRET and ELISA. The CD sensing technique was previously utilized to detect RNA and small molecules such as ATP and cocaine.[276,277]

Although previously used to a lesser extent than DNA nanostructures, dynamic RNA origami platforms have recently shown great potential for biosensing. In 2018, Andersen's group developed a fluorescent RNA aptamer-embedded ssRNA origami scaffold for nucleic acid and small molecule detection (Figure 20).[104] Fluorescent spinach and mango RNA aptamers were integrated into the RNA origami nanostructure. RNA detection was achieved by toehold-mediated interactions between the RNA and a hairpin loop in the nanostructure that induced a conformational change, resulting in a low FRET signal. Furthermore, detection of *S*-adenosylmethionine (SAM) was accomplished by incorporating an SAM aptamer into the RNA origami frame. The presence of SAM induced a conformational change, altering the separation and increasing the fluorescence emission of the FRET pair. The authors further demonstrated the capability of this apta-FRET RNA system to be expressed and cotranscriptionally folded inside *E. coli* cells, opening a wide range of applications for the use of RNA origami for *in vivo* sensing and synthetic biology.

5.1.2.2. Disassembly Based Sensing. Unlike aptasensor platforms for protein detection, aptamer−small molecule binding is extremely difficult to directly observe using AFM. Thus, in order to employ DNA origami-based aptasensors for small molecule detection, it is crucial to couple target binding to large conformational changes of the origami platforms. In 2015, Mao's group fabricated nanostructure "cages" comprised of multiple layers of TDNs (Figure 21A).[278] The layers were joined by dsDNA comprised of an ATP-binding aptamer. The presence of ATP triggered a conformational change in the nanostructure and disassembly of its layers in proportion to the ATP concentration, measurable by gel electrophoresis. Two years later, Willner's group reported the use of DNA origami dimers and trimers connected by dsDNA comprised of ATP and cocaine-binding aptamers (Figure 21B).[279] In the presence of either target, the multimerized hexagonal origami dissociated. AFM and gel electrophoresis confirmed that the decrease in amount of the multimerized origami structures was proportional to the ATP or cocaine concentration. Importantly, this work demonstrated the ability to detect two targets simultaneously by manipulating target-induced DNA origami dissociation.

5.1.3. Dynamic Nucleic Acid Nanotechnology for Signal Amplification. Dynamic nucleic acid nanotechnology includes reconfigurable nanodevices and nanocircuits that have been used in far-reaching applications, from nanoelectronics to nanosensing. Dynamic nucleic acid nanostructures include DNA and RNA nanocircuits and nanomachines as well as enzyme-free and enzyme-driven signal amplification processes. For example, isothermal nucleic acid hybridization processes such as hybridization chain reactions (HCR) and rolling circle amplification (RCA) are intriguing tools for use in signal amplification in biochemical sensing applications. Recent

https://doi.org/10.1021/acs.chemrev.0c01332
Chem. Rev. XXXX, XXX, XXX−XXX

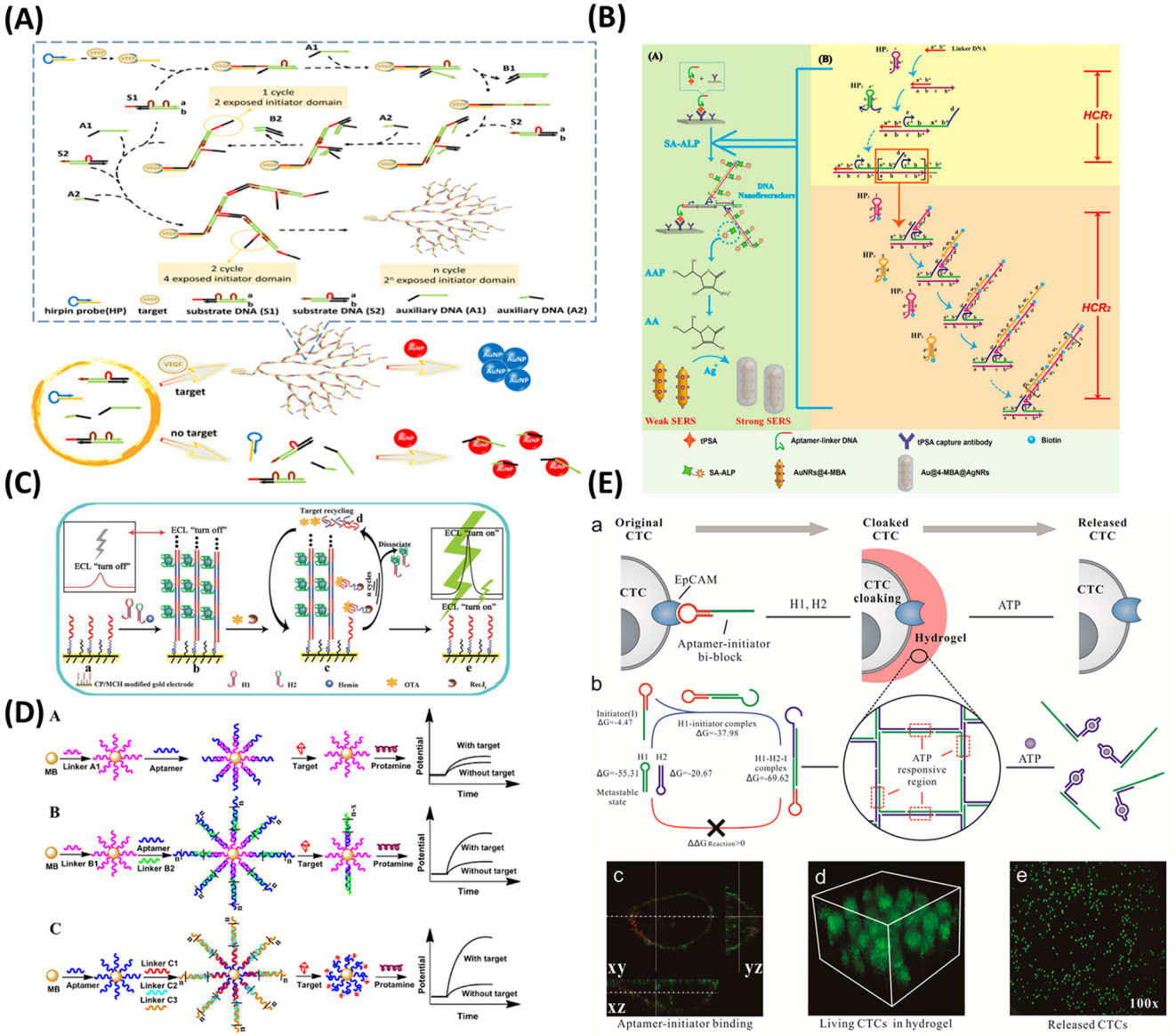

Figure 22. Dynamic nucleic acid nanostructures for signal amplification in chemo- and biosensing platforms. (A) Branched aptamer-functionalized DNA nanostructure for NLHCR-based detection of vascular endothelial growth factor. Reprinted with permission from ref 283. Copyright 2015 Elsevier. (B) Hyperbranched aptamer-decorated DNA nanostructure for detection of total prostate antigen using concatenated-HCR. Reprinted from ref 285. Copyright 2020 American Chemical Society. (C) Aptamer−DNAzyme supersandwich nanostructures for detection of ochratoxin A. OTA-induced disassembly of the nanostructures triggers ECL emission. Reprinted with permission from ref 286. Copyright 2013 Royal Society of Chemistry. (D) Label-free, HCR-based detection of bisphenol A using aptamer-functionalized nanostructures self-assembled on magnetic beads. Reprinted from ref 287. Copyright 2015 American Chemical Society. (E) Target-responsive DNA hydrogel for whole-cell detection of tumor cells. Aptamers are used to control cloaking and decloaking, with ATP as an external stimulus. Reprinted from ref 289. Copyright 2017 American Chemical Society.

advances in the use of HCR in biosensing and bioimaging are summarized by Bi, Yue, and Zhang.[280] In this review, we focus on aptasensor-based dynamic nucleic acid nanotechnology for signal amplification.

5.1.3.1. Enzyme-Free Signal Amplification. 5.1.3.1.1. Hybridization Chain Reaction. HCR is a versatile tool that has been used in various application such as bioimaging, biomedicine, and biosensing.[280−282] To improve the sensitivity of sensing platforms, high signaling output is generally needed for diagnostic and clinical applications, but linear HCR can take a prohibitively long time to acquire such a signal.[283] Therefore, a form of nonlinear HCR (NLHCR) involving exponential formation of hyperbranched DNA nanostructures was developed by Xuan and Hsing.[284] This technique was used in 2015 by Chang et al. to develop an enzyme-free, branched DNA aptasensor that targeted vascular endothelial growth factor (VEGF), as shown in Figure 22A.[283] Once aptamer−VEGF binding occurred, a conformational change in the aptamer probe occurred and consequently triggered NLHCR. Salt-induced gold nanoparticle aggregation was used for colorimetric output. A visible color change from red to blue occurred due to surface plasmon coupling induced by AuNP aggregation. This aptasensor was highly sensitive, detecting VEGF at femtomolar concentrations. In 2020, Wang et al. used a concatenated hybridization chain reaction (C-HCR) to produce a large, highly branched DNA nanostructure functionalized with an aptamer

https://doi.org/10.1021/acs.chemrev.0c01332
Chem. Rev. XXXX, XXX, XXX−XXX

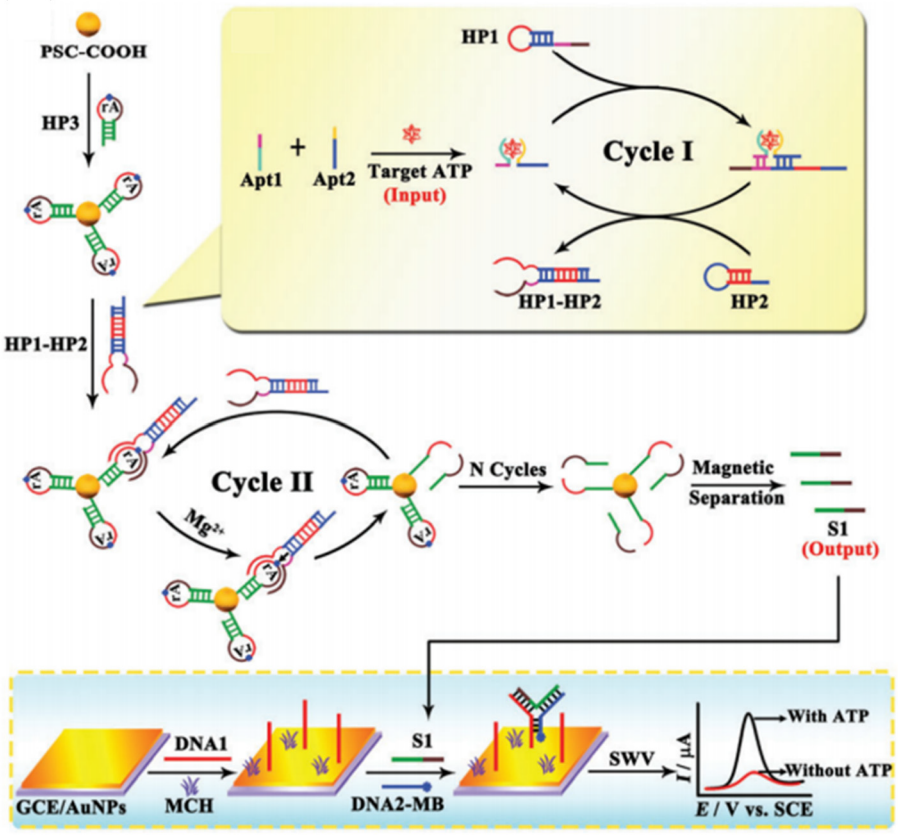

Figure 23. CHA-based method for ATP sensing. A split ATP aptamer is used to bind to ATP and trigger CHA. Magnetic separation of hairpin loops allows hybridization with MB-tagged reporters. Electrochemical signal increases with concentration of ATP. Adapted with permission from ref 292. Copyright 2017 Royal Society of Chemistry.

that bound to total prostate specific antigen (tPSA), a prostate cancer biomarker (Figure 22B).[285] The aptamer linked the nanostructure to the antigen/antibody complex, triggering NLHCR. The nanostructure was labeled with streptavidin-modified alkaline phosphatase, which catalytically reduced Ag^+ and deposited silver on gold nanorods. Sensing efficacy could thus be measured using a surface-enhanced Raman scattering (SERS) immunoassay. The limit of detection of this biosensor was only 0.94 fg/mL, and measurement of tPSA concentrations from Raman spectra closely fit the values given for the human blood serum samples used, indicating this method's potential utility for early cancer diagnosis.

Target-induced HCR-based nanostructure disassembly has been applied in other biosensing settings. In 2014, Chen and colleagues fabricated aptamer−DNAzyme supersandwich nanostructures capable of detecting the toxic fungal metabolite ochratoxin A (OTA) via electrochemiluminescent (ECL) sensing (Figure 22C).[286] These nanostructures were preassembled by HCR on a gold electrode, forming aptamer−DNAzyme complexes that effectively quenched the ECL emission of dissolved oxygen. However, the presence of OTA and the DNA exonuclease $RecJ_f$ induced disassembly of the nanostructures, strengthening the ECL emission. A year later, Qin's group used the same principle to pioneer the first aptamer-functionalized DNA nanostructures self-assembled by HCR on magnetic beads that did not require signaling tags for bisphenol A detection (Figure 22D).[287] Specific binding of bisphenol A to the aptamer induced disassembly of the HCR-based nanostructures from the magnetic nanoparticles, resulting in a detectable change in the particles' surface charge that was measured using a polycation-sensitive electrode and protamine indicator. In 2016, the same group expanded their method to whole cell detection, using DNA nanostructures decorated on magnetic beads to potentiometrically detect *Vibrio alginolyticus*, with a limit of detection of only 10 CFU/mL.[288]

Combining aptamer-triggered HCR formation and target-induced HCR product deformation has been used to improve both sensitivity and specificity in biosensing. For example, in 2017, Song et al. synthesized a DNA hydrogel to detect circulating tumor cells (CTCs) (Figure 22E).[289] An aptamer biblock specifically bound to epithelial cell adhesion molecule (EpCAM) on the CTC surface, triggering HCR and cloaking the cells. Furthermore, the HCR product contained an ATP-binding aptamer and disassembled in the presence of ATP, allowing decloaking of the CTCs and their release into the surrounding solution. This method had a detection limit of only ten cancer cells, and its carefully modulated cloaking and decloaking processes are promising tools for whole-cell analysis in clinical settings.

5.1.3.1.2. Nucleic Acid Circuits. Nucleic acid nanocircuits based on catalytic hairpin assembly reactions have served as common signal amplification tools in various biosensors. Catalytic hairpin assembly (CHA) is an enzyme-free isothermal amplification technique, often involving the opening of hairpin loops when bound to a single-stranded nucleic acid analyte. This results in exponential formation of stable, double-stranded products. The method was first introduced by Yin et al. in 2008,[290] and has since been applied in various *in vitro* and *in vivo* applications owing to its high signal amplification efficiency.[291]

https://doi.org/10.1021/acs.chemrev.0c01332
Chem. Rev. XXXX, XXX, XXX−XXX

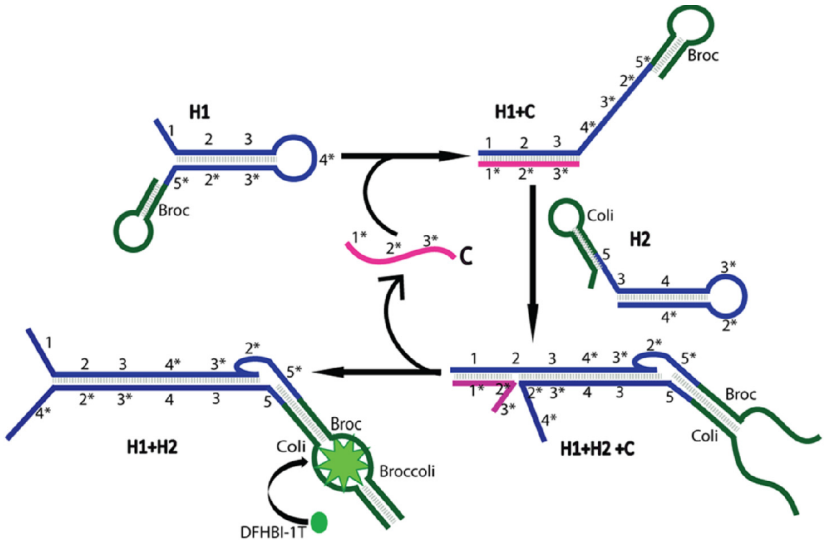

Figure 24. CHA-based RNA nanocircuit for RNA biosensing in living cells. CHA produces hairpin loop duplexes, and a fluorescent broccoli aptamer undergoes conformation change in the presence of the RNA target. Reprinted from ref 296. Copyright 2018 American Chemical Society.

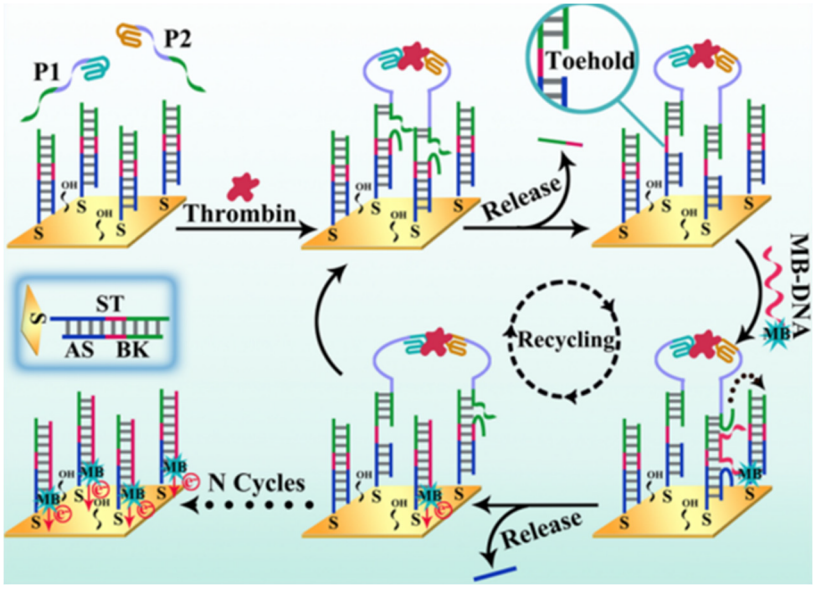

Figure 25. Diagram of sequential steps in the mechanism of the TSDR-based thrombin aptasensor. P1 and P2 represent the two thrombin-binding aptamers. The three strand DNA capture probes are assembled on a gold electrode surface. In the presence of thrombin, one strand is released, exposing a toehold. Methylene blue-tagged DNA (MB-DNA) can then invade, resulting in an electrochemical response. The released target−capture probe complexes can be recycled. Reprinted from ref 301. Copyright 2017 American Chemical Society.

In 2017, Xie and colleagues developed an ultrasensitive electrochemical biosensor for ATP based on CHA signal amplification (Figure 23).[292] Target binding to an ATP split aptamer triggered CHA, and the resulting products hybridized with hairpin loops to form DNAzymes via a toehold-mediated strand displacement reaction. Magnetic separation of these hairpin loops formed ssDNA that could hybridize with MB-tagged DNA, generating an electrochemical signal. One year later, Liu et al. expanded the use of CHA to detect cancer cells through a fast and sensitive method.[293] They incorporated an aptamer that both bound to the target cells and initiated CHA. This caused fluorophore−quencher separation and thus a detectable fluorescent signal. The detection technique was applied to clinical samples, with a detection limit of 10 cells/mL, better than previous aptasensor whole-cell detection methods. CHA thus shows promise for signal amplification in the sensing of various targets, from small molecules to whole cells.

DNA nanocircuits have inspired the development of RNA-based circuits for signal amplification. In 2014, Bhadra and Ellington designed a CHA-based RNA nanocircuit with detection of CHA-produced hairpin loop duplexes provided by the DFHBI fluorophore-binding spinach aptamer.[294] The spinach aptamer was sequence-specific, only undergoing a conformational change in the presence of the nucleic acid target. The authors applied their method to detect ssDNA products from an isothermal strand displacement amplification reaction, demonstrating nanomolar sensitivity. This work showed that RNA nanocircuits could be transcribed from DNA templates without purification, with detection efficacy comparable to traditional DNA circuits. One year later, Akter and Yokobayashi also applied an RNA nanocircuit to nucleic acid detection.[295]

https://doi.org/10.1021/acs.chemrev.0c01332
Chem. Rev. XXXX, XXX, XXX−XXX

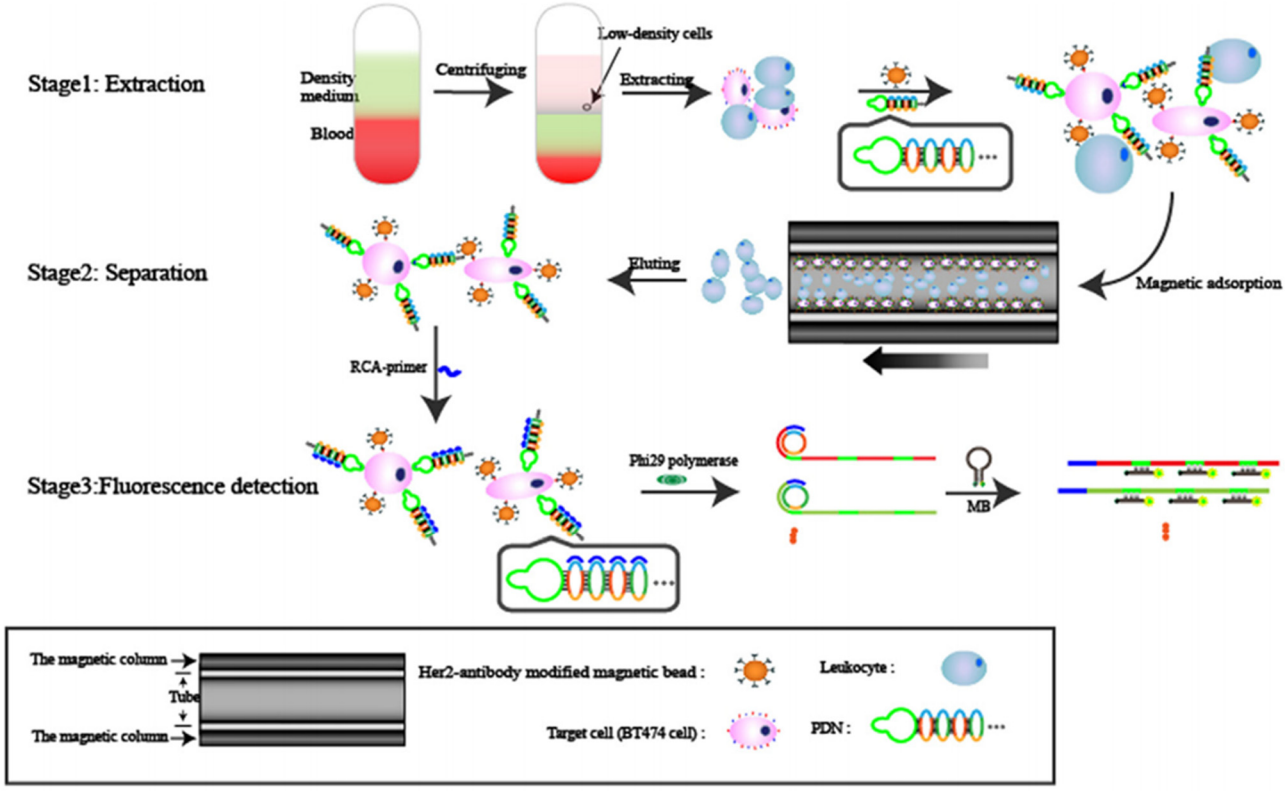

Figure 26. RCA-based detection of circulating tumor cells (CTCs). Antibody-conjugated magnetic beads are used to separate the CTCs from blood samples, an EpCAM-binding aptamer is used for target capture, and RCA is used to amplify the fluorescent signal. Adapted with permission from ref 303. Copyright 2018 Elsevier.

Their design was composed of an initially blocked spinach aptamer, a fuel strand, and an input strand. The input strand hybridized with the aptamer at its toehold, triggering fluorescence, while the fuel strand displaced the input strand through toehold-mediated strand displacement, allowing recycling of the input strand. In 2018, Karunanayake Mudiyanselage et al. expanded the use of CHA-based RNA nanocircuit biosensors to *in vivo* whole-cell detection, as shown in Figure 24.[296] They genetically encoded and transcribed the RNA circuit, demonstrating cellular permeability and sensitive intracellular RNA sensing. The RNA analyte triggered the nanocircuit and activated the fluorescent split broccoli aptamer.

5.1.3.1.3. Nucleic Acid Nanomachines. Nucleic acid nanomachines have been applied in numerous biomedical engineering and clinical settings, from drug transport to biosensing.[297−299] In sensing applications, DNA walkers and other nanomachines have been used for signal amplification and transduction through a variety of processes, including toehold-mediated strand displacement (TMSD).[300] In 2017, Yang and colleagues used a TMSD-based DNA nanomachine as an aptasensor to detect thrombin in blood serum (Figure 25).[301] Three aptamer-functionalized DNA strands were immobilized on a gold electrode surface, and two aptamers that bound different exosites of thrombin aided the target capture process. Binding triggered displacement of one of the three strands and exposure of a toehold that could hybridize with a ssDNA conjugated with a methylene blue (MB) dye. The nanomachine's mechanism was based on TMSD of the aptamer−thrombin complex by the MB-tagged DNA. In this way, the complex could be recycled and the MB-tagged ssDNA could be captured on the electrode surface in sufficient quantity to generate an electrochemical signal. Using this method, the authors demonstrated amplified signaling output and improved detection limits of thrombin in serum.

5.1.3.2. Enzyme-Driven Nanostructure Formation for Signal Amplification. Rolling circle amplification (RCA) has recently been applied, among other applications, to clinical biosensing, where it can serve as a powerful signal amplifier to improve limits of target detection.[302]

In 2018, Wang et al. developed a biosensing system comprised of magnetic beads conjugated with HER2 antibodies and an anti-EpCAM SYL3C aptamer-functionalized DNA nanocatenane consisting of three circular DNA structures as shown in Figure 26.[303] The beads were used to separate breast cancer circulating tumor cells (CTCs) in whole blood. Aptamer−target binding triggered RCA to bind the CTCs together, generating and amplifying a fluorescent signal transduced by a molecular beacon conjugated with 4-(dimethylaminoazo)benzene-4-carboxylic acid (DABCYL) and fluorescein (FAM) fluorophores, a FRET pair. The authors demonstrated a limit of detection of under 10 CTCs/mL of blood. Recently, Gao et al. further used RCA to achieve photoelectrochemical detection of cancer biomarkers.[304] They fabricated a DNA nanosphere functionalized with an aptamer that targeted carcinoembryonic antigen (CEA). The structure was self-assembled by RCA on a glass electrode and, when present, quenched photocurrent from Au nanoparticles and ZnSe QDs. On aptamer−CEA binding, the hairpin loop in the nanostructure opened, triggering enzyme-free strand displacement amplification, which produced large amounts ssDNA that competitively bound and released the nanospheres. This increased the photoelectric signal in

https://doi.org/10.1021/acs.chemrev.0c01332
Chem. Rev. XXXX, XXX, XXX−XXX

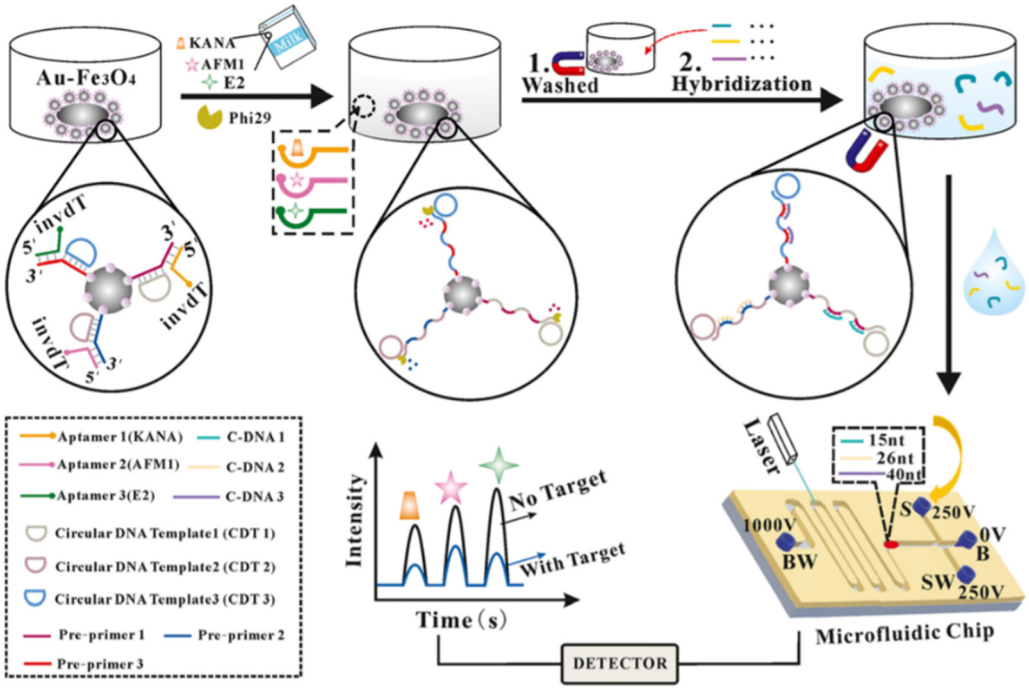

Figure 27. Representation of the overall process to sense multiple pollutants simultaneously. The magnetic DNA nanocomposite was added to a milk sample, aptamers bound to the three targets in the supernatant fluid, and RCA was initiated. Subsequently, the solution was magnetically separated, and microchip laser-induced fluorescence was used to quantify the intensity changes when the RCA products were added to a solution containing their complementary strands. Reprinted with permission from ref 306. Copyright 2020 Springer Nature.

proportion to the CEA concentration. A low detection limit of 0.12 fg/mL in blood serum samples was achieved.

Aptamer-functionalized nanostructures have proved to be valuable chemosensors to detect potential toxins in food samples. Recently, Hao et al. used an aptamer-functionalized DNA hydrogel to detect the concentration of the fungal toxin ochratoxin A (OTA) in beer.[305] To overcome the issue of low sensitivity that often plagues hydrogel sensing applications, RCA was used as a signal amplifier. In the absence of OTA, the aptamer hybridized with the RCA primer, inhibiting RCA. Once present, OTA bound the aptamer and released the primer, allowing the RCA reaction to occur and amplify the fluorescent signal. Fluorescence intensity was amplified in proportion to the OTA concentration, and was measured by adding Cy3−dUTP to the hydrogel. In the same year, He et al. reported the development of an aptasensor involving a microfluidic chip and a three-part DNA nanostructure comprising an aptamer component as well as preprimers and circular DNA templates (Figure 27).[306] The authors used this sensor to measure the concentrations of three potential toxins in milk, namely, kanamycin (KANA), aflatoxin M1 (AFM1), and 17β-estradiol (E2). The aptamers targeted these three molecules, while the preprimer and circular DNA templates were used to start rolling circle amplification (RCA) of the products in solution. Importantly, the DNA nanostructure was conjugated with a magnetic nanocomposite, consisting of gold nanoparticles and ferrosoferric oxide, allowing magnetic separation of the sample. Upon addition to a solution containing DNA strands complementary to the RCA products, a marked decrease in the number of complementary strands was observed due to the presence of the targets. This was quantified using microchip laser-induced fluorescence, and linear regression was used to obtain the original target concentration. The advantages of this method include high sensitivity, fast response time, convenience, and simultaneous multiplex target detection.

The functionalization of nucleic acid nanostructure sensors with aptamer bioreceptors and bioreporters has taken great strides in the direction of improved analyte specificity and sensitivity for nanosensors. Tetrahedral DNA nanostructures have been assembled on electrodes to enable better target accessibility for target capture probes and facilitate electrochemical signal transduction by redox probes, while DNA/RNA origami has been utilized to optimize bioreceptor−target interactions through precise spatial control of aptamer orientation. Optical-based dynamic biosensors combined with FRET reporting systems have been used to quickly generate fluorescent signals for analyte detection, and processes such as hybridization chain reactions and rolling circle amplification have been applied for signal amplification to obtain ultrasensitive platforms. Aptamer-decorated nucleic acid nanostructures have been utilized to detect a wide variety of analytes, including nucleic acids, proteins, inorganic and organic small molecules, whole cells, and viruses. We expect that the range of detectable analytes will grow broader, encompassing virtually any biochemical target. However, one of the most challenging issues facing the field of nanosensing lies in fabricating practical sensors that can be applied in real-world settings, such as clinical diagnostics or food safety inspections. Several groups have demonstrated the ability to detect analytes in complex biosamples including food, whole blood, and urine samples. Furthermore, some groups have developed universal biosensors, capable of detecting many different types of analytes by simple reprogramming of the same central sensing platform. In order to realize the practical utility of these sensors, it is necessary to find a balance between the convenience of the sensing method and its sensitivity of detection. For example, static electrochemical biosensors have achieved femtomolar limits of detection for

https://doi.org/10.1021/acs.chemrev.0c01332
Chem. Rev. XXXX, XXX, XXX−XXX

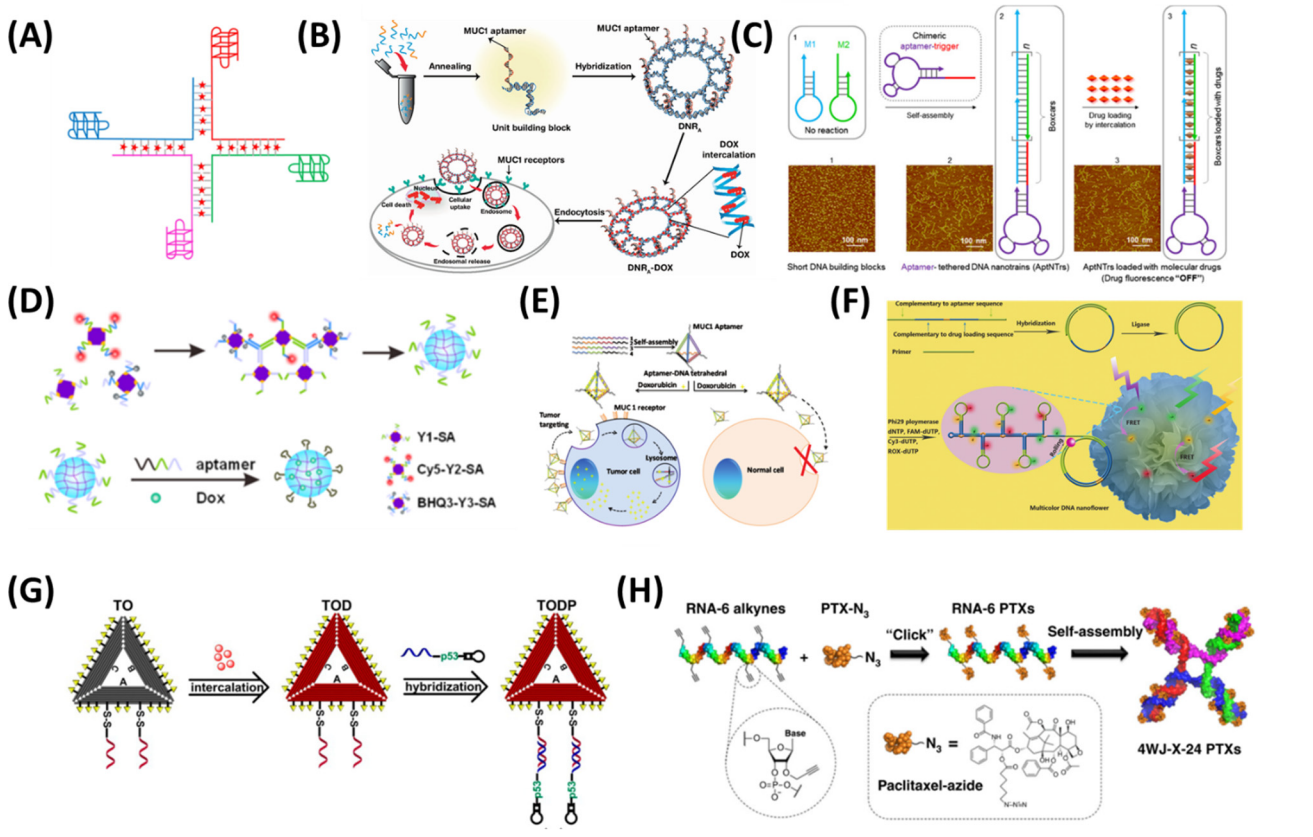

Figure 28. Chemical therapeutic drug loading aptamer-tethered nucleic acid nanostructure for targeted delivery. (A) 4-WJ DNA nanostructure bearing multivalent aptamers as a DOX carrier. Adapted with permission from ref 324. Copyright 2020 Dove Medical Press. (B) Self-assembled aptamer/DNA nanoring drug carrier. Adapted with permission from ref 328. Copyright 2018 IOP Publishing. (C) Drug loaded on aptamer-decorated DNA nanotrains. Adapted with permission from ref 331. Copyright 2013 National Academy of Sciences. (D) Protein-scaffolded DNA nanohydrogel harboring dual aptamers to transport DOX. Adapted from ref 334. Copyright 2019 American Chemical Society. (E) DOX-loaded, multivalent aptamer-decorated tetrahedral DNA nanostructures. Adapted with permission from ref 339. Copyright 2019 Royal Society of Chemistry. (F) RCA-based DNA nanoparticles. Reprinted with permission from ref 342. Copyright 2014 John Wiley and Sons. (G) Triangular DNA origami bearing DNA aptamers with DOX loading. Adapted from ref 350. Copyright 2018 American Chemical Society. (H) Chemical therapeutic drug covalently conjugated on 4-WJ RNA nanoparticle. Adapted from ref 353. Published 2020 Springer Nature. Licensed under a Creative Commons agreement (https://creativecommons.org/licenses/by/4.0/).

biomolecules, but they often require laborious multistep sample preparations as well as expensive labeling processes, making them infeasible for some clinical applications. Advances have been made to reduce the expense and time scale of detection without compromising on sensitivity, but this will be an ongoing challenge as groups continue to develop convenient and sensitive sensors for a multitude of applications.

5.2. Targeted Delivery and Controlled Release

Many effective therapeutic agents have been comprehensively developed from bench to bedside to treat human diseases, such as cancers. However, most therapeutic agents cause unwanted side effects such as severe cytotoxicity to healthy cells due to their nonspecific interactions. To circumvent problems associated with these undesired effects, the targeted delivery of therapeutic drugs is crucial.

Nucleic acid aptamers specifically bind to their targets with high affinity. Additionally, aptamers can bind to a wide range of targets including small molecules, proteins, viruses, and cancer biomarkers. With these properties, aptamers can be used as targeting molecules for selective drug delivery.[307−309] Several methods have been developed to conjugate therapeutic agents to aptamers for targeted delivery. Covalent and noncovalent conjugations of chemotherapeutic drugs on aptamers have been demonstrated and have shown selective delivery to target cells.[133,177] Furthermore, oligonucleotide-based therapeutic agents such as siRNA and miRNA can be combined with cell-targeting aptamers via sticky-end hybridization[310−313] or sequence extension.[314,315] However, the loading efficiency associated with direct conjugation of therapeutic agents on stand-alone aptamers is low. To increase loading capacity, many drug carriers, including liposomes and polymeric nanoparticles, have been utilized for targeted delivery. Cancer-targeting, aptamer-modified nanocarriers for targeted delivery have been extensively developed and previously reviewed.[133,309,316,317]

With programmability, controllable size and shape, biocompatibility, and addressability, nucleic acid nanostructures can be used as biomolecular platforms for functionalization with targeting aptamers and carriers of therapeutic molecules for targeted delivery. Taking advantage of both nucleic acid nanostructures and aptamers, many targeted delivery platforms have been developed. In this section, we focus on the progressive development of nucleic acid nanostructures bearing aptamers for targeted delivery and classify them based on the molecules they deliver, including chemical drugs, oligonucleotides, peptides and proteins, inorganic nanomaterials, and multi-therapeutic agents.

https://doi.org/10.1021/acs.chemrev.0c01332
Chem. Rev. XXXX, XXX, XXX−XXX

5.2.1. Chemical Molecules. *5.2.1.1. Chemotherapeutic Drugs.* Doxorubicin (DOX) is a common chemotherapeutic agent and has been widely used from research to clinical areas for treatment of a large range of solid and liquid tumors.[318,319] DOX intercalates between DNA base pairs and inhibits topoisomerase II, causing DNA replication to stop and consequently promoting cell death.[320] This intercalation property of DOX offers the potential for co-delivery with nucleic acid aptamers that selectively bind cancer cells. For targeted delivery, aptamers serve as targeting molecules and DOX serves as the chemotherapeutic anticancer agent. Targeted delivery of DOX−aptamer complexes has been developed and successfully demonstrated to treat cancers.[309,316] To enhance efficacy of treatment and minimize cytotoxicity to nontarget cells, a high loading capacity of chemotherapeutic agents into drug carriers that are specific and enable internalization to target cells is crucial. The loading amount of DOX into DNA structures depends on the length and size of DNA nanostructures. Nucleic acid nanostructures not only offer biomolecular platforms to decorate multivalent targeting aptamers, but also can be used as promising carriers for the targeted delivery of chemotherapeutic agents with high loading capacity. With biocompatibility, modularity, and programmable properties, nucleic acid nanostructures provide a great tool for targeted delivery of chemotherapeutic drugs, especially DOX. During the past decade, many research groups have developed various designs of nucleic acid nanostructures, including branch-junction structures, tetrahedral DNA nanostructures, DNA origami, and RNA/DNA hybrid nanoparticle, to serve as carriers for chemotherapeutic drugs and increase treatment efficiency.

Multiarm junction nucleic acid nanostructures have been developed and utilized in a wide range of applications from sensing to targeted delivery. These topologically branched structures allow decoration of multivalent functional motifs, such as aptamers, which opens opportunities for targeted delivery purposes. Yang constructed aptamer−dendrimer DNA nanostructures using Y-DNA as a building block for the targeted delivery of DOX to cancer cells. The dendrimer nanostructures allow decoration of multiple Sgc8 aptamers, targeting the human T-cell acute lymphoblastic leukemia cell line, and can be loaded with DOX.[321] Abnous et al. designed 3WJ pocket DNA nanostructures containing three strands of AS1411 aptamers to target prostate and breast cancer cells.[322] The DOX-loaded DNA nanostructures were more effective for inhibition of tumor growth compared to free DOX. Additionally, the DOX/aptamer-conjugated DNA nanostructures have high cytotoxicity specific to target cells compared with nontarget cells. Using 4WJ-DNA nanostructures, targeted co-delivery of chemotherapeutic drugs (DOX) and therapeutic aptamers (FOXM1 aptamer) was developed.[323] With a similar strategy, Yao et al. constructed four AS1411 aptamers decorated on a 4WJ-DNA nanostructure that carries approximately 17 DOX molecules, as shown in Figure 28A.[324] The DOX-loaded, aptamer-decorated DNA nanostructures showed selective delivery to CT26 colon cancer cells. Recently, Sun et al. demonstrated targeted delivery of DOX on aptamer-functionalized 3D DNA nanostructures based on the self-assembly of four-way junctions.[325] They appended an AS1411 aptamer, targeting MCT-7 breast cancer cells, on one end of the 4WJ and sticky-ends on the other three arms to form a cocklebur-like DNA nanostructure via sticky-end hybridization. This aptamer/3D nanostructure selectively transported DOX to target cells and showed higher cytotoxicity than a DOX-loaded DNA nanostructure without aptamers. Furthermore, complex 3D DNA nanostructures can be formed by using junction motifs as building blocks.[326] For example, icosahedral DNA nanostructures have been constructed by self-assembly of five- and six-point star motifs. Huang developed aptamer-conjugated icosahedral DNA nanostructures as a carrier of DOX to kill epithelial cancer cells.[327] Furthermore, DNA nanorings have been created by self-assembly of T-shaped junctions. The DNA nanorings were decorated with mucin aptamers (MUC1) to selectively deliver chemotherapeutic anticancer drugs to MCF-7 breast cancer cells (Figure 28B).[328] Recently, Xue et al. developed a nuclease-resistant DNA nanowire decorated with multivalent Sgc8 aptamers, cancer-targeting aptamers, for the targeted delivery of DOX.[329] Two short DNA strands formed a dsDNA core structure that could form DNA nanowires via four sticky-ends that enable connections between monomer units. The 4WJ-like DNA nanowires display multiple ssDNA anchor points, allowing decoration of aptamers via DNA/DNA hybridization. To enhance the stability of nanostructures in nuclease conditions, the researchers designed nick-hidden DNA nanowires. The DNA nanowires were stable in serum after over 24 h of incubation and had a long blood circulation time. The DOX-loaded aptamer/DNA nanowires specifically bound to target cells and induced cancer cell apoptosis.

To obtain a high loading capacity of chemical agents, large and complex DNA nanostructures have been utilized as vesicles for targeted delivery. Hybridization chain reaction (HCR) is a method to form long dsDNA with a few strands of DNA.[280,330] Due to simplicity of design, capability of self-polymerization, and synthesis of long dsDNA products, HCR has shown great potential for creating carriers for therapeutic drugs. In 2013, Tan developed aptamer-tethered DNA nanotrains for the targeted delivery of cancer-treating drugs. They employed Sgc8 aptamer as a targeting molecule and constructed HCR-based nanotrains as carriers for loading DOX (Figure 28C).[331] An artificially expanded genetic information system allows the addition of four synthetic nucleobases to the genetic code to produce an eight-letter alphabet named hachimoji.[332] In 2020, Tan further developed aptamer-tethered DNA nanotrains to deliver DOX by using six nucleotides, comprising four natural bases (A:T and C:G pairs) and two unnatural bases (P:Z pair).[333] Liver cancer aptamers were selected from a six-letter DNA library. The six letter-based aptamer/DNA nanotrains were used as a carrier for DOX and demonstrated selective cytotoxicity for liver cells.

To construct nucleic acid nanostructures as carriers for targeted delivery, proteins such as streptavidin have been used as linker molecules to form protein/DNA hybrid nanostructures. In 2019, Jiang developed protein-scaffolded DNA nanohydrogels bearing MUC1 and ATP aptamers to transport DOX (Figure 28D).[334] The hybrid DNA nanohydrogel was constructed via sticky-end hybridization of ssDNA-linked streptavidin and Y-shaped DNA. The DOX-loaded nanoparticles targeted cancer cells via MUC1 aptamer; once internalized, the ATP aptamer allowed controlled release of DOX in ATP-rich environments inside the target cells. In the presence of intracellular ATP, the ATP aptamers underwent conformational changes, resulting in disassembly of the nanostructures and the release of intercalated drugs within the target cells. With a similar strategy, Prasad et al. successfully loaded DOX into Sgc8 aptamer-decorated, streptavidin−DNA hybrid nanohydrogels for the targeting CCRF-CEM and HeLa cell lines.[335]

https://doi.org/10.1021/acs.chemrev.0c01332
Chem. Rev. XXXX, XXX, XXX−XXX

Tetrahedral DNA nanostructures are one of the most widely used DNA nanostructures because they are easy to construct using only a few oligonucleotides, are well-studied, have controllable size, and have reasonably high stability at low salt concentration. With these advantages, they have been immensely utilized in various applications including sensing, bioimaging, and drug delivery.[217,250,336] In 2016, Yang developed a MUC1 aptamer-decorated tetrahedral DNA nanostructure capable of carrying 25 DOX molecules.[337] Using a similar strategy, Lin developed Sgc8c DNA aptamer-decorated DNA tetrahedra to transport DOX to CCPR-CEM PKT7-positive tumor cells.[338] A tetrahedral DNA nanostructure contains four vertices that provide four decoration points that allow four possible locations to decorate with multivalent cancer-targeting aptamers. Taking advantage of this strategy, Han et al. constructed multivalent aptamer-functionalized tetrahedral DNA nanostructure capable of loading DOX (Figure 28E).[339] They decorated different numbers of MUC1 aptamers on nanostructures to target MCF-7 tumor cells. Their results showed that increasing the number of aptamers displayed on DNA nanostructure had a significant impact on uptake efficiency into targeted cells but did not increase uptake into nontarget cells. Other chemical drugs such as epirubicin have been selectively delivered by aptamer-conjugated DNA nanostructure carriers. Taghdisi et al. loaded epirubicin into DNA nanodiamonds labeled with dual aptamers.[340] They decorated DNA nanostructures with MUC1 aptamers targeting C26 (murine colon carcinoma) and MCF-7 (breast cancer) cells and ATP aptamers for controlled release of the drug.

To enhance the loading capacity of intercalated chemical drugs, researchers have developed a high-molecular weight, inexpensive DNA nanostructure for drug carriers. Rolling circle amplification (RCA) is an isothermal enzymatic reaction that enables DNA synthesis and has been utilized to construct DNA particles from nano- to sub-micrometer-sized particles.[302,341] RCA-based DNA synthesis produces a densely packed DNA nanostructure that provides nuclease resistance and offers a large loading capacity of chemical drugs, such as DOX. With these features, an RCA-synthesized DNA particle is a promising candidate for targeted delivery. In 2014, Tan developed RCA-DNA nanoflowers bearing two types of DNA aptamers, Sgc8 and MUC1 (Figure 28F).[342] The dual aptamer-DNA nanoflowers were stable in DNase I for 24 h. They loaded DOX into DNA nanoflowers and successfully delivered DOX to target cancer cells. Using a similar strategy, Wang developed RCA-produced DNA nanosponges decorated with Sgc-8C aptamers as carriers for two cancer therapeutic agents, ZnO and DOX.[343]

With programmable sizes and shapes, biocompatibility, and availability for chemical molecule conjugation, self-assembled DNA origami is another promising carrier for therapeutic drugs. Additionally, DNA origami can be used as a biomolecular platform for decoration of multivalent and multifunctional molecules, has stability in cell lysate for 12 h, and is degraded slowly in living cells.[344,345] The stability and slow degradation of DNA origami promotes the potential of DNA origami as drug carriers for controlled release. Many research groups have developed diverse origami designs for high drug loading efficiency, demonstrating controlled release of drugs in various systems.[346−348] Högberg and colleagues designed straight and twisted 18-helix bundle DNA nanotubes to deliver DOX to human breast cancer cells *in vitro*.[347] They found that the DNA origami designs impacted drug loading efficiency and release rate. The DNA origami is an effective carrier and promotes higher cellular internalization of DOX compared with free DOX. Du et al. further performed systematic studies on DNA origami's shape-dependent tumor accumulation *in vivo*.[348] They designed three DNA origami nanostructures (triangle, square, and 6-helix nanotubes). The fluorescently labeled DNA origami were administered into MB231 subcutaneous tumor-bearing nude mice. Twenty-four hours after injection, they examined biodistribution using fluorescence imaging. The *ex vivo* fluorescence imaging revealed that the triangular DNA origami had high accumulation at the tumor site and low accumulation in liver, while the squares and nanotubes accumulated in the tumor, kidney, and liver. Using DNA origami as a multifunctional biomolecular platform, Ding demonstrated targeted, co-delivery of DOX and gold nanorods on MUC1 aptamer-decorated triangular DNA origami to improve cancer treatments by circumventing drug resistance in cancer cells.[349] One triangular DNA origami could load approximately 2000 DOX molecules. Gold nanorods immobilized on the DNA origami via sticky-end hybridization were co-delivered for use in photothermal cancer therapy. In 2018, Ding et al. further developed combined delivery of chemotherapeutic drugs and tumor therapeutic genes by using triangular DNA origami bearing multivalent MUC1 aptamers as a nanocarrier, as shown in Figure 28G.[350] Additionally, hollow-structured DNA nanospheres have recently been constructed and decorated with MUC1 aptamers for the selective delivery of DOX to three cancer cell lines (MCF-7, HACaT, and MDA-MB-231).[351]

The interaction of DOX with DNA is well-known. However, the DOX/RNA interaction remains unclear. To load DOX into RNA nanostructures for targeted delivery, Guo and colleagues developed DNA/RNA hybrid nanoparticles.[352] The thermally stable pRNA-3WJ motif served as the core structure to form the nanoparticles. To construct the DNA/RNA hybrid nanoparticles, chemically synthesized phosphothioate-modified Endo 28 DNA aptamers, targeting annexin A2, and 2′-fluoro-modified RNA were assembled. To increase the loading capacity of DOX into the nanoparticles, they extended one arm of the pRNA-3WJ with a GC-rich sequence, allowing loading of 10 DOX molecules per particle. The DOX-loaded Endo28 aptamer-decorated hybrid nanoparticle was able to selectively bind and internalize into target cells and showed a slow DOX release profile. Recently, Guo and colleagues further developed a 4WJ bearing an anti-EGRP RNA aptamer for the delivery of paclitaxel to treat breast cancer (Figure 28H).[353] Paclitaxel is a chemotherapeutic anticancer drug that has been widely used for cancer treatments despite its low water solubility. To improve solubility and achieve targeted delivery, they covalently conjugated paclitaxel on 4WJ. Chemically synthesized ssRNAs containing six alkyne moieties were made. The 4WJ nanostructures were assembled with four alkyne-modified RNAs, yielding 24 reactive alkyne groups per structure. To load paclitaxel, azide-modified paclitaxel was covalently conjugated to alkyne-4WJ via click chemistry. With drug-conjugated RNA nanoparticles, the water solubility of paclitaxel was significantly increased, opening possibilities for targeted delivery of hydrophobic drugs.

5.2.1.2. Photosensitizers. Reactive oxygen species (ROS) are chemically reactive products made from partial reduction of molecular oxygen (O_2) that include peroxide (O_2^{2-}), superoxide ($O_2^{\bullet -}$), hydroxyl radical ($HO^{\bullet}$), and singlet oxygen ($^1O_2$).[354−356] In nature, ROS are continuously produced inside cells during cellular processes such as the electron transport chain.[357,358] However, high levels of ROS inside cells cause

https://doi.org/10.1021/acs.chemrev.0c01332
Chem. Rev. XXXX, XXX, XXX−XXX

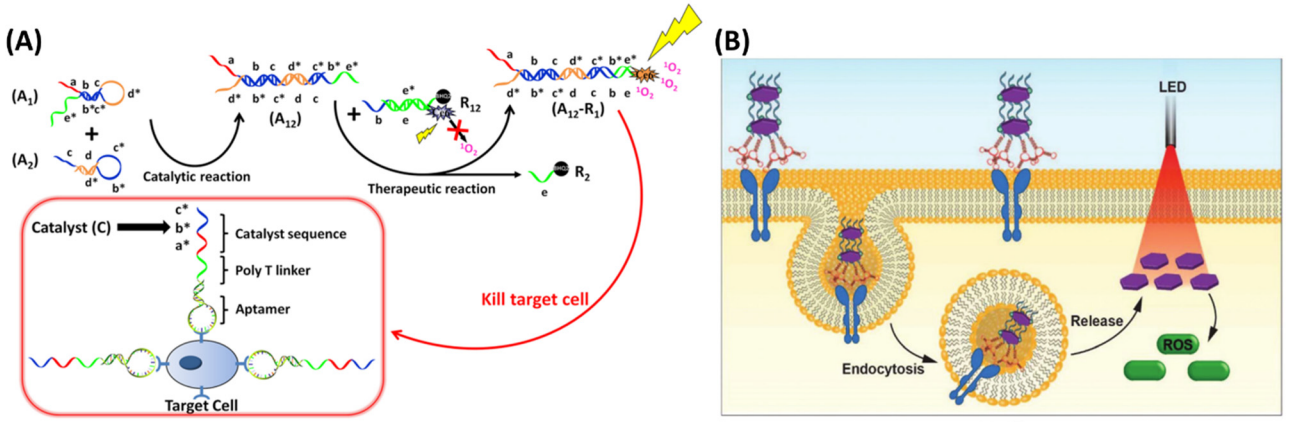

Figure 29. Aptamer-decorated DNA nanostructures for selective photodynamic therapy. (A) Targeted delivery and controllable activation of photodynamic therapy by an aptamer-based DNA nanocircuit. Adapted from ref 363. Copyright 2013 American Chemical Society. (B) Multivalent aptamer-decorated DNA nanostructure for the targeted delivery of methylene blue. Adapted with permission from ref 369. Copyright 2018 Royal Society of Chemistry.

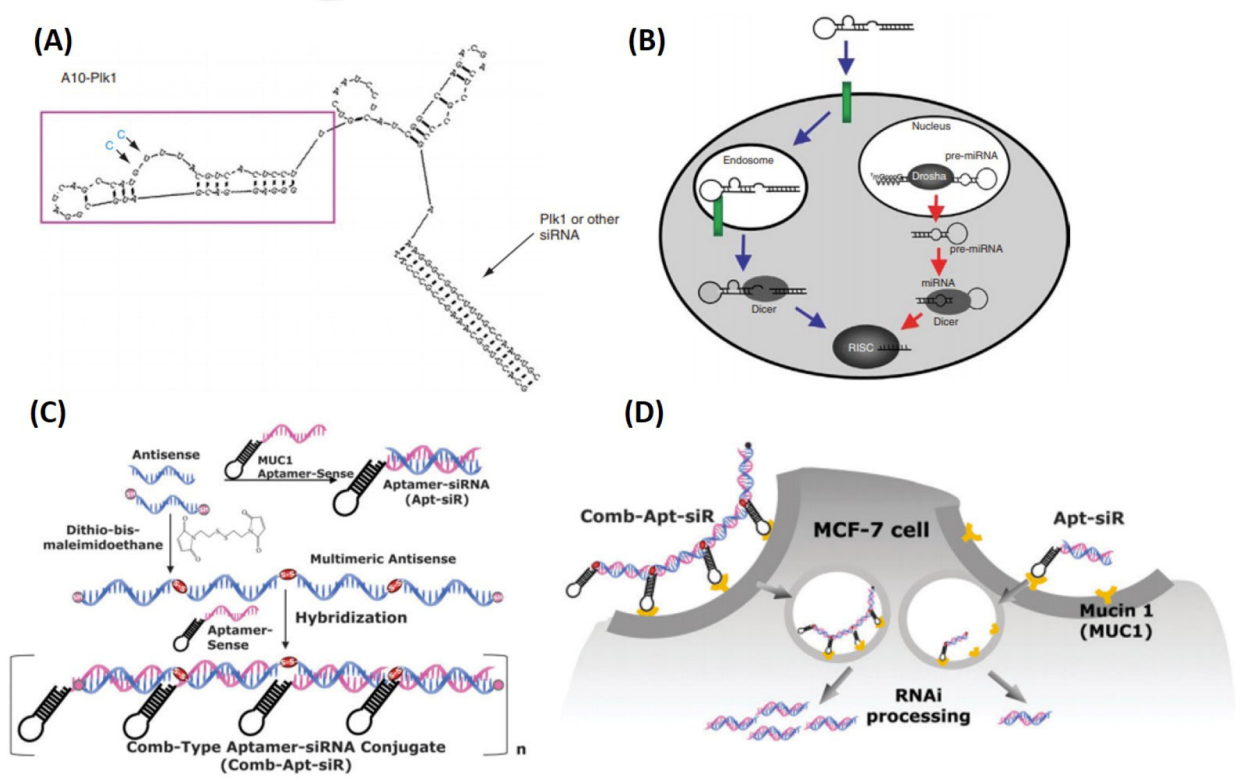

Figure 30. Aptamer–siRNA chimeras. (A) Predicted secondary structure of A10 aptamer–siRNA chimera. The PSMA binding region of the A10 aptamer is outlined in magenta. (B) Endocytosis and RNAi pathway for aptamer–siRNA chimeras (green arrows) compared with endogenous microRNA silencing pathway (red arrows). Adapted with permission from ref 310. Copyright 2006 Springer Nature. (C) Synthesis of multivalent comb-type aptamer–siRNA structure. (D) Cellular uptake of multivalent aptamer–siRNA structure versus single aptamer–siRNA chimera. Adapted with permission from ref 376. Copyright 2014 Royal Society of Chemistry.

damage to cellular components such as lipids, proteins, and DNA, resulting in cell apoptosis and mutation-induced cancers.[359−361] Cell damage caused by ROS can trigger programmed cell death, offering a potential approach for cancer therapy.[362] However, ROS have a short half-life and travel distance, meaning targeted delivery is crucial to achieve effective treatment.

Photodynamic therapy has been used for cancer treatment. To promote cell damage through photodynamic therapy, ROS can be generated by irradiating a photosensitizer. Many research groups have developed methods to selectively deliver photosensitizers by using aptamer-conjugated DNA nanostructures as carriers. In 2013, an aptamer-based DNA circuit was developed to selectively target cancer cells, with controllable activation of the photosensitizer chlorin 6 resulting in amplification of therapeutic effects (Figure 29A).[363] The DNA circuit was composed of two DNA hairpins that did not initially hybridize with each other. In the presence of a catalyst sequence, the hybridization reaction of the DNA circuit was triggered, resulting in activation of the photosensitizer via toehold-

https://doi.org/10.1021/acs.chemrev.0c01332
Chem. Rev. XXXX, XXX, XXX−XXX

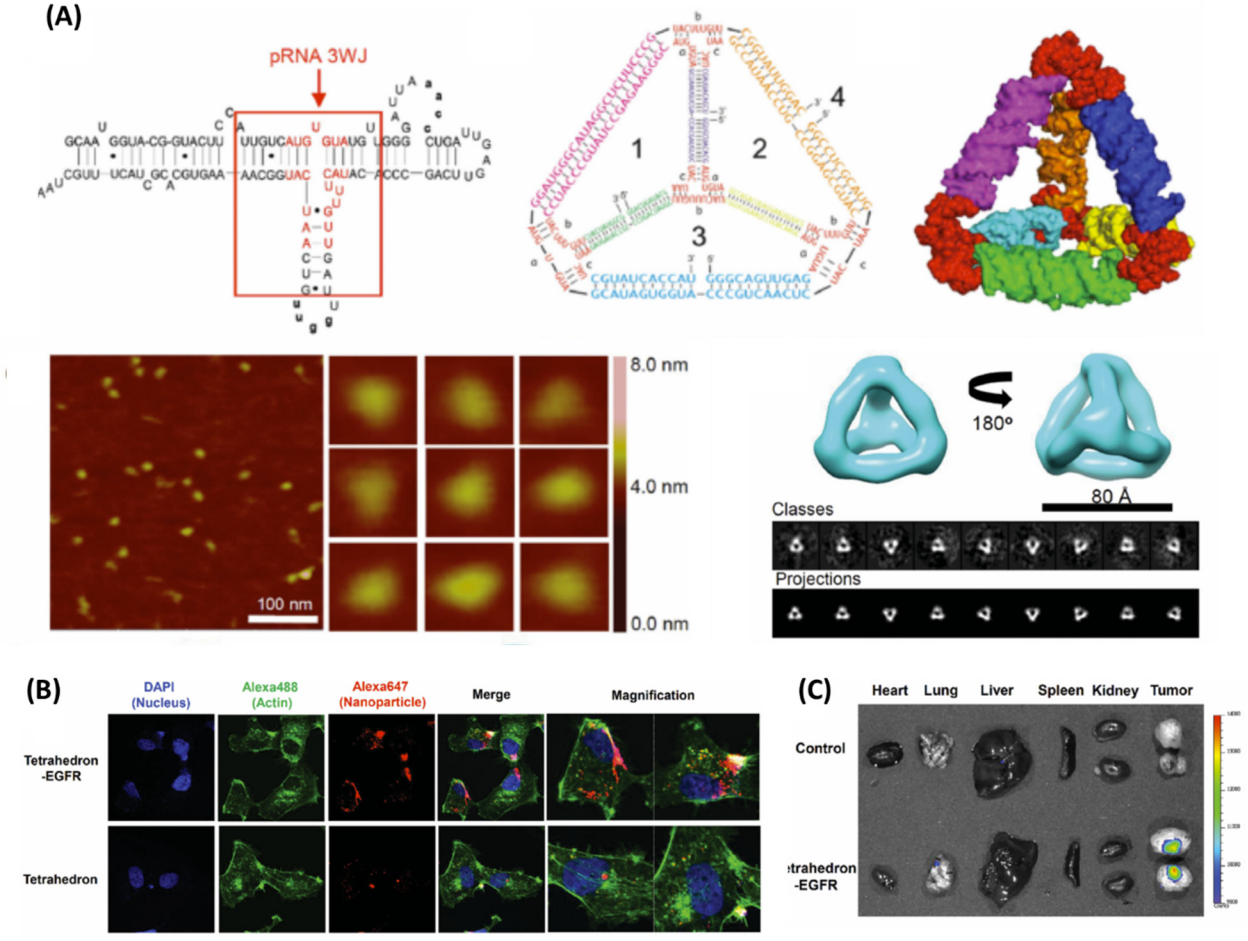

Figure 31. Bacteriophage phi29 pRNA−siRNA chimeras. (A) Bacteriophage phi29 pRNA secondary structure and self-assembled tetrahedral RNA nanostructure. Characterization of tetrahedral RNA nanoparticles using AFM and cryo-EM. (B) Confocal image comparison of cellular binding of RNA tetrahedrons with and without aptamers. (C) Biodistribution assay in tumor-bearing mice after systemic tail vein injection of tetrahedrons both with and without EGFR aptamers. Adapted with permission from ref 379. Copyright 2016 John Wiley and Sons.

meditated strand displacement interactions. Using this method, a high local concentration of ROS, produced via irradiating photosensitizers, occurs only near the target cells and increases the potential of killing the cancer cells.

Methylene blue (MB) is an effective photosensitizer that intercalates with DNA.[364−366] Because of these features, MB-loaded DNA nanostructures have been used for a wide range of applications, from sensing to photodynamic therapy.[367,368] Jin et al. constructed DNA nanostructures as carriers to selective deliver MB to target cancer cells. PTK7-specific DNA aptamers linked with 15 guanines were self-assembled to form stem-like DNA nanostructures via G-quadruplex formation (Figure 29B).[369] MB-loaded DNA nanostructures selectively bound to and internalized into target cells. By light irradiation, ROS were generated via photodynamic effect and killed the cancer cells. In 2018, MUC1 and AS1411 aptamer-decorated tetrahedral DNA nanostructures used as carriers for the anticancer metal complex, $[Ir(ppy_2)phen]^+PF_6$, were constructed by Tian et al.[370] They successfully loaded IrPP into DNA nanostructures via non-covalent interactions. The IrPP-loaded aptamer-DNA nanostructure selectively targeted and was internalized into glioma cells and localized in the cell nucleus. The IrPP metal complex promoted a high level of ROS inside the cells, causing mitochondrial fragmentation and cell apoptosis.

5.2.2. Oligonucleotides. Aptamer-directed nucleic acid nanostructures can be used to deliver therapeutic oligonucleotides, such as siRNAs, miRNAs, DNAzymes, aptamers, and antisense DNAs. Although many oligonucleotides can be delivered using aptamers alone, the addition of nucleic acid platforms allows for the delivery of multiple therapeutic strands using a single aptamer.

5.2.2.1. RNA Interference. RNA interference (RNAi) is the process of promoting mRNA degradation to prevent or minimize translation, also known as gene silencing. RNAi occurs naturally in mammalian cells through the binding of small interfering RNAs (siRNAs) or microRNAs (miRNAs) with mRNA, creating a double-stranded RNA. The double-stranded RNA is processed by degradation enzymes in the cytoplasm, namely, Dicer and RISC.[371] For the RNAi-based down-regulation of gene expression to be successful, the small RNAs must be able to cross the plasma membrane of target cells, survive nuclease degradation, and migrate into the appropriate cell compartments.[372] These requirements are well met by engineered lipid vesicles as one potential solution to help pilot and protect therapeutic RNAs.

In 2006, McNamara et al. developed a solely RNA chimera (Figure 30A) consisting of an A10 aptamer that binds the prostate specific membrane antigen (PSMA) and siRNAs that target mitotic regulator polo-like kinase 1 (PLK1) and apoptosis

https://doi.org/10.1021/acs.chemrev.0c01332
Chem. Rev. XXXX, XXX, XXX−XXX

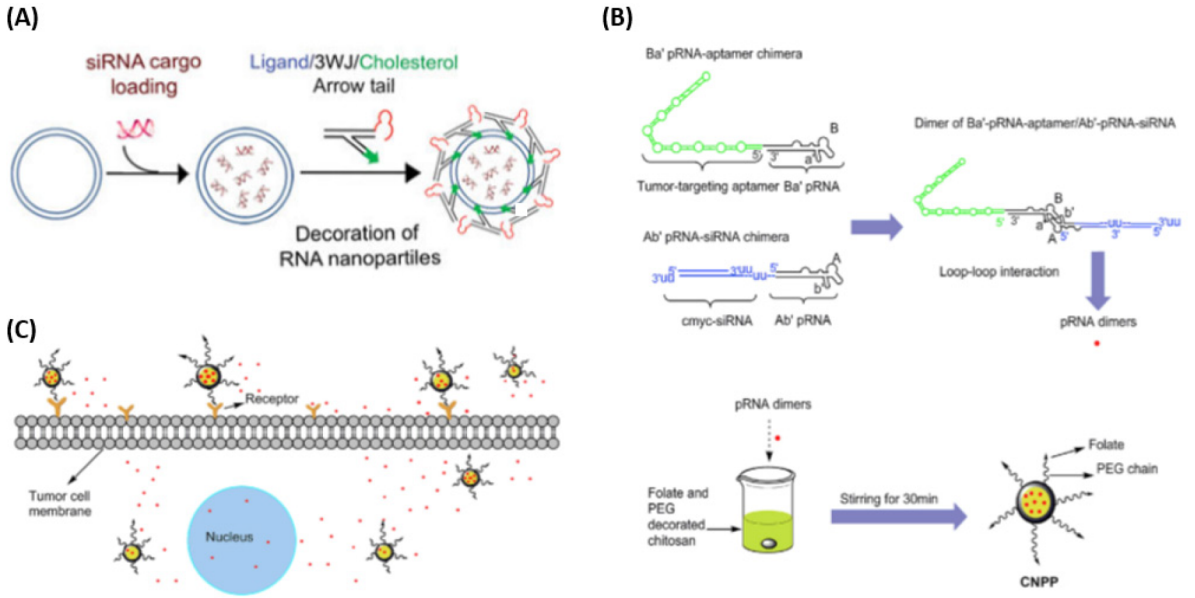

Figure 32. Delivery of aptamer-decorated nucleic acids with non-nucleic acid components. (A) siRNA loading into EVs and display of cholesterol conjugated aptamers. Adapted with permission from ref 382. Copyright 2017 Springer Nature. (B) Preparation of PEGylated chitosan nanoparticles containing pRNA aptamer/siRNA dimers. (C) Cellular delivery of chitosan nanoparticles containing pRNA aptamer/siRNA dimers. pRNA/aptamer dimers released extracellularly enter via receptor-mediated endocytosis or intercellular penetration due to small particle size. Adapted from ref 383. Copyright 2017 Elsevier. Licensed under a Creative Commons agreement (https://creativecommons.org/licenses/by/4.0/).

regulator BCL2.[310] The RNA chimera is able to specifically bind and be endocytosed by target cells before entering the RNAi pathway (Figure 30B). Additionally, the chimera appears to have low immunogenicity and can be chemically modified during production to increase nuclease resistance. Similarly, in 2008, Zhou et al. linked an anti-gp120 aptamer with anti-human immunodeficiency virus (HIV) siRNA.[373] The chimera was found to inhibit HIV replication *in vitro*. The inhibition of HIV was also demonstrated *in vivo* using a CD4 aptamer−siRNA complex.[374] This therapeutic complex was applied intravaginally to humanized mice and protected against HIV vaginal transmission. In 2020, suppression of HER2+ breast cancer was observed in mouse models using aptamer conjugated siRNA to target a protein responsible for the chemoresistance of triple-negative breast cancer.[375] Although these siRNA−aptamer conjugates are useful for targeting specific cellular functions, larger, more complex nucleic acid structures have the potential to increase targeting efficacy and efficiency.

In 2014, Mok's group developed the first multivalent structure that consisted only of aptamers and siRNAs linked by hybridization and chemical conjugation (Figure 30C).[376] The comb-like structure was designed to target cancer cells overexpressing mucin-1 and absorbed intracellularly (Figure 30D). Previous studies showed that endocytosis occurs more rapidly when multiple ligands are locally bound to receptors, so it was predicted that the comb-like aptamer structure would increase cellular uptake. The group found that the structure was absorbed via clathrin-dependent endocytosis and that uptake was greater for the multivalent comb structure compared to mono- or bivalent aptamer−siRNA structures.

Bacteriophage phi29 packaging RNA (pRNA) is a 117-nucleotide motor RNA that dimerizes and assembles into a hexameric ring.[77,96,372] The ring is used to propel the DNA-packaging motor. Using RNA nanotechnology, the pRNA can be arranged into dimers, trimers, and hexamers via hand−hand interactions (Figure 5E,F). The pRNA consists of two independently folding functional domains, a double-stranded helical domain and an intermolecular binding domain. The helical domain can be replaced by other components, such as aptamers or siRNA, allowing the pRNA to function as a delivery vector. In 2005, Guo's group fused pRNAs with either a cancer targeting CD4 aptamer or survivin siRNA, which induces apoptosis.[372] These siRNA and CD4 aptamer conjugated nanostructures were able to dimerize by left- and right-hand loop interactions. The dimer was delivered to CD4+ cells and processed by Dicer, increasing the probability of cell death by 30%. Bacteriophage pRNA dimerization has been utilized for the delivery of a variety of siRNA−aptamer chimeras to inhibit diseases, such as HIV.[377] In 2014, Hao's group developed a bacteriophage phi29 pRNA heterodimer to treat neuro-inflammatory diseases.[378] The heterodimer contained FB4 aptamers for targeted delivery to the transferrin receptor, as well as an siRNA sequence to silence intercellular adhesion molecule-1 (ICAM-1), an important component of the inflammatory response. Guo's group used bacteriophage phi29 pRNA to develop a 3D RNA tetrahedron (Figure 31A).[379] The tetrahedron was decorated with siRNA as well as a cancer targeting aptamer, EGFR. The aptamer-decorated tetrahedron was studied *in vivo* using breast cancer mouse models. Following injection, the tetrahedron−aptamer complexes were found in the breast cancer cells, while the tetrahedrons lacking aptamers were not (Figure 31B). Additionally, biodistribution studies showed that the complex was found in the tumor site but not in other organs, indicating that the method is promising for targeted delivery of 3D pRNA nanostructures to cancer cells (Figure 31C). Zhang et al. used a three-way junction (3WJ) pRNA motif to treat HER2-overexpressing breast cancer cells.[380] The 3WJ combined a HER2 aptamer and siRNA targeting the estrogen receptor alpha cofactor, mediator subunit 1 (MED1). The complex demonstrated specific targeting of HER2 overexpressing cancer cells both *in vitro* and *in vivo*. In addition to siRNA, aptamer/pRNA conjugates can be used to

https://doi.org/10.1021/acs.chemrev.0c01332
Chem. Rev. XXXX, XXX, XXX−XXX

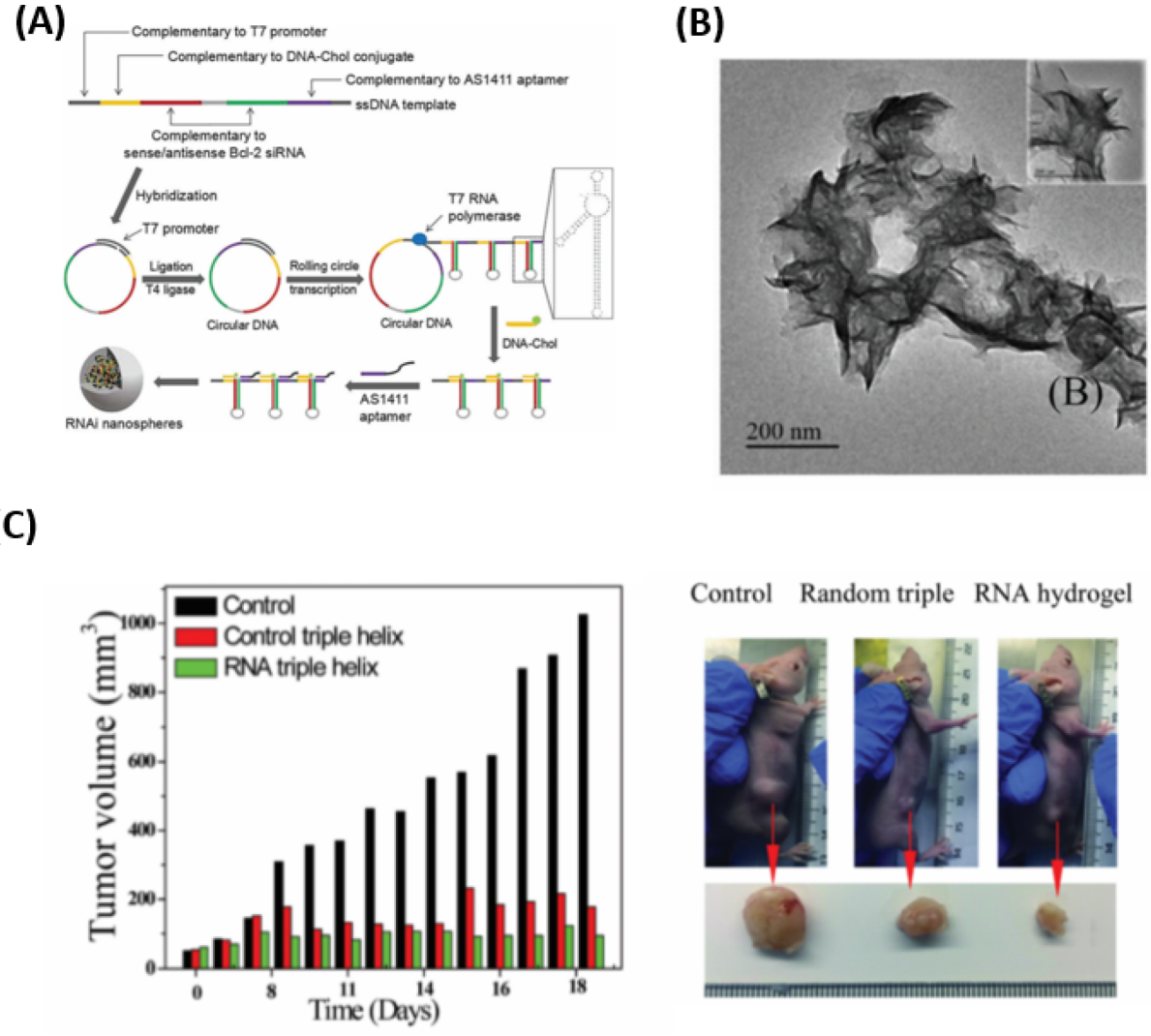

Figure 33. RNAi structures produced by rolling circle transcription. (A) Production of RCT self-assembled RNAi nanospheres. Adapted with permission from ref 111. Copyright 2018 Royal Society of Chemistry. (B) TEM image of RNA transcripts containing miRNAs and aptamer−DNA−cholesterol strands. (C) Volume of tumors after treatment with incubation buffer, triple helix control hydrogel, and therapeutic RNA triple-helix hydrogel over a 19-day period. Tumors removed from mice after 19 days of treatment. Adapted with permission from ref 384. Copyright 2020 Royal Society of Chemistry.

deliver other RNAi agents, such as miRNA and locked nucleic acids.[83,381]

Aptamer-mediated RNA nanostructures have also been conjugated to other delivery vehicles, such as extracellular vesicles (EVs), to enhance their function. EVs can cross cell membranes via natural routes such as endocytosis, making them promising candidates for cellular delivery. However, once inside the cell, EVs are not target specific. In 2018, Pi et al. combined extracellular vesicles with 3WJ pRNA motifs that contained both cancer-targeting aptamers and cholesterol to create a target specific vesicle that could easily enter cells.[382] The cholesterol autonomously merged with the surface of the EV and was used as an anchor for the 3WJ/aptamer construct. Furthermore, the cancer targeting aptamers faced outward at angles controlled by the pRNA 3WJ, making the vesicle target specific (Figure 32A). Vesicles loaded with survivin siRNA were shown to be effective in targeting a variety of cancer cells both *in vitro* and *in vivo*, demonstrating how aptamer-guided nucleic acid nanostructures can increase the efficacy of *in vivo* delivery systems. In addition, chitosan is considered an apt *in vivo* carrier due to its positive charge, biocompatibility, and available chemical modifications; however, it is limited in its ability to deliver contents intracellularly. Li et al. created a dual delivery system consisting of folate-conjugated and PEGylated chitosan nanoparticles containing pRNA aptamer/siRNA dimers (Figure 32B).[383] The outer chitosan shell was used to protect the pRNA contents and bring the nanoparticle near target cells. The nanoparticles could then be endocytosed, or the contents diffused out near the cell surface (Figure 32C). It was shown that the released contents could be delivered intracellularly via receptor mediated endocytosis. This demonstrates the potential that aptamer-guided nucleic acid nanostructures have for enhancing the efficiency of established intracellular delivery systems.

Many RNAi studies have focused on the development of delivery vesicles, many of which introduce reagents, particularly polycationic reagents, that can have unwanted immune or toxic effects. In 2018, Pei and colleagues developed a new approach: creating clusters of siRNA that functioned as both the therapeutic agent and nanovesicle.[111] The group used rolling circle transcription (RCT) to create siRNA microspheres, which

https://doi.org/10.1021/acs.chemrev.0c01332
Chem. Rev. XXXX, XXX, XXX−XXX

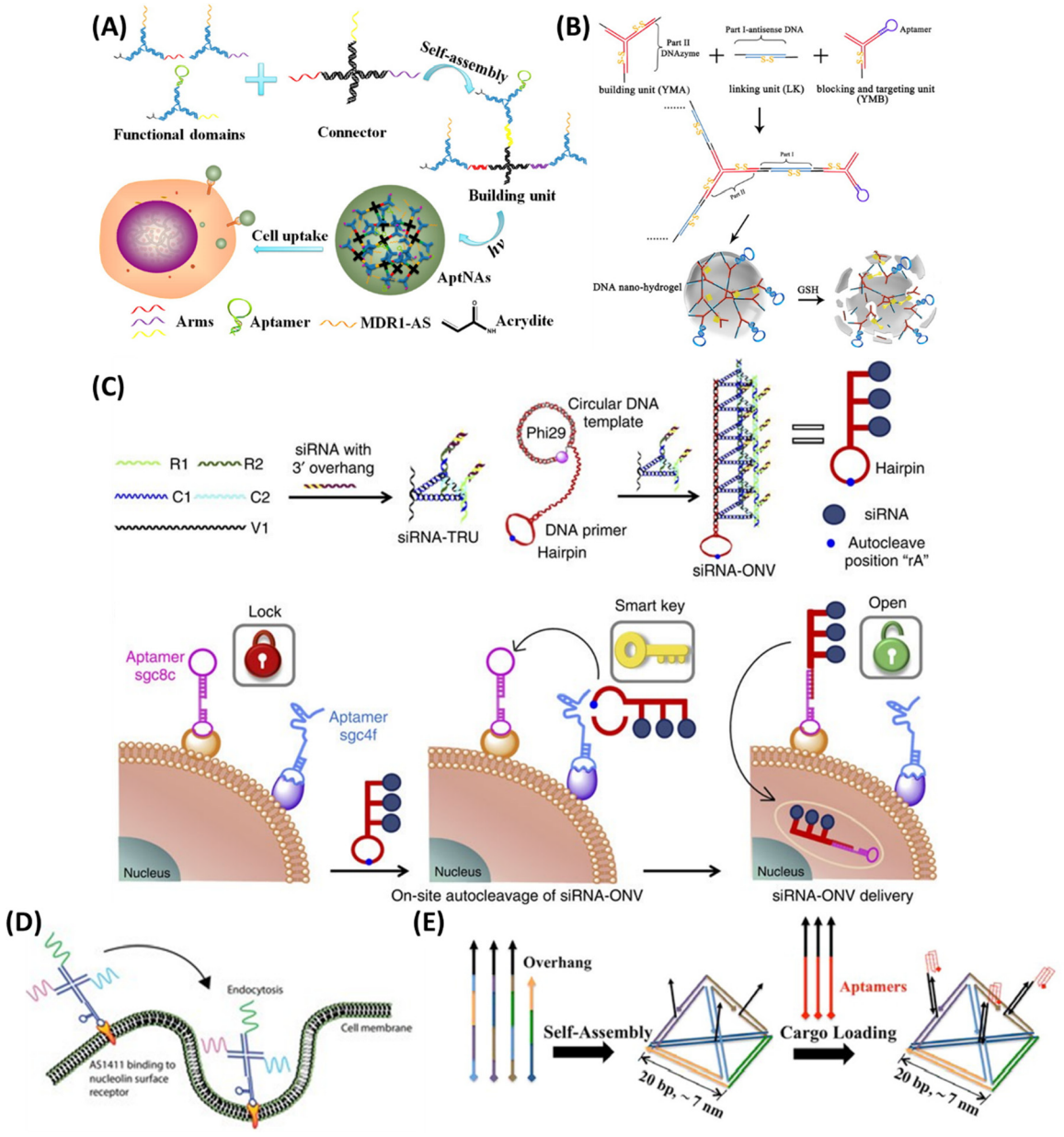

Figure 34. Aptamer decorated DNA nanostructures for oligonucleotide delivery. (A) Illustration of aptamer-based DNA nanoparticle assembled via self-assembly and photo-cross-linking. Adapted from ref 385. Copyright 2013 American Chemical Society. (B) Construction of a stimuli-responsive DNA nanohydrogel. Adapted from ref 386. Copyright 2015 American Chemical Society. (C) Schematic of aptamer lock and hairpin key activated by cell surface markers. Adapted from ref 387. Published 2016 Springer Nature. Licensed under a Creative Commons agreement (https://creativecommons.org/licenses/by/4.0/). (D) Holliday junction DNA nanoconstruct mode of transfection. After entering cells, the construct disassembles into its subsequent parts. Adapted from ref 388. Published 2017 Springer Nature. Licensed under a Creative Commons agreement (https://creativecommons.org/licenses/by/4.0/). (E) Self-assembly of pyramidal DNA nanostructures. Overhangs allow for the addition of aptamers along three pyramid edges. Adapted from ref 392. Copyright 2014 American Chemical Society.

were packed into nanospheres using cholesterol-modified DNA and functionalized with AS1411 aptamers (Figure 33A). With this method, large amounts of RNAi agents can be delivered specifically to target cells using only nucleic acid components, resulting in minimal immunogenicity and cytotoxicity. In 2019, Zhang and colleagues developed a self-assembling RNA-triple-helix hydrogel, free of polycationic reagents, to deliver RNAi components for breast cancer therapy.[384] The triple helix consisted of two antitumor miRNA sequences and siRNA duplexes embedded into the RNA hydrogel. The therapeutic hydrogel was characterized by TEM (Figure 33B), tested *in vivo*, and compared to a control (incubation buffer) and a random triple-helix hydrogel. As shown in Figure 33C, the therapeutic RNA hydrogel significantly limited tumor growth *in vivo* and showed no signs of toxicity or side effects.

In addition to RNA nanostructures, aptamer-based DNA nanoassemblies have also been reported to aid in RNAi therapies. In 2013, Wu et al. developed an aptamer-based DNA nanoparticle to target leukemia cancer cells.[385] Y-shaped functional DNA domains were constructed using base pair hybridization and combined with targeting aptamers, intercalated anticancer drugs, and antisense sequences. The Y domains were linked using an X-shaped DNA connector. These units were modified with 5′ acrydite groups and photo-cross-linked to

https://doi.org/10.1021/acs.chemrev.0c01332
Chem. Rev. XXXX, XXX, XXX−XXX

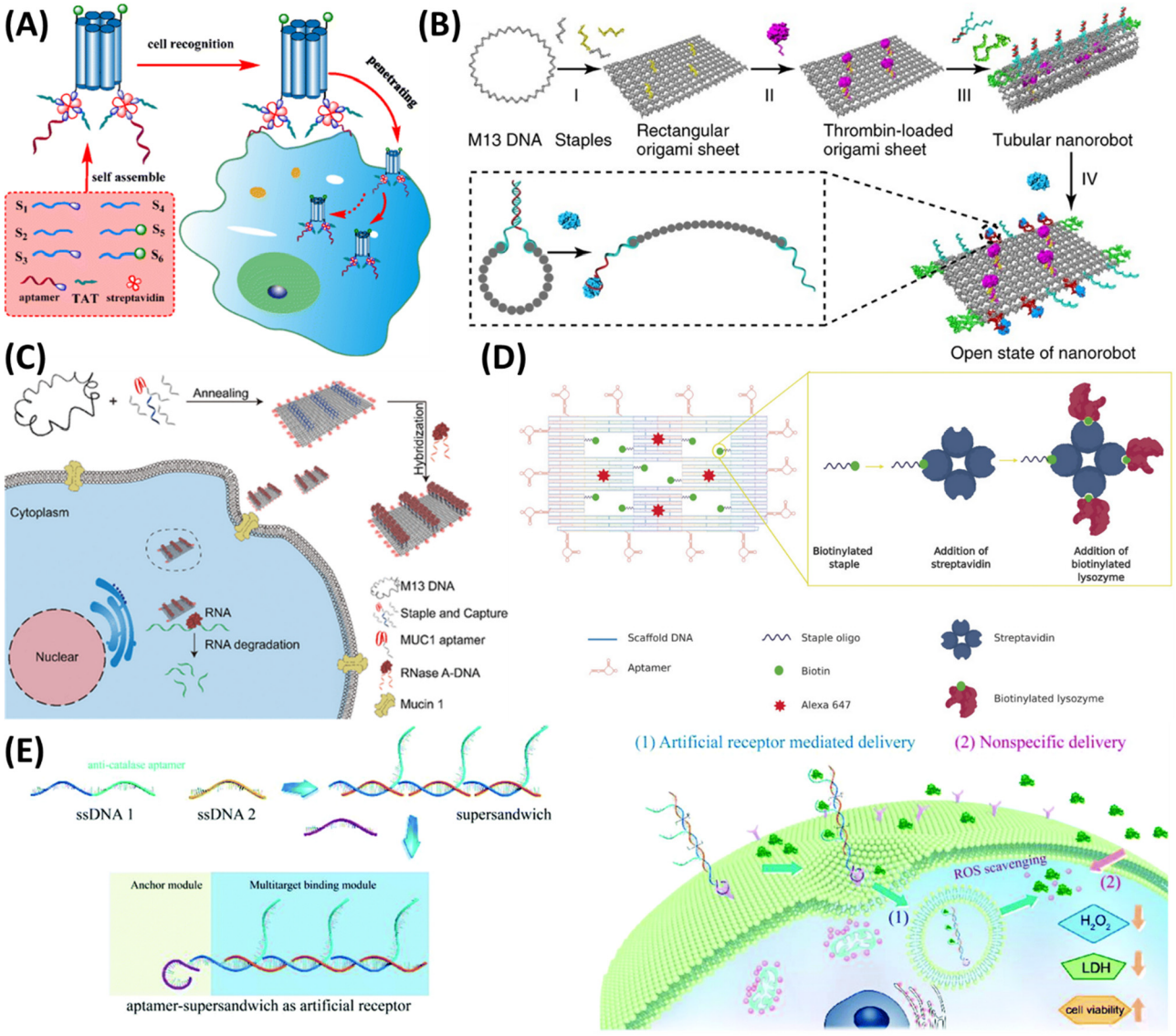

Figure 35. Targeted delivery of therapeutic proteins using aptamer-guided DNA nanostructures. (A) CPP-functionalized DNA nanopore guided by Ramos cell targeting aptamer. Adapted with permission from ref 394. Copyright 2017 Springer Nature. (B) Synthesis and unfolding of tubular DNA nanorobot loaded with thrombin. Adapted with permission from ref 395. Copyright 2018 Springer Nature. (C) DNA nanosheet decorated with MUC1 aptamers to carry RNase A. Adapted from ref 396. Copyright 2019 American Chemical Society. (D) Aptamer-decorated DNA nanosheet consisting of 5 internal wells for antibacterial components. Adapted from ref 397. Published 2020 Wiley-VCH Verlag GmbH & Co. KGaA, Weinheim. Licensed under a Creative Commons agreement (https://creativecommons.org/licenses/by/4.0/). (E) DNA supersandwich used as an artificial receptor for catalase proteins. Adapted with permission from ref 398. Copyright 2019 Royal Society of Chemistry.

create 3D nanoparticles (Figure 34A). The nanoparticles demonstrated multifunctionality, programmability, biostability, and biocompatibility while also having targeted cytotoxicity for leukemia cells. DNA hydrogels are yet another method that has shown potential for drug delivery and immunotherapy applications; however, the bulky size of these hydrogels have limited their practical use. In 2014, Li et al. reported a size-controllable and stimulus-responsive DNA nanohydrogel decorated with aptamers for targeted gene delivery.[386] The hydrogel consists of three DNA building units, seen in (Figure 34B), that link via sticky-end hybridization. The ratio of the building units can be used to control the size of the hydrogel.

Many cell targeting therapies focus on the binding of one cell receptor to induce release or endocytosis of therapeutics, such as siRNA. Most target cells, such as cancer cells, overexpress certain types of surface markers; however, many of these markers are also expressed in lower concentrations on normal cell surfaces, creating the possibility of off-target delivery. To combat this problem, Ju and colleagues created the first reported siRNA delivery method requiring participation of multiple cell membrane receptors by assembling a dual lock-and-key system.[387] The system consists of aptamer "locks" and a hairpin "key" that is activated by two cell surface markers prior to siRNA delivery. The hairpin "key" must be sequentially activated by aptamers bound to surface receptors and can then enter target cells (Figure 34C). In 2017, Tung et al. used a DNA Holliday junction to link three siRNA strands with an AS1411 cell-targeting aptamer (Figure 34D).[388] The siRNA strands were used to induce apoptosis in triple negative breast cancer cells, and reduced cell viability by approximately 82% within 24 h. Similarly, Jeong et al. used the DNA Holliday junction to create a radially symmetric aptamer−siRNA structure.[389] The structure

https://doi.org/10.1021/acs.chemrev.0c01332
Chem. Rev. XXXX, XXX, XXX−XXX

consists of a Holliday junction at the center, siRNA at each of the four junctions, and MUC1 aptamer caps on each strand. The Holliday−aptamer−siRNA structures proved superior to aptamer−siRNA duplexes in cellular uptake and gene silencing.

Although RNAi is a promising therapeutic for many diseases, few RNAi agents have been approved by the FDA due to the poor properties of bare RNAi agents.[390] A key challenge for clinical application of RNAi therapy is delivery specificity. The addition of aptamer-directed nucleic acid nanostructures provides degradation protection and targeting efficiency without compromising biocompatibility, increasing the viability of RNAi agents in clinical settings.

5.2.2.2. Gene Therapy. Mutations in the p53 tumor suppressor gene occur in approximately 50% of tumors of all cancer types. Gene therapies have been used to deliver corrected versions of the p53 gene, but delivery of the gene without inducing an immune response remains a challenge. In 2018, Ding's group constructed a self-assembled DNA nanokite led by aptamers to deliver p53 genes, as well as potential anticancer drugs.[350] The DNA kite was shown to achieve gene delivery and inhibit tumor growth both *in vitro* and *in vivo*. This structure design provides a general method for delivery of gene therapies and drugs that could be used to treat a wide range of disease.

5.2.2.3. DNAzymes. Deoxyribozymes (DNAzymes) are self-folding, single-strand DNA molecules that can catalyze specific reactions with other nucleic acid targets. DNAzymes are more stable, easier to produce, and less expensive than other targeting agents such as siRNA, ribozymes, or antisense oligonucleotides; however, to be effective DNAzymes need a targeted delivery system. In 2015, Krishnakumar's group developed a delivery method for survivin DNAzymes using AS1411 aptamers and poly-T linkers.[391] Their chimera was found to internalize specifically into cancer cells and was particularly useful for inducing apoptosis in retinoblastoma cells, which are responsible for most childhood eye cancers.

5.2.2.4. Aptamers. Targeting aptamers not only can be used to aid in the delivery of other therapeutic aptamers but also can act simultaneously as therapeutic aptamers themselves. For example, in 2014 Charoenphol and Bermudez developed DNA pyramids displaying the AS1411 aptamer, which were shown to both act as a delivery aptamer and decrease HeLa cell viability (Figure 34E).[392] Additionally, AS1411 has been shown to escape degradation in cancer cells but be degraded by regular pathways in noncancerous cells. Based on trends observed in the uptake of AS1411-pyramids, the nanostructures are predicted to follow the same trend in uptake as AS1411 aptamers, but further investigation of the uptake pathways and intracellular effects of the decorated pyramids was needed. In 2017, Lin's group further investigated the effect of AS1411-tetrahedral DNA nanostructures (Apt-TDNs) on both cancerous and normal cells under hypoxic conditions.[393] The group confirmed that the Apt-TDNs inhibited tumor cells and promoted cell growth of normal cells in hypoxic conditions. The Apt-TDNs were also found to enter tumor cells more regularly than normal cells, suggesting high potential for delivering anticancer drugs as well.

Nucleic acid nanostructures as a whole are useful as vehicles *in vivo* due to their programmable self-assembly into compact structures and excellent biocompatibility, but it is important to note that these structures often have lackluster cellular uptake due to their dependence on passive delivery or the enhanced permeability and retention effect. The addition of targeting aptamers onto nucleic acid assemblies creates targeted therapies with the potential to attach to and enter cells via active methods such as receptor mediated endocytosis, enhancing the therapeutic power of the delivered cargos and limiting off-target damage.

5.2.3. Peptides. A DNA nanopore functionalized with a Ramos cell-targeting aptamer and cell-penetrating peptide (CPP) was constructed.[394] CPPs have been shown to increase cellular uptake via pinocytosis, but this uptake is not cell-specific; for this reason, aptamers were used to specifically target the Ramos cells (Figure 35A). The dual-functional DNA nanopore was shown to have high cellular uptake specifically in Ramos cells, while DNA nanopores functionalized with only CPP did not show specificity for Ramos cells. This cell-specific DNA nanopore is a promising platform for targeted delivery of drugs that have harmful off-target effects. Additionally, multiple aptamers could potentially be added to steer the internalized nanopore for specific organelle delivery.

5.2.4. Proteins. Protein therapy is the delivery of proteins to achieve a desired biological effect and can be used to treat many diseases; however, intracellular delivery of proteins is difficult because there are not many pathways by which proteins themselves can cross cell membranes. However, DNA nanostructures can be used to carry large payloads, such as proteins, across membranes. DNA nanorobots are self-assembling DNA nanostructures that have been transformed into mechanical devices to serve a variety of roles, such as delivery vesicles and probes. In 2018, Zhao and colleagues demonstrated the first DNA nanorobot for targeted delivery and controlled release in mammals.[395] The group created a tubular DNA origami with thrombin proteins loaded in the inner cavity and aptamers targeting nucleolin on the outer surface (Figure 35B). In the presence of nucleolin, the tube unfolds, exposing the thrombin, and clotting is induced. The robot was tested in both mice and miniature pigs and proven to induce necrosis in cancerous tumors without compromising healthy tissue in the animals. The group also tested a targeted nanotube, a tube decorated with nucleolin aptamers that does not unfold, and a nontargeted nanotube that lacked aptamers. The targeted nanotube demonstrated weak thrombotic activity due to the lack of thrombin exposure and the nontargeted aptamer showed little to no activity at the tumor site. This highlights the importance of both the presence of aptamers for targeted delivery of nucleic acid nanostructures, and the importance of the nanostructure design itself for effective cellular protein delivery. In 2019, Jiang and Ding used a static DNA origami nanosheet to deliver RNase A into cancer cells to induce cell death.[396] The nanosheet was decorated with MUC1 aptamers along the edges, and RNase proteins were attached to the face of the nanosheet using hybridized DNA strands (Figure 35C). The therapeutic nanosheet was successful in inducing cell death in human breast cancer cells *in vitro*; however, neither *in vitro* nor *in vivo* effects on healthy cells were studied. In comparison with the DNA nanorobot produced by Zhao, the nanosheet structure is more likely to have off-target complications due to the constant exposure to RNase in the surrounding environment prior to binding with target cells. In 2020, Mela et al. used aptamer functionalized DNA origami nanostructures as delivery vehicles for lysozymes to bacterial cells.[397] The origami structure resembled the aptamer-decorated nanosheet presented by Jiang and Ding, with the addition of five wells in the interior of the sheet to carry antibacterial components (Figure 35D). The structure used aptamers that were able to target both Gram-positive and Gram-negative bacteria. It was shown that the origami-delivered antibacterial enzyme lysozyme was more

https://doi.org/10.1021/acs.chemrev.0c01332
Chem. Rev. XXXX, XXX, XXX−XXX

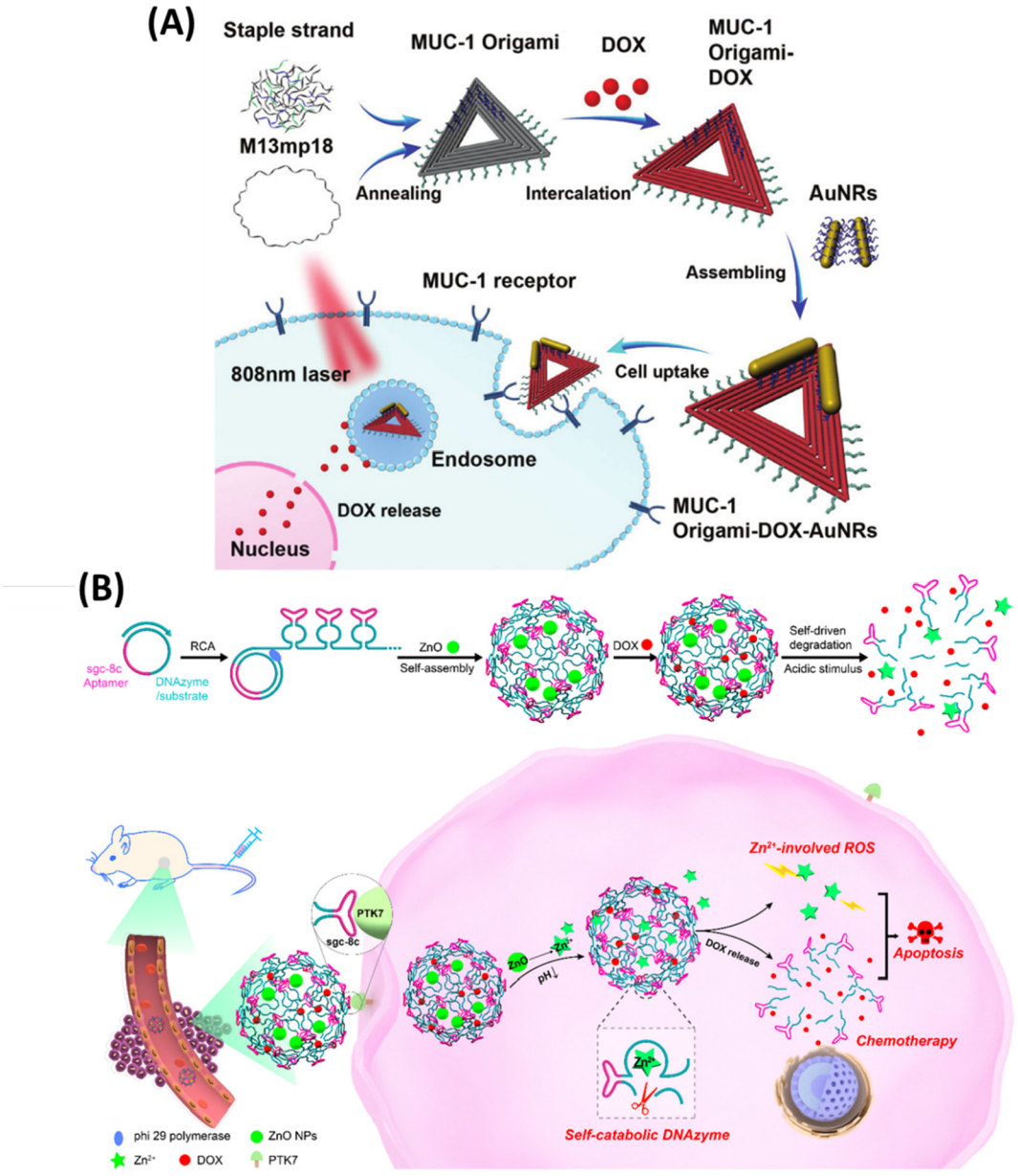

Figure 36. Targeted delivery of aptamer−DNA nanostructure for inorganic nanomaterial delivery. (A) DOX and gold nanorods decorated on an aptamer−DNA nanotriangle for photothermal therapy and chemotherapy. Reprinted with permission from ref 349. Copyright 2017 Royal Society of Chemistry. (B) Dual delivery of ZnO and DOX-embedded DNA nanoparticles. Reprinted from ref 343. Copyright 2019 American Chemical Society.

effective than free lysozyme in killing Gram-positive bacteria. It was also shown that the aptamer-decorated origami without lysozyme had antimicrobial properties against Gram-negative bacteria. However, lysozyme was found to be relatively ineffective on Gram-negative bacteria due to the presence of an outer lipid membrane, at least partially explaining why the presence of lysozyme on the origami did not increase antibacterial activity. For future studies on the effect of targeted delivery to Gram-negative bacteria, it may be necessary to use an antibacterial agent that naturally inhibits the growth of the bacteria in order to clearly see the effects of the novel delivery system.

Rather than using DNA nanostructures directly for drug delivery, Liu and Wang used a DNA supersandwich assembly as an artificial receptor to enable protein transfection.[398] The supersandwich consisted of an anchor domain for embedding in the cell membrane and catalase aptamers for recruitment of catalase, a protein enzyme that protects cells from peroxide damage (Figure 35E). Laser scanning confocal microscopy confirmed cellular uptake of the DNA−catalase complexes and suggested that the DNA was endocytosed via a transferrin receptor (TfR)-involved route. This method demonstrated that using aptamer-based DNA nanostructures as artificial receptors locally concentrates naturally present proteins rather than delivering loaded protein cargos, eliminating the need to introduce foreign proteins into living organisms during protein therapy.

5.2.5. Inorganic Nanomaterials. Many cancer cells require a very high dose of chemotherapeutic anticancer drugs for treatment due to multidrug resistance. However, a high level of chemotherapeutic drug will cause additional unwanted cytotoxicity for healthy cells, highlighting the need for more effective

https://doi.org/10.1021/acs.chemrev.0c01332
Chem. Rev. XXXX, XXX, XXX−XXX

therapeutic methods. Delivery of functional inorganic nanomaterials using the organizational and targeting abilities of self-assembled DNA nanostructures represents a possible path forward. Gold nanorods are promising nanomaterials for photothermal cancer therapy due to their tunable and strong localized surface plasmon resonance.[399,400] In 2017, Ding developed multivalent MUC1 aptamer-conjugated triangular DNA origami for the co-delivery of therapeutic agents to treat multidrug-resistant cancer cells (Figure 36A).[349] Chemotherapeutic drugs were loaded into DNA nanostructures while ssDNA-modified gold nanorods were decorated on the triangular DNA origami through DNA/DNA hybridization. The dual delivery of aptamer−DNA origami was internalized into target cells and irradiation with near-infrared laser light activated the photothermal effect of gold nanorods. It was found that the expression of P-glycoprotein, a pump found in drug-resistant tumors, was downregulated.[401] This dual delivery system thus provides an effective approach to treat multidrug-resistant cancers.

Cellular free Zn^{2+} is important for many cellular functions. However, high concentrations of cellular free Zn^{2+} can cause cell death due to the excessive accumulation of intracellular ROS.[402−404] In 2019, Wang developed RCT-based DNA nanoparticles for the dual delivery of zinc oxide nanoparticles (ZnO) and DOX (Figure 36B).[343] The DNA nanoparticle carrier contained targeting aptamers and a self-catalytic DNAzyme that served as a controlled releasing unit. The ZnO- and DOX-containing multivalent aptamer nanoparticles showed effective delivery to target cells. In the acidic conditions inside lysosomes, dissolution of ZnO occurs, releasing Zn^{2+}, a cofactor for DNAzyme and promoting ROS production. The Zn^{2+}/DNAzyme complex promoted DNA nanoparticle cleavage and resulted in release of DOX and production of ROS, resulting in cell apoptosis.

5.2.6. Multicomponent Platforms. A major advantage of using aptamer-conjugated nanostructures rather than stand-alone aptamers is the opportunity to deliver multiple components with one targeted platform. Many combinations of therapeutic agents have been delivered using aptamer−DNA nanoconstructs to target cancer cells. Chemotherapy drug resistance is a major cause of cancer treatment failure, so most treatments consist of a "cocktail" of drugs to circumvent the drug resistant nature of cancer cells. It follows that combining multiple therapeutic agents onto a single targeted treatment platform would prove beneficial in treating cancer. For example, DNA nanoplatforms have been developed to deliver cancer drugs in tandem with oligonucleotides such as shRNA,[405] antisense oligos,[406] therapeutic genes,[350] therapeutic aptamers,[407] peptides,[408] and ROS-producing nanoparticles.[343] Liu and Ding developed a DNA tetrahedron to induce apoptosis using both antisense oligos and a protein drug for photodynamic therapy.[409] RNA nanostructures have also been developed to specifically deliver multiple cancer therapeutics at once to lessen the effect of drug resistance. In 2005, a pRNA trimer was used to deliver two targeting aptamers along with a siRNA,[410] and in 2014, an RNA nanoring was created that contained 6 "arms" that could house a variety of therapeutics, including aptamers and RNAi sequences.[93] These applications indicate that using aptamer decorated nucleic acid nanostructures to co-deliver both traditional cancer drugs and other therapeutic molecules can greatly enhance therapeutic efficacy by utilizing both targeted delivery and multiple treatment combinations.

Another approach to circumvent cancer cell drug resistance is to downregulate protein pumps that expel drugs from the cell. A DNA origami nanostructure decorated with a MUC1 aptamer, gold nanorods, and DOX followed this approach by utilizing the photothermal inhibiting effects of the gold nanorods while simultaneously delivering DOX to the targeted cancer cells.[349] The simultaneous, targeted delivery of these cargos ensures that the proper cells are targeted and that protein pumps continue to be downregulated while chemotherapeutic drugs are present in the cell.

Taking advantage of the combined benefit of nucleic acid nanostructures and aptamers, many strategies for the development of aptamer-decorated nucleic acid nanostructures have been successfully demonstrated and utilized for the selective delivery of a wide range of therapeutic agents including chemotherapeutic anticancer drugs, oligonucleotides, peptides and proteins, and photodynamic and photothermal therapeutic agents. To achieve high efficiency treatment with targeted delivery, there are many aspects that must be considered when using nucleic acid nanostructures as drug carriers such as drug−nucleic acid compatibility, loading capacity, stability in physiological conditions, internalization and cellular uptake, toxicity, blood half-life, and undesired immunogenicity. To conjugate therapeutic agents, such as proteins, chemotherapeutic drugs, and nanomaterials, into DNA nanostructures, Gothelf's and Medintz's group have recently published a review article that provides information on drug/DNA nanostructure conjugations.[195,411]

There are many systemic and intracellular barriers that must be overcome for the successful delivery of nucleic acid therapeutics. Poor cellular uptake can cause lack of therapeutic effect; therefore, methods have been established that aid in cellular delivery of nucleic acids. These methods include, but are not limited to, controlling particle size and charge, lipid particle encapsulation, and viral delivery. One of the many factors that influences cellular uptake and the stability of nanostructures under physiological conditions is the size and shape of the nucleic acid nanostructures. The stability and internalization of various nucleic acid nanostructures have been studied and previously reviewed.[250,411−414] Chemical modifications of RNA nanostructures have helped to significantly improve stability of the RNA nanostructures in biological environments.[412,415] Furthermore, size and surface functionalization of nanostructures play important roles in biodistribution and the circulation half-life of nanoparticles.[416,417] Small particles below 10 nm are swiftly removed from the body via kidney clearance, while large particles (100−200 nm) are cleared by the spleen and reticuloendothelial system;[416,418] therefore, surface modified nanostructures of the optimal size and shape are crucial to increase circulation lifetimes.

The immune and inflammatory systems help protect the body from invaders such as pathogens and viruses. Although nucleic acids are natural biopolymers, nucleic acids appearing at wrong locations inside the body can stimulate immune responses and activate inflammatory reactions. Exogenous nucleic acids, unnatural nucleic acid nanostructures, and virus-inspired nanostructure designs (pRNA) can potentially contribute to the activation of immune and inflammatory responses. To avoid this problem, chemically modified nucleotides offer a reduction in immune response activation.[419,420] Krishnan has summarized how cells respond to exogenous or endogenous DNA to understand and provide insight for the design of DNA nanostructures with immune-compatibility.[421] Recently, Afonin

https://doi.org/10.1021/acs.chemrev.0c01332
Chem. Rev. XXXX, XXX, XXX−XXX

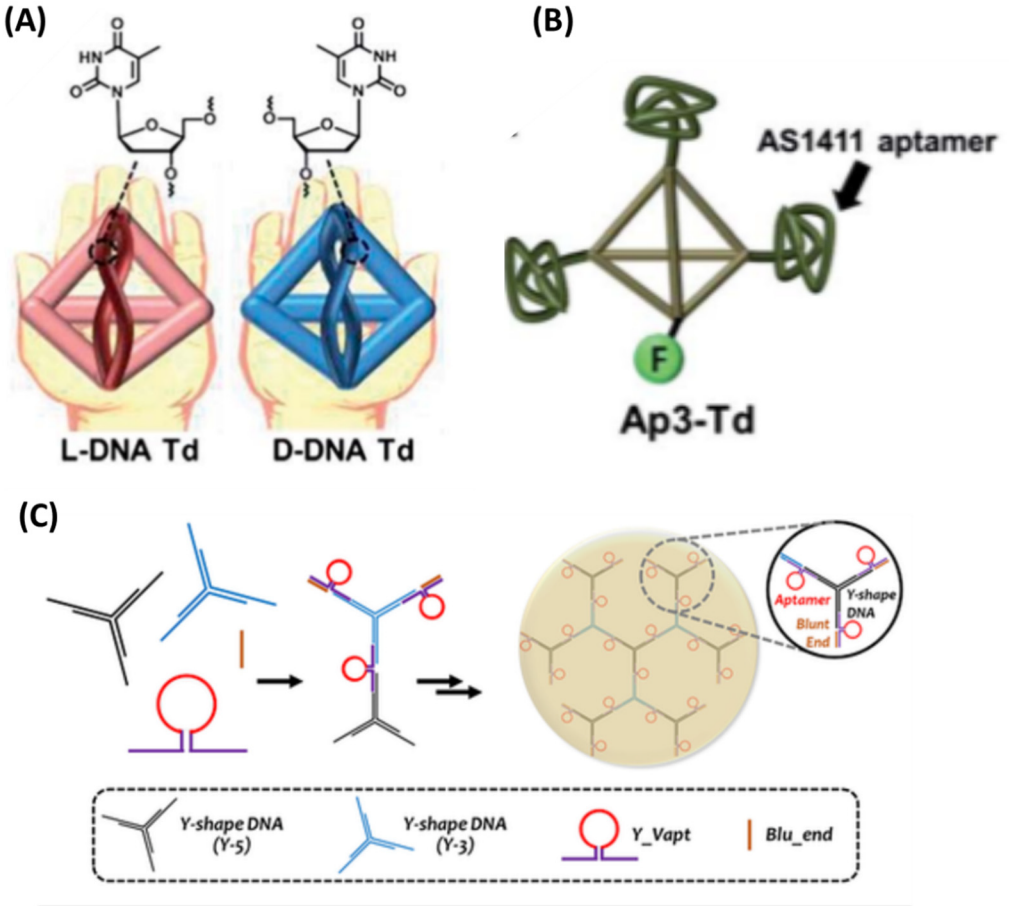

Figure 37. Aptamer-based nucleic acid nanostructure cancer therapy. (A) Depiction of L-DNA tetrahedral nanostructure mirror form versus D-DNA tetrahedral nanostructure native form. (B) Illustration of DNA tetrahedron decorated with multivalent AS1411 aptamers. Adapted from ref 424. Published 2014 Royal Society of Chemistry. Licensed under a Creative Commons Attribution-NonCommercial 3.0 Unported License (https://creativecommons.org/licenses/by-nc/3.0/). (C) Schematic of antiangiogenesis aptamer-decorated DNA construct. Sticky-ends are used to polymerize the network, while blunt ends are used to protect the construct from enzymatic degradation. Adapted with permission from ref 427. Copyright 2018 John Wiley and Sons.

also published a review article describing how different sizes and shapes of nucleic acid nanostructures are associated with varying degrees of immune stimulation.[422]

In summary, aptamer decorated nucleic acid nanostructures are a promising method for targeted delivery, but to achieve effective targeted delivery, optimal designs and surface functionalization of the nucleic acid nanostructure-based nanocarriers are crucial.

5.3. Therapeutics

In addition to being used as targeting agents, aptamers can be used as therapeutic agents to treat a range of diseases and disorders, including eye disorders, thrombosis and vascular disease, and cancer.[140] The placement of aptamers on nucleic acid nanostructures has overcome many pharmacokinetic challenges associated with stand-alone aptamer therapeutics, such as renal filtration and metabolic instability. Additionally, nucleic acid structures can function as carriers for molecular cargos or as the cargo itself to be delivered. Delivery of therapeutic nucleic acid cargos using nucleic acid nanocarriers is a promising method due to their ability to self-assemble into one structure without the use of additional conjugation chemistry. In this section, we will cover four main therapeutic applications for aptamer-decorated nucleic acid nanostructures: cancer therapies, anticoagulants, viral inhibition, and neurodegeneration.

5.3.1. Cancer Therapy. For cancer therapy applications, most nucleic acid aptamers have been utilized as targeting agents for the delivery of chemotherapeutic drugs.[423] Some aptamers can be used as both targeting agents and therapeutic agents such as the AS1411 and C2NP aptamers. There are several approaches for aptamer-based cancer therapy including antiproliferation, antiangiogenesis, aptamer-induced cell apoptosis, and immunotherapy. In this section, we focus on therapeutic aptamers decorated on nucleic acid nanostructures for cancer therapy.

5.3.1.1. Antiproliferation. One way to combat cancer growth is to inhibit proliferation of cancer cells using antiproliferation therapeutics. Ahn's group reported an antiproliferation system using nucleic acid nanostructures as carriers and aptamers as cargo, creating a tetrahedral DNA nanocarrier for delivery of the AS1411 antiproliferative aptamer.[424] This aptamer binds with nucleolin, a cell-surface protein that is overexpressed on rapidly growing cancer cells, and inhibits DNA replication.[425] The group discovered that the oligonucleotide cargo could disrupt the folding of the DNA nanostructure during the self-assembling process. To address this problem, they created a carrier that would properly fold, regardless of the number and sequence of cargo molecules. Using a biorthogonal base pairing system, they constructed an L-DNA tetrahedron that could be decorated with therapeutic aptamers at its vertices (Figure 37A,B). The

https://doi.org/10.1021/acs.chemrev.0c01332
Chem. Rev. XXXX, XXX, XXX−XXX

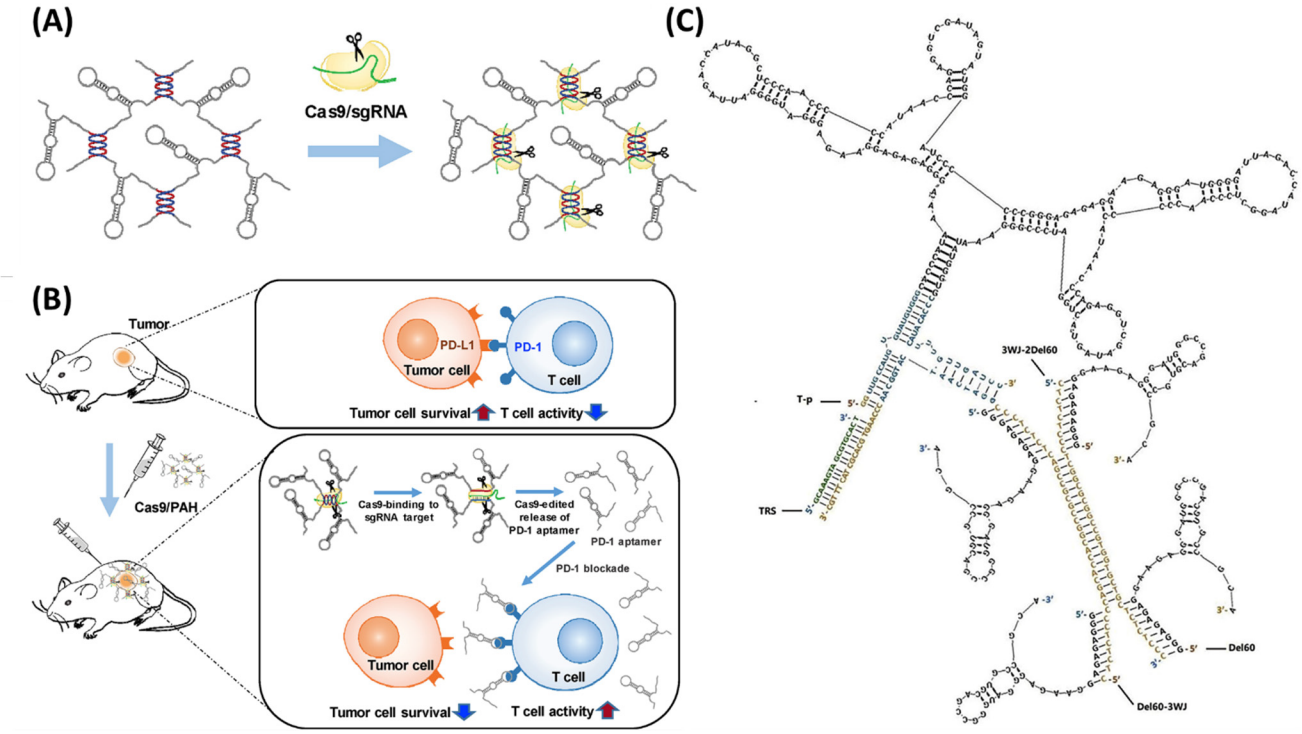

Figure 38. Aptamer-based nucleic acid nanostructures for immunotherapy applications. (A) Cleavage of DNA polyaptamer hydrogel containing sgRNA sequences using Cas9/sgRNA systems to release individual aptamers. (B) Blockage of PD-1 immune cell and tumor cell interactions via Cas9/sgRNA system. Adapted with permission from ref 432. Copyright 2019 Elsevier. (C) Diagram of self-assembled X-polymer nanoparticle consisting of one CD28Apt-dimer and four Del60 aptamers. Adapted from ref 433. Published 2017 Elsevier. Licensed under a Creative Commons agreement (https://creativecommons.org/licenses/by/4.0/).

aptamer-functionalized tetrahedrons were found to have more cytotoxicity toward cancer cells compared to free aptamers. Additionally, the L-DNA carriers were found to have similar thermodynamic stability but higher cancer cell cytotoxicity than their D-DNA tetrahedral enantiomers. In 2018, Taghdisi's group developed a synergistic cancer therapy approach by using a 4WJ that carried DOX and two different types of therapeutic aptamers. Specifically, AS1411 aptamers and FOXM1 aptamers, which inhibit an overexpressed protein associated with cancer cell proliferation, were decorated on the nanostructure.[323] The therapeutic combination of the cargo was found to decrease tumor proliferation and lower off-target toxicity, enhancing both the efficiency and efficacy of cancer treatment.

5.3.1.2. Antiangiogenesis. Rapidly growing cancer cells rely on angiogenesis, or the formation of new blood vessels, to supply oxygen to tumor sites. Nanotechnology-based therapeutics to stunt angiogenesis have been developed to starve cancer cells and induce tumor necrosis.[426] Human vascular endothelial growth factor (hVEGF) is a molecule known for promoting angiogenesis. In 2018, Kim and colleagues developed an antiangiogenesis platform by incorporating hVEGF aptamers into Y-shaped DNA nanostructures.[427] The group incorporated the aptamers into the backbone of the DNA nanostructure to overcome the loading capacity limitations found when incorporating aptamers at the end groups of a structure (Figure 37C). The nanoconstructs were stable in serum for over 3 days, attributed to entanglements that lowered nuclease access. In comparison, free aptamers had a serum degradation time of 12 hours. The antiangiogenesis construct was evaluated by immunohistochemical methods and was found to prevent significant tumor growth by inhibiting VEGF.

5.3.1.3. Induced Cell Apoptosis. Another method to treat tumors is by inducing cell apoptosis, which can be done using a variety of cell pathways. Like the AS1411 antiproliferative aptamer, the C2NP aptamer possesses both targeting and therapeutic properties. C2NP aptamers can both target a cancer cell marker and induce apoptosis in T-cell lymphoma cells.[428] Zhou and Zhao used DNA origami to deliver DOX synergistically with C2NP to cancer cells to increase cell death.[429] The origami provided a platform to anchor varied numbers of the multivalent aptamers. The anticancer activity was tested *in vitro*; it was found that the DOX loaded C2NP−DNA origami structure had much higher activity compared with free DOX. Additionally, the origami decorated with 16 aptamers was found to induce greater rates of cancer cell apoptosis compared to the origami decorated with 4 aptamers. The use of DNA origami allowed exploitation of the anticancer activity of both DOX and C2NP aptamers and further enabled stability as well as controlled release of the molecular cargo.

5.3.1.4. Cancer Immunotherapy. The human immune system naturally possesses the ability to recognize as foreign mutated cell markers, also known as neoantigens, produced by tumor cells often leading to destruction of the unhealthy cells. However, tumor cells can also evade recognition by the immune system, resulting in immune tolerance. Cancer immunotherapy is a technique used to ensure that the immune system recognizes and attacks immune system-evading cancer cells. Many strategies have been proposed and used, including nonspecific immune stimulation, T-cell transfer therapy, and immune checkpoint inhibitors. To avoid recognition by the immune system, cancer cells can overexpress immune checkpoint inhibitory receptors in order to suppress normal immune cell function.[430] Fortunately, drugs that interrupt immune check-

https://doi.org/10.1021/acs.chemrev.0c01332
Chem. Rev. XXXX, XXX, XXX−XXX

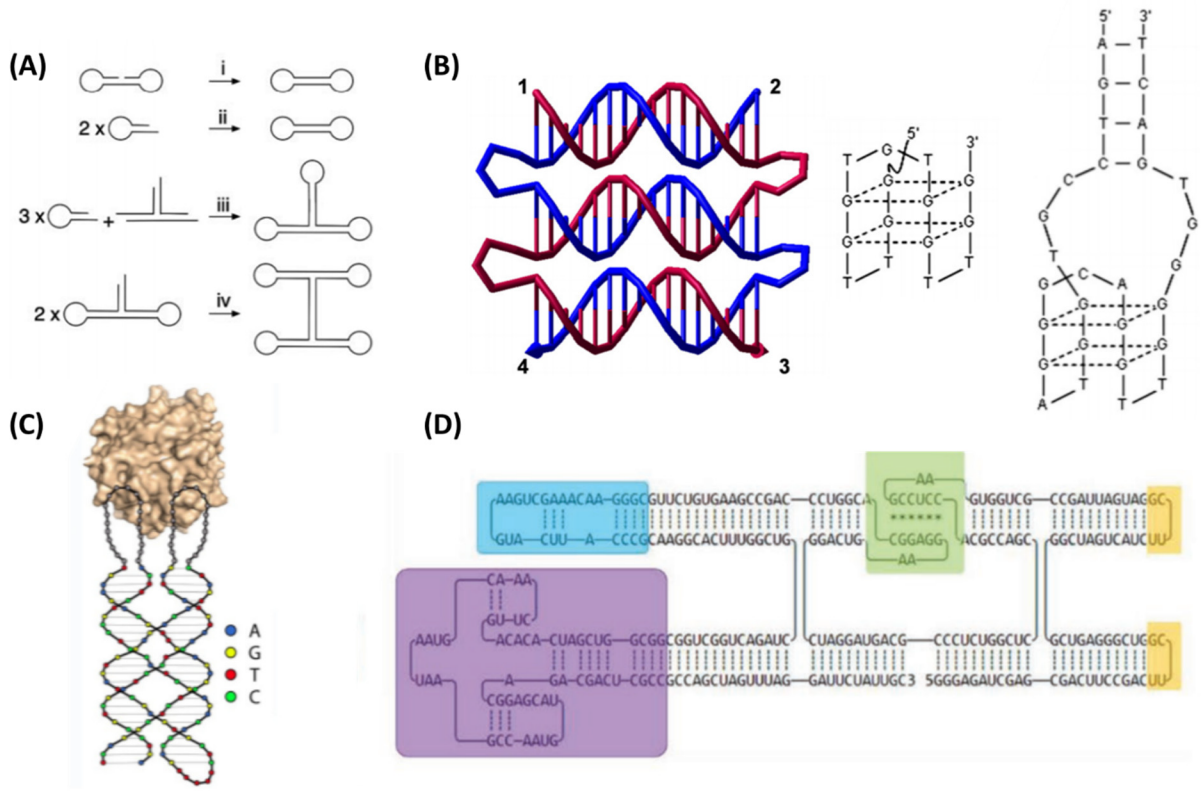

Figure 39. Aptamer-decorated nucleic acid nanostructures functioning as anticoagulants. (A) Construction of DNA duplex bearing multiple aptamers. Adapted with permission from ref 436. Copyright 2004 American Society for Biochemistry and Molecular. (B) DNA 3-helix weave tile designed to serve as biomolecular platform for multivalent aptamer display. Sequences and structures of thrombin exosite-1 and exosite-2 binding aptamers used to decorate DNA weave tiles. Adapted with permission from ref 438. Copyright 2012 Elsevier. (C) Design of conserved parallel DNA 2-helix structure (colored markers) bearing two randomized aptamer loops (gray markers) composing SELEX library. Adapted with permission from ref 180. Copyright 2019 John Wiley and Sons. (D) RNA origami anticoagulant produced via in vitro transcription consisting of tetraloops (yellow), kissing loops (green), exosite 1-binding aptamer (purple), and exosite-2 binding aptamer (blue). Adapted with permission from ref 106. Copyright 2019 John Wiley and Sons.

points can be used to help counteract this immune suppression, and some immune checkpoint inhibitors have been approved for clinical trials, such as anti-PD-1 antibodies that inhibit PD-L1, a ligand that weakens T-cell function and is overexpressed on cancer cells. However, problems such as rapid tumor clearance and high manufacturing costs pose challenges for practical use. Anti-PD-1 aptamers have also been developed to provide lower cost production and better tumor penetration, but their short *in vivo* retention time is a major hurdle.[431] To overcome these challenges, in 2019, Oh and colleagues developed a new immunotherapy drug using RCA to produce DNA hydrogels containing multivalent PD-1 aptamers.[432] The hydrogel also contained sgRNA-targeting sequences to allow controlled release of PD-1 aptamers from the hydrogel using a Cas9/sgRNA cleavage system (Figure 38A). The programmed release of PD-1 aptamers resulted in activation of T-cells and lowered tumor survival rate (Figure 38B). The Cas9/aptamer-hydrogel was found to remain at the tumor injection site longer and have higher antitumor effects due to increased immune cell filtration compared with free aptamers or hydrogel alone.

Chimeric antigen receptor T cells (CAR-Ts) yield another immunotherapeutic tool that has been used in clinical settings to aid in the immune recognition of cancer cells. In this type of therapy, a patient's own immune cells are modified to produce CARs on their surface, enabling them to better recognize and target tumor cell antigens and promote T cell proliferation. In 2020, Bai et al. created self-assembled multivalent CAR-like aptamer nanoparticles that were designed to perform similar functions seen in CAR-Ts, such as identifying cancer cells and activating T cells.[433] The nanoparticles were made using a 3WJ to connect a dimer of CD28 RNA aptamers for promoting T cell proliferation, a tetramer of CTLA-4 aptamers for immune checkpoint blockade, and folic-acid-labeled ssDNA for cancer cell targeting (Figure 38C). The nanoparticles were able to inhibit the growth of melanoma B16 cells both *in vitro* and in mouse models by activating T cells.

5.3.2. Anticoagulants. DNA and RNA aptamer-based anticoagulants have also been developed and used for therapeutic applications. This is made possible through the selection of aptamers that specifically inhibit proteins involved in the coagulation cascade, as previously reviewed by Woodruff and Sullenger.[434] Nucleic acid nanostructures have been used to organize these aptamers to increase their local concentration and optimize distances between aptamers to enhance interactions with their target proteins. Due to these benefits, aptamers on nucleic acid nanostructures provide various advantages over stand-alone aptamers, including improvement of pharmacokinetic properties and enhancement of anticoagulant activity. Even simple structures, such as ssDNA linkers, have been used to connect aptamers and have resulted in enhanced anticoagulation activity.[435] Giusto and King developed the first multivalent DNA anticoagulants by constructing duplexes bearing two aptamers, a 3WJ bearing three aptamers and connecting two 3WJ to host four aptamers (Figure 39A).[436] The

https://doi.org/10.1021/acs.chemrev.0c01332
Chem. Rev. XXXX, XXX, XXX−XXX

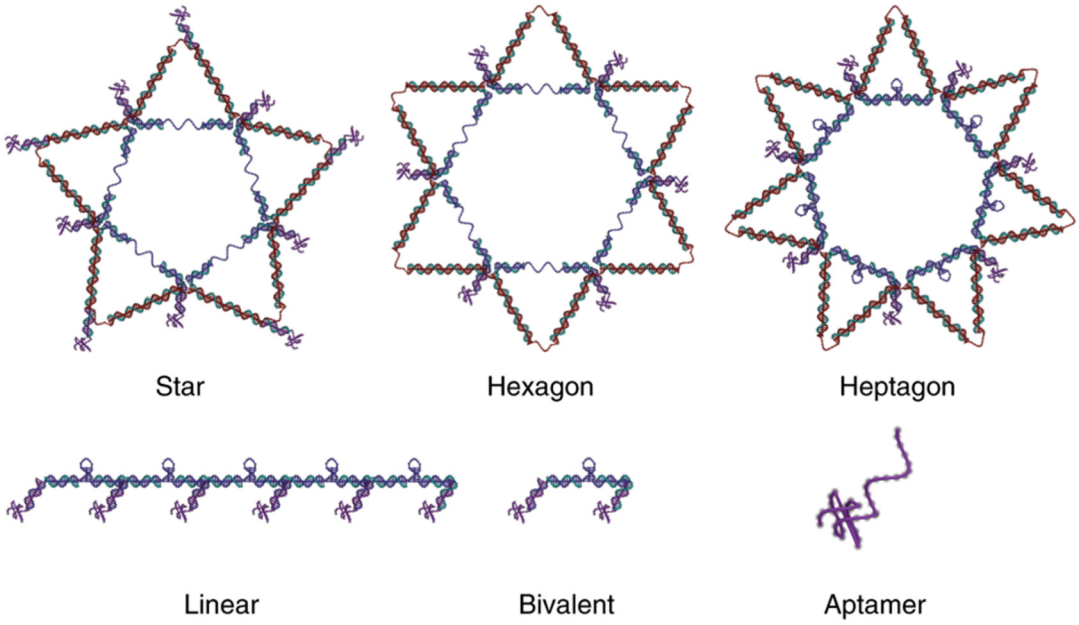

Figure 40. Various 1-D and 2-D DNA structures used to sense and inhibit DENV. The structures consist of a fluorescent component as well as therapeutic aptamers that inhibit viral activity. Adapted with permission from ref 242. Copyright 2019 Springer Nature.

structures showed promise for clinical development as a result of their resistance to nuclease degradation and long half-lives in blood serum and plasma. Additionally, they were found to increase anticoagulation activity 2−3-fold compared to free aptamer therapeutics.

LaBean further improved the anticoagulation activity of aptamer-decorated DNA nanostructures through the construction of an anticoagulant DNA weave tile.[437] Weave tiles hosting up to four copies of thrombin binding aptamers and were tested using aPTT coagulation assays and were found to increase anticoagulation activity by nearly 5-fold compared to free aptamers. LaBean's group further developed this technology by optimizing the distance between the thrombin binding aptamers, as well as incorporating two different aptamer sequences, one for exosite 1 on thrombin and the other for exosite 2, into the same structure (Figure 39B).[438] Two-, three-, four-, and five-helix weave tiles were constructed and had varying anticoagulation effects. This demonstrated the ability to control anticoagulation activity by varying the spatial separation between the aptamers to find the optimal distance for thrombin interaction and inhibition. Additionally, the activity of these structures could be reversed by complementary single-stranded DNA sequences. In 2016, they continued optimizing the weave tile platform, resulting in a 16-fold increase in anticoagulation activity compared to free aptamers in aPTT assays.[439] With aid from molecular dynamic simulations, it was shown that a certain level of flexibility in the weave tile configurations provided the highest observed thrombin inhibition. The large variety of aptamer-decorated weave tile anticoagulant nanostructures emphasizes the diverse toolkit available for optimizing anticoagulant activity when aptamers are decorated on nucleic acid nanostructure platforms.

Bivalent aptamers are known to demonstrate stronger affinities compared to monovalent ones, resulting in higher inhibition activity, especially when they undergo simultaneous selection. Therefore, Zhang and Yan created a SELEX library based on bivalent aptamers attached to a predefined DNA structure to select thrombin binders.[180] The SELEX library design contained two randomized loop sequences for bivalent aptamer selection, as shown in Figure 39C. This was the first reported successful selection of heterobivalent aptamers on a predefined DNA structure using a simple SELEX process. Selected bivalent aptamer nanostructures were found to have dissociation constants as low as 321 fM and demonstrated higher anticoagulation activity than free aptamers when tested using fibrin generation assays.

In 2019, LaBean's group reported the first RNA origami anticoagulant, consisting of a 2-helix origami bearing two thrombin binding aptamers (Figure 39D).[106] The group developed the ssRNA origami anticoagulant to circumvent the multistrand folding challenges found in the weave-tile designs.[437−439] The RNA anticoagulant was produced by *in vitro* transcription and had higher activity compared to both free aptamers and equivalent DNA weave tile designs. 2′F-modified pyrimidines were incorporated to provide nuclease resistance, making the structure more stable in plasma compared to weave tiles and for at least 3 months at 4 °C storage. Furthermore, DNA antidotes were designed that could reverse anticoagulation activity. Currently, they enhanced anticoagulation activities of RNA origami by decorating four thrombin binding aptamers into a RNA origami structure and improved reversal activity up to 95% using PNA antidotes. Importantly, freeze-dried and freshly produced RNA origami showed same coagulation activities.[181]

5.3.3. Viral Inhibition. In 2020, the first aptamer-decorated DNA nanostructure for simultaneous virus sensing and inhibition was reported by Wang and colleagues.[242] The group created various DNA architectures that carried molecular beacon-like motifs, as well as Dengue virus (DENV) envelope protein domain III (ED3) targeting aptamers. Once the nanostructures bound to the virus, they would fluoresce, sensing the virus while also inhibiting the virus from interacting with and infecting living cells. Both 2D structures, such as stars, hexagons, and heptagons, and 1D structures were constructed to determine the optimal shape and spacing for DENV inhibition (Figure 40). It was determined that optimal inhibition of DENV

https://doi.org/10.1021/acs.chemrev.0c01332
Chem. Rev. XXXX, XXX, XXX−XXX

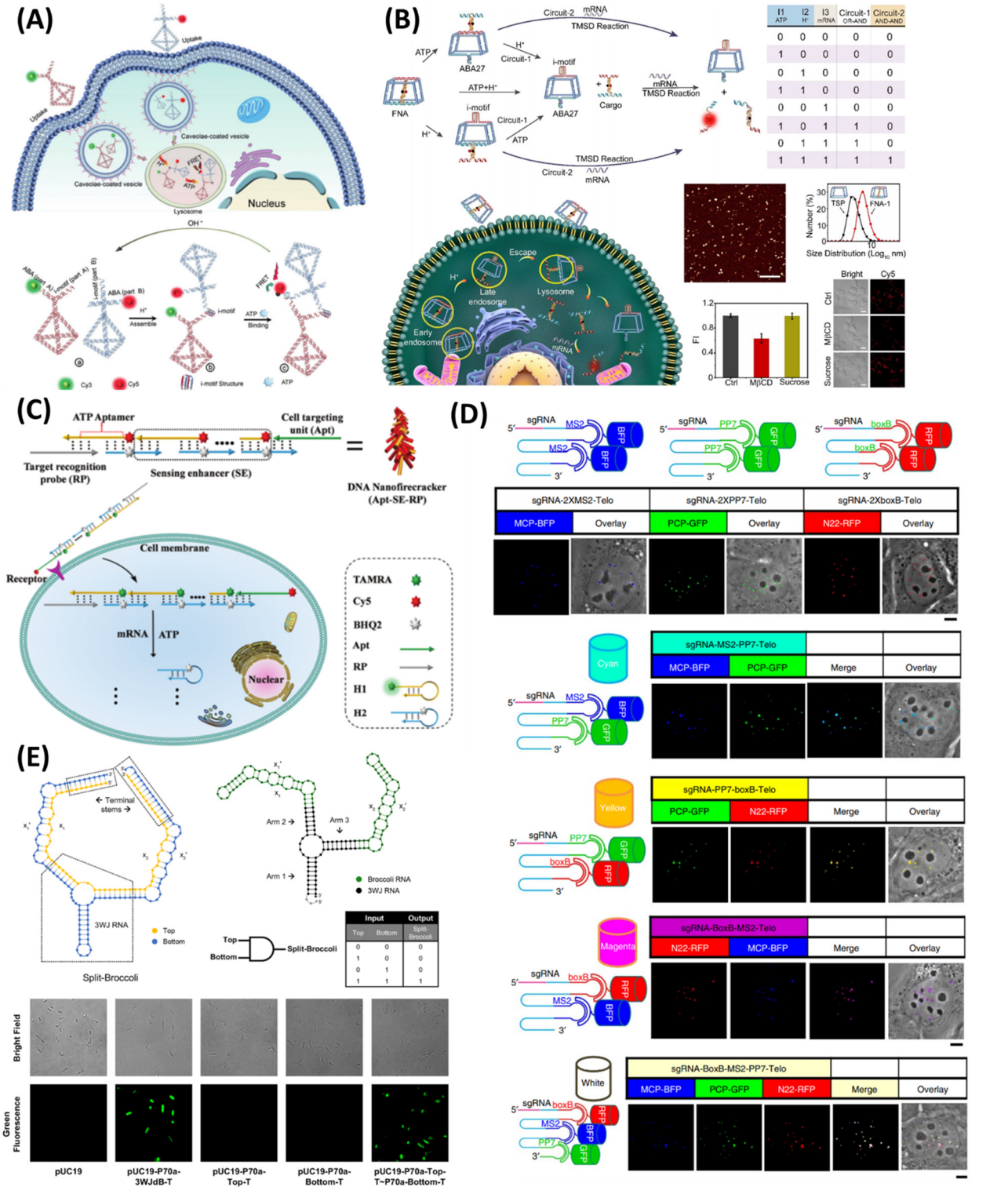

Figure 41. In vitro imaging using aptamer-decorated nucleic acid nanostructures. (A) Schematic illustration of intracellular ATP imaging using self-assembled heterodimer tetrahedral DNA nanostructure bearing split ATP aptamers and i-motifs. Adapted with permission from ref 440. Copyright 2019 John Wiley and Sons. (B) Three input logic gate DNA nanodevice for mRNA imaging. Adapted with permission from ref 442. Copyright 2020 John Wiley and Sons. (C) DNA nanostructure dissociation-based signal amplification for mRNA imaging in living cells. Adapted with permission from ref 443. Copyright 2020 Royal Society of Chemistry (D) Multiplexed genome loci imaging using CRISPRainbow, dCas9 combined with engineered sgRNA containing fluorescent protein-binding RNA aptamers (scale bar = 5 μm). Adapted with permission from ref 444. Copyright 2016 Springer Nature. (E) Split-broccoli fluorescent system expressed inside living cells, enabling real-time visualization of RNA assembly inside cells. Adapted from ref 128. Copyright 2017 American Chemical Society.

was achieved for the star-shaped configuration. However, two-dimensional structures that were not close to the optimal shape, namely, the heptagon, proved to be less effective than one-dimensional structures such as linear or bivalent aptamers. This

https://doi.org/10.1021/acs.chemrev.0c01332
Chem. Rev. XXXX, XXX, XXX−XXX

technology holds therapeutic potential for many infectious diseases, as the therapeutic aptamer can be selected to target a variety of viruses and the DNA structure can be optimized based on viral surface geometry.

5.3.4. Neurodegeneration. Neurodegeneration is the cause of many devastating diseases such has Alzheimer's disease, dementia, and Parkinson's disease. Neurodegeneration is thought to be linked to abnormal deposition of neuronal proteins, such as the tau protein, but many therapies for these diseases are not target specific and have problems crossing the blood−brain barrier. To address these problems, in 2020, Wang and Tan developed a bifunctional aptamer complex that would aid in both crossing the BBB using a transferrin receptor aptamer and inhibiting tau phosphorylation and other tauopathy-related pathological events using a tau protein aptamer.[313] The structure was found to improve cognition and memory deficits found in tau-overexpressing mice.

5.4. Bioimaging

Bioimaging techniques provide understanding and insight into biological processes, and track the localization of targeted delivery materials from the cellular level to the whole organism level using noninvasive methods including optical and magnetic resonance imaging. Static and dynamic nucleic acid nanostructures incorporated with functional motifs, such as aptamers and DNAzymes, have been developed and utilized in bioimaging applications. Furthermore, programmable nucleic acid nanostructures have served as biomolecular platforms for decoration of multiple imaging materials such as bright fluorescent dyes, photostable nanomaterials, radioactive isotopes, and magnetic resonance imaging materials, resulting in signal enhancement and high-resolution image quality. In this section, we focus on aptamer-conjugated nucleic acid nanostructures for bioimaging applications and categorize them into two groups: *in vitro* and *in vivo* imaging.

5.4.1. In Vitro Bioimaging. The programmability, functionality, and biocompatibility of nucleic acid nanostructures offer great tools for bioimaging platforms. To this end, aptamer-decorated nucleic acid nanostructures for *in vitro* fluorescent bioimaging have been developed. Fan's group constructed reconfigurable tetrahedral DNA nanostructures containing ATP aptamers.[267] Using FRET pair labeled ATP aptamers on the tetrahedral DNA, ATP imaging in living cells was demonstrated. Dendrimer DNA nanostructures bearing multiple ATP aptamers were further developed and utilized for intracellular imaging of ATP.[248] In the presence of intracellular ATP, a fluorescence signal could be detected. The aptamer-functionalized DNA dendrimer showed biocompatibility and intracellular stability. In 2017, Zhang demonstrated FRET-based ATP imaging in living cells by using a split ATP aptamer decorated on a DNA triangular prism.[241] The FRET signal increase corresponded to the ATP level. Notably, aptamer-decorated DNA nanostructures showed higher efficiency over the traditional molecular beacon system.

Nucleic acid nanostructures allow conjugation of multivalent functional motifs, including i-motifs, DNAzymes and aptamers, and offer logic gate-based bioimaging platforms. In 2019, Li demonstrated pH-induced DNA nanostructure formation for ATP intracellular imaging.[440] Two tetrahedral DNA nanostructures bearing i-motif and split ATP aptamers were constructed. In the acidic environment inside lysosomes, the heterodimeric tetrahedral DNA nanostructures were assembled via i-motif interaction (Figure 41 A). In the presence of endogenous ATP, the binding interactions of ATP and split ATP aptamers resulted in FRET signal enhancement. With this system, they successfully demonstrated two-input AND gate-based subcellular imaging. Moreover, a DNA triangular prism incorporating i-motifs and ATP aptamers preforming a DNA logic gate nanodevice for cellular imaging has been developed.[441] Recently, Li further developed three-input logic gate nanodevices for intracellular imaging.[442] To sense mRNA, they constructed a truncated square pyramid DNA nanocage carrying an i-motif, ATP aptamer, and duplex DNA. They reported two cascade logic gates (OR−AND and AND−AND) that responded to acidic environments in lysosomes and intracellular ATP that enabled controlled release of duplex DNA cargo for mRNA imaging (Figure 41B). This functional, logic gate-controlled DNA nanodevice has the potential to be applied in various applications including bioimaging, sensing, and targeted drug delivery with controlled release of molecular cargo.

Nucleic acid aptamers have also been employed as targeting molecules for the specific transport of imaging materials into target cells. Recently, Tan developed signal-enhancing mRNA imaging in living cells using aptamer-functionalized DNA nanofirecrackers.[443] AS141 aptamers specifically target cancer cells and allow internalization of the DNA nanostructures. The HCR-based DNA nanofirecrackers contain multiple ATP aptamers and a toehold region, complementary to the target mRNA. Intracellular mRNA and ATP trigger rapid dissociation of the DNA nanofirecrackers and subsequent enhancement of the fluorescence signal. (Figure 41C).

Fluorescent protein-binding RNA aptamers have been developed and utilized in bioimaging applications. In 2016, Pederson developed a multiplexed chromosomal imaging method called CRISPRainbow, using dCas9 associated with engineered sgRNA scaffolds that bound with multiple fluorescent proteins expressed inside the cells and displayed seven distinguished colors (Figure 41 D).[444] They successfully demonstrated intracellular, simultaneous imaging of six chromosomal loci by coexpression of six sgRNA scaffolds. A few years later, they further developed a bright multicolor system for genome imaging using a CRISPR guide RNA scaffold carrying multiple fluorescent protein-binding RNA aptamers.[445]

Fluorescent RNA aptamers are biocompatible and can be expressed inside many cells. For these reasons, many research groups have developed and employed RNA aptamers for intracellular imaging and monitoring of RNA transcripts, gene expression, and metabolites.[446−450] For example, Aoyama developed a light-up fluorescent RNA aptamer tag to monitor mRNA during *in vitro* transcription.[451] Within the realm of RNA nanotechnology, RNA could be transcribed and self-assembled into sophisticated RNA nanostructures inside living cells.[104,452] Understanding and monitoring the self-assembly and stability of RNA nanostructures without disrupting the native designed geometries and conformations are crucial. Fluorescence and radioisotope labeling are commonly used to monitor and track nucleic acid nanostructures; however these labeling techniques potentially cause RNA misfolding. Incorporation of fluorescent RNA aptamers into RNA nanostructures as reporters maintains the natural folding of RNA during imaging, providing great bioimaging tools for probing RNA nanostructure formation and degradation inside the cells. With this goal, Guo designed fluorogenic RNA nanoparticles to monitor RNA folding and degradation in living cells.[453] The RNA nanoparticles were made of pRNA 3WJ motif core structures fused with a malachite green aptamer (fluorogenic aptamer), ribozyme, and luciferase

https://doi.org/10.1021/acs.chemrev.0c01332
Chem. Rev. XXXX, XXX, XXX−XXX

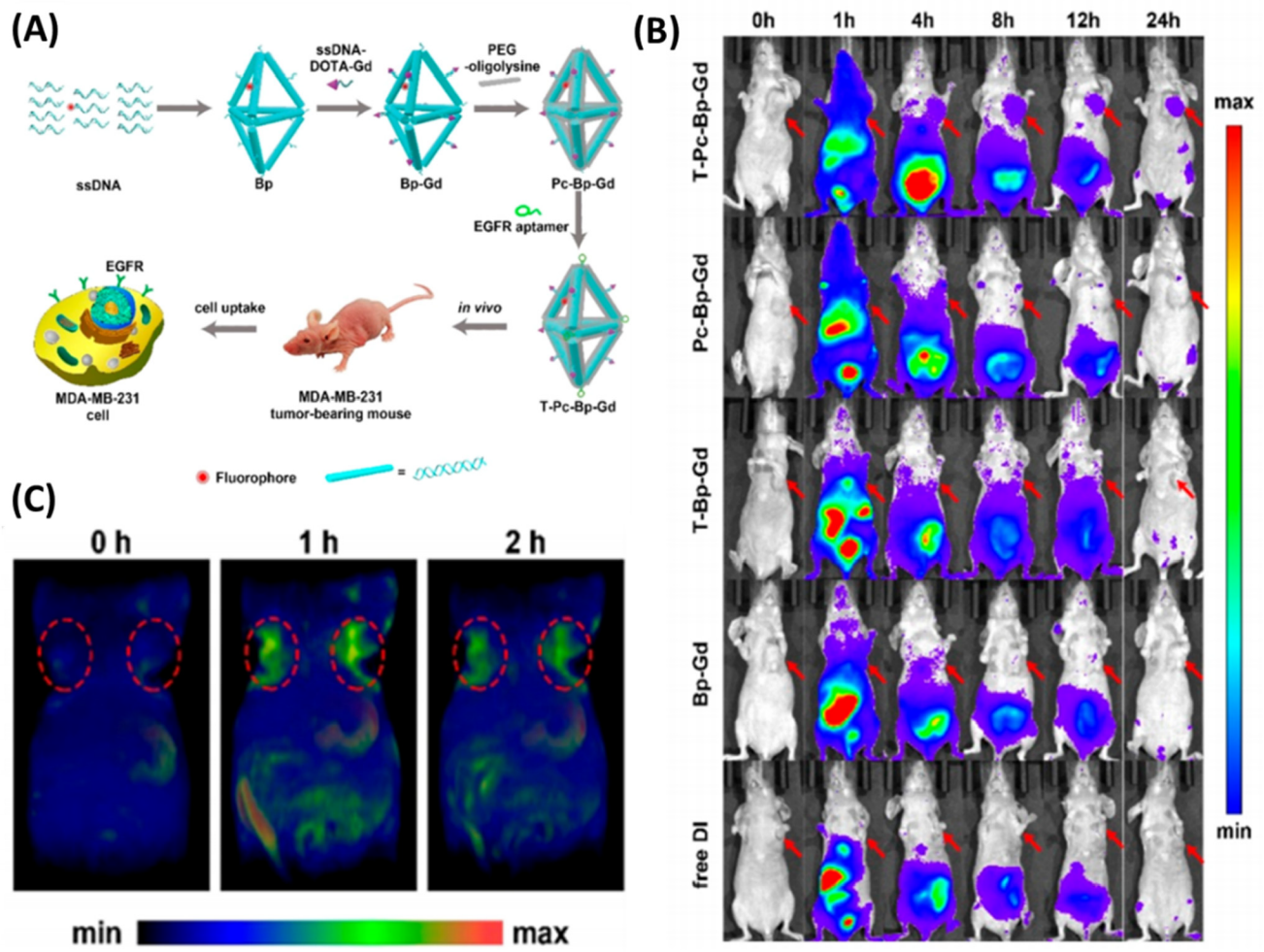

Figure 42. Self-assembled DNA nanostructures for *in vivo* imaging. (A) Construction of dual-labeled, multivalent tumor-targeting aptamer-decorated DNA bipyramid nanostructures. (B) Fluorescence imaging and (C) magnetic resonance imaging of DNA nanostructures in tumor-bearing mice postinjection. Red circles indicate tumor sites. Adapted from ref 457. Copyright 2020 American Chemical Society.

siRNA. When the RNA nanostructures correctly folded, the aptamers fluoresced, while the fluorescence signal disappeared in degraded, denatured, or misfolded RNA nanoparticles. This fluorogenic aptamer-modified RNA nanoparticle allowed monitoring of the folding and degrading RNA nanostructure, enabling estimation of RNA nanoparticle half-life inside living cells. Furthermore, Burke developed a split-broccoli system as a RNA logic gate for real-time visualization of RNA−RNA assembly in living cells.[128] This system required two strands of RNA to form a 3WJ RNA nanostructure, resulting in fluorescence activation (Figure 41E). Both strands of RNA were expressed inside living cells and formed RNA nanostructures, creating an AND gate for monitoring RNA assembly in real-time.

5.4.2. *In Vivo* Bioimaging. Fluorescently labeled nucleic acid nanostructures have been commonly used for tracking and monitoring the localization of the delivered nanostructures *in vivo* due to their convenience and low costs.[339,343,350,395] However, fluorescence-based optical imaging suffers from low resolution and permeability limiting the application of *in vivo* imaging in preclinical and clinical studies. Therefore, advanced, high-resolution bioimaging techniques and microscopies have been developed.[454] In 2016, radiolabeled DNA bipyramid nanostructures were designed, constructed, and utilized for *in vivo* bioimaging in mice using single-photon emission computed tomography imaging (SPECT).[455] Fan further developed multiarmed tetrahedral DNA nanostructures for *in vivo* imaging by utilizing dual decorations of near-infrared fluorescence dye and the radioactive isotope, ^{99m}Tc.[456] These dual-labeled DNA nanostructures were employed for tumor imaging in mice by using both near-IR optical imaging and SPECT. Magnetic resonance imaging (MRI) is a promising technique for *in vivo* bioimaging and has been widely used in preclinical and clinical studies for cancer diagnostics. Recently, Ding developed a tumor-targeting DNA nanostructure with dual-modality bioimaging.[457] The DNA bipyramid nanostructures were decorated with a tumor-targeting aptamer and two types of imaging molecules, magnetic resonance contrast agents (Gd-DOTA) and near-IR fluorescence imaging dye (Dylight800) (Figure 42A). The DNA nanostructures were intravenously injected into tumor-bearing nude mice. Fluorescence imaging and MRI results showed that the tumor-targeting, aptamer-conjugated DNA nanostructures accumulated at the tumor site (Figure 42B,C). This DNA nanostructure platform decorated with aptamers and different imaging molecules shows great potential for applications in bioimaging and disease diagnostics.

https://doi.org/10.1021/acs.chemrev.0c01332
Chem. Rev. XXXX, XXX, XXX−XXX

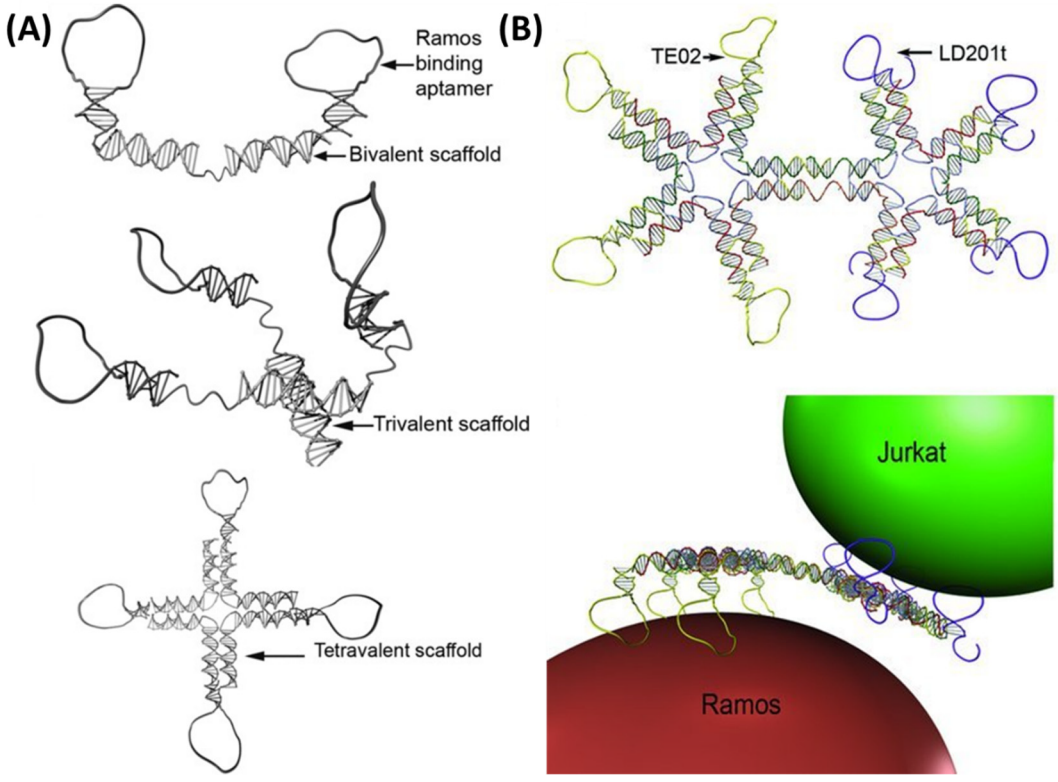

Figure 43. DNA scaffolds for multivalent aptamer decoration. (A) Schematic design of bivalent, trivalent, and tetravalent DNA nanostructures. The bivalent and trivalent designs are considered flexible due to their single-stranded five-thymine linker. (B) Schematic representation of rigid, dimerized five-point star DNA nanostructure harboring four aptamers targeting both Ramos and Jurkat cells. Illustration of DNA structure facilitating Ramos and Jurkat cell−cell conjugates. Adapted with permission from ref 460. Copyright 2011 John Wiley and Sons.

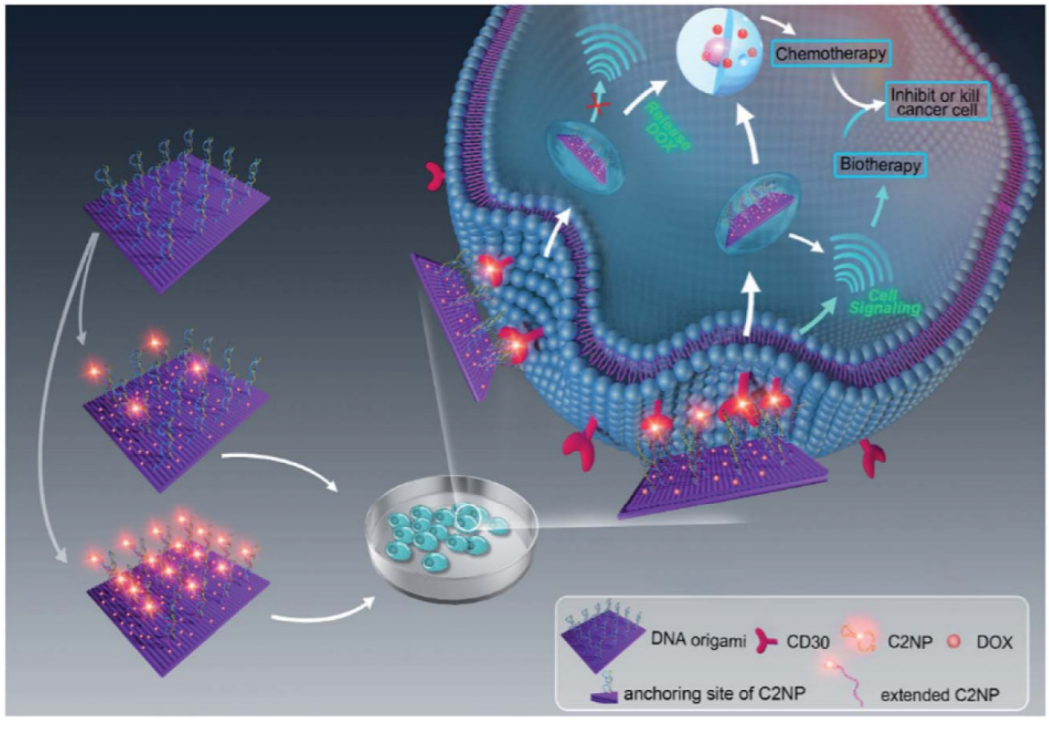

Figure 44. Illustration of DNA origami cellular interaction pathways. C2NP aptamers interact with CD30 receptors to aid in endocytosis of chemotherapy drugs as well as induce cell signaling, leading to apoptosis. Reprinted from ref 429. Published 2018 Royal Society of Chemistry. Licensed under a Creative Commons Attribution-NonCommercial 3.0 Unported License (https://creativecommons.org/licenses/by-nc/3.0/).

https://doi.org/10.1021/acs.chemrev.0c01332
Chem. Rev. XXXX, XXX, XXX−XXX

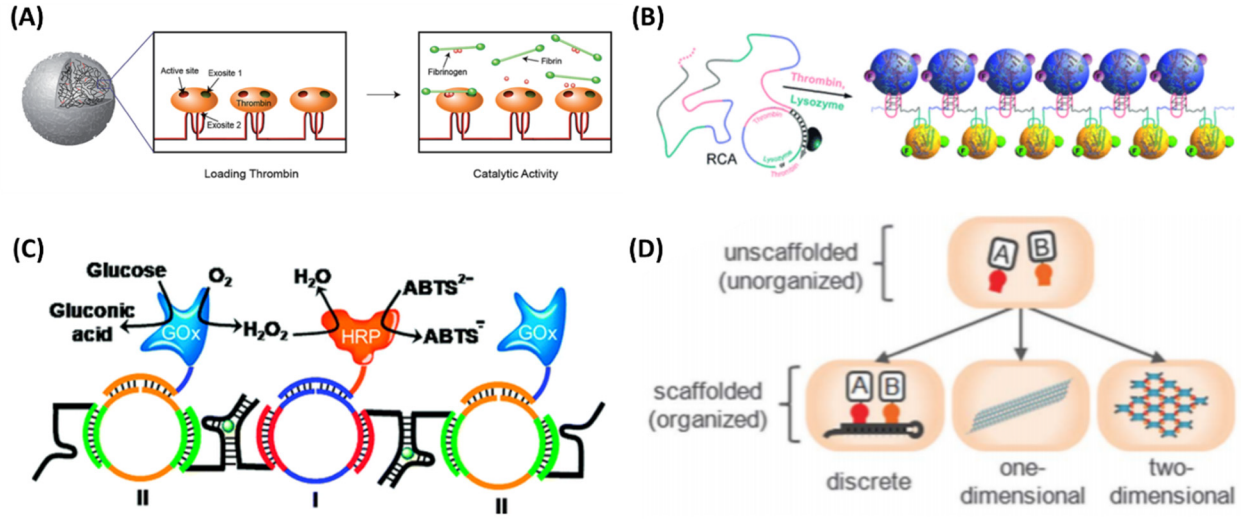

Figure 45. Aptamer-decorated nanostructures for enhanced enzymatic reactions. (A) Schematic of interactions of thrombin binding particles with thrombin exosite 2, followed by catalytic conversion of fibrinogen into fibrin. Adapted from ref 468. Published 2017 Royal Society of Chemistry. Licensed under a Creative Commons agreement (https://creativecommons.org/licenses/by/3.0/). (B) DNA tapes decorated by both thrombin and lysozyme binding aptamers created by RCA. Adapted with permission from ref 469. Copyright 2007 John Wiley and Sons. (C) Catalytic activity of GOx and HRP decorated DNA nanowires. Aptamers (black) self-assemble in the presence of cocaine (green circles). Reprinted from ref 470. Copyright 2009 American Chemical Society. (D) 0D, 1D, and 2D RNA scaffolds containing proteins A and B. Adapted with permission from ref 471. Copyright 2011 The American Association for the Advancement of Science.

5.5. Cell Reprogramming

5.5.1. Cell–Cell Interactions. Multicellular organisms rely on cell–cell interactions for tissue development and organization, cell communication, and immune response.[458] Many efforts have been made to synthetically construct tissues *ex vivo* through bottom-up strategies, including cell linkage by hybridization of DNA sequences attached to cell surfaces; however, most of these efforts lack specificity in the cell–cell interactions seen in native tissues.[459] Liu and Chang developed a DNA scaffold decorated with bispecific aptamers to bring two specific cell types in proximity to promote cell–cell interactions.[460] The aptamers targeted naturally occurring cell surface markers, eliminating the need for synthetic surface decoration. The group used a variety of branched DNA scaffolds to create multivalent structures as shown in Figure 43A. They showed that more rigid structures promoted higher aptamer binding affinity; thus, a rigid five-point-star dimer was used to connect a Ramos B cell and Jurkat T cell (Figure 43B). The multivalent star dimer DNA nanostructure increased aptamer affinity by around 4-fold compared to monovalent aptamers and was found to be the most efficient in inducing cell–cell conjugates. This work demonstrated a proof-of-concept for the potential use of aptamer-decorated DNA nanostructures to specifically mediate cell–cell interactions without the need for synthetic cell surface modifications. This technology could be developed for a variety of applications, from increasing tissue development on *ex vivo* scaffolds to mediating T-cell recognition of cancer cells in living organisms.

5.5.2. Cell Signaling. In addition to contact communication via cell–cell interactions, cells can also communicate through complex signaling processes. During many of these processes, an external stimulus binds to a cell surface receptor and triggers a cascade of reactions within the cell that lead to a desired outcome. Some aptamers have been selected to bind to cell surface receptors and can serve as external stimuli to induce downstream signaling. For example, the C2NP aptamer binds to CD30 cell markers and can activate signaling that induces apoptosis in T-cell lymphoma cells.[461] In 2018, Zhao developed a rectangular DNA origami nanostructure harboring C2NP aptamers and DOX for a dual approach cancer therapy (Figure 44).[429] The C2NP aptamers allow cellular penetration of the DOX-loaded DNA origami while also inducing cell signals that result in cancer cell apoptosis. The aptamer-induced biotherapy was only significant after 72 h of treatment with high concentrations. The aptamer-decorated DNA nanostructures were found to induce cell apoptosis by arresting the cell cycle in the G2 phase and upregulating ROS levels, a common cause of DNA damage. Higher activity was observed for aptamers decorated on the DNA nanostructures and was attributed to increased stability. This work further emphasizes the value of using aptamer-enhanced DNA nanostructures to target diseased cells, through both delivery of drug cargos and direct signaling cascades via receptor-mediated cell communication.

5.6. Enhanced Enzymatic Reactions

Many nanostructures are found in nature that specifically arrange biomolecules to mediate functions such as biomolecular synthesis, gene regulation, and signal transduction. Enzymes involved in these processes are often highly organized and require precise positioning and orientation to expedite the metabolism of substrates. Spatial organization of enzymes helps facilitate sequential reactions by helping direct substrate flow in these so-called enzyme cascades. Synthetic precise arrangement of such sets of biomolecules can be used to optimize catalytic efficiency and specificity. A variety of nanostructures have been used to influence metabolic pathways, including synthetic protein scaffolds[462−464] and plasmid DNA.[465] Compared to these scaffolds, nucleic acid nanostructures present more predictable and programmable interactions that can precisely position other materials. Inorganic nanomaterials, such as gold nanoparticles and quantum dots, as well as biological molecules, such as proteins, have been arranged using nucleic acid nanostructures.[466,467] Additionally, aptamer docking sites have

https://doi.org/10.1021/acs.chemrev.0c01332
Chem. Rev. XXXX, XXX, XXX−XXX

been integrated into nucleic acid scaffolds to aid in the precise arrangement of many nanomaterials.

The enzymatic activity of a protein can be enhanced by increasing the local concentration of that protein in a defined area. Enzymes organized using DNA nanostructures have been used to increase enzymatic activity for *in vitro* applications. In 2017, Lee used RCA, an important tool for creating many tandem repeat copies concentrated in a small area, to synthesize DNA microparticles with thrombin-binding aptamers.[468] Two particle designs were tested, one containing exosite 1 binding aptamers and the other containing exosite 2 binding aptamers. As shown in Figure 45A, exosite 1 is attributed to most fibrinogen cleavage and is in proximity to the thrombin active site; therefore, it was found that the particles containing aptamers that bound exosite 2, leaving exosite 1 unbound, did not block the active site and had the greatest increase in thrombin activity. Compared to free thrombin activity, the activity of DNA particle-concentrated thrombin was found to improve up to 1.7 times. This study emphasizes the importance of the synergistic effect between the DNA nanostructure and the enzyme-binding aptamers to both increase local concentration and optimally orient enzymes for increased activity.

In addition to increasing local concentration of a single enzyme type, colocalization of multiple enzymes can be used to influence metabolic flux. DNA nanostructures have been used to achieve this by arranging proteins periodically using RCA. Willner and colleagues used RCA to create linear ssDNA tapes that consisted of periodic repeats of aptamers targeting both thrombin and lysozyme (Figure 45B).[469] Using a single-step synthesis, the group was able to create bifunctional, 1D DNA nanostructures with potential for scaffolding multiple proteins with precise spatial control. This bifunctional system could be modified to control larger metabolic processes by incorporating aptamers for a variety of cascading enzymes.

Typically, aptamers are used to recruit enzymes to nucleic acid scaffolds; however, aptamers can also be used as connectors between structural components of the scaffolds. The ability of aptamers to aid both in the recruitment of proteins and in structural functions demonstrates the versatility of aptamer−nucleic acid nanostructure combinations. Willner continued the use of RCA to produce anticocaine aptamer-decorated DNA nanostructures. Interestingly, the aptamers self-assembled in the presence of cocaine and acted as connectors attaching the DNA nanounits into nanowires.[470] To functionalize the nanowires with proteins, horseradish peroxidase (HRP) and glucose oxidase (GOx) were linked to thiolated nucleic acids that hybridized to the circular DNA nanounits (Figure 45C). The oxidization activity of the enzymes increased by 6-fold compared to a disorganized solution of the two free enzymes. The improved catalytic activity was attributed to an increase in local concentration of the two interdependent components and enhanced substrate shuttling of the first reaction product to the second reactive site.

Compared to DNA nanostructures, RNA nanostructures are more compatible for *in vivo* applications. In 2011, Delebecque and colleagues created the first aptamer-decorated RNA nanostructures to influence metabolic processes *in vivo*.[471] The group created RNA components that assembled into 0D, 1D, and 2D scaffolds in bacterial cells (Figure 45D). These scaffolds contained two aptamers that functioned as docking sites for enzymes involved in a hydrogen-producing pathway. Hydrogen biosynthesis was analyzed by gas chromatography, and it was shown that hydrogen production could be controlled via scaffold architecture *in vivo* and scaffolded hydrogen production could be increased up to 1.4 times higher than unscaffolded production. This work was furthered in 2014 by the construction of RNA nanostructures with the ability to colocalize two, three, and four enzymes using aptamer docking sites *in vivo*.[472] The two-enzyme system was organized on 0D, 1D, and 2D scaffolds to influence the pentadecane production pathway in *E. coli*. The metabolic activity increased with structural complexity, with the 2D scaffold leading to 2.4-fold higher production levels compared to nonscaffolded enzymes. The three- and four-enzyme systems were assembled on 2D scaffolds to increase metabolic output from the succinate production pathway. The three-enzyme system on the 2D scaffold was found to cause an 83% increase in succinate production compared to enzymes with no scaffold, while the four-enzyme system on the 2D scaffold caused an 88% increase. This technology presents the potential for aptamer-functionalized RNA nanostructures to enhance periodic protein processes *in vivo* and could be advantageous in areas such as biofuels, biosensing, and biocatalysis.

5.7. Control of Gene Expression

Control of gene expression is critical for many biological applications, from protein level optimization to disease prevention. Gene expression begins with transcription, and consequently, many technologies have focused on targeting transcription processes. Both activation and deactivation of transcription processes have been achieved using a myriad of technologies, including aptamer-mediated RNA nanotechnology. Transcription activators are known to be involved in the recruitment of RNA polymerase to specific DNA locations and turn on gene expression. Shi developed an RNA-based activator by converting an inhibitory aptamer into an activation aptamer and placing it on a 3WJ nanostructure that also contained an indirect DNA binding domain (Figure 46).[473] The RNA construct was able to increase transcription activity, was easy to design, and had less immunogenicity *in vivo* compared to its protein equivalents. This paved the way for the use of RNA aptamer nanostructures to modify genetic processes.

CRISPR−Cas9 systems are used to directly modify DNA genetic code, and deactivated Cas9 (CRISPR−dCas9) can be used to moderate transcription and epigenetic processes. These systems consist of single guide RNAs (sgRNAs) that direct the Cas protein to promoter regions of genes to regulate gene expression; however, the targeting capabilities of sgRNAs are limited. Thus, in 2015, Konermann and colleagues developed a transcription activating CRISPR−dCas9 system led by an aptamer-decorated sgRNA to upregulate transcription more efficiently than typical sgRNA sequences.[474] The aptamers were used to recruit effectors that increase transcription activity, and aptamer-decorated systems resulted in up to a 12-fold increase in upregulation compared to nonaptamer systems.

5.8. Logic Gate-Based Smart Nanodevices

Aptamer-based logic gates are promising nanodevices for creating advanced targeted delivery systems and multiplexed biosensing platforms. Logic gates of varying degrees of complexity have been designed for molecular computation, and the use of DNA as a construction material has been a valuable development in the field of smart nanodevices. Decoration of multivalent aptamers on self-assembled DNA nanostructures has the potential to create logic gate-based devices that can be employed in far-reaching applications, from neural network computations using strand displacement

https://doi.org/10.1021/acs.chemrev.0c01332
Chem. Rev. XXXX, XXX, XXX−XXX

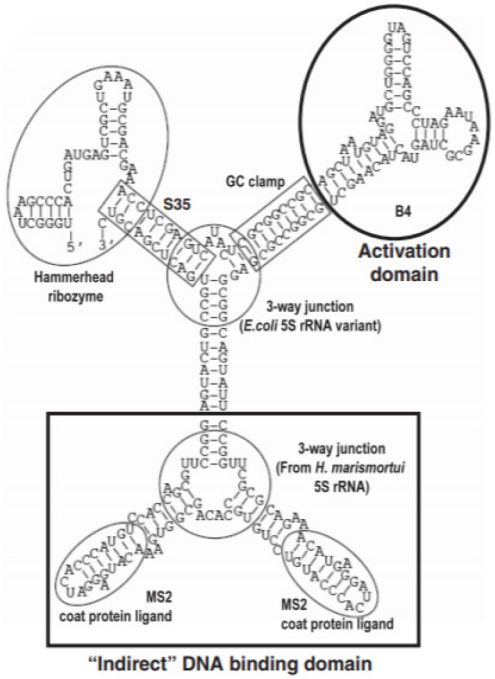

Figure 46. Transcription activator RNA structure predicted by mfold. The structure consists of a 3WJ, activation domain (indicated by a circle), and indirect DNA binding domain (indicated by a square). Adapted from ref 473. Published 2010 Oxford University Press. Licensed under the terms of the Creative Commons Attribution Non-Commercial License (http://creativecommons.org/licenses/by-nc/2.5).

reactions to controlled and programmable delivery of molecular cargo such as therapeutic drugs *in vivo*.[267,475] A crucial property of *in vivo* nucleic acid logic gates is their ability to be functionalized with multiple aptamers, which allows target cell identification based on multiple cell surface markers. This provides several advantages, including improved accuracy of cellular delivery and comprehensive disease diagnosis and treatment.[476]

Nucleic acid nanostructures provide an ideal biocompatible and modularizable platform for biomedical applications, since they can be decorated with several functional motifs, such as aptamers, well-suited for logic gate-based applications. In this section, we focus on the use of logic gate-based, aptamer-functionalized DNA nanostructures as smart nanodevices for targeted delivery and biosensing.

5.8.1. Logic Gate-Based Cell Identification and Smart Targeted Delivery. Multivalent aptamers have been decorated on DNA nanostructures to form target-specific logic gate-based nanorobots and nanomachines. In 2012, Church's group pioneered the use of logic gate-based nanorobots that used aptamers for specific delivery of molecular cargo (Figure 47A).[477] They designed a hollow DNA origami nanostructure self-assembled in a one-pot reaction with an aptamer-based lock mechanism, testing their construct with three well-known aptamers targeting platelet-derived growth factor (PDGF), CCRF-CEM cells, and tyrosine-protein kinase-like 7 (PTK7). The aptamer-complement duplexes functioned as locks on the nanostructure and dissociated in the presence of the targets, unlocking the nanobox and triggering release of the payloads, which were covalently attached to ssDNA linkers. To test opening and closing of the nanomachine, AuNP payloads were used. Later, fluorescently labeled Fab′ antibody fragments were loaded. The nanomachine was only activated in the presence of certain cells expressing human leukocyte antigen, and antibody−antigen binding triggered fluorescence emission. Six nanorobots were designed for six different cell types, and construction of AND logic gates was demonstrated, whereby two different protein inputs were needed to open the aptamer locks. Two years later, the same group designed DNA origami nanorobots for *in vitro* flow cytometric analysis of hemocytes from living cockroaches, *Blaberus discoidalis*.[478] Several different logic gates were constructed using many nanorobots, including AND, OR, NOR, NAND, NOT, CNOT, and half-adder gates, where PDGF and vascular endothelial growth factor (VEGF) were used as inputs. The robot was mechanized by target-induced strand displacement of aptamer−complement duplexes. Inspired by this approach involving strand displacement, You et al. developed AND and INH logic gates functionalized with Sgc8c, Sgc4f, and TC01 aptamers to target cancer biomarkers that were overexpressed on carcinogenic cells, such as CCRF-CEM cells (Figure 47B).[476] Two different shapes of nanostructures were fabricated: a Y-shaped DNA "nanoclaw" carried Sgc8c and TC01 aptamers and an X-shaped nanostructure carrying three aptamers. Both constructs had one end connected to a therapeutic drug or fluorescent reporting dye for biosensing. Specifically, successful photodynamic therapy was demonstrated using a photosensitizer payload.

Various aptamers can be used simultaneously to bind to multiple cell surface markers and activate logic gated DNA nanostructures. This helps to ensure target cells are recognized appropriately without false positives. In 2019, Chang et al. developed aptamer-based DNA nanodevices acting as AND logic gates for single-step cancer cell identification (Figure 47C).[479] Using two and three aptamers targeting different biomarkers on cancer cell membranes, the authors could detect and isolate target cells *in vivo*, using hybridization chain reaction (HCR) mediated by associative toehold activation for fluorescent signal amplification. Importantly, this work demonstrated for the first time isolation of target cells in samples with more than three similar cell types using an AND logic gate, as well as maintenance of signal strength by HCR. Using a similar idea, Ouyang and colleagues have recently developed a dual-purpose logic gate-based DNA nanostructure for cancer cell identification and targeted cancer therapy (Figure 47D).[480] AND logic gates were constructed and functionalized with three aptamer bioreceptors, which guided the rod-shaped nanostructure to the appropriate target cells and triggered its disassembly, resulting in release of the doxorubicin payload. Target binding and identification was confirmed using fluorescence labeling. The nanotubes exhibited excellent biostability and efficient cellular penetration, and the aptamer-integrated logic gate-based approach helped maintain target specificity and avoid off-target effects.

5.8.2. Logic Gate-Based Smart Biosensors. Logic gate-based smart biosensors have been developed for programmed recognition of biochemical analytes. In 2012, Fan's group designed tetrahedral DNA nanostructures (TDNs) for intracellular ATP detection.[267] By integrating different functional motifs into edges of the tetrahedron, such as anti-ATP aptamers and i-motifs, the authors constructed AND, OR, XOR, INH, and half-adder logic gates for multiplex intelligent sensing of small molecules. Four years later, Yang et al. constructed AND, OR, and YES DNA origami tile-based logic gates functionalized with aptamers and DNAzymes for simultaneous detection of ATP

https://doi.org/10.1021/acs.chemrev.0c01332
Chem. Rev. XXXX, XXX, XXX−XXX

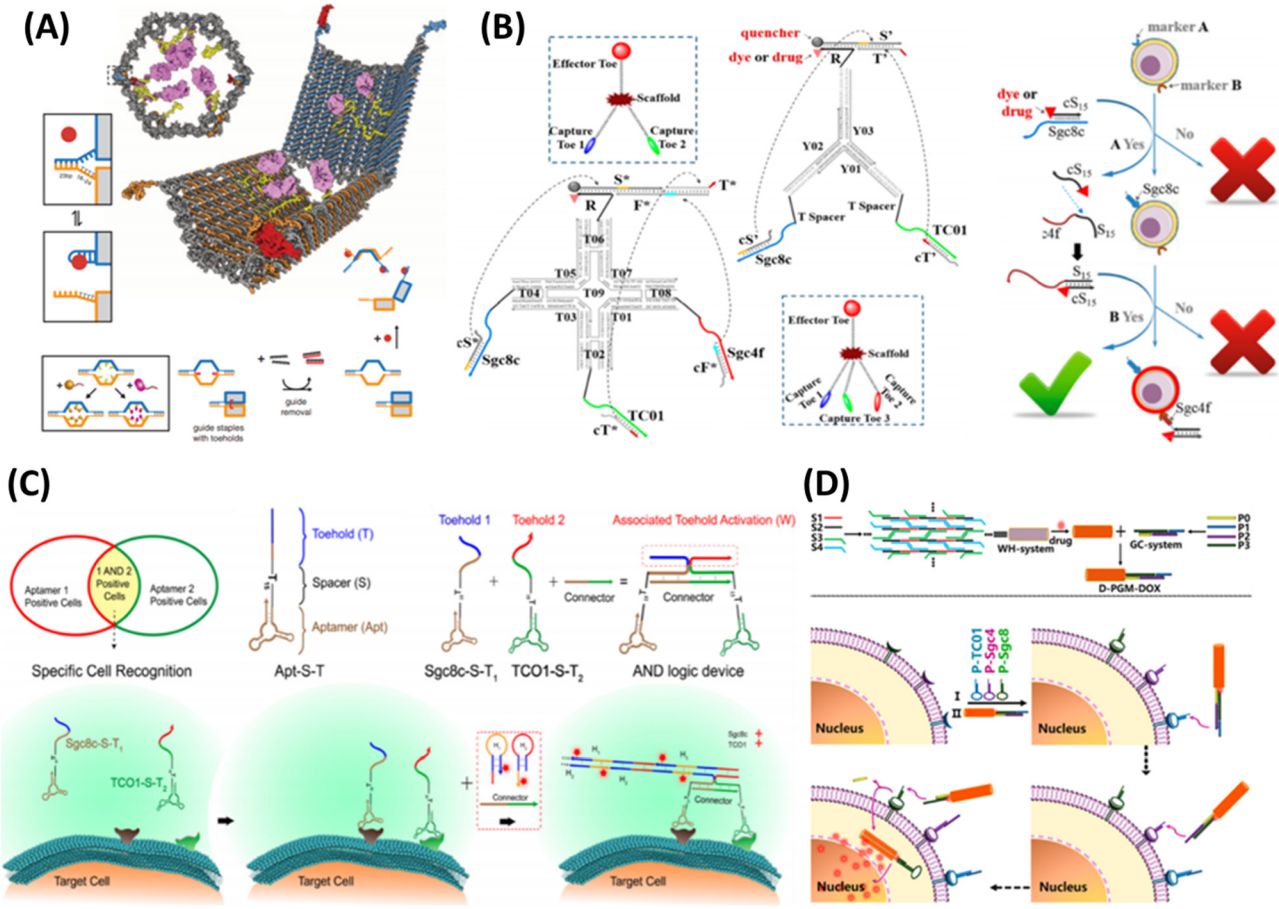

Figure 47. Multivalent aptamer-decorated DNA nanodevices acting as logic gates. (A) DNA nanorobot functionalized with antibody payload and locks consisting of aptamers binding PDGF, PTK7, and CCRF-CEM cells. Adapted with permission from ref 477. Copyright 2012 The American Association for the Advancement of Science. (B) DNA "nanoclaw" for cancer cell identification and photodynamic therapy. Adapted from ref 476. Copyright 2014 American Chemical Society. (C) AND logic gate for separation and identification of cancer cells in vivo. HCR was applied for signal amplification. Adapted from ref 479. Copyright 2019 American Chemical Society. (D) Three-input AND logic gate-based drug delivery system for cancer therapeutics. Rod-shaped nanostructures carry a doxorubicin payload for targeted cancer therapy. Adapted from ref 480. Copyright 2020 American Chemical Society.

and cocaine,[259] and in 2017, Willner's group used multimerized DNA origami smart nanodevices for the same two targets.[279] These works have demonstrated the potential of logic gate-based smart sensing for specific detection of multiple targets.

The application of aptamer-based logic gates in biomedical applications has taken great strides in the past decade. Many groups have successfully fabricated smart aptasensors and aptamer-decorated nucleic acid nanorobots for targeted delivery. The nucleic acid platform allows for decoration with multiple aptamers to operate complex logic gates, resulting in sensitive identification of various targets as well as accurate delivery of precisely guided molecular cargo. However, many of these approaches remain cost- and time-ineffective. For example, most logic gate-based aptasensors still require laborious and expensive sample preparation steps and labeling processes. Furthermore, more work will need to be done to examine the efficacy of aptamer-based smart delivery systems in biological fluids such as whole blood samples. Overcoming these challenges, aptamer-based smart devices could emerge as valuable clinical and biomedical tools for applications ranging from disease diagnosis to therapeutics.

5.9. Stimuli-Responsive Nucleic Acid Hydrogels

Hydrogels are excellent materials that have found application in numerous avenues of research, including therapy and biosensing. They have been extensively developed, given that they were the first biomaterials fabricated for use inside the human body.[481] Traditional hydrogels have been synthesized using cross-linking copolymerization, and polyacrylamide has served as an ideal polymer for hydrogels due to its high water content. More recently, aptamers have been used as cross-linkers in acrylamide hydrogels to provide stimulus-induced hydrogels for biosensing, therapeutic, and drug delivery applications. Conjugation of aptamers with polyacrylamide structures to form hydrogels has allowed detection of small molecules and biomolecules, including adenosine,[482] ATP,[483,484] cocaine,[483,485] and aflatoxin B1.[486]

Recently, DNA has emerged as a promising scaffold for hydrogel formation due to its biocompatibility, biodegradability, inexpensiveness, stability, and multifunctionality.[487] The first hydrogel comprised purely of DNA was developed in 2006 by Um et al.[488] Importantly, DNA hydrogels can easily integrate functional nucleic acids such as DNAzymes, i-motifs, and aptamers, resulting in smart, target-responsive hydrogels that undergo gel-to-sol or sol-to-gel phase changes when the target is

https://doi.org/10.1021/acs.chemrev.0c01332
Chem. Rev. XXXX, XXX, XXX−XXX

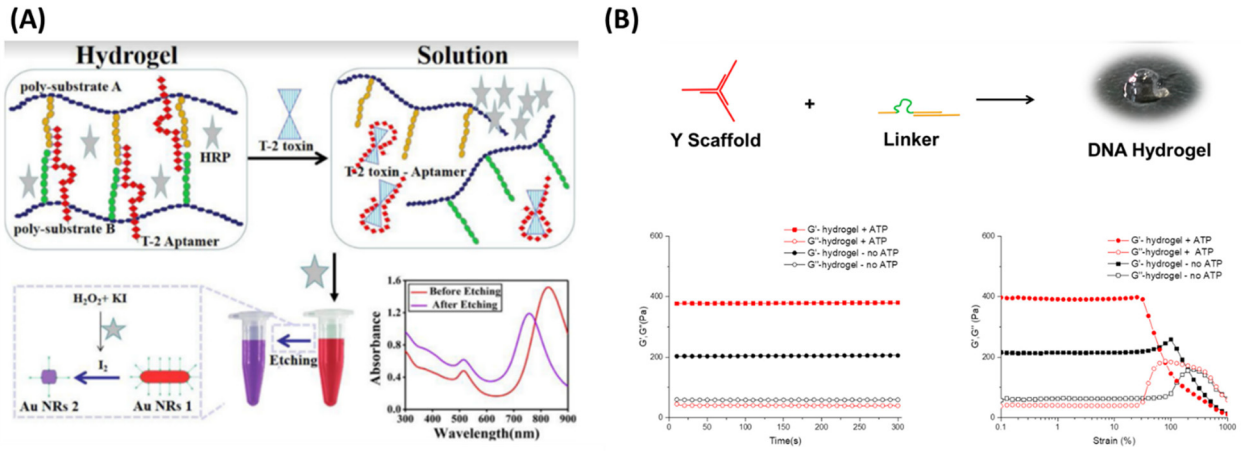

Figure 48. Aptamer-integrated DNA hydrogels. (A) DNA hydrogel with T-2 toxin-targeting aptamer cross-linkers for sensitive fluorescent detection of T-2 toxin. Adapted with permission from ref 491. Copyright 2020 Elsevier. (B) Tunable DNA hydrogel designed from Y-shaped DNA monomer and ATP aptamer with three phases of mechanical strength. Adapted from ref 493. Published 2018 Multidisciplinary Digital Publishing Institute. Licensed under a Creative Commons agreement (http://creativecommons.org/licenses/by/4.0/).

present.[489] Due to the gelling process, they can also bypass the need for explicit cargo loading in drug delivery applications. Furthermore, they can be easily modified for different applications by changing the concentration or type of the monomers that initiate ligation-catalyzed hydrogel synthesis. Given these advantages, it is no surprise that DNA hydrogels have emerged as promising candidates for a variety of biomedical applications, from biosensing and drug delivery to cancer therapy. In this section, we focus on aptamer-conjugated nucleic acid nanostructures that serve as target-responsive hydrogels.

5.9.1. Aptamer-Functionalized DNA Hydrogels for Sensing Applications. DNA hydrogels that use aptamers as cross-linkers have been utilized by multiple groups for biosensing applications. In 2019, Oishi and Nakatani synthesized an aptamer-functionalized DNA hydrogel for ATP sensing.[490] The hydrogel was constructed with a DNA nanocircuit using toehold-mediated strand displacement reactions and underwent a target-responsive phase transition from gel to solution form. As a proof of concept, the authors incorporated cross-linking ATP aptamers and PEGylated gold nanoparticle (AuNP) payloads. ATP presence triggered collapse of the hydrogel and release of the AuNPs from the hydrogel, resulting in a detectable colorimetric signal with a detection limit of approximately 5 μM. Inspired by this work, Sun and colleagues developed a DNA hydrogel biosensor for T-2 mycotoxin, testing detection efficacy in coffee, corn, and soybean samples (Figure 48A).[491] T-2 toxin-binding aptamers served as cross-linkers, and gold nanorods (AuNRs) were integrated into the hydrogel. Toxin−aptamer binding induced dissociation of the hydrogel and release of horseradish peroxidase. The resulting catalysis of AuNR etching caused a detectable shift in the UV spectral peak, which scaled logarithmically with toxin concentration. Importantly, this method demonstrated detection of T-2 mycotoxin over a wide range of concentrations, 0.01−10000 ng/mL, with a detection limit of only 0.87 pg/mL. These works demonstrate the viability of aptamer-integrated DNA hydrogel-based biosensing.

5.9.2. Improvement of Mechanical and Thermodynamic Properties of Nucleic Acid Based Hydrogels. To improve the value of aptamer-functionalized DNA hydrogels in biomedical applications, various groups have worked to enhance the mechanical and thermodynamic properties of these hydrogels. In 2012, Lee and colleagues developed the first DNA hydrogel-based metamaterial.[492] Although no aptamers were used, the authors demonstrated a change in the hydrogel's mechanical properties in the presence or absence of water. Specifically, the hydrogel exhibited a novel hierarchical structure that enabled integration in a circuit using water as a switch. In 2018, Liu et al. integrated ATP aptamers into a previously developed DNA hydrogel (Figure 48B).[493] The hydrogel was comprised of Y-shaped DNA nanostructures joined by ATP aptamers. Importantly, the authors demonstrated tunability of the hydrogel's mechanical strength. ATP binding triggered a conformational change of the aptamer to a more rigid secondary structure that increased mechanical strength nearly 2-fold, and further increases in mechanical strength were observed on addition of the aptamer's complementary strand. Given this tunability, DNA hydrogels could serve as valuable biomaterials in tissue engineering. Using a similarly structured hydrogel, Plaxco's group investigated the effects of changing the thermodynamic stability of an adenosine aptamer-functionalized DNA hydrogel.[494] By varying the degree of hybridization between the gel's Y-shaped DNA monomer and the aptamer, the cross-linking stability was changed. This allowed control over the kinetics of target-induced dissolution as well as the gel's mechanical strength. Specifically, greater cross-linking stability corresponded to greater mechanical strength and longer dissolution times. Together, these works represent successes in modulating thermodynamic and mechanical stability for greater control in developing target-responsive hydrogels.

5.9.3. Nanohydrogels for Biomedical Applications. Many therapeutic agents are successful *in vitro* but fail *in vivo* due to degradation in harsh environments or failure to efficiently find their target. Delivery vectors therefore largely determine the safety, efficiency, and success of therapeutic agents. To combat the nuclease degradation and short retention times observed for therapeutic nucleic acids, DNA nanohydrogels have been constructed for biomedical application and are being developed as replacements for traditional vectors, such as viral vectors, due to their safety. For example, most gene therapies utilize viral vectors for delivery, but there has been a push for nonviral vectors due to the risks of viral delivery, such as unintended genome alterations.[495] Unfortunately, many nonviral vectors

https://doi.org/10.1021/acs.chemrev.0c01332
Chem. Rev. XXXX, XXX, XXX−XXX

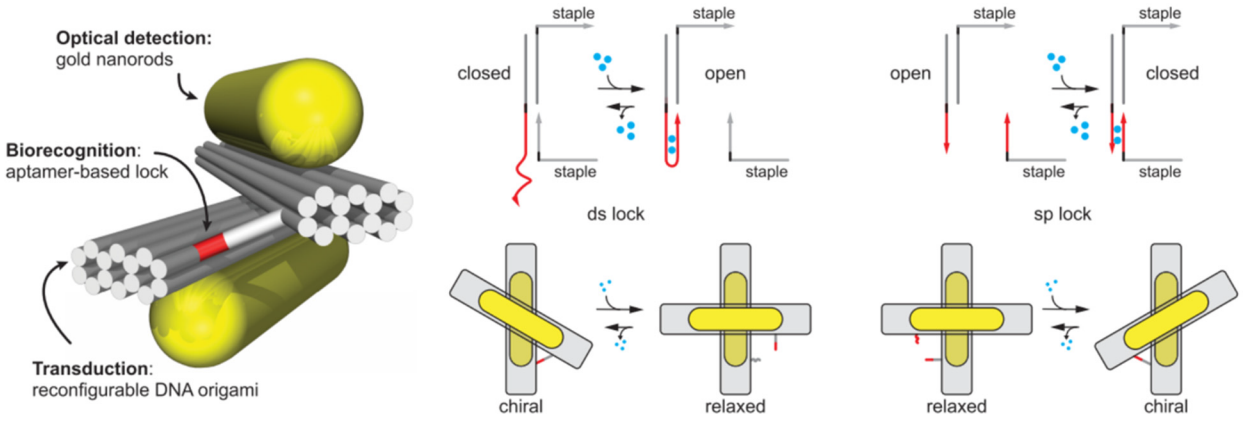

Figure 49. Reconfigurable aptamer-decorated DNA origami nanoplasmonic architecture for adenosine sensing. The orientation of the gold nanorods is sensitively modulated by an aptamer lock mechanism and directly determines the chiral configuration of the nanostructure and its CD spectral strength. Adapted from ref 500. Copyright 2018 American Chemical Society.

have lower transfection rate compared to their viral counterparts, creating the need for more effective nonviral options. Yang, Tan, and co-workers developed a DNA nanohydrogel that functioned as a gene therapy vector.[386] Their hydrogel consisted of two Y-shaped monomers and a dsDNA cross-linker that were joined by hybridization (Figure 34B). Many DNA hydrogels are difficult to use due to their bulky size, thus the group's approach included hydrogel size control through the adjustment of the ratio between the two Y-DNA monomers. The hydrogel was also made to be target-specific by the inclusion of cancer targeting aptamers used a disulfide linkage for controlled release inside the cytosol, resulting in fine-tuned gene delivery. Nanogels have also been developed as carriers for chemotherapeutics. In 2019, Varghese's group created a DNA−protein hybrid nanogel for targeted cancer therapy.[335] The hydrogel consisted of biotin-modified X-DNA building blocks that were polymerized using streptavidin. The hydrogels also contained cell-specific sgc8 aptamers and were used to load doxorubicin for targeted cancer therapy. DNA nanohydrogels have also been employed for immunotherapy vehicles. In 2019, Lee et al. used RCA to develop an advanced DNA hydrogel for blocking immune checkpoints.[432] The hydrogel consisted of PD-1 aptamers and sgRNA-targeting sequences (Figure 38A). Once delivered, the hydrogel could be dissolved using a Cas9/sgRNA complex, resulting in release of anticancer immunotherapeutic aptamers. The hydrogel allowed the aptamers to remain at the injection site longer and provided higher antitumor effects compared to free aptamers. DNA nanohydrogels have been used as vectors to deliver gene therapeutic, chemotherapeutic, and immunotherapeutic cargos. The hydrogels are safe and effective alternatives to many common delivery vehicles, such as virions, due to their low immunogenicity, lack of genomic incorporation, increased nuclease resistance, and targeted delivery with aptamer incorporation.

5.10. Nanoplasmonic Devices

The field of nanoplasmonics has focused on the development of devices that uniquely optimize the interaction between light and matter at the nanoscale. Recently, much work has been conducted in applying nanoplasmonic devices to biosensing applications. These plasmonic-based sensing devices offer benefits of signal-enhanced and label-free optical detection. They have been applied as portable, cost-effective, and real-time biosensors in a variety of clinical applications.[496,497] Although nanoplasmonic devices offer structure tunability, their fabrication can sometimes be a tedious process.[498] To overcome this challenge, DNA origami has provided a promising method to self-assemble reconfigurable and controllable nucleic acid-based nanoplasmonic devices. The DNA origami platform allows decoration with target-specific functional modules for biosensing applications. DNA "locks" have been decorated on origami for nucleic acid sensing, but aptamer-integrated DNA origami nanoplasmonic systems allow expansion to biomolecule and small molecule analytes, with decoration of multiple aptamers permitting simultaneous detection of different targets.[499,500] These systems often consist of conformation-changing chiral assemblies that change circular dichroism (CD) spectral strength in response to aptamer−target binding. This sensing method offers high signal-to-noise ratios and allows for analyte detection even in strongly absorbing biological fluids.[501]

DNA origami-based plasmonic nanodevices have served as valuable light-responsive nanosensors with unique optical properties. However, most architectures are responsive only to single stimuli. In 2018, to design a plasmonic system responsive to multiple stimuli, Zhou and colleagues integrated split ATP and cocaine aptamers and two gold nanorods (AuNRs) on a rectangular DNA origami plate and rotary bundle.[277] The aptamers enabled target-specific sensing, while the orientation of the AuNRs directly determined the chiral state and thus optical response. The origami was sensitive to both temperature changes and aptamer-target binding. Specifically, stronger circular dichroism (CD) spectra were observed for lower temperatures and ATP/cocaine presence. By decorating both types of split aptamers on the DNA origami, the authors demonstrated multiplex sensing of ATP and cocaine. Inspired by this work, Huang and colleagues used a similar construct to detect adenosine (Figure 49).[500] Their DNA origami plasmonic nanostructure consisted of two helix bundles and two AuNRs functionalized with two kinds of aptamer locks: double-stranded locks, consisting of an aptamer and its complementary strand, and split aptamer locks. CD spectral strength was observed to decrease with increasing adenosine concentration, due to conformational changes to a more relaxed state. The plasmonic system had a response time of tens of minutes and a detection limit of 270 μM. In order to expand to protein analytes, Funck et al. functionalized their DNA origami with two thrombin-binding aptamers.[275] Aptamer−thrombin binding was found to cause an inversion of chirality and a quantitative change in CD spectra.

https://doi.org/10.1021/acs.chemrev.0c01332
Chem. Rev. XXXX, XXX, XXX−XXX

The authors achieved a detection limit comparable to thrombin sensing using traditional assays such as FRET and ELISA.

Together, the results of these studies demonstrate the growing potential of nucleic acid origami-based plasmonic nanosensors, which offer the possibility of light-responsive and label-free biosensing. These nanoplasmonic devices based on aptamer-bearing DNA nanostructures are not limited to sensing applications but also show promise for various applications in optoelectronics, optomechanics, and photovoltaic devices.

6. CONCLUSION AND OUTLOOK

In this review, we have attempted to summarize the relevant literature and convey the scientific advances and technological promise of self-assembling nucleic acid nanostructures decorated with aptamers as functional affinity handles. Obviously, this topic is currently large enough that we have been unable to refer specifically to every published report within every subtopic, and for this we apologize to any authors whose papers have been neglected here. However, we believe that we have adequately pointed out the historical trends and potential application areas, such that the avid reader now possesses sufficient signposts from which to dig deeper into the primary literature. We have reviewed application areas for this technology including as smart drug delivery vehicles, therapeutics, biosensing and bioimaging agents, cell signaling complexes, stimulus-responsive materials, enzyme cascade organizers, and even molecular computing devices.

Nucleic acid nanotechnology offers a highly useful biomolecular platform shown to function well with appended aptamers and can be applied in wide ranging application areas, as described in this review. However, many factors, including stability, freedom of designs, design tools, cost of production, and chemical modifications also need to be considered when choosing materials (DNA, RNA, and DNA/RNA hybrid) with which to construct nanomaterials. Stability of nucleic acids is one of the main issues of concern. Both DNA and RNA are swiftly degraded in the presence of nuclease enzymes; however, nucleic acid nanostructures have been successfully redesigned and developed specifically to minimize degradation by nucleases.[502,503] Additionally, chemical modifications on nucleic acid nanostructures enhancing nuclease resistance activity have been developed.[412,415,504] For freedom of design, DNA nanostructures have been created with a wide range of architectures, in arbitrary shapes (from rigid to wireframe structures) and many length scales (from nano- to micrometer size) that are versatile and provide larger and more sophisticated designs than RNA or DNA/RNA hybrid nanostructures.[4,8,505−507] Computer-aided design software is crucial for spreading design skills and experience to a wider community and for moving the field forward. User-friendly semiautomated and automated software tools for designing DNA nanostructures, in particular DNA origami have been extensively developed and are available online.[39,41,508−510] However, software customized for designing RNA and DNA/RNA hybrid materials are, thus far, limited. For example, semi- and automated computer-aided design for RNA origami is currently not available.[511] When dedicated RNA design software does become available, the ever expanding library of natural and artificial motifs and secondary and tertiary structures of RNA will make available the large design space and accessible complexity of RNA structures to biomolecular engineers. The cost of production of DNA via chemical synthesis has rapidly decreased over the past decade, offering economical advantage for construction of DNA nanostructures, while the synthesis cost of RNA still remains relatively high. With current technology, chemical synthesis of long ssDNA (larger than 200 nt) and ssRNA (more than 120 nt) remains very challenging. However, ultralong, single-stranded RNA can be produced via *in vitro* transcription, thus reducing the cost of production.[103,107,181] A potential benefit of RNA for nanostructure fabrication is that it can be transcribed and cotranscriptionally folded inside cells isothermally, without the need for thermal annealing, providing great benefit over DNA nanostructures for *in vivo* applications including biosensors and metabolic engineering.[104,471,512] Both DNA and RNA nanostructures offer different advantages and disadvantages; therefore choosing which type of nucleic acid is best for particular studies or applications will remain a necessary part of the design process.

The pace of development in this field has been accelerated by the modularity of functional nucleic acid structures, where subunits created along independent pathways have been shown to maintain structure and function when integrated into larger molecular systems. We have seen designable modules such as the double-crossover motifs of structural DNA nanotechnology as well as selectable modules such as RNA and DNA aptamers combined almost seamlessly with structural and functional substructures copied directly from biology, such as RNA kissing-loops. Researchers have referred to this third set of modules as "biokleptic" or stolen directly from nature to highlight the comparison with "bioinspired" or "biomimetic" designs. We have also touched briefly on the ability to integrate modules from different biopolymer types including peptides and proteins. Elucidation of further natural and artificial molecular structures at atomic resolution will likely add to our toolbox of substructures useful for future modular design efforts.

Future development of structural nucleic acid nanotechnology could be expected to follow the established trend of increasing length scale and complexity. Bottom-up assembly of programmed macromolecules began at the low nanoscale but is rapidly approaching the macroscale in both two and three dimensions. Hierarchically assembled 3D molecular materials hold promise for a wide range of programmable fabrication efforts in application areas as diverse as biological tissue engineering and nanoelectronics production. Molecular-level control of self-assembling materials might provide access to previously unavailable points of interest for nanoelectronics along the quantum/classical continuum. The DNA hydrogels mentioned briefly above will probably gain complexity of function and control and be applied to new practical uses. The obvious biocompatibility of nucleic acid-based materials also suggests increased use in future biomedical applications. Overall, the highly successful engineering of artificial nucleic acid assemblies observed thus far suggests a bright future for this line of research.

AUTHOR INFORMATION

Corresponding Author

Thomas H. LaBean − *Department of Materials Science and Engineering, College of Engineering, North Carolina State University, Raleigh, North Carolina 27695, United States;* orcid.org/0000-0002-6739-2059; Email: thlabean@ncsu.edu

https://doi.org/10.1021/acs.chemrev.0c01332
Chem. Rev. XXXX, XXX, XXX−XXX

Authors

Abhichart Krissanaprasit − *Department of Materials Science and Engineering, College of Engineering, North Carolina State University, Raleigh, North Carolina 27695, United States*

Carson M. Key − *Department of Biomedical Engineering, Duke University, Durham, North Carolina 27708, United States*

Sahil Pontula − *Department of Physics and Department of Electrical Engineering and Computer Science, Massachusetts Institute of Technology, Cambridge, Massachusetts 02139, United States;* orcid.org/0000-0002-0230-0176

Complete contact information is available at: https://pubs.acs.org/10.1021/acs.chemrev.0c01332

Notes

The authors declare no competing financial interest.

Biographies

Abhichart Krissanaprasit obtained his Ph.D. in Biotechnology from the lab of Prof. W. Surareungchai at King Mongkut's University of Technology Thonburi, Thailand. His Ph.D. dissertation focused on utilizing DNA nanostructures for development of multiplexed biosensing platforms and molecular machines. He then became a postdoctoral researcher in Prof. Gothelf's group at Aarhus University, Denmark, where he developed programmable polymer−DNA conjugates on DNA origami. Currently, he is a postdoctoral researcher in the LaBean group, a Biomolecular Materials lab, at North Carolina State University. His current research focuses on nucleic acid nanotechnology for therapeutic applications.

Carson M. Key obtained her B.S. degree in Materials Science and Engineering from North Carolina State University. During her time at NC State, she was a member of the LaBean lab where she focused on the development of nucleic acid origami anticoagulants. In 2020, she was awarded an NSF Graduate Research Fellowship for biomedical engineering. Carson Key is currently a graduate student in the Gersbach Lab, a part of the Center for Advanced Genomic Technologies at Duke University. Her current research focuses on viral delivery of genetic engineering technologies.

Sahil Pontula is a first-year undergraduate student at the Massachusetts Institute of Technology (MIT) majoring in Physics and Electrical Engineering. As a high school student, he was a National Science Olympiad gold medalist and a bronze medalist at the International Olympiad on Astronomy and Astrophysics. At the 2019 Research Science Institute at MIT, he was awarded the Regeneron top research paper award for his computational physics research on applying machine learning to parameter extraction and inverse design. He was also selected as a Regeneron Science Talent Search Top 300 scholar for applying this research to pollutant models. He has been a member of North Carolina State University's LaBean lab since 2017, working to develop RNA origami anticoagulants and was a member of the lab's second-place team at the 2018 International BIOMOD competition.

Thomas H. LaBean is a Professor in the Department of Materials Science and Engineering at North Carolina State University. He received his B.S. in biochemistry from Michigan State University and his Ph.D. in biochemistry from the University of Pennsylvania. He spent many years at Duke University, starting as a postdoctoral researcher working on protein design in the Biochemistry Department and finally as a Research Professor pursuing nucleic acid engineering with appointments in the Departments of Computer Science, Chemistry, and Biomedical Engineering. He has been at NCSU since 2011 and was awarded tenure there in 2012. His research group currently focuses on design and implementation of self-assembling macromolecular systems for biomedical applications and for the bottom-up fabrication of nanoelectronics.

ACKNOWLEDGMENTS

The authors acknowledge support from the National Science Foundation including recent grants to T.H.L. (1559077, 1603179, 1709010, and 1825398), as well as funding from the North Carolina Biotechnology Center (NCBC-2021-TRG-6705), and a 2020 award from the NCSU Chancellor's Innovation Fund.

LIST OF ABBREVIATIONS

3WJ	three-way junction
AFB1	aflatoxin B1
AFM	atomic force microscope
AMP	adenosine monophosphate
AuNP	gold nanoparticle
BHQ	black hole quencher
bp	base pairing
CHA	catalytic hairpin assembly
DNA	deoxyribonucleic acid
DNAzymes	deoxyribozymes
DOX	doxorubicin
dsDNA	double-stranded DNA
dsRNA	double-stranded RNA
DX	double crossover
FRET	Förster resonance energy transfer
hAGT	human O6-alkylguanine-DNA alkyltransferase enzyme
HCR	hybridization chain reaction
HCV	hepatitis C virus
HIV	human immunodeficiency virus
HRP	horseradish peroxidase
hVEGF	vascular endothelial growth factor
IRES	internal ribosomal entry site
KL	kissing loop
LR	loop-receptor
MB	methylene blue
MGA	malachite green aptamer
MSO	mercury-specific oligonucleotide
N-WJ	*N*-way junction
NAN	nucleic acid nanoparticle
PCR	polymerase chain reaction
PLK1	polo-like kinase 1
pRNA	packaging RNA
PSMA	prostate specific membrane antigen
PTK7	protein tyrosine kinase 7
RA	right angle
RCA	rolling circle amplification
RCR	rolling circle replication
RCT	rolling circle transcription
RNA	ribonucleic acid
RNAi	RNA interference
RNP	RNA−protein complex
ROS	reactive oxygen species
RT-PCR	reverse transcription polymerase chain reaction
SELEX	systematic evolution of ligands by exponential enrichment
sgRNA	single guide RNA
siRNA	small interfering RNA
ssDNA	single-stranded DNA
ssRNA	single-stranded RNA

https://doi.org/10.1021/acs.chemrev.0c01332
Chem. Rev. XXXX, XXX, XXX−XXX

SVV	Seneca Valley virus
TDN	tetrahedral DNA nanostructure
TEM	transmission electron microscope

REFERENCES

(1) Seeman, N. C. DNA in a Material World. *Nature* **2003**, *421*, 427−431.
(2) Li, H.; Carter, J. D.; LaBean, T. H. Nanofabrication by DNA Self-Assembly. *Mater. Today* **2009**, *12*, 24−32.
(3) Tørring, T.; Voigt, N. V.; Nangreave, J.; Yan, H.; Gothelf, K. V. DNA Origami: A Quantum Leap for Self-Assembly of Complex Structures. *Chem. Soc. Rev.* **2011**, *40*, 5636−5646.
(4) Hong, F.; Zhang, F.; Liu, Y.; Yan, H. DNA Origami: Scaffolds for Creating Higher Order Structures. *Chem. Rev.* **2017**, *117*, 12584−12640.
(5) Ishikawa, J.; Furuta, H.; Ikawa, Y. RNA Tectonics (TectoRNA) for RNA Nanostructure Design and Its Application in Synthetic Biology. *Wiley Interdiscip. Rev. RNA* **2013**, *4*, 651−664.
(6) Grabow, W. W.; Jaeger, L. RNA Self-Assembly and RNA Nanotechnology. *Acc. Chem. Res.* **2014**, *47*, 1871−1880.
(7) Haque, F.; Pi, F.; Zhao, Z.; Gu, S.; Hu, H.; Yu, H.; Guo, P. RNA Versatility, Flexibility, and Thermostability for Practice in RNA Nanotechnology and Biomedical Applications. *Wiley Interdiscip. Rev. RNA* **2018**, *9*, e1452.
(8) Ohno, H.; Akamine, S.; Saito, H. RNA Nanostructures and Scaffolds for Biotechnology Applications. *Curr. Opin. Biotechnol.* **2019**, *58*, 53−61.
(9) Osborne, S. E.; Ellington, A. D. Nucleic Acid Selection and the Challenge of Combinatorial Chemistry. *Chem. Rev.* **1997**, *97*, 349−370.
(10) Famulok, M.; Hartig, J. S.; Mayer, G. Functional Aptamers and Aptazymes in Biotechnology, Diagnostics, and Therapy. *Chem. Rev.* **2007**, *107*, 3715−3743.
(11) Tan, W.; Donovan, M. J.; Jiang, J. Aptamers from Cell-Based Selection for Bioanalytical Applications. *Chem. Rev.* **2013**, *113*, 2842−2862.
(12) Wilner, O. I.; Willner, I. Functionalized DNA Nanostructures. *Chem. Rev.* **2012**, *112*, 2528−2556.
(13) Krishnan, Y.; Seeman, N. C. Introduction: Nucleic Acid Nanotechnology. *Chem. Rev.* **2019**, *119*, 6271−6272.
(14) Pedersen, R.; Marchi, A. N.; Majikes, J.; Nash, J. A.; Estrich, N. A.; Courson, D. S.; Hall, C. K.; Craig, S. L.; LaBean, T. H. *Properties of DNA*; Springer-Verlag: Berlin Heidelberg, 2014.
(15) Seeman, N. C. Nucleic Acid Junctions and Lattices. *J. Theor. Biol.* **1982**, *99*, 237−247.
(16) Seeman, N. C.; Kallenbach, N. R. Design of Immobile Nucleic Acid Junctions. *Biophys. J.* **1983**, *44*, 201−209.
(17) Li, X.; Yang, X.; Qi, J.; Seeman, N. C. Antiparallel DNA Double Crossover Molecules as Components for Nanoconstruction. *J. Am. Chem. Soc.* **1996**, *118*, 6131−6140.
(18) Winfree, E.; Liu, F.; Wenzler, L. A.; Seeman, N. C. Design and Self-Assembly of Two-Dimensional DNA Crystals. *Nature* **1998**, *394*, 539−544.
(19) Yan, H.; Park, S. H.; Finkelstein, G.; Reif, J. H.; LaBean, T. H. DNA-Templated Self-Assembly of Protein Arrays and Highly Conductive Nanowires. *Science* **2003**, *301*, 1882−1884.
(20) Liu, D.; Wang, M.; Deng, Z.; Walulu, R.; Mao, C. Tensegrity: Construction of Rigid DNA Triangles with Flexible Four-Arm DNA Junctions. *J. Am. Chem. Soc.* **2004**, *126*, 2324−2325.
(21) Ke, Y.; Liu, Y.; Zhang, J.; Yan, H. A Study of DNA Tube Formation Mechanisms Using 4-, 8-, and 12-Helix DNA Nanostructures. *J. Am. Chem. Soc.* **2006**, *128*, 4414−4421.
(22) Majumder, U.; Rangnekar, A.; Gothelf, K. V.; Reif, J. H.; LaBean, T. H. Design and Construction of Double-Decker Tile as a Route to Three-Dimensional Periodic Assembly of DNA. *J. Am. Chem. Soc.* **2011**, *133*, 3843−3845.
(23) Hansma, P.; Elings, V.; Marti, O.; Bracker, C. Scanning Tunneling Microscopy and Atomic Force Microscopy: Application to Biology and Technology. *Science* **1988**, *242*, 209−216.
(24) Shih, W. M.; Quispe, J. D.; Joyce, G. F. A 1.7-Kilobase Single-Stranded DNA that Folds into a Nanoscale Octahedron. *Nature* **2004**, *427*, 618−621.
(25) Rothemund, P. W. K. Folding DNA to Create Nanoscale Shapes and Patterns. *Nature* **2006**, *440*, 297−302.
(26) Marchi, A. N.; Saaem, I.; Vogen, B. N.; Brown, S.; LaBean, T. H. Toward Larger DNA Origami. *Nano Lett.* **2014**, *14*, 5740−5747.
(27) Rajendran, A.; Endo, M.; Katsuda, Y.; Hidaka, K.; Sugiyama, H. Programmed Two-Dimensional Self-Assembly of Multiple DNA Origami Jigsaw Pieces. *ACS Nano* **2011**, *5*, 665−671.
(28) Liu, W.; Zhong, H.; Wang, R.; Seeman, N. C. Crystalline Two-Dimensional DNA-Origami Arrays. *Angew. Chem., Int. Ed.* **2011**, *50*, 264−267.
(29) Tikhomirov, G.; Petersen, P.; Qian, L. Fractal Assembly of Micrometre-Scale DNA Origami Arrays with Arbitrary Patterns. *Nature* **2017**, *552*, 67−71.
(30) Yin, P.; Hariadi, R. F.; Sahu, S.; Choi, H. M. T.; Park, S. H.; LaBean, T. H.; Reif, J. H. Programming DNA Tube Circumferences. *Science* **2008**, *321*, 824−826.
(31) Wei, B.; Dai, M.; Yin, P. Complex Shapes Self-Assembled from Single-Stranded DNA Tiles. *Nature* **2012**, *485*, 623−626.
(32) Ke, Y.; Ong, L. L.; Shih, W. M.; Yin, P. Three-Dimensional Structures Self-Assembled from DNA Bricks. *Science* **2012**, *338*, 1177−1183.
(33) He, Y.; Ye, T.; Su, M.; Zhang, C.; Ribbe, A. E.; Jiang, W.; Mao, C. Hierarchical Self-Assembly of DNA into Symmetric Supramolecular Polyhedra. *Nature* **2008**, *452*, 198−201.
(34) Douglas, S. M.; Dietz, H.; Liedl, T.; Högberg, B.; Graf, F.; Shih, W. M. Self-Assembly of DNA into Nanoscale Three-Dimensional Shapes. *Nature* **2009**, *459*, 414−418.
(35) Dietz, H.; Douglas, S. M.; Shih, W. M. Folding DNA into Twisted and Curved Nanoscale Shapes. *Science* **2009**, *325*, 725−730.
(36) Han, D.; Pal, S.; Nangreave, J.; Deng, Z.; Liu, Y.; Yan, H. DNA Origami with Complex Curvatures in Three-Dimensional Space. *Science* **2011**, *332*, 342−346.
(37) Andersen, E. S.; Dong, M.; Nielsen, M. M.; Jahn, K.; Subramani, R.; Mamdouh, W.; Golas, M. M.; Sander, B.; Stark, H.; Oliveira, C. L. P.; et al. Self-Assembly of a Nanoscale DNA Box with a Controllable Lid. *Nature* **2009**, *459*, 73−76.
(38) Wagenbauer, K. F.; Sigl, C.; Dietz, H. Gigadalton-Scale Shape-Programmable DNA Assemblies. *Nature* **2017**, *552*, 78−83.
(39) Benson, E.; Mohammed, A.; Gardell, J.; Masich, S.; Czeizler, E.; Orponen, P.; Högberg, B. DNA Rendering of Polyhedral Meshes at the Nanoscale. *Nature* **2015**, *523*, 441−444.
(40) Zhang, F.; Jiang, S.; Wu, S.; Li, Y.; Mao, C.; Liu, Y.; Yan, H. Complex Wireframe DNA Origami Nanostructures with Multi-Arm Junction Vertices. *Nat. Nanotechnol.* **2015**, *10*, 779−784.
(41) Veneziano, R.; Ratanalert, S.; Zhang, K.; Zhang, F.; Yan, H.; Chiu, W.; Bathe, M. Designer Nanoscale DNA Assemblies Programmed from the Top Down. *Science* **2016**, *352*, 1534−1534.
(42) Zheng, J.; Birktoft, J. J.; Chen, Y.; Wang, T.; Sha, R.; Constantinou, P. E.; Ginell, S. L.; Mao, C.; Seeman, N. C. From Molecular to Macroscopic via the Rational Design of a Self-Assembled 3D DNA Crystal. *Nature* **2009**, *461*, 74−77.
(43) Chen, J.; Seeman, N. C. Synthesis from DNA of a Molecule with the Connectivity of a Cube. *Nature* **1991**, *350*, 631−633.
(44) Zhang, Y.; Seeman, N. C. Construction of a DNA-Truncated Octahedron. *J. Am. Chem. Soc.* **1994**, *116*, 1661−1669.
(45) Yan, H.; Zhang, X.; Shen, Z.; Seeman, N. C. A Robust DNA Mechanical Device Controlled by Hybridization Topology. *Nature* **2002**, *415*, 62−65.
(46) Goodman, R. P.; Berry, R. M.; Turberfield, A. J. The Single-Step Synthesis of a DNA Tetrahedron. *Chem. Commun.* **2004**, *12*, 1372−1373.
(47) Erben, C. M.; Goodman, R. P.; Turberfield, A. J. Single-Molecule Protein Encapsulation in a Rigid DNA Cage. *Angew. Chem., Int. Ed.* **2006**, *45*, 7414−7417.
(48) Manuguerra, I.; Croce, S.; El-Sagheer, A. H.; Krissanaprasit, A.; Brown, T.; Gothelf, K. V.; Manetto, A. Gene Assembly via One-Pot

https://doi.org/10.1021/acs.chemrev.0c01332
Chem. Rev. XXXX, XXX, XXX−XXX

Chemical Ligation of DNA Promoted by DNA Nanostructures. *Chem. Commun.* **2018**, *54*, 4529−4532.
(49) Afonin, K. A.; Bindewald, E.; Yaghoubian, A. J.; Voss, N.; Jacovetty, E.; Shapiro, B. A.; Jaeger, L. In Vitro Assembly of Cubic RNA-Based Scaffolds Designed In Silico. *Nat. Nanotechnol.* **2010**, *5*, 676−682.
(50) Khisamutdinov, E. F.; Jasinski, D. L.; Li, H.; Zhang, K.; Chiu, W.; Guo, P. Fabrication of RNA 3D Nanoprisms for Loading and Protection of Small RNAs and Model Drugs. *Adv. Mater.* **2016**, *28*, 10079−10087.
(51) Stewart, J. M.; Viard, M.; Subramanian, H. K. K.; Roark, B. K.; Afonin, K. A.; Franco, E. Programmable RNA Microstructures for Coordinated Delivery of siRNAs. *Nanoscale* **2016**, *8*, 17542−17550.
(52) Stewart, J. M.; Geary, C.; Franco, E. Design and Characterization of RNA Nanotubes. *ACS Nano* **2019**, *13*, 5214−5221.
(53) Halman, J. R.; Satterwhite, E.; Roark, B.; Chandler, M.; Viard, M.; Ivanina, A.; Bindewald, E.; Kasprzak, W. K.; Panigaj, M.; Bui, M. N.; et al. Functionally-Interdependent Shape-Switching Nanoparticles with Controllable Properties. *Nucleic Acids Res.* **2017**, *45*, 2210−2220.
(54) Monferrer, A.; Zhang, D.; Lushnikov, A. J.; Hermann, T. Versatile Kit of Robust Nanoshapes Self-Assembling from RNA and DNA Modules. *Nat. Commun.* **2019**, *10*, 608.
(55) Chen, S.; Hermann, T. RNA-DNA Hybrid Nanoshapes that Self-Assemble Dependent on Ligand Binding. *Nanoscale* **2020**, *12*, 3302−3307.
(56) Ko, S. H.; Su, M.; Zhang, C.; Ribbe, A. E.; Jiang, W.; Mao, C. Synergistic Self-Assembly of RNA and DNA Molecules. *Nat. Chem.* **2010**, *2*, 1050−1055.
(57) Green, L. N.; Subramanian, H. K. K.; Mardanlou, V.; Kim, J.; Hariadi, R. F.; Franco, E. Autonomous Dynamic Control of DNA Nanostructure Self-Assembly. *Nat. Chem.* **2019**, *11*, 510−520.
(58) Agarwal, S.; Franco, E. Enzyme-Driven Assembly and Disassembly of Hybrid DNA-RNA Nanotubes. *J. Am. Chem. Soc.* **2019**, *141*, 7831−7841.
(59) Westhof, E.; Masquida, B.; Jaeger, L. RNA Tectonics: Towards RNA Design. *Folding Des.* **1996**, *1*, R78−R88.
(60) Jaeger, L.; Chworos, A. The Architectonics of Programmable RNA and DNA Nanostructures. *Curr. Opin. Struct. Biol.* **2006**, *16*, 531−543.
(61) Leontis, N. B.; Lescoute, A.; Westhof, E. The Building Blocks and Motifs of RNA Architecture. *Curr. Opin. Struct. Biol.* **2006**, *16*, 279−287.
(62) Chworos, A.; Severcan, I.; Koyfman, A. Y.; Weinkam, P.; Oroudjev, E.; Hansma, H. G.; Jaeger, L. Building Programmable Jigsaw Puzzles with RNA. *Science* **2004**, *306*, 2068−2072.
(63) Severcan, I.; Geary, C.; Verzemnieks, E.; Chworos, A.; Jaeger, L. Square-Shaped RNA Particles from Different RNA Folds. *Nano Lett.* **2009**, *9*, 1270−1277.
(64) Boerneke, M. A.; Dibrov, S. M.; Hermann, T. Crystal-Structure-Guided Design of Self-Assembling RNA Nanotriangles. *Angew. Chem., Int. Ed.* **2016**, *55*, 4097−4100.
(65) Yu, J.; Liu, Z.; Jiang, W.; Wang, G.; Mao, C. De Novo Design of an RNA Tile that Self-Assembles into a Homo-Octameric Nanoprism. *Nat. Commun.* **2015**, *6*, 5724.
(66) Nissen, P.; Hansen, J.; Ban, N.; Moore, P. B.; Steitz, T. A. The Structural Basis of Ribosome Activity in Peptide Bond Synthesis. *Science* **2000**, *289*, 920−930.
(67) Wimberly, B. T.; Brodersen, D. E.; Clemons, W. M.; Morgan-Warren, R. J.; Carter, A. P.; Vonrhein, C.; Hartsch, T.; Ramakrishnan, V. Structure of the 30S Ribosomal Subunit. *Nature* **2000**, *407*, 327−339.
(68) Dibrov, S. M.; Johnston-Cox, H.; Weng, Y. H.; Hermann, T. Functional Architecture of HCV IRES Domain II Stabilized by Divalent Metal Ions in the Crystal and in Solution. *Angew. Chem., Int. Ed.* **2007**, *46*, 226−229.
(69) Dibrov, S. M.; McLean, J.; Parsons, J.; Hermann, T. Self-Assembling RNA Square. *Proc. Natl. Acad. Sci. U. S. A.* **2011**, *108*, 6405−6408.
(70) Ohno, H.; Kobayashi, T.; Kabata, R.; Endo, K.; Iwasa, T.; Yoshimura, S. H.; Takeyasu, K.; Inoue, T.; Saito, H. Synthetic RNA-Protein Complex Shaped Like an Equilateral Triangle. *Nat. Nanotechnol.* **2011**, *6*, 116−120.
(71) Ohno, H.; Inoue, T. Designed Regular Tetragon-Shaped RNA-Protein Complexes with Ribosomal Protein L1 for Bionanotechnology and Synthetic Biology. *ACS Nano* **2015**, *9*, 4950−4956.
(72) Bindewald, E.; Afonin, K.; Jaeger, L.; Shapiro, B. A. Multistrand RNA Secondary Structure Prediction and Nanostructure Design including Pseudoknots. *ACS Nano* **2011**, *5*, 9542−9551.
(73) Parlea, L.; Bindewald, E.; Sharan, R.; Bartlett, N.; Moriarty, D.; Oliver, J.; Afonin, K. A.; Shapiro, B. A. Ring Catalog: A Resource for Designing Self-Assembling RNA Nanostructures. *Methods* **2016**, *103*, 128−137.
(74) Nissan, T. A.; Oliphant, B.; Perona, J. J. An Engineered Class I Transfer RNA with a Class II Tertiary Fold. *RNA* **1999**, *5*, 434−445.
(75) Severcan, I.; Geary, C.; Chworos, A.; Voss, N.; Jacovetty, E.; Jaeger, L. A Polyhedron Made of tRNAs. *Nat. Chem.* **2010**, *2*, 772−779.
(76) Biou, V.; Yaremchuk, A.; Tukalo, M.; Cusack, S. The 2.9 Å Crystal Structure of T. Thermophilus Seryl-tRNA Synthetase Complexed with tRNA(Ser). *Science* **1994**, *263*, 1404−1410.
(77) Shu, D.; Moll, W.-D.; Deng, Z.; Mao, C.; Guo, P. Bottom-up Assembly of RNA Arrays and Superstructures as Potential Parts in Nanotechnology. *Nano Lett.* **2004**, *4*, 1717−1723.
(78) Khisamutdinov, E. F.; Jasinski, D. L.; Guo, P. RNA as a Boiling-Resistant Anionic Polymer Material to Build Robust Structures with Defined Shape and Stoichiometry. *ACS Nano* **2014**, *8*, 4771−4781.
(79) Khisamutdinov, E. F.; Li, H.; Jasinski, D. L.; Chen, J.; Fu, J.; Guo, P. Enhancing Immunomodulation on Innate Immunity by Shape Transition among RNA Triangle, Square and Pentagon Nanovehicles. *Nucleic Acids Res.* **2014**, *42*, 9996−10004.
(80) Jasinski, D. L.; Khisamutdinov, E. F.; Lyubchenko, Y. L.; Guo, P. Physicochemically Tunable Polyfunctionalized RNA Square Architecture with Fluorogenic and Ribozymatic Properties. *ACS Nano* **2014**, *8*, 7620−7629.
(81) Feng, L.; Li, S. K.; Liu, H.; Liu, C. Y.; LaSance, K.; Haque, F.; Shu, D.; Guo, P. Ocular Delivery of pRNA Nanoparticles: Distribution and Clearance after Subconjunctival Injection. *Pharm. Res.* **2014**, *31*, 1046−1058.
(82) Shu, D.; Li, H.; Shu, Y.; Xiong, G.; Carson, W. E., 3rd; Haque, F.; Xu, R.; Guo, P. Systemic Delivery of Anti-miRNA for Suppression of Triple Negative Breast Cancer Utilizing RNA Nanotechnology. *ACS Nano* **2015**, *9*, 9731−9740.
(83) Binzel, D. W.; Shu, Y.; Li, H.; Sun, M.; Zhang, Q.; Shu, D.; Guo, B.; Guo, P. Specific Delivery of miRNA for High Efficient Inhibition of Prostate Cancer by RNA Nanotechnology. *Mol. Ther.* **2016**, *24*, 1267−1277.
(84) Haque, F.; Shu, D.; Shu, Y.; Shlyakhtenko, L. S.; Rychahou, P. G.; Mark Evers, B.; Guo, P. Ultrastable Synergistic Tetravalent RNA Nanoparticles for Targeting to Cancers. *Nano Today* **2012**, *7*, 245−257.
(85) Sharma, A.; Haque, F.; Pi, F.; Shlyakhtenko, L. S.; Evers, B. M.; Guo, P. Controllable Self-Assembly of RNA Dendrimers. *Nanomedicine* **2016**, *12*, 835−844.
(86) Koyfman, A. Y.; Braun, G.; Magonov, S.; Chworos, A.; Reich, N. O.; Jaeger, L. Controlled Spacing of Cationic Gold Nanoparticles by Nanocrown RNA. *J. Am. Chem. Soc.* **2005**, *127*, 11886−11887.
(87) Jaeger, L.; Leontis, N. B. Tecto-RNA: One-Dimensional Self-Assembly through Tertiary Interactions. *Angew. Chem., Int. Ed.* **2000**, *39*, 2521−2524.
(88) Nasalean, L.; Baudrey, S.; Leontis, N. B.; Jaeger, L. Controlling RNA Self-Assembly to Form Filaments. *Nucleic Acids Res.* **2006**, *34*, 1381−1392.
(89) Novikova, I. V.; Hassan, B. H.; Mirzoyan, M. G.; Leontis, N. B. Engineering Cooperative Tecto-RNA Complexes Having Programmable Stoichiometries. *Nucleic Acids Res.* **2011**, *39*, 2903−2917.
(90) Hong, E.; Halman, J. R.; Shah, A. B.; Khisamutdinov, E. F.; Dobrovolskaia, M. A.; Afonin, K. A. Structure and Composition Define Immunorecognition of Nucleic Acid Nanoparticles. *Nano Lett.* **2018**, *18*, 4309−4321.

https://doi.org/10.1021/acs.chemrev.0c01332
Chem. Rev. XXXX, XXX, XXX−XXX

(91) Liu, D.; Geary, C. W.; Chen, G.; Shao, Y.; Li, M.; Mao, C.; Andersen, E. S.; Piccirilli, J. A.; Rothemund, P. W. K.; Weizmann, Y. Branched Kissing Loops for the Construction of Diverse RNA Homooligomeric Nanostructures. *Nat. Chem.* **2020**, *12*, 249−259.
(92) Grabow, W. W.; Zakrevsky, P.; Afonin, K. A.; Chworos, A.; Shapiro, B. A.; Jaeger, L. Self-Assembling RNA Nanorings Based on RNAI/II Inverse Kissing Complexes. *Nano Lett.* **2011**, *11*, 878−887.
(93) Afonin, K. A.; Viard, M.; Koyfman, A. Y.; Martins, A. N.; Kasprzak, W. K.; Panigaj, M.; Desai, R.; Santhanam, A.; Grabow, W. W.; Jaeger, L.; et al. Multifunctional RNA Nanoparticles. *Nano Lett.* **2014**, *14*, 5662−5671.
(94) Guo, P. X.; Erickson, S.; Anderson, D. A Small Viral RNA is Required for In Vitro Packaging of Bacteriophage Phi 29 DNA. *Science* **1987**, *236*, 690−694.
(95) Guo, P.; Zhang, C.; Chen, C.; Garver, K.; Trottier, M. Inter-RNA Interaction of Phage Phi29 pRNA to Form a Hexameric Complex for Viral DNA Transportation. *Mol. Cell* **1998**, *2*, 149−155.
(96) Shu, Y.; Haque, F.; Shu, D.; Li, W.; Zhu, Z.; Kotb, M.; Lyubchenko, Y.; Guo, P. Fabrication of 14 Different RNA Nanoparticles for Specific Tumor Targeting without Accumulation in Normal Organs. *RNA* **2013**, *19*, 767−777.
(97) Hao, C.; Li, X.; Tian, C.; Jiang, W.; Wang, G.; Mao, C. Construction of RNA Nanocages by Re-Engineering the Packaging RNA of Phi29 Bacteriophage. *Nat. Commun.* **2014**, *5*, 3890.
(98) Endo, M.; Yamamoto, S.; Tatsumi, K.; Emura, T.; Hidaka, K.; Sugiyama, H. RNA-Templated DNA Origami Structures. *Chem. Commun.* **2013**, *49*, 2879−2881.
(99) Wang, P.; Hyeon Ko, S.; Tian, C.; Hao, C.; Mao, C. RNA-DNA Hybrid Origami: Folding of a Long RNA Single Strand into Complex Nanostructures Using Short DNA Helper Strands. *Chem. Commun.* **2013**, *49*, 5462−5464.
(100) Zheng, H.-N.; Ma, Y.-Z.; Xiao, S.-J. Periodical Assembly of Repetitive RNA Sequences Synthesized by Rolling Circle Transcription with Short DNA Staple Strands to RNA-DNA Hybrid Nanowires. *Chem. Commun.* **2014**, *50*, 2100−2103.
(101) Endo, M.; Takeuchi, Y.; Emura, T.; Hidaka, K.; Sugiyama, H. Preparation of Chemically Modified RNA Origami Nanostructures. *Chem. - Eur. J.* **2014**, *20*, 15330−15333.
(102) Høiberg, H. C.; Sparvath, S. M.; Andersen, V. L.; Kjems, J.; Andersen, E. S. An RNA Origami Octahedron with Intrinsic siRNAs for Potent Gene Knockdown. *Biotechnol. J.* **2019**, *14*, No. 1700634.
(103) Geary, C.; Rothemund, P. W. K.; Andersen, E. S. A Single-Stranded Architecture for Cotranscriptional Folding of RNA Nanostructures. *Science* **2014**, *345*, 799−804.
(104) Jepsen, M. D. E.; Sparvath, S. M.; Nielsen, T. B.; Langvad, A. H.; Grossi, G.; Gothelf, K. V.; Andersen, E. S. Development of a Genetically Encodable FRET System Using Fluorescent RNA Aptamers. *Nat. Commun.* **2018**, *9*, 18.
(105) Chopra, A.; Sagredo, S.; Grossi, G.; Andersen, E. S.; Simmel, F. C. Out-of-Plane Aptamer Functionalization of RNA Three-Helix Tiles. *Nanomaterials* **2019**, *9*, 507.
(106) Krissanaprasit, A.; Key, C.; Fergione, M.; Froehlich, K.; Pontula, S.; Hart, M.; Carriel, P.; Kjems, J.; Andersen, E. S.; LaBean, T. H. Genetically Encoded, Functional Single-Strand RNA Origami: Anticoagulant. *Adv. Mater.* **2019**, *31*, No. 1808262.
(107) Han, D.; Qi, X.; Myhrvold, C.; Wang, B.; Dai, M.; Jiang, S.; Bates, M.; Liu, Y.; An, B.; Zhang, F.; et al. Single-Stranded DNA and RNA Origami. *Science* **2017**, *358*, No. eaao2648.
(108) Fu, X.; Peng, F.; Lee, J.; Yang, Q.; Zhang, F.; Xiong, M.; Kong, G.; Meng, H.-M.; Ke, G.; Zhang, X.-B. Aptamer-Functionalized DNA Nanostructures for Biological Applications. *Top. Curr. Chem.* **2020**, *378*, 21.
(109) Daubendiek, S. L.; Ryan, K.; Kool, E. T. Rolling-Circle RNA Synthesis: Circular Oligonucleotides as Efficient Substrates for T7 RNA Polymerase. *J. Am. Chem. Soc.* **1995**, *117*, 7818−7819.
(110) Lee, J. B.; Hong, J.; Bonner, D. K.; Poon, Z.; Hammond, P. T. Self-Assembled RNA Interference Microsponges for Efficient siRNA Delivery. *Nat. Mater.* **2012**, *11*, 316−322.
(111) Cheng, H.; Hong, S.; Wang, Z.; Sun, N.; Wang, T.; Zhang, Y.; Chen, H.; Pei, R. Self-Assembled RNAi Nanoflowers via Rolling Circle Transcription for Aptamer-Targeted siRNA Delivery. *J. Mater. Chem. B* **2018**, *6*, 4638−4644.
(112) Lee, J. H.; Ku, S. H.; Kim, M. J.; Lee, S. J.; Kim, H. C.; Kim, K.; Kim, S. H.; Kwon, I. C. Rolling Circle Transcription-Based Polymeric siRNA Nanoparticles for Tumor-Targeted Delivery. *J. Controlled Release* **2017**, *263*, 29−38.
(113) Tuerk, C.; Gold, L. Systematic Evolution of Ligands by Exponential Enrichment: RNA Ligands to Bacteriophage T4 DNA Polymerase. *Science* **1990**, *249*, 505−510.
(114) Ellington, A. D.; Szostak, J. W. In Vitro Selection of RNA Molecules that Bind Specific Ligands. *Nature* **1990**, *346*, 818−822.
(115) Tan, W.; Wang, H.; Chen, Y.; Zhang, X.; Zhu, H.; Yang, C.; Yang, R.; Liu, C. Molecular Aptamers for Drug Delivery. *Trends Biotechnol.* **2011**, *29*, 634−640.
(116) Reverdatto, S.; Burz, D. S.; Shekhtman, A. Peptide Aptamers: Development and Applications. *Curr. Top. Med. Chem.* **2015**, *15*, 1082−1101.
(117) Szeto, K.; Latulippe, D. R.; Ozer, A.; Pagano, J. M.; White, B. S.; Shalloway, D.; Lis, J. T.; Craighead, H. G. Rapid-SELEX for RNA Aptamers. *PLoS One* **2013**, *8*, No. e82667.
(118) Dunn, M. R.; Jimenez, R. M.; Chaput, J. C. Analysis of Aptamer Discovery and Technology. *Nat. Rev. Chem.* **2017**, *1*, 0076.
(119) Panigaj, M.; Johnson, M. B.; Ke, W.; McMillan, J.; Goncharova, E. A.; Chandler, M.; Afonin, K. A. Aptamers as Modular Components of Therapeutic Nucleic Acid Nanotechnology. *ACS Nano* **2019**, *13*, 12301−12321.
(120) White, R.; Rusconi, C.; Scardino, E.; Wolberg, A.; Lawson, J.; Hoffman, M.; Sullenger, B. Generation of Species Cross-Reactive Aptamers Using "Toggle" SELEX. *Mol. Ther.* **2001**, *4*, 567−573.
(121) Odeh, F.; Nsairat, H.; Alshaer, W.; Ismail, M. A.; Esawi, E.; Qaqish, B.; Bawab, A. A.; Ismail, S. I. Aptamers Chemistry: Chemical Modifications and Conjugation Strategies. *Molecules* **2020**, *25*, 3.
(122) McGown, L. B.; Joseph, M. J.; Pitner, J. B.; vonk, G. P.; Linn, C. P. The Nucleic Acid Ligand. A New Tool for Molecular Recognition. *Anal. Chem.* **1995**, *67*, 663A−668A.
(123) Debiais, M.; Lelievre, A.; Smietana, M.; Müller, S. Splitting Aptamers and Nucleic Acid Enzymes for the Development of Advanced Biosensors. *Nucleic Acids Res.* **2020**, *48*, 3400−3422.
(124) Bhattacharyya, D.; Mirihana Arachchilage, G.; Basu, S. Metal Cations in G-Quadruplex Folding and Stability. *Front. Chem.* **2016**, *4*, 38.
(125) Mergny, J.-L.; Sen, D. DNA Quadruple Helices in Nanotechnology. *Chem. Rev.* **2019**, *119*, 6290−6325.
(126) Kolpashchikov, D. M. Binary Malachite Green Aptamer for Fluorescent Detection of Nucleic Acids. *J. Am. Chem. Soc.* **2005**, *127*, 12442−12443.
(127) Rogers, T. A.; Andrews, G. E.; Jaeger, L.; Grabow, W. W. Fluorescent Monitoring of RNA Assembly and Processing Using the Split-Spinach Aptamer. *ACS Synth. Biol.* **2015**, *4*, 162−166.
(128) Alam, K. K.; Tawiah, K. D.; Lichte, M. F.; Porciani, D.; Burke, D. H. A Fluorescent Split Aptamer for Visualizing RNA-RNA Assembly In Vivo. *ACS Synth. Biol.* **2017**, *6*, 1710−1721.
(129) Adachi, T.; Nakamura, Y. Aptamers: A Review of Their Chemical Properties and Modifications for Therapeutic Application. *Molecules* **2019**, *24*, 4229.
(130) Griffin, L. C.; Tidmarsh, G. F.; Bock, L. C.; Toole, J. J.; Leung, L. L. In Vivo Anticoagulant Properties of a Novel Nucleotide-Based Thrombin Inhibitor and Demonstration of Regional Anticoagulation in Extracorporeal Circuits. *Blood* **1993**, *81*, 3271−3276.
(131) Maasch, C.; Buchner, K.; Eulberg, D.; Vonhoff, S.; Klussmann, S. Physicochemical Stability of NOX-E36, a 40mer L-RNA (Spiegelmer) for Therapeutic Applications. *Nucleic acids Symp. Ser.* **2008**, *52*, 61−62.
(132) Thiviyanathan, V.; Somasunderam, A. D.; Gorenstein, D. G. Combinatorial Selection and Delivery of Thioaptamers. *Biochem. Soc. Trans.* **2007**, *35*, 50−52.

https://doi.org/10.1021/acs.chemrev.0c01332
Chem. Rev. XXXX, XXX, XXX−XXX

(133) Zhou, J.; Rossi, J. Aptamers as Targeted Therapeutics: Current Potential and Challenges. *Nat. Rev. Drug Discovery* **2017**, *16*, 181−202.
(134) Rohloff, J. C.; Gelinas, A. D.; Jarvis, T. C.; Ochsner, U. A.; Schneider, D. J.; Gold, L.; Janjic, N. Nucleic Acid Ligands with Protein-Like Side Chains: Modified Aptamers and Their Use as Diagnostic and Therapeutic Agents. *Mol. Ther.–Nucleic Acids* **2014**, *3*, No. e201.
(135) Waring, M. J. Lipophilicity in Drug Discovery. *Expert Opin. Drug Discovery* **2010**, *5*, 235−248.
(136) Ganson, N. J.; Povsic, T. J.; Sullenger, B. A.; Alexander, J. H.; Zelenkofske, S. L.; Sailstad, J. M.; Rusconi, C. P.; Hershfield, M. S. Pre-Existing Anti-Polyethylene Glycol Antibody Linked to First-Exposure Allergic Reactions to Pegnivacogin, a PEGylated RNA Aptamer. *J. Allergy Clin. Immunol.* **2016**, *137*, 1610−1613.
(137) Groff, K.; Brown, J.; Clippinger, A. J. Modern Affinity Reagents: Recombinant Antibodies and Aptamers. *Biotechnol. Adv.* **2015**, *33*, 1787−1798.
(138) Lakhin, A. V.; Tarantul, V. Z.; Gening, L. V. Aptamers: Problems, Solutions and Prospects. *Acta Naturae* **2013**, *5*, 34−43.
(139) Kedzierski, S.; Khoshnejad, M.; Caltagirone, G. T. Synthetic Antibodies: The Emerging Field of Aptamers. *BioProcess. J.* **2013**, *11*, 46−49.
(140) Nimjee, S. M.; White, R. R.; Becker, R. C.; Sullenger, B. A. Aptamers as Therapeutics. *Annu. Rev. Pharmacol. Toxicol.* **2017**, *57*, 61−79.
(141) Cai, S.; Yan, J.; Xiong, H.; Liu, Y.; Peng, D.; Liu, Z. Investigations on the Interface of Nucleic Acid Aptamers and Binding Targets. *Analyst* **2018**, *143*, 5317−5338.
(142) Mairal, T.; Ozalp, V. C.; Lozano Sánchez, P.; Mir, M.; Katakis, I.; O'Sullivan, C. K. Aptamers: Molecular Tools for Analytical Applications. *Anal. Bioanal. Chem.* **2008**, *390*, 989−1007.
(143) Nagatoishi, S.; Isono, N.; Tsumoto, K.; Sugimoto, N. Loop Residues of Thrombin-Binding DNA Aptamer Impact G-Quadruplex Stability and Thrombin Binding. *Biochimie* **2011**, *93*, 1231−1238.
(144) Pagano, B.; Martino, L.; Randazzo, A.; Giancola, C. Stability and Binding Properties of a Modified Thrombin Binding Aptamer. *Biophys. J.* **2008**, *94*, 562−569.
(145) Aviñó, A.; Mazzini, S.; Ferreira, R.; Gargallo, R.; Marquez, V. E.; Eritja, R. The Effect on Quadruplex Stability of North-Nucleoside Derivatives in the Loops of the Thrombin-Binding Aptamer. *Bioorg. Med. Chem.* **2012**, *20*, 4186−4193.
(146) Hermann, T. Strategies for the Design of Drugs Targeting RNA and RNA-Protein Complexes. *Angew. Chem., Int. Ed.* **2000**, *39*, 1890−1904.
(147) Davies, D. R.; Gelinas, A. D.; Zhang, C.; Rohloff, J. C.; Carter, J. D.; O'Connell, D.; Waugh, S. M.; Wolk, S. K.; Mayfield, W. S.; Burgin, A. B.; et al. Unique Motifs and Hydrophobic Interactions Shape the Binding of Modified DNA Ligands to Protein Targets. *Proc. Natl. Acad. Sci. U. S. A.* **2012**, *109*, 19971−19976.
(148) Gupta, S.; Drolet, D. W.; Wolk, S. K.; Waugh, S. M.; Rohloff, J. C.; Carter, J. D.; Mayfield, W. S.; Otis, M. R.; Fowler, C. R.; Suzuki, T.; et al. Pharmacokinetic Properties of DNA Aptamers with Base Modifications. *Nucleic Acid Ther.* **2017**, *27*, 345−353.
(149) Flinders, J.; DeFina, S. C.; Brackett, D. M.; Baugh, C.; Wilson, C.; Dieckmann, T. Recognition of Planar and Nonplanar Ligands in the Malachite Green-RNA Aptamer Complex. *ChemBioChem* **2004**, *5*, 62−72.
(150) Bjerregaard, N.; Andreasen, P. A.; Dupont, D. M. Expected and Unexpected Features of Protein-Binding RNA Aptamers. *Wiley Interdiscip. Rev. RNA* **2016**, *7*, 744−757.
(151) Lang, P. T.; Brozell, S. R.; Mukherjee, S.; Pettersen, E. F.; Meng, E. C.; Thomas, V.; Rizzo, R. C.; Case, D. A.; James, T. L.; Kuntz, I. D. DOCK 6: Combining Techniques to Model RNA-Small Molecule Complexes. *RNA* **2009**, *15*, 1219−1230.
(152) Ghosh, G.; Huang, D.-B.; Huxford, T. Molecular Mimicry of the NF-Kb DNA Target Site by a Selected RNA Aptamer. *Curr. Opin. Struct. Biol.* **2004**, *14*, 21−27.
(153) Amano, R.; Takada, K.; Tanaka, Y.; Nakamura, Y.; Kawai, G.; Kozu, T.; Sakamoto, T. Kinetic and Thermodynamic Analyses of Interaction between a High-Affinity RNA Aptamer and Its Target Protein. *Biochemistry* **2016**, *55*, 6221−6229.
(154) Lin, P.-H.; Chen, R.-H.; Lee, C.-H.; Chang, Y.; Chen, C.-S.; Chen, W.-Y. Studies of the Binding Mechanism between Aptamers and Thrombin by Circular Dichroism, Surface Plasmon Resonance and Isothermal Titration Calorimetry. *Colloids Surf., B* **2011**, *88*, 552−558.
(155) Tan, S. Y.; Acquah, C.; Sidhu, A.; Ongkudon, C. M.; Yon, L. S.; Danquah, M. K. SELEX Modifications and Bioanalytical Techniques for Aptamer-Target Binding Characterization. *Crit. Rev. Anal. Chem.* **2016**, *46*, 521−537.
(156) Li, T.; Dong, S.; Wang, E. Label-Free Colorimetric Detection of Aqueous Mercury Ion (Hg^{2+}) Using Hg^{2+}-Modulated G-Quadruplex-Based Dnazymes. *Anal. Chem.* **2009**, *81*, 2144−2149.
(157) Chung, C. H.; Kim, J. H.; Jung, J.; Chung, B. H. Nuclease-Resistant DNA Aptamer on Gold Nanoparticles for the Simultaneous Detection of Pb^{2+} and Hg^{2+} in Human Serum. *Biosens. Bioelectron.* **2013**, *41*, 827−832.
(158) Jiang, L.; Suri, A. K.; Fiala, R.; Patel, D. J. Saccharide-RNA Recognition in an Aminoglycoside Antibiotic-RNA Aptamer Complex. *Chem. Biol.* **1997**, *4*, 35−50.
(159) Lin, P. H.; Chen, R. H.; Lee, C. H.; Chang, Y.; Chen, C. S.; Chen, W. Y. Studies of the Binding Mechanism between Aptamers and Thrombin by Circular Dichroism, Surface Plasmon Resonance and Isothermal Titration Calorimetry. *Colloids Surf., B* **2011**, *88*, 552−558.
(160) Morris, K. N.; Jensen, K. B.; Julin, C. M.; Weil, M.; Gold, L. High Affinity Ligands from In Vitro Selection: Complex Targets. *Proc. Natl. Acad. Sci. U. S. A.* **1998**, *95*, 2902−2907.
(161) Shangguan, D.; Li, Y.; Tang, Z.; Cao, Z. C.; Chen, H. W.; Mallikaratchy, P.; Sefah, K.; Yang, C. J.; Tan, W. Aptamers Evolved from Live Cells as Effective Molecular Probes for Cancer Study. *Proc. Natl. Acad. Sci. U. S. A.* **2006**, *103*, 11838−11843.
(162) Chen, C.-H. B.; Chernis, G. A.; Hoang, V. Q.; Landgraf, R. Inhibition of Heregulin Signaling by an Aptamer that Preferentially Binds to the Oligomeric Form of Human Epidermal Growth Factor Receptor-3. *Proc. Natl. Acad. Sci. U. S. A.* **2003**, *100*, 9226−9231.
(163) Dollins, C. M.; Nair, S.; Boczkowski, D.; Lee, J.; Layzer, J. M.; Gilboa, E.; Sullenger, B. A. Assembling OX40 Aptamers on a Molecular Scaffold to Create a Receptor-Activating Aptamer. *Chem. Biol.* **2008**, *15*, 675−682.
(164) McNamara, J. O.; Kolonias, D.; Pastor, F.; Mittler, R. S.; Chen, L.; Giangrande, P. H.; Sullenger, B.; Gilboa, E. Multivalent 4-1BB Binding Aptamers Costimulate CD8+ T Cells and Inhibit Tumor Growth in Mice. *J. Clin. Invest.* **2008**, *118*, 376−386.
(165) Pratico, E. D.; Sullenger, B. A.; Nair, S. K. Identification and Characterization of an Agonistic Aptamer against the T Cell Costimulatory Receptor, OX40. *Nucleic Acid Ther.* **2013**, *23*, 35−43.
(166) Pastor, F.; Soldevilla, M. M.; Villanueva, H.; Kolonias, D.; Inoges, S.; de Cerio, A. L.; Kandzia, R.; Klimyuk, V.; Gleba, Y.; Gilboa, E.; et al. CD28 Aptamers as Powerful Immune Response Modulators. *Mol. Ther.–Nucleic Acids* **2013**, *2*, No. e98.
(167) Soldevilla, M. M.; Villanueva, H.; Bendandi, M.; Inoges, S.; López-Díaz de Cerio, A.; Pastor, F. 2-Fluoro-RNA Oligonucleotide CD40 Targeted Aptamers for the Control of B Lymphoma and Bone-Marrow Aplasia. *Biomaterials* **2015**, *67*, 274−285.
(168) Ramaswamy, V.; Monsalve, A.; Sautina, L.; Segal, M. S.; Dobson, J.; Allen, J. B. DNA Aptamer Assembly as a Vascular Endothelial Growth Factor Receptor Agonist. *Nucleic Acid Ther.* **2015**, *25*, 227−234.
(169) Yunn, N. O.; Koh, A.; Han, S.; Lim, J. H.; Park, S.; Lee, J.; Kim, E.; Jang, S. K.; Berggren, P. O.; Ryu, S. H. Agonistic Aptamer to the Insulin Receptor Leads to Biased Signaling and Functional Selectivity through Allosteric Modulation. *Nucleic Acids Res.* **2015**, *43*, 7688−7701.
(170) Nudler, E.; Mironov, A. S. The Riboswitch Control of Bacterial Metabolism. *Trends Biochem. Sci.* **2004**, *29*, 11−17.
(171) Serganov, A.; Nudler, E. A Decade of Riboswitches. *Cell* **2013**, *152*, 17−24.
(172) Paige, J. S.; Wu, K. Y.; Jaffrey, S. R. RNA Mimics of Green Fluorescent Protein. *Science* **2011**, *333*, 642−646.

https://doi.org/10.1021/acs.chemrev.0c01332
Chem. Rev. XXXX, XXX, XXX−XXX

(173) Dolgosheina, E. V.; Jeng, S. C.; Panchapakesan, S. S.; Cojocaru, R.; Chen, P. S.; Wilson, P. D.; Hawkins, N.; Wiggins, P. A.; Unrau, P. J. RNA Mango Aptamer-Fluorophore: A Bright, High-Affinity Complex for RNA Labeling and Tracking. *ACS Chem. Biol.* **2014**, *9*, 2412−2420.
(174) Figueroa-Miranda, G.; Feng, L.; Shiu, S. C.-C.; Dirkzwager, R. M.; Cheung, Y.-W.; Tanner, J. A.; Schöning, M. J.; Offenhäusser, A.; Mayer, D. Aptamer-Based Electrochemical Biosensor for Highly Sensitive and Selective Malaria Detection with Adjustable Dynamic Response Range and Reusability. *Sens. Actuators, B* **2018**, *255*, 235−243.
(175) Wang, R. E.; Zhang, Y.; Cai, J.; Cai, W.; Gao, T. Aptamer-Based Fluorescent Biosensors. *Curr. Med. Chem.* **2011**, *18*, 4175−4184.
(176) Goldsworthy, V.; LaForce, G.; Abels, S.; Khisamutdinov, E. F. Fluorogenic RNA Aptamers: A Nano-Platform for Fabrication of Simple and Combinatorial Logic Gates. *Nanomaterials* **2018**, *8*, 984.
(177) You, M.; Zhu, G.; Chen, T.; Donovan, M. J.; Tan, W. Programmable and Multiparameter DNA-Based Logic Platform for Cancer Recognition and Targeted Therapy. *J. Am. Chem. Soc.* **2015**, *137*, 667−674.
(178) Dhar, P.; Samarasinghe, R. M.; Shigdar, S. Antibodies, Nanobodies, or Aptamers—Which is Best for Deciphering the Proteomes of Non-Model Species? *Int. J. Mol. Sci.* **2020**, *21*, 2485.
(179) Kushwaha, A.; Takamura, Y.; Nishigaki, K.; Biyani, M. Competitive Non-SELEX for the Selective and Rapid Enrichment of DNA Aptamers and Its Use in Electrochemical Aptasensor. *Sci. Rep.* **2019**, *9*, 6642.
(180) Zhou, Y.; Qi, X.; Liu, Y.; Zhang, F.; Yan, H. DNA-Nanoscaffold-Assisted Selection of Femtomolar Bivalent Human A-Thrombin Aptamers with Potent Anticoagulant Activity. *ChemBioChem* **2019**, *20*, 2494−2503.
(181) Krissanaprasit, A.; Key, C. M.; Froehlich, K.; Pontula, S.; Mihalko, E.; Dupont, D. M.; Andersen, E. S.; Kjems, J.; Brown, A. C.; LaBean, T. H. Multivalent Aptamer-Functionalized Single-Strand RNA Origami as Effective, Target-Specific Anticoagulants with Corresponding Reversal Agents. *Adv. Healthcare Mater.* **2021**, 2001826.
(182) Keefe, A. D.; Pai, S.; Ellington, A. Aptamers as Therapeutics. *Nat. Rev. Drug Discovery* **2010**, *9*, 537−550.
(183) Rusconi, C. P.; Scardino, E.; Layzer, J.; Pitoc, G. A.; Ortel, T. L.; Monroe, D.; Sullenger, B. A. RNA Aptamers as Reversible Antagonists of Coagulation Factor IXa. *Nature* **2002**, *419*, 90−94.
(184) Rusconi, C. P.; Roberts, J. D.; Pitoc, G. A.; Nimjee, S. M.; White, R. R.; Quick, G.; Scardino, E.; Fay, W. P.; Sullenger, B. A. Antidote-Mediated Control of an Anticoagulant Aptamer In Vivo. *Nat. Biotechnol.* **2004**, *22*, 1423−1428.
(185) Nimjee, S. M.; Keys, J. R.; Pitoc, G. A.; Quick, G.; Rusconi, C. P.; Sullenger, B. A. A Novel Antidote-Controlled Anticoagulant Reduces Thrombin Generation and Inflammation and Improves Cardiac Function in Cardiopulmonary Bypass Surgery. *Mol. Ther.* **2006**, *14*, 408−415.
(186) Guan, B.; Zhang, X. Aptamers as Versatile Ligands for Biomedical and Pharmaceutical Applications. *Int. J. Nanomed.* **2020**, *15*, 1059−1071.
(187) Chen, K.; Liu, B.; Yu, B.; Zhong, W.; Lu, Y.; Zhang, J.; Liao, J.; Liu, J.; Pu, Y.; Qiu, L. Advances in the Development of Aptamer Drug Conjugates for Targeted Drug Delivery. *Wiley Interdiscip. Rev. Nanomed. Nanobiotechnol.* **2017**, *9*, e1438.
(188) Yang, Y.; Yang, X.; Yang, Y.; Yuan, Q. Aptamer-Functionalized Carbon Nanomaterials Electrochemical Sensors for Detecting Cancer Relevant Biomolecules. *Carbon* **2018**, *129*, 380−395.
(189) Ding, P.; Wang, Z.; Wu, Z.; Zhu, W.; Liu, L.; Sun, N.; Pei, R. Aptamer-Based Nanostructured Interfaces for the Detection and Release of Circulating Tumor Cells. *J. Mater. Chem. B* **2020**, *8*, 3408−3422.
(190) Ren, Q.; Ga, L.; Lu, Z.; Ai, J.; Wang, T. Aptamer-Functionalized Nanomaterials for Biological Applications. *Mater. Chem. Front.* **2020**, *4*, 1569−1585.
(191) Meng, H.-M.; Liu, H.; Kuai, H.; Peng, R.; Mo, L.; Zhang, X.-B. Aptamer-Integrated DNA Nanostructures for Biosensing, Bioimaging and Cancer Therapy. *Chem. Soc. Rev.* **2016**, *45*, 2583−2602.
(192) Sakai, Y.; Islam, M. S.; Adamiak, M.; Shiu, S. C.-C.; Tanner, J. A.; Heddle, J. G. DNA Aptamers for the Functionalisation of DNA Origami Nanostructures. *Genes* **2018**, *9*, 571.
(193) Hasegawa, H.; Savory, N.; Abe, K.; Ikebukuro, K. Methods for Improving Aptamer Binding Affinity. *Molecules* **2016**, *21*, 421.
(194) Sakamoto, T.; Ennifar, E.; Nakamura, Y. Thermodynamic Study of Aptamers Binding to Their Target Proteins. *Biochimie* **2018**, *145*, 91−97.
(195) Madsen, M.; Gothelf, K. V. Chemistries for DNA Nanotechnology. *Chem. Rev.* **2019**, *119*, 6384−6458.
(196) Krissanaprasit, A.; Somasundrum, M.; Surareungchai, W. RGB Colour Coding of Y-Shaped DNA for Simultaneous Tri-Analyte Solid Phase Hybridization Detection. *Biosens. Bioelectron.* **2011**, *26*, 2183−2187.
(197) Campuzano, S.; Yáez-Sedeño, P.; Pingarrón, J. M. Electrochemical Affinity Biosensors in Food Safety. *Chemosensors* **2017**, *5*, 8.
(198) Metkar, S. K.; Girigoswami, K. Diagnostic Biosensors in Medicine - A Review. *Biocatal. Agric. Biotechnol.* **2019**, *17*, 271−283.
(199) Lertanantawong, B.; Krissanaprasit, A.; Chaibun, T.; Gothelf, K. V.; Surareungchai, W. Multiplexed DNA Detection with DNA Tweezers in a One-Pot Reaction. *Mater. Sci. Technol.* **2019**, *2*, 503−508.
(200) Mehrotra, P. Biosensors and Their Applications - A Review. *J. Oral Biol. Craniofac. Res.* **2016**, *6*, 153−159.
(201) Song, S.; Wang, L.; Li, J.; Fan, C.; Zhao, J. Aptamer-Based Biosensors. *TrAC, Trends Anal. Chem.* **2008**, *27*, 108−117.
(202) Ouellet, J. RNA Fluorescence with Light-up Aptamers. *Front. Chem.* **2016**, *4*, 29.
(203) Mishra, G. K.; Sharma, V.; Mishra, R. K. Electrochemical Aptasensors for Food and Environmental Safeguarding: A Review. *Biosensors* **2018**, *8*, 28.
(204) Forouzanfar, S.; Alam, F.; Pala, N.; Wang, C. Review—a Review of Electrochemical Aptasensors for Label-Free Cancer Diagnosis. *J. Electrochem. Soc.* **2020**, *167*, 067511.
(205) Wang, Z.; Yu, J.; Gui, R.; Jin, H.; Xia, Y. Carbon Nanomaterials-Based Electrochemical Aptasensors. *Biosens. Bioelectron.* **2016**, *79*, 136−149.
(206) Xu, Y.; Cheng, G.; He, P.; Fang, Y. A Review: Electrochemical Aptasensors with Various Detection Strategies. *Electroanalysis* **2009**, *21*, 1251−1259.
(207) Xiao, Y.; Piorek, B. D.; Plaxco, K. W.; Heeger, A. J. A Reagentless Signal-on Architecture for Electronic, Aptamer-Based Sensors via Target-Induced Strand Displacement. *J. Am. Chem. Soc.* **2005**, *127*, 17990−17991.
(208) Farjami, E.; Campos, R.; Nielsen, J. S.; Gothelf, K. V.; Kjems, J.; Ferapontova, E. E. RNA Aptamer-Based Electrochemical Biosensor for Selective and Label-Free Analysis of Dopamine. *Anal. Chem.* **2013**, *85*, 121−128.
(209) Zhang, Z.; Zhao, X.; Liu, J.; Yin, J.; Cao, X. Highly Sensitive Sandwich Electrochemical Sensor Based on DNA-Scaffolded Bivalent Split Aptamer Signal Probe. *Sens. Actuators, B* **2020**, *311*, 127920.
(210) Feng, C.; Dai, S.; Wang, L. Optical Aptasensors for Quantitative Detection of Small Biomolecules: A Review. *Biosens. Bioelectron.* **2014**, *59*, 64−74.
(211) Nutiu, R.; Li, Y. Structure-Switching Signaling Aptamers. *J. Am. Chem. Soc.* **2003**, *125*, 4771−4778.
(212) Liu, J.; Lee, J. H.; Lu, Y. Quantum Dot Encoding of Aptamer-Linked Nanostructures for One-Pot Simultaneous Detection of Multiple Analytes. *Anal. Chem.* **2007**, *79*, 4120−4125.
(213) Saha, S.; Prakash, V.; Halder, S.; Chakraborty, K.; Krishnan, Y. A pH-Independent DNA Nanodevice for Quantifying Chloride Transport in Organelles of Living Cells. *Nat. Nanotechnol.* **2015**, *10*, 645−651.
(214) Ping, J.; Zhou, Y.; Wu, Y.; Papper, V.; Boujday, S.; Marks, R. S.; Steele, T. W. J. Recent Advances in Aptasensors Based on Graphene and Graphene-Like Nanomaterials. *Biosens. Bioelectron.* **2015**, *64*, 373−385.
(215) Yang, D.; Liu, X.; Zhou, Y.; Luo, L.; Zhang, J.; Huang, A.; Mao, Q.; Chen, X.; Tang, L. Aptamer-Based Biosensors for Detection of Lead(II) Ion: A Review. *Anal. Methods* **2017**, *9*, 1976−1990.

https://doi.org/10.1021/acs.chemrev.0c01332
Chem. Rev. XXXX, XXX, XXX−XXX

(216) Mao, K.; Zhang, H.; Wang, Z.; Cao, H.; Zhang, K.; Li, X.; Yang, Z. Nanomaterial-Based Aptamer Sensors for Arsenic Detection. *Biosens. Bioelectron.* **2020**, *148*, 111785.
(217) Xie, N.; Liu, S.; Yang, X.; He, X.; Huang, J.; Wang, K. DNA Tetrahedron Nanostructures for Biological Applications: Biosensors and Drug Delivery. *Analyst* **2017**, *142*, 3322−3332.
(218) Li, S.; Tian, T.; Zhang, T.; Cai, X.; Lin, Y. Advances in Biological Applications of Self-Assembled DNA Tetrahedral Nanostructures. *Mater. Today* **2019**, *24*, 57−68.
(219) Pei, H.; Lu, N.; Wen, Y.; Song, S.; Liu, Y.; Yan, H.; Fan, C. A DNA Nanostructure-Based Biomolecular Probe Carrier Platform for Electrochemical Biosensing. *Adv. Mater.* **2010**, *22*, 4754−4758.
(220) Poturnayová, A.; Snejdárková, M.; Castillo, G.; Rybár, P.; Leitner, M.; Ebner, A.; Hianik, T. Aptamer-Based Detection of Thrombin by Acoustic Method Using DNA Tetrahedrons as Immobilisation Platform. *Chem. Papers* **2015**, *69*, 211.
(221) Wen, Y.; Pei, H.; Wan, Y.; Su, Y.; Huang, Q.; Song, S.; Fan, C. DNA Nanostructure-Decorated Surfaces for Enhanced Aptamer-Target Binding and Electrochemical Cocaine Sensors. *Anal. Chem.* **2011**, *83*, 7418−7423.
(222) Lin, M.; Song, P.; Zhou, G.; Zuo, X.; Aldalbahi, A.; Lou, X.; Shi, J.; Fan, C. Electrochemical Detection of Nucleic Acids, Proteins, Small Molecules and Cells Using a DNA-Nanostructure-Based Universal Biosensing Platform. *Nat. Protoc.* **2016**, *11*, 1244−1263.
(223) Jiang, J.; Yu, Y.; Zhang, H.; Cai, C. Electrochemical Aptasensor for Exosomal Proteins Profiling Based on DNA Nanotetrahedron Coupled with Enzymatic Signal Amplification. *Anal. Chim. Acta* **2020**, *1130*, 1−9.
(224) Faria, A. M.; Peixoto, E. B. M. I.; Adamo, C. B.; Flacker, A.; Longo, E.; Mazon, T. Controlling Parameters and Characteristics of Electrochemical Biosensors for Enhanced Detection of 8-Hydroxy-2′-Deoxyguanosine. *Sci. Rep.* **2019**, *9*, 7411.
(225) Fan, J.; Liu, Y.; Xu, E.; Zhang, Y.; Wei, W.; Yin, L.; Pu, Y.; Liu, S. A Label-Free Ultrasensitive Assay of 8-Hydroxy-2′-Deoxyguanosine in Human Serum and Urine Samples via Polyaniline Deposition and Tetrahedral DNA Nanostructure. *Anal. Chim. Acta* **2016**, *946*, 48−55.
(226) Li, C.; Hu, X.; Lu, J.; Mao, X.; Xiang, Y.; Shu, Y.; Li, G. Design of DNA Nanostructure-Based Interfacial Probes for the Electrochemical Detection of Nucleic Acids Directly in Whole Blood. *Chem. Sci.* **2018**, *9*, 979−984.
(227) Eisenstein, M. Growing Pains. *Nature* **2006**, *444*, 959−959.
(228) Hucknall, A.; Rangarajan, S.; Chilkoti, A. In Pursuit of Zero: Polymer Brushes that Resist the Adsorption of Proteins. *Adv. Mater.* **2009**, *21*, 2441−2446.
(229) Ryu, J. Y.; Song, I. T.; Lau, K. H. A.; Messersmith, P. B.; Yoon, T.-Y.; Lee, H. New Antifouling Platform Characterized by Single-Molecule Imaging. *ACS Appl. Mater. Interfaces* **2014**, *6*, 3553−3558.
(230) Chen, D.; Sun, D.; Wang, Z.; Qin, W.; Chen, L.; Zhou, L.; Zhang, Y. A DNA Nanostructured Aptasensor for the Sensitive Electrochemical Detection of HepG2 Cells Based on Multibranched Hybridization Chain Reaction Amplification Strategy. *Biosens. Bioelectron.* **2018**, *117*, 416−421.
(231) Liu, Y.; Chen, D.; Zhang, W.; Zhang, Y. Mobile DNA Tetrahedron on Ultra-Low Adsorption Lipid Membrane for Directional Control of Cell Sensing. *Sens. Actuators, B* **2020**, *307*, 127570.
(232) Sun, D.; Luo, Z.; Lu, J.; Zhang, S.; Che, T.; Chen, Z.; Zhang, L. Electrochemical Dual-Aptamer-Based Biosensor for Nonenzymatic Detection of Cardiac Troponin I by Nanohybrid Electrocatalysts Labeling Combined with DNA Nanotetrahedron Structure. *Biosens. Bioelectron.* **2019**, *134*, 49−56.
(233) Luo, Z.; Sun, D.; Tong, Y.; Zhong, Y.; Chen, Z. DNA Nanotetrahedron Linked Dual-Aptamer Based Voltammetric Aptasensor for Cardiac Troponin I Using a Magnetic Metal-Organic Framework as a Label. *Microchim. Acta* **2019**, *186*, 374.
(234) Ou, D.; Sun, D.; Lin, X.; Liang, Z.; Zhong, Y.; Chen, Z. A Dual-Aptamer-Based Biosensor for Specific Detection of Breast Cancer Biomarker HER2 via Flower-Like Nanozymes and DNA Nanostructures. *J. Mater. Chem. B* **2019**, *7*, 3661−3669.
(235) Taghdisi, S. M.; Danesh, N. M.; Nameghi, M. A.; Ramezani, M.; Alibolandi, M.; Abnous, K. An Electrochemical Sensing Platform Based on Ladder-Shaped DNA Structure and Label-Free Aptamer for Ultrasensitive Detection of Ampicillin. *Biosens. Bioelectron.* **2019**, *133*, 230−235.
(236) Taghdisi, S. M.; Danesh, N. M.; Ramezani, M.; Abnous, K. A Novel M-Shape Electrochemical Aptasensor for Ultrasensitive Detection of Tetracyclines. *Biosens. Bioelectron.* **2016**, *85*, 509−514.
(237) Abnous, K.; Danesh, N. M.; Alibolandi, M.; Ramezani, M.; Sarreshtehdar Emrani, A.; Zolfaghari, R.; Taghdisi, S. M. A New Amplified Π-Shape Electrochemical Aptasensor for Ultrasensitive Detection of Aflatoxin B1. *Biosens. Bioelectron.* **2017**, *94*, 374−379.
(238) Abnous, K.; Danesh, N. M.; Ramezani, M.; Taghdisi, S. M.; Emrani, A. S. A Novel Electrochemical Aptasensor Based on H-Shape Structure of Aptamer-Complimentary Strands Conjugate for Ultrasensitive Detection of Cocaine. *Sens. Actuators, B* **2016**, *224*, 351−355.
(239) Mohammad Danesh, N.; Ramezani, M.; Sarreshtehdar Emrani, A.; Abnous, K.; Taghdisi, S. M. A Novel Electrochemical Aptasensor Based on Arch-Shape Structure of Aptamer-Complimentary Strand Conjugate and Exonuclease I for Sensitive Detection of Streptomycin. *Biosens. Bioelectron.* **2016**, *75*, 123−128.
(240) Li, Z.; Zhao, B.; Wang, D.; Wen, Y.; Liu, G.; Dong, H.; Song, S.; Fan, C. DNA Nanostructure-Based Universal Microarray Platform for High-Efficiency Multiplex Bioanalysis in Biofluids. *ACS Appl. Mater. Interfaces* **2014**, *6*, 17944−17953.
(241) Zheng, X.; Peng, R.; Jiang, X.; Wang, Y.; Xu, S.; Ke, G.; Fu, T.; Liu, Q.; Huan, S.; Zhang, X. Fluorescence Resonance Energy Transfer-Based DNA Nanoprism with a Split Aptamer for Adenosine Triphosphate Sensing in Living Cells. *Anal. Chem.* **2017**, *89*, 10941−10947.
(242) Kwon, P. S.; Ren, S.; Kwon, S.-J.; Kizer, M. E.; Kuo, L.; Xie, M.; Zhu, D.; Zhou, F.; Zhang, F.; Kim, D.; et al. Designer DNA Architecture Offers Precise and Multivalent Spatial Pattern-Recognition for Viral Sensing and Inhibition. *Nat. Chem.* **2020**, *12*, 26−35.
(243) Shiu, S. C.-C.; Fraser, L. A.; Ding, Y.; Tanner, J. A. Aptamer Display on Diverse DNA Polyhedron Supports. *Molecules* **2018**, *23*, 1695.
(244) Bu, N. N.; Gao, A.; He, X. W.; Yin, X. B. Electrochemiluminescent Biosensor of ATP Using Tetrahedron Structured DNA and a Functional Oligonucleotide for Ru(Phen)3(2+) Intercalation and Target Identification. *Biosens. Bioelectron.* **2013**, *43*, 200−204.
(245) Wang, S.; Dong, Y.; Liang, X. Development of a SPR Aptasensor Containing Oriented Aptamer for Direct Capture and Detection of Tetracycline in Multiple Honey Samples. *Biosens. Bioelectron.* **2018**, *109*, 1−7.
(246) Antiochia, R.; Bollella, P.; Favero, G.; Mazzei, F. Nanotechnology-Based Surface Plasmon Resonance Affinity Biosensors for In Vitro Diagnostics. *Int. J. Anal. Chem.* **2016**, *2016*, 2981931.
(247) Yang, D.; Campolongo, M. J.; Nhi Tran, T. N.; Ruiz, R. C. H.; Kahn, J. S.; Luo, D. Novel DNA Materials and Their Applications. *Wiley Interdiscip. Rev.: Nanomed. Nanobiotechnol.* **2010**, *2*, 648−669.
(248) Meng, H. M.; Zhang, X.; Lv, Y.; Zhao, Z.; Wang, N. N.; Fu, T.; Fan, H.; Liang, H.; Qiu, L.; Zhu, G.; et al. DNA Dendrimer: An Efficient Nanocarrier of Functional Nucleic Acids for Intracellular Molecular Sensing. *ACS Nano* **2014**, *8*, 6171−6181.
(249) Norouzi, A.; Ravan, H.; Mohammadi, A.; Hosseinzadeh, E.; Norouzi, M.; Fozooni, T. Aptamer-Integrated DNA Nanoassembly: A Simple and Sensitive DNA Framework to Detect Cancer Cells. *Anal. Chim. Acta* **2018**, *1017*, 26−33.
(250) Bujold, K. E.; Lacroix, A.; Sleiman, H. F. DNA Nanostructures at the Interface with Biology. *Chem.* **2018**, *4*, 495−521.
(251) Lin, C.; Katilius, E.; Liu, Y.; Zhang, J.; Yan, H. Self-Assembled Signaling Aptamer DNA Arrays for Protein Detection. *Angew. Chem., Int. Ed.* **2006**, *45*, 5296−5301.
(252) Kikuchi, N.; Kolpashchikov, D. M. A Universal Split Spinach Aptamer (USSA) for Nucleic Acid Analysis and DNA Computation. *Chem. Commun.* **2017**, *53*, 4977−4980.

https://doi.org/10.1021/acs.chemrev.0c01332
Chem. Rev. XXXX, XXX, XXX−XXX

(253) Rinker, S.; Ke, Y.; Liu, Y.; Chhabra, R.; Yan, H. Self-Assembled DNA Nanostructures for Distance-Dependent Multivalent Ligand-Protein Binding. *Nat. Nanotechnol.* **2008**, *3*, 418−422.
(254) Mei, Q.; Johnson, R. H.; Wei, X.; Su, F.; Liu, Y.; Kelbauskas, L.; Lindsay, S.; Meldrum, D. R.; Yan, H. On-Chip Isotachophoresis Separation of Functional DNA Origami Capture Nanoarrays from Cell Lysate. *Nano Res.* **2013**, *6*, 712−719.
(255) Tintoré, M.; Gállego, I.; Manning, B.; Eritja, R.; Fàbrega, C. DNA Origami as a DNA Repair Nanosensor at the Single-Molecule Level. *Angew. Chem., Int. Ed.* **2013**, *52*, 7747−7750.
(256) Godonoga, M.; Lin, T.-Y.; Oshima, A.; Sumitomo, K.; Tang, M. S. L.; Cheung, Y.-W.; Kinghorn, A. B.; Dirkzwager, R. M.; Zhou, C.; Kuzuya, A.; et al. A DNA Aptamer Recognising a Malaria Protein Biomarker can Function as Part of a DNA Origami Assembly. *Sci. Rep.* **2016**, *6*, 21266.
(257) Lu, Z.; Wang, Y.; Xu, D.; Pang, L. Aptamer-Tagged DNA Origami for Spatially Addressable Detection of Aflatoxin B1. *Chem. Commun.* **2017**, *53*, 941−944.
(258) Takeuchi, Y.; Endo, M.; Suzuki, Y.; Hidaka, K.; Durand, G.; Dausse, E.; Toulmé, J.-J.; Sugiyama, H. Single-Molecule Observations of RNA-RNA Kissing Interactions in a DNA Nanostructure. *Biomater. Sci.* **2016**, *4*, 130−135.
(259) Yang, J.; Jiang, S.; Liu, X.; Pan, L.; Zhang, C. Aptamer-Binding Directed DNA Origami Pattern for Logic Gates. *ACS Appl. Mater. Interfaces* **2016**, *8*, 34054−34060.
(260) Duanghathaipornsuk, S.; Shen, B.; Cameron, B. D.; Ijäs, H.; Linko, V.; Kostiainen, M. A.; Kim, D.-S. Aptamer-Embedded DNA Origami Cage for Detecting (Glycated) Hemoglobin with a Surface Plasmon Resonance Sensor. *Mater. Lett.* **2020**, *275*, 128141.
(261) Rafati, A.; Zarrabi, A.; Gill, P. DNA Nanotubes Coupled with Magnetic Nanoparticles as a Platform for Colorimetric Biosensors. *Nanomed. Research J.* **2020**, *5*, 63−74.
(262) Rutten, I.; Daems, D.; Lammertyn, J. Boosting Biomolecular Interactions through DNA Origami Nano-Tailored Biosensing Interfaces. *J. Mater. Chem. B* **2020**, *8*, 3606−3615.
(263) Zhang, D. Y.; Seelig, G. Dynamic DNA Nanotechnology Using Strand-Displacement Reactions. *Nat. Chem.* **2011**, *3*, 103−113.
(264) DeLuca, M.; Shi, Z.; Castro, C. E.; Arya, G. Dynamic DNA Nanotechnology: Toward Functional Nanoscale Devices. *Nanoscale Horiz.* **2020**, *5*, 182−201.
(265) Sheng, Q.; Liu, R.; Zhang, S.; Zheng, J. Ultrasensitive Electrochemical Cocaine Biosensor Based on Reversible DNA Nanostructure. *Biosens. Bioelectron.* **2014**, *51*, 191−194.
(266) Chen, X.; Shi, X.; Liu, Y.; Lu, L.; Lu, Y.; Xiong, X.; Liu, Y.; Xiong, X. Impedimetric Determination of Staphylococcal Enterotoxin B Using Electrochemical Switching with DNA Triangular Pyramid Frustum Nanostructure. *Microchim. Acta* **2018**, *185*, 460.
(267) Pei, H.; Liang, L.; Yao, G.; Li, J.; Huang, Q.; Fan, C. Reconfigurable Three-Dimensional DNA Nanostructures for the Construction of Intracellular Logic Sensors. *Angew. Chem., Int. Ed.* **2012**, *51*, 9020−9024.
(268) Shiu, S. C.-C.; Cheung, Y.-W.; Dirkzwager, R. M.; Liang, S.; Kinghorn, A. B.; Fraser, L. A.; Tang, M. S. L.; Tanner, J. A. Aptamer-Mediated Protein Molecular Recognition Driving a DNA Tweezer Nanomachine. *Adv. Biosyst.* **2017**, *1*, 1600006.
(269) Yurke, B.; Turberfield, A. J.; Mills, A. P.; Simmel, F. C.; Neumann, J. L. A DNA-Fuelled Molecular Machine Made of DNA. *Nature* **2000**, *406*, 605−608.
(270) Kuzuya, A.; Sakai, Y.; Yamazaki, T.; Xu, Y.; Komiyama, M. Nanomechanical DNA Origami 'Single-Molecule Beacons' Directly Imaged by Atomic Force Microscopy. *Nat. Commun.* **2011**, *2*, 449.
(271) Walter, H.-K.; Bauer, J.; Steinmeyer, J.; Kuzuya, A.; Niemeyer, C. M.; Wagenknecht, H.-A. DNA Origami Traffic Lights" with a Split Aptamer Sensor for a Bicolor Fluorescence Readout. *Nano Lett.* **2017**, *17*, 2467−2472.
(272) Zadegan, R. M.; Jepsen, M. D. E.; Thomsen, K. E.; Okholm, A. H.; Schaffert, D. H.; Andersen, E. S.; Birkedal, V.; Kjems, J. Construction of a 4 Zeptoliters Switchable 3D DNA Box Origami. *ACS Nano* **2012**, *6*, 10050−10053.
(273) Zadegan, R. M.; Jepsen, M. D. E.; Hildebrandt, L. L.; Birkedal, V.; Kjems, J. Construction of a Fuzzy and Boolean Logic Gates Based on DNA. *Small* **2015**, *11*, 1811−1817.
(274) Tang, M. S. L.; Shiu, S. C.; Godonoga, M.; Cheung, Y. W.; Liang, S.; Dirkzwager, R. M.; Kinghorn, A. B.; Fraser, L. A.; Heddle, J. G.; Tanner, J. A. An Aptamer-Enabled DNA Nanobox for Protein Sensing. *Nanomedicine* **2018**, *14*, 1161−1168.
(275) Funck, T.; Liedl, T.; Bae, W. Dual Aptamer-Functionalized 3D Plasmonic Metamolecule for Thrombin Sensing. *Appl. Sci.* **2019**, *9*, 3006.
(276) Funck, T.; Nicoli, F.; Kuzyk, A.; Liedl, T. Sensing Picomolar Concentrations of RNA Using Switchable Plasmonic Chirality. *Angew. Chem., Int. Ed.* **2018**, *57*, 13495−13498.
(277) Zhou, C.; Xin, L.; Duan, X.; Urban, M. J.; Liu, N. Dynamic Plasmonic System that Responds to Thermal and Aptamer-Target Regulations. *Nano Lett.* **2018**, *18*, 7395−7399.
(278) Liu, Z.; Tian, C.; Yu, J.; Li, Y.; Jiang, W.; Mao, C. Self-Assembly of Responsive Multilayered DNA Nanocages. *J. Am. Chem. Soc.* **2015**, *137*, 1730−1733.
(279) Wu, N.; Willner, I. Programmed Dissociation of Dimer and Trimer Origami Structures by Aptamer-Ligand Complexes. *Nanoscale* **2017**, *9*, 1416−1422.
(280) Bi, S.; Yue, S.; Zhang, S. Hybridization Chain Reaction: A Versatile Molecular Tool for Biosensing, Bioimaging, and Biomedicine. *Chem. Soc. Rev.* **2017**, *46*, 4281−4298.
(281) Chen, J.; Tang, L.; Chu, X.; Jiang, J. Enzyme-Free, Signal-Amplified Nucleic Acid Circuits for Biosensing and Bioimaging Analysis. *Analyst* **2017**, *142*, 3048−3061.
(282) Augspurger, E. E.; Rana, M.; Yigit, M. V. Chemical and Biological Sensing Using Hybridization Chain Reaction. *ACS Sens.* **2018**, *3*, 878−902.
(283) Chang, C. C.; Chen, C. Y.; Chuang, T. L.; Wu, T. H.; Wei, S. C.; Liao, H.; Lin, C. W. Aptamer-Based Colorimetric Detection of Proteins Using a Branched DNA Cascade Amplification Strategy and Unmodified Gold Nanoparticles. *Biosens. Bioelectron.* **2016**, *78*, 200−205.
(284) Xuan, F.; Hsing, I. M. Triggering Hairpin-Free Chain-Branching Growth of Fluorescent DNA Dendrimers for Nonlinear Hybridization Chain Reaction. *J. Am. Chem. Soc.* **2014**, *136*, 9810−9813.
(285) Wang, J. R.; Xia, C.; Yang, L.; Li, Y. F.; Li, C. M.; Huang, C. Z. DNA Nanofirecrackers Assembled through Hybridization Chain Reaction for Ultrasensitive SERS Immunoassay of Prostate Specific Antigen. *Anal. Chem.* **2020**, *92*, 4046−4052.
(286) Chen, Y.; Yang, M.; Xiang, Y.; Yuan, R.; Chai, Y. Binding-Induced Autonomous Disassembly of Aptamer-DNAzyme Super-sandwich Nanostructures for Sensitive Electrochemiluminescence Turn-on Detection of Ochratoxin A. *Nanoscale* **2014**, *6*, 1099−1104.
(287) Ding, J.; Gu, Y.; Li, F.; Zhang, H.; Qin, W. DNA Nanostructure-Based Magnetic Beads for Potentiometric Aptasensing. *Anal. Chem.* **2015**, *87*, 6465−6469.
(288) Zhao, G.; Ding, J.; Yu, H.; Yin, T.; Qin, W. Potentiometric Aptasensing of Vibrio alginolyticus Based on DNA Nanostructure-Modified Magnetic Beads. *Sensors* **2016**, *16*, 2052.
(289) Song, P.; Ye, D.; Zuo, X.; Li, J.; Wang, J.; Liu, H.; Hwang, M. T.; Chao, J.; Su, S.; Wang, L.; et al. DNA Hydrogel with Aptamer-Toehold-Based Recognition, Cloaking, and Decloaking of Circulating Tumor Cells for Live Cell Analysis. *Nano Lett.* **2017**, *17*, 5193−5198.
(290) Yin, P.; Choi, H. M. T.; Calvert, C. R.; Pierce, N. A. Programming Biomolecular Self-Assembly Pathways. *Nature* **2008**, *451*, 318−322.
(291) Liu, J.; Zhang, Y.; Xie, H.; Zhao, L.; Zheng, L.; Ye, H. Applications of Catalytic Hairpin Assembly Reaction in Biosensing. *Small* **2019**, *15*, 1902989.
(292) Xie, H.; Chai, Y.; Yuan, Y.; Yuan, R. Highly Effective Molecule Converting Strategy Based on Enzyme-Free Dual Recycling Amplification for Ultrasensitive Electrochemical Detection of Atp. *Chem. Commun.* **2017**, *53*, 8368−8371.

https://doi.org/10.1021/acs.chemrev.0c01332
Chem. Rev. XXXX, XXX, XXX−XXX

(293) Liu, J.; Zhang, Y.; Zhao, Q.; Situ, B.; Zhao, J.; Luo, S.; Li, B.; Yan, X.; Vadgama, P.; Su, L.; et al. Bifunctional Aptamer-Mediated Catalytic Hairpin Assembly for the Sensitive and Homogenous Detection of Rare Cancer Cells. *Anal. Chim. Acta* **2018**, *1029*, 58−64.
(294) Bhadra, S.; Ellington, A. D. Design and Application of Cotranscriptional Non-Enzymatic RNA Circuits and Signal Transducers. *Nucleic Acids Res.* **2014**, *42*, No. e58.
(295) Akter, F.; Yokobayashi, Y. RNA Signal Amplifier Circuit with Integrated Fluorescence Output. *ACS Synth. Biol.* **2015**, *4*, 655−658.
(296) Karunanayake Mudiyanselage, A.; Yu, Q.; Leon-Duque, M. A.; Zhao, B.; Wu, R.; You, M. Genetically Encoded Catalytic Hairpin Assembly for Sensitive RNA Imaging in Live Cells. *J. Am. Chem. Soc.* **2018**, *140*, 8739−8745.
(297) Bath, J.; Turberfield, A. J. DNA Nanomachines. *Nat. Nanotechnol.* **2007**, *2*, 275−284.
(298) Lund, K.; Manzo, A. J.; Dabby, N.; Michelotti, N.; Johnson-Buck, A.; Nangreave, J.; Taylor, S.; Pei, R.; Stojanovic, M. N.; Walter, N. G.; et al. Molecular Robots Guided by Prescriptive Landscapes. *Nature* **2010**, *465*, 206−210.
(299) Pan, J.; Li, F.; Cha, T.-G.; Chen, H.; Choi, J. H. Recent Progress on DNA Based Walkers. *Curr. Opin. Biotechnol.* **2015**, *34*, 56−64.
(300) Mason, S. D.; Tang, Y.; Li, Y.; Xie, X.; Li, F. Emerging Bioanalytical Applications of DNA Walkers. *TrAC, Trends Anal. Chem.* **2018**, *107*, 212−221.
(301) Yang, J.; Dou, B.; Yuan, R.; Xiang, Y. Aptamer/Protein Proximity Binding-Triggered Molecular Machine for Amplified Electrochemical Sensing of Thrombin. *Anal. Chem.* **2017**, *89*, 5138−5143.
(302) Ali, M. M.; Li, F.; Zhang, Z.; Zhang, K.; Kang, D.-K.; Ankrum, J. A.; Le, X. C.; Zhao, W. Rolling Circle Amplification: A Versatile Tool for Chemical Biology, Materials Science and Medicine. *Chem. Soc. Rev.* **2014**, *43*, 3324−3341.
(303) Wang, J.; Dong, H.-y.; Zhou, Y.; Han, L.-y.; Zhang, T.; Lin, M.; Wang, C.; Xu, H.; Wu, Z.-S.; Jia, L. Immunomagnetic Antibody Plus Aptamer Pseudo-DNA Nanocatenane Followed by Rolling Circle Amplication for Highly-Sensitive CTC Detection. *Biosens. Bioelectron.* **2018**, *122*, 239−246.
(304) Gao, X.; Niu, S.; Ge, J.; Luan, Q.; Jie, G. 3D DNA Nanosphere-Based Photoelectrochemical Biosensor Combined with Multiple Enzyme-Free Amplification for Ultrasensitive Detection of Cancer Biomarkers. *Biosens. Bioelectron.* **2020**, *147*, 111778.
(305) Hao, L.; Wang, W.; Shen, X.; Wang, S.; Li, Q.; An, F.; Wu, S. A Fluorescent DNA Hydrogel Aptasensor Based on the Self-Assembly of Rolling Circle Amplification Products for Sensitive Detection of Ochratoxin A. *J. Agric. Food Chem.* **2020**, *68*, 369−375.
(306) He, L.; Shen, Z.; Wang, J.; Zeng, J.; Wang, W.; Wu, H.; Wang, Q.; Gan, N. Simultaneously Responsive Microfluidic Chip Aptasensor for Determination of Kanamycin, Aflatoxin M1, and 17β-Estradiol Based on Magnetic Tripartite DNA Assembly Nanostructure Probes. *Microchim. Acta* **2020**, *187*, 176.
(307) Ray, P.; White, R. R. Aptamers for Targeted Drug Delivery. *Pharmaceuticals* **2010**, *3*, 1761−1778.
(308) Zhou, J.; Rossi, J. J. Cell-Specific Aptamer-Mediated Targeted Drug Delivery. *Oligonucleotides* **2011**, *21*, 1−10.
(309) Kim, M.; Kim, D. M.; Kim, K. S.; Jung, W.; Kim, D. E. Applications of Cancer Cell-Specific Aptamers in Targeted Delivery of Anticancer Therapeutic Agents. *Molecules* **2018**, *23*, 830.
(310) McNamara, J. O., II; Andrechek, E. R.; Wang, Y.; Viles, K. D.; Rempel, R. E.; Gilboa, E.; Sullenger, B. A.; Giangrande, P. H. Cell Type-Specific Delivery of siRNAs with Aptamer-siRNA Chimeras. *Nat. Biotechnol.* **2006**, *24*, 1005−1015.
(311) Liu, J.; Wei, T.; Zhao, J.; Huang, Y.; Deng, H.; Kumar, A.; Wang, C.; Liang, Z.; Ma, X.; Liang, X. J. Multifunctional Aptamer-Based Nanoparticles for Targeted Drug Delivery to Circumvent Cancer Resistance. *Biomaterials* **2016**, *91*, 44−56.
(312) Liu, J.; Ma, X.; Lei, C.; Xue, X.; Wei, T.; Zhao, J.; Li, S.; Liang, X.-J. A Self-Assembled DNA Nanostructure for Targeted and pH-Triggered Drug Delivery to Combat Doxorubicin Resistance. *J. Mater. Chem. B* **2016**, *4*, 3854−3858.
(313) Li, X.; Yang, Y.; Zhao, H.; Zhu, T.; Yang, Z.; Xu, H.; Fu, Y.; Lin, F.; Pan, X.; Li, L.; et al. Enhanced In Vivo Blood-Brain Barrier Penetration by Circular Tau-Transferrin Receptor Bifunctional Aptamer for Tauopathy Therapy. *J. Am. Chem. Soc.* **2020**, *142*, 3862−3872.
(314) Ni, X.; Zhang, Y.; Ribas, J.; Chowdhury, W. H.; Castanares, M.; Zhang, Z.; Laiho, M.; DeWeese, T. L.; Lupold, S. E. Prostate-Targeted Radiosensitization via Aptamer-shRNA Chimeras in Human Tumor Xenografts. *J. Clin. Invest.* **2011**, *121*, 2383−2390.
(315) Liu, N.; Zhou, C.; Zhao, J.; Chen, Y. Reversal of Paclitaxel Resistance in Epithelial Ovarian Carcinoma Cells by a MUC1 Aptamer-Let-7i Chimera. *Cancer Invest.* **2012**, *30*, 577−582.
(316) Catuogno, S.; Esposito, C. L.; de Franciscis, V. Aptamer-Mediated Targeted Delivery of Therapeutics: An Update. *Pharmaceuticals* **2016**, *9*, 69.
(317) Zhou, J.; Rossi, J. J. Cell-Type-Specific, Aptamer-Functionalized Agents for Targeted Disease Therapy. *Mol. Ther.–Nucleic Acids* **2014**, *3*, No. e169.
(318) Carvalho, C.; Santos, R. X.; Cardoso, S.; Correia, S.; Oliveira, P. J.; Santos, M. S.; Moreira, P. I. Doxorubicin: The Good, the Bad and the Ugly Effect. *Curr. Med. Chem.* **2009**, *16*, 3267−3285.
(319) Yang, F.; Teves, S. S.; Kemp, C. J.; Henikoff, S. Doxorubicin, DNA Torsion, and Chromatin Dynamics. *Biochim. Biophys. Acta, Rev. Cancer* **2014**, *1845*, 84−89.
(320) Pommier, Y.; Leo, E.; Zhang, H.; Marchand, C. DNA Topoisomerases and Their Poisoning by Anticancer and Antibacterial Drugs. *Chem. Biol.* **2010**, *17*, 421−433.
(321) Zhang, H.; Ma, Y.; Xie, Y.; An, Y.; Huang, Y.; Zhu, Z.; Yang, C. J. A Controllable Aptamer-Based Self-Assembled DNA Dendrimer for High Affinity Targeting, Bioimaging and Drug Delivery. *Sci. Rep.* **2015**, *5*, 10099.
(322) Taghdisi, S. M.; Danesh, N. M.; Ramezani, M.; Yazdian-Robati, R.; Abnous, K. A Novel AS1411 Aptamer-Based Three-Way Junction Pocket DNA Nanostructure Loaded with Doxorubicin for Targeting Cancer Cells In Vitro and In Vivo. *Mol. Pharmaceutics* **2018**, *15*, 1972−1978.
(323) Abnous, K.; Danesh, N. M.; Ramezani, M.; Charbgoo, F.; Bahreyni, A.; Taghdisi, S. M. Targeted Delivery of Doxorubicin to Cancer Cells by a Cruciform DNA Nanostructure Composed of AS1411 and FOXM1 Aptamers. *Expert Opin. Drug Delivery* **2018**, *15*, 1045−1052.
(324) Yao, F.; An, Y.; Li, X.; Li, Z.; Duan, J.; Yang, X. D. Targeted Therapy of Colon Cancer by Aptamer-Guided Holliday Junctions Loaded with Doxorubicin. *Int. J. Nanomed.* **2020**, *15*, 2119−2129.
(325) Sun, S.; Cheraga, N.; Jiang, H.-N.; Xiao, Q.-R.; Gao, P.-C.; Wang, Y.; Wei, Y.-Y.; Wang, X.-W.; Jiang, Y. Bioinspired DNA Nanocockleburs for Targeted Delivery of Doxorubicin. *Colloids Surf., B* **2020**, *186*, 110733.
(326) Zhang, C.; Su, M.; He, Y.; Zhao, X.; Fang, P.-A.; Ribbe, A. E.; Jiang, W.; Mao, C. Conformational Flexibility Facilitates Self-Assembly of Complex DNA Nanostructures. *Proc. Natl. Acad. Sci. U. S. A.* **2008**, *105*, 10665−10669.
(327) Chang, M.; Yang, C.-S.; Huang, D.-M. Aptamer-Conjugated DNA Icosahedral Nanoparticles as a Carrier of Doxorubicin for Cancer Therapy. *ACS Nano* **2011**, *5*, 6156−6163.
(328) Srivithya, V.; Roun, H.; Sekhar Babu, M.; Jae Hyung, P.; Sung Ha, P. Aptamer-Conjugated DNA Nano-Ring as the Carrier of Drug Molecules. *Nanotechnology* **2018**, *29*, 095602.
(329) Xue, C.; Zhang, S.; Yu, X.; Hu, S.; Lu, Y.; Wu, Z.-S. Periodically Ordered, Nuclease-Resistant DNA Nanowires Decorated with Cell-Specific Aptamers as Selective Theranostic Agents. *Angew. Chem., Int. Ed.* **2020**, *59*, 17540−17547.
(330) Dirks, R. M.; Pierce, N. A. Triggered Amplification by Hybridization Chain Reaction. *Proc. Natl. Acad. Sci. U. S. A.* **2004**, *101*, 15275−15278.
(331) Zhu, G.; Zheng, J.; Song, E.; Donovan, M.; Zhang, K.; Liu, C.; Tan, W. Self-Assembled, Aptamer-Tethered DNA Nanotrains for Targeted Transport of Molecular Drugs in Cancer Theranostics. *Proc. Natl. Acad. Sci. U. S. A.* **2013**, *110*, 7998−8003.

https://doi.org/10.1021/acs.chemrev.0c01332
Chem. Rev. XXXX, XXX, XXX−XXX

(332) Hoshika, S.; Leal, N. A.; Kim, M.-J.; Kim, M.-S.; Karalkar, N. B.; Kim, H.-J.; Bates, A. M.; Watkins, N. E.; SantaLucia, H. A.; Meyer, A. J.; et al. Hachimoji DNA and RNA: A Genetic System with Eight Building Blocks. *Science* **2019**, *363*, 884−887.
(333) Zhang, L.; Wang, S.; Yang, Z.; Hoshika, S.; Xie, S.; Li, J.; Chen, X.; Wan, S.; Li, L.; Benner, S. A.; et al. An Aptamer-Nanotrain Assembled from Six-Letter DNA Delivers Doxorubicin Selectively to Liver Cancer Cells. *Angew. Chem., Int. Ed.* **2020**, *59*, 663−668.
(334) Li, N.; Wang, X.-Y.; Xiang, M.-H.; Liu, J.-W.; Yu, R.-Q.; Jiang, J.-H. Programmable Self-Assembly of Protein-Scaffolded DNA Nanohydrogels for Tumor-Targeted Imaging and Therapy. *Anal. Chem.* **2019**, *91*, 2610−2614.
(335) Thelu, H. V. P.; Atchimnaidu, S.; Perumal, D.; Harikrishnan, K. S.; Vijayan, S.; Varghese, R. Self-Assembly of an Aptamer-Decorated, DNA-Protein Hybrid Nanogel: A Biocompatible Nanocarrier for Targeted Cancer Therapy. *ACS Appl. Bio Mater.* **2019**, *2*, 5227−5234.
(336) Duangrat, R.; Udomprasert, A.; Kangsamaksin, T. Tetrahedral DNA Nanostructures as Drug Delivery and Bioimaging Platforms in Cancer Therapy. *Cancer Sci.* **2020**, *111*, 3164−3173.
(337) Dai, B.; Hu, Y.; Duan, J.; Yang, X. D. Aptamer-Guided DNA Tetrahedron as a Novel Targeted Drug Delivery System for MUC1-Expressing Breast Cancer Cells In Vitro. *Oncotarget* **2016**, *7*, 38257−38269.
(338) Liu, M.; Ma, W.; Li, Q.; Zhao, D.; Shao, X.; Huang, Q.; Hao, L.; Lin, Y. Aptamer-Targeted DNA Nanostructures with Doxorubicin to Treat Protein Tyrosine Kinase 7-Positive Tumours. *Cell Proliferation* **2019**, *52*, No. e12511.
(339) Han, X.; Jiang, Y.; Li, S.; Zhang, Y.; Ma, X.; Wu, Z.; Wu, Z.; Qi, X. Multivalent Aptamer-Modified Tetrahedral DNA Nanocage Demonstrates High Selectivity and Safety for Anti-Tumor Therapy. *Nanoscale* **2019**, *11*, 339−347.
(340) Abnous, K.; Danesh, N. M.; Ramezani, M.; Lavaee, P.; Jalalian, S. H.; Yazdian-Robati, R.; Emrani, A. S.; Hassanabad, K. Y.; Taghdisi, S. M. A Novel Aptamer-Based DNA Diamond Nanostructure for In Vivo Targeted Delivery of Epirubicin to Cancer Cells. *RSC Adv.* **2017**, *7*, 15181−15188.
(341) Zhu, G.; Hu, R.; Zhao, Z.; Chen, Z.; Zhang, X.; Tan, W. Noncanonical Self-Assembly of Multifunctional DNA Nanoflowers for Biomedical Applications. *J. Am. Chem. Soc.* **2013**, *135*, 16438−16445.
(342) Hu, R.; Zhang, X.; Zhao, Z.; Zhu, G.; Chen, T.; Fu, T.; Tan, W. DNA Nanoflowers for Multiplexed Cellular Imaging and Traceable Targeted Drug Delivery. *Angew. Chem., Int. Ed.* **2014**, *53*, 5821−5826.
(343) Wang, J.; Wang, H.; Wang, H.; He, S.; Li, R.; Deng, Z.; Liu, X.; Wang, F. Nonviolent Self-Catabolic DNAzyme Nanosponges for Smart Anticancer Drug Delivery. *ACS Nano* **2019**, *13*, 5852−5863.
(344) Mei, Q.; Wei, X.; Su, F.; Liu, Y.; Youngbull, C.; Johnson, R.; Lindsay, S.; Yan, H.; Meldrum, D. Stability of DNA Origami Nanoarrays in Cell Lysate. *Nano Lett.* **2011**, *11*, 1477−1482.
(345) Shen, X.; Jiang, Q.; Wang, J.; Dai, L.; Zou, G.; Wang, Z.-G.; Chen, W.-Q.; Jiang, W.; Ding, B. Visualization of the Intracellular Location and Stability of DNA Origami with a Label-Free Fluorescent Probe. *Chem. Commun.* **2012**, *48*, 11301−11303.
(346) Jiang, Q.; Song, C.; Nangreave, J.; Liu, X.; Lin, L.; Qiu, D.; Wang, Z.-G.; Zou, G.; Liang, X.; Yan, H.; et al. DNA Origami as a Carrier for Circumvention of Drug Resistance. *J. Am. Chem. Soc.* **2012**, *134*, 13396−13403.
(347) Zhao, Y.-X.; Shaw, A.; Zeng, X.; Benson, E.; Nyström, A. M.; Högberg, B. DNA Origami Delivery System for Cancer Therapy with Tunable Release Properties. *ACS Nano* **2012**, *6*, 8684−8691.
(348) Zhang, Q.; Jiang, Q.; Li, N.; Dai, L.; Liu, Q.; Song, L.; Wang, J.; Li, Y.; Tian, J.; Ding, B.; et al. DNA Origami as an In Vivo Drug Delivery Vehicle for Cancer Therapy. *ACS Nano* **2014**, *8*, 6633−6643.
(349) Song, L.; Jiang, Q.; Liu, J.; Li, N.; Liu, Q.; Dai, L.; Gao, Y.; Liu, W.; Liu, D.; Ding, B. DNA Origami/Gold Nanorod Hybrid Nanostructures for the Circumvention of Drug Resistance. *Nanoscale* **2017**, *9*, 7750−7754.
(350) Liu, J.; Song, L.; Liu, S.; Jiang, Q.; Liu, Q.; Li, N.; Wang, Z.-G.; Ding, B. A DNA-Based Nanocarrier for Efficient Gene Delivery and Combined Cancer Therapy. *Nano Lett.* **2018**, *18*, 3328−3334.
(351) Chaithongyot, S.; Duangrat, R.; Wootthichairangsan, C.; Hanchaina, R.; Udomprasert, A.; Kangsamaksin, T. Selective Delivery of Doxorubicin Using the Biomarker-Specific, Aptamer-Functionalized DNA Nanosphere. *Mater. Lett.* **2020**, *260*, 126952.
(352) Pi, F.; Zhang, H.; Li, H.; Thiviyanathan, V.; Gorenstein, D. G.; Sood, A. K.; Guo, P. RNA Nanoparticles Harboring Annexin A2 Aptamer Can Target Ovarian Cancer for Tumor-Specific Doxorubicin Delivery. *Nanomedicine* **2017**, *13*, 1183−1193.
(353) Guo, S.; Vieweger, M.; Zhang, K.; Yin, H.; Wang, H.; Li, X.; Li, S.; Hu, S.; Sparreboom, A.; Evers, B. M.; et al. Ultra-Thermostable RNA Nanoparticles for Solubilizing and High-Yield Loading of Paclitaxel for Breast Cancer Therapy. *Nat. Commun.* **2020**, *11*, 972.
(354) Apel, K.; Hirt, H. Reactive Oxygen Species: Metabolism, Oxidative Stress, and Signal Transduction. *Annu. Rev. Plant Biol.* **2004**, *55*, 373−399.
(355) Dickinson, B. C.; Chang, C. J. Chemistry and Biology of Reactive Oxygen Species in Signaling or Stress Responses. *Nat. Chem. Biol.* **2011**, *7*, 504−511.
(356) Zhou, Z.; Song, J.; Nie, L.; Chen, X. Reactive Oxygen Species Generating Systems Meeting Challenges of Photodynamic Cancer Therapy. *Chem. Soc. Rev.* **2016**, *45*, 6597−6626.
(357) Murphy, M. P. How Mitochondria Produce Reactive Oxygen Species. *Biochem. J.* **2009**, *417*, 1−13.
(358) Tong, L.; Chuang, C. C.; Wu, S.; Zuo, L. Reactive Oxygen Species in Redox Cancer Therapy. *Cancer Lett.* **2015**, *367*, 18−25.
(359) Simon, H. U.; Haj-Yehia, A.; Levi-Schaffer, F. Role of Reactive Oxygen Species (ROS) in Apoptosis Induction. *Apoptosis* **2000**, *5*, 415−418.
(360) Waris, G.; Ahsan, H. Reactive Oxygen Species: Role in the Development of Cancer and Various Chronic Conditions. *J. Carcinog.* **2006**, *5*, 14.
(361) Circu, M. L.; Aw, T. Y. Reactive Oxygen Species, Cellular Redox Systems, and Apoptosis. *Free Radical Biol. Med.* **2010**, *48*, 749−762.
(362) Perillo, B.; Di Donato, M.; Pezone, A.; Di Zazzo, E.; Giovannelli, P.; Galasso, G.; Castoria, G.; Migliaccio, A. ROS in Cancer Therapy: The Bright Side of the Moon. *Exp. Mol. Med.* **2020**, *52*, 192−203.
(363) Han, D.; Zhu, G.; Wu, C.; Zhu, Z.; Chen, T.; Zhang, X.; Tan, W. Engineering a Cell-Surface Aptamer Circuit for Targeted and Amplified Photodynamic Cancer Therapy. *ACS Nano* **2013**, *7*, 2312−2319.
(364) Rohs, R.; Sklenar, H.; Lavery, R.; Röder, B. Methylene Blue Binding to DNA with Alternating GC Base Sequence: A Modeling Study. *J. Am. Chem. Soc.* **2000**, *122*, 2860−2866.
(365) Rohs, R.; Sklenar, H. Methylene Blue Binding to DNA with Alternating Gc Base Sequence: Continuum Treatment of Salt Effects. *Indian J. Biochem. Biophys.* **2001**, *38*, 1−6.
(366) Hossain, M.; Suresh Kumar, G. DNA Intercalation of Methylene Blue and Quinacrine: New Insights into Base and Sequence Specificity from Structural and Thermodynamic Studies with Polynucleotides. *Mol. BioSyst.* **2009**, *5*, 1311−1322.
(367) Furst, A. L.; Hill, M. G.; Barton, J. K. Electrocatalysis in DNA Sensors. *Polyhedron* **2014**, *84*, 150−159.
(368) Kim, K. R.; Bang, D.; Ahn, D. R. Nano-Formulation of a Photosensitizer Using a DNA Tetrahedron and Its Potential for In Vivo Photodynamic Therapy. *Biomater. Sci.* **2016**, *4*, 605−609.
(369) Jin, H.; Kim, M. G.; Ko, S. B.; Kim, D. H.; Lee, B. J.; Macgregor, R. B., Jr.; Shim, G.; Oh, Y. K. Stemmed DNA Nanostructure for the Selective Delivery of Therapeutics. *Nanoscale* **2018**, *10*, 7511−7518.
(370) Tian, Y.; Huang, Y.; Gao, P.; Chen, T. Nucleus-Targeted DNA Tetrahedron as a Nanocarrier of Metal Complexes for Enhanced Glioma Therapy. *Chem. Commun.* **2018**, *54*, 9394−9397.
(371) Tijsterman, M.; Plasterk, R. H. Dicers at Risc; the Mechanism of RNAi. *Cell* **2004**, *117*, 1−3.
(372) Guo, S.; Tschammer, N.; Mohammed, S.; Guo, P. Specific Delivery of Therapeutic RNAs to Cancer Cells via the Dimerization Mechanism of Phi29 Motor pRNA. *Hum. Gene Ther.* **2005**, *16*, 1097−1109.

https://doi.org/10.1021/acs.chemrev.0c01332
Chem. Rev. XXXX, XXX, XXX−XXX

(373) Zhou, J.; Li, H.; Li, S.; Zaia, J.; Rossi, J. J. Novel Dual Inhibitory Function Aptamer-siRNA Delivery System for HIV-1 Therapy. *Mol. Ther.* **2008**, *16*, 1481−1489.
(374) Wheeler, L. A.; Trifonova, R.; Vrbanac, V.; Basar, E.; McKernan, S.; Xu, Z.; Seung, E.; Deruaz, M.; Dudek, T.; Einarsson, J. I.; et al. Inhibition of HIV Transmission in Human Cervicovaginal Explants and Humanized Mice Using CD4 Aptamer-siRNA Chimeras. *J. Clin. Invest.* **2011**, *121*, 2401−2412.
(375) Zhang, L.; Mu, C.; Zhang, T.; Wang, Y.; Wang, Y.; Fan, L.; Liu, C.; Chen, H.; Shen, J.; Wei, K.; et al. Systemic Delivery of Aptamer-Conjugated XBP1 siRNA Nanoparticles for Efficient Suppression of HER2+ Breast Cancer. *ACS Appl. Mater. Interfaces* **2020**, *12*, 32360−32371.
(376) Yoo, H.; Jung, H.; Kim, S. A.; Mok, H. Multivalent Comb-Type Aptamer-siRNA Conjugates for Efficient and Selective Intracellular Delivery. *Chem. Commun.* **2014**, *50*, 6765−6767.
(377) Zhou, J.; Shu, Y.; Guo, P.; Smith, D. D.; Rossi, J. J. Dual Functional RNA Nanoparticles Containing Phi29 Motor pRNA and Anti-GP120 Aptamer for Cell-Type Specific Delivery and HIV-1 Inhibition. *Methods* **2011**, *54*, 284−294.
(378) Hu, J.; Xiao, F.; Hao, X.; Bai, S.; Hao, J. Inhibition of Monocyte Adhesion to Brain-Derived Endothelial Cells by Dual Functional RNA Chimeras. *Mol. Ther.–Nucleic Acids* **2014**, *3*, No. e209.
(379) Li, H.; Zhang, K.; Pi, F.; Guo, S.; Shlyakhtenko, L.; Chiu, W.; Shu, D.; Guo, P. Controllable Self-Assembly of RNA Tetrahedrons with Precise Shape and Size for Cancer Targeting. *Adv. Mater.* **2016**, *28*, 7501−7507.
(380) Zhang, Y.; Leonard, M.; Shu, Y.; Yang, Y.; Shu, D.; Guo, P.; Zhang, X. Overcoming Tamoxifen Resistance of Human Breast Cancer by Targeted Gene Silencing Using Multifunctional pRNA Nanoparticles. *ACS Nano* **2017**, *11*, 335−346.
(381) Yin, H.; Xiong, G.; Guo, S.; Xu, C.; Xu, R.; Guo, P.; Shu, D. Delivery of Anti-miRNA for Triple-Negative Breast Cancer Therapy Using RNA Nanoparticles Targeting Stem Cell Marker CD133. *Mol. Ther.* **2019**, *27*, 1252−1261.
(382) Pi, F.; Binzel, D. W.; Lee, T. J.; Li, Z.; Sun, M.; Rychahou, P.; Li, H.; Haque, F.; Wang, S.; Croce, C. M.; et al. Nanoparticle Orientation to Control RNA loading and Ligand Display on Extracellular Vesicles for Cancer Regression. *Nat. Nanotechnol.* **2018**, *13*, 82−89.
(383) Li, L.; Hu, X.; Zhang, M.; Ma, S.; Yu, F.; Zhao, S.; Liu, N.; Wang, Z.; Wang, Y.; Guan, H.; et al. Dual Tumor-Targeting Nanocarrier System for siRNA Delivery Based on pRNA and Modified Chitosan. *Mol. Ther.–Nucleic Acids* **2017**, *8*, 169−183.
(384) Ding, L.; Li, J.; Wu, C.; Yan, F.; Li, X.; Zhang, S. A Self-Assembled RNA-Triple Helix Hydrogel Drug Delivery System Targeting Triple-Negative Breast Cancer. *J. Mater. Chem. B* **2020**, *8*, 3527−3533.
(385) Wu, C.; Han, D.; Chen, T.; Peng, L.; Zhu, G.; You, M.; Qiu, L.; Sefah, K.; Zhang, X.; Tan, W. Building a Multifunctional Aptamer-Based DNA Nanoassembly for Targeted Cancer Therapy. *J. Am. Chem. Soc.* **2013**, *135*, 18644−18650.
(386) Li, J.; Zheng, C.; Cansiz, S.; Wu, C.; Xu, J.; Cui, C.; Liu, Y.; Hou, W.; Wang, Y.; Zhang, L.; et al. Self-Assembly of DNA Nanohydrogels with Controllable Size and Stimuli-Responsive Property for Targeted Gene Regulation Therapy. *J. Am. Chem. Soc.* **2015**, *137*, 1412−1415.
(387) Ren, K.; Liu, Y.; Wu, J.; Zhang, Y.; Zhu, J.; Yang, M.; Ju, H. A DNA Dual Lock-and-Key Strategy for Cell-Subtype-Specific siRNA Delivery. *Nat. Commun.* **2016**, *7*, 13580.
(388) Tung, J.; Tew, L. S.; Hsu, Y. M.; Khung, Y. L. A Novel 4-Arm DNA/RNA Nanoconstruct Triggering Rapid Apoptosis of Triple Negative Breast Cancer Cells within 24 h. *Sci. Rep.* **2017**, *7*, 793.
(389) Jeong, E. H.; Jeong, H.; Jang, B.; Kim, B.; Kim, M.; Kwon, H.; Lee, K.; Lee, H. Aptamer-Incorporated DNA Holliday Junction for the Targeted Delivery of siRNA. *J. Ind. Eng. Chem.* **2017**, *56*, 55−61.
(390) Second RNAi drug approved. *Nat. Biotechnol.* **2020**, *38*, 385.
(391) Subramanian, N.; Kanwar, J. R.; Akilandeswari, B.; Kanwar, R. K.; Khetan, V.; Krishnakumar, S. Chimeric Nucleolin Aptamer with Survivin Dnazyme for Cancer Cell Targeted Delivery. *Chem. Commun.* **2015**, *51*, 6940−6943.
(392) Charoenphol, P.; Bermudez, H. Aptamer-Targeted DNA Nanostructures for Therapeutic Delivery. *Mol. Pharmaceutics* **2014**, *11*, 1721−1725.
(393) Li, Q.; Zhao, D.; Shao, X.; Lin, S.; Xie, X.; Liu, M.; Ma, W.; Shi, S.; Lin, Y. Aptamer-Modified Tetrahedral DNA Nanostructure for Tumor-Targeted Drug Delivery. *ACS Appl. Mater. Interfaces* **2017**, *9*, 36695−36701.
(394) Guo, X. L.; Yuan, D. D.; Song, T.; Li, X. M. DNA Nanopore Functionalized with Aptamer and Cell-Penetrating Peptide for Tumor Cell Recognition. *Anal. Bioanal. Chem.* **2017**, *409*, 3789−3797.
(395) Li, S.; Jiang, Q.; Liu, S.; Zhang, Y.; Tian, Y.; Song, C.; Wang, J.; Zou, Y.; Anderson, G. J.; Han, J.-Y.; et al. A DNA Nanorobot Functions as a Cancer Therapeutic in Response to a Molecular Trigger In Vivo. *Nat. Biotechnol.* **2018**, *36*, 258−264.
(396) Zhao, S.; Duan, F.; Liu, S.; Wu, T.; Shang, Y.; Tian, R.; Liu, J.; Wang, Z.-G.; Jiang, Q.; Ding, B. Efficient Intracellular Delivery of RNase a Using DNA Origami Carriers. *ACS Appl. Mater. Interfaces* **2019**, *11*, 11112−11118.
(397) Mela, I.; Vallejo-Ramirez, P. P.; Makarchuk, S.; Christie, G.; Bailey, D.; Henderson, R. M.; Sugiyama, H.; Endo, M.; Kaminski, C. F. DNA Nanostructures for Targeted Antimicrobial Delivery. *Angew. Chem., Int. Ed.* **2020**, *59*, 12698−12702.
(398) Chen, Q.; Zhou, S.; Li, C.; Guo, Q.; Yang, X.; Huang, J.; Liu, J.; Wang, K. DNA Supersandwich Assemblies as Artificial Receptors to Mediate Intracellular Delivery of Catalase for Efficient Ros Scavenging. *Chem. Commun.* **2019**, *55*, 4242−4245.
(399) Elahi, N.; Kamali, M.; Baghersad, M. H. Recent Biomedical Applications of Gold Nanoparticles: A Review. *Talanta* **2018**, *184*, 537−556.
(400) Doughty, A. C. V.; Hoover, A. R.; Layton, E.; Murray, C. K.; Howard, E. W.; Chen, W. R. Nanomaterial Applications in Photothermal Therapy for Cancer. *Materials* **2019**, *12*, 779.
(401) Cancer multidrug resistance. *Nat. Biotechnol.* **2000**, *18*, IT18−IT20.
(402) Ayaz, M.; Turan, B. Selenium Prevents Diabetes-Induced Alterations in $[Zn^{2+}]$I and Metallothionein Level of Rat Heart via Restoration of Cell Redox Cycle. *Am. J. Physiol. Heart Circ. Physiol.* **2006**, *290*, H1071−H1080.
(403) Slepchenko, K. G.; Lu, Q.; Li, Y. V. Cross Talk between Increased Intracellular Zinc (Zn^{2+}) and Accumulation of Reactive Oxygen Species in Chemical Ischemia. *Am. J. Physiol. Cell Physiol.* **2017**, *313*, C448−C459.
(404) Lopes-Pires, M. E.; Ahmed, N. S.; Vara, D.; Gibbins, J. M.; Pula, G.; Pugh, N. Zinc Regulates Reactive Oxygen Species Generation in Platelets. *Platelets* **2021**, *32*, 368.
(405) Liu, J.; Song, L.; Liu, S.; Zhao, S.; Jiang, Q.; Ding, B. A Tailored DNA Nanoplatform for Synergistic RNAi-/Chemotherapy of Multidrug-Resistant Tumors. *Angew. Chem., Int. Ed.* **2018**, *57*, 15486−15490.
(406) Yu, S.; Wang, Y.; Li, Y.; Jiang, L.-P.; Bi, S.; Zhu, J.-J. Multifunctional DNA Polycatenane Nanocarriers for Synergistic Targeted Therapy of Multidrug-Resistant Human Leukemia. *Adv. Funct. Mater.* **2019**, *29*, 1905659.
(407) Zhan, Y.; Ma, W.; Zhang, Y.; Mao, C.; Shao, X.; Xie, X.; Wang, F.; Liu, X.; Li, Q.; Lin, Y. DNA-Based Nanomedicine with Targeting and Enhancement of Therapeutic Efficacy of Breast Cancer Cells. *ACS Appl. Mater. Interfaces* **2019**, *11*, 15354−15365.
(408) Charbgoo, F.; Alibolandi, M.; Taghdisi, S. M.; Abnous, K.; Soltani, F.; Ramezani, M. Muc1 Aptamer-Targeted DNA Micelles for Dual Tumor Therapy Using Doxorubicin and Kla Peptide. *Nanomedicine* **2018**, *14*, 685−697.
(409) Wu, T.; Liu, Q.; Cao, Y.; Tian, R.; Liu, J.; Ding, B. Multifunctional Double-Bundle DNA Tetrahedron for Efficient Regulation of Gene Expression. *ACS Appl. Mater. Interfaces* **2020**, *12*, 32461−32467.
(410) Khaled, A.; Guo, S.; Li, F.; Guo, P. Controllable Self-Assembly of Nanoparticles for Specific Delivery of Multiple Therapeutic Molecules to Cancer Cells Using RNA Nanotechnology. *Nano Lett.* **2005**, *5*, 1797−1808.

https://doi.org/10.1021/acs.chemrev.0c01332
Chem. Rev. XXXX, XXX, XXX−XXX

(411) Mathur, D.; Medintz, I. L. The Growing Development of DNA Nanostructures for Potential Healthcare-Related Applications. *Adv. Healthcare Mater.* **2019**, *8*, No. 1801546.
(412) Parlea, L.; Puri, A.; Kasprzak, W.; Bindewald, E.; Zakrevsky, P.; Satterwhite, E.; Joseph, K.; Afonin, K. A.; Shapiro, B. A. Cellular Delivery of RNA Nanoparticles. *ACS Comb. Sci.* **2016**, *18*, 527−547.
(413) Green, C. M.; Mathur, D.; Medintz, I. L. Understanding the Fate of DNA Nanostructures inside the Cell. *J. Mater. Chem. B* **2020**, *8*, 6170−6178.
(414) Weng, Y.; Huang, Q.; Li, C.; Yang, Y.; Wang, X.; Yu, J.; Huang, Y.; Liang, X.-J. Improved Nucleic Acid Therapy with Advanced Nanoscale Biotechnology. *Mol. Ther.–Nucleic Acids* **2020**, *19*, 581−601.
(415) Jasinski, D.; Haque, F.; Binzel, D. W.; Guo, P. Advancement of the Emerging Field of RNA Nanotechnology. *ACS Nano* **2017**, *11*, 1142−1164.
(416) Petros, R. A.; DeSimone, J. M. Strategies in the Design of Nanoparticles for Therapeutic Applications. *Nat. Rev. Drug Discovery* **2010**, *9*, 615−627.
(417) Blanco, E.; Shen, H.; Ferrari, M. Principles of Nanoparticle Design for Overcoming Biological Barriers to Drug Delivery. *Nat. Biotechnol.* **2015**, *33*, 941−951.
(418) Xu, C.-f.; Wang, J. Delivery Systems for siRNA Drug Development in Cancer Therapy. *Asian J. Pharm. Sci.* **2015**, *10*, 1−12.
(419) Sioud, M. Single-Stranded Small Interfering RNA are More Immunostimulatory Than Their Double-Stranded Counterparts: A Central Role for 2′-Hydroxyl Uridines in Immune Responses. *Eur. J. Immunol.* **2006**, *36*, 1222−1230.
(420) Meng, Z.; Lu, M. RNA Interference-Induced Innate Immunity, Off-Target Effect, or Immune Adjuvant? *Front. Immunol.* **2017**, *8*, 331.
(421) Surana, S.; Shenoy, A. R.; Krishnan, Y. Designing DNA Nanodevices for Compatibility with the Immune System of Higher Organisms. *Nat. Nanotechnol.* **2015**, *10*, 741−747.
(422) Chandler, M.; Johnson, M. B.; Panigaj, M.; Afonin, K. A. Innate Immune Responses Triggered by Nucleic Acids Inspire the Design of Immunomodulatory Nucleic Acid Nanoparticles (NANPS). *Curr. Opin. Biotechnol.* **2020**, *63*, 8−15.
(423) Zhang, Y.; Hong, H.; Cai, W. Tumor-Targeted Drug Delivery with Aptamers. *Curr. Med. Chem.* **2011**, *18*, 4185−4194.
(424) Kim, K.-R.; Lee, T.; Kim, B.-S.; Ahn, D.-R. Utilizing the Bioorthogonal Base-Pairing System of L-DNA to Design Ideal DNA Nanocarriers for Enhanced Delivery of Nucleic Acid Cargos. *Chem. Sci.* **2014**, *5*, 1533−1537.
(425) Ireson, C. R.; Kelland, L. R. Discovery and Development of Anticancer Aptamers. *Mol. Cancer Ther.* **2006**, *5*, 2957−2962.
(426) Banerjee, D.; Harfouche, R.; Sengupta, S. Nanotechnology-Mediated Targeting of Tumor Angiogenesis. *Vasc. Cell* **2011**, *3*, 3−3.
(427) Lee, J.; Lee, J.; Ree, B. J.; Lee, Y. M.; Park, H.; Lee, T. G.; Kim, J. H.; Kim, W. J. Self-Assembled Aptamer Nanoconstruct: A Highly Effective Molecule-Capturing Platform Having Therapeutic Applications. *Adv. Ther.* **2019**, *2*, 1800111.
(428) Parekh, P.; Kamble, S.; Zhao, N.; Zeng, Z.; Portier, B. P.; Zu, Y. Immunotherapy of CD30-Expressing Lymphoma Using a Highly Stable ssDNA Aptamer. *Biomaterials* **2013**, *34*, 8909−8917.
(429) Sun, P.; Zhang, N.; Tang, Y.; Yang, Y.; Zhou, J.; Zhao, Y. Site-Specific Anchoring Aptamer C2NP on DNA Origami Nanostructures for Cancer Treatment. *RSC Adv.* **2018**, *8*, 26300−26308.
(430) Topalian, S. L.; Drake, C. G.; Pardoll, D. M. Immune Checkpoint Blockade: A Common Denominator Approach to Cancer Therapy. *Cancer Cell* **2015**, *27*, 450−461.
(431) Prodeus, A.; Abdul-Wahid, A.; Fischer, N. W.; Huang, E. H.; Cydzik, M.; Gariépy, J. Targeting the PD-1/PD-L1 Immune Evasion Axis with DNA Aptamers as a Novel Therapeutic Strategy for the Treatment of Disseminated Cancers. *Mol. Ther.–Nucleic Acids* **2015**, *4*, No. e237.
(432) Lee, J.; Le, Q.-V.; Yang, G.; Oh, Y.-K. Cas9-Edited Immune Checkpoint Blockade PD-1 DNA Polyaptamer Hydrogel for Cancer Immunotherapy. *Biomaterials* **2019**, *218*, 119359.
(433) Bai, C.; Gao, S.; Hu, S.; Liu, X.; Li, H.; Dong, J.; Huang, A.; Zhu, L.; Zhou, P.; Li, S.; et al. Self-Assembled Multivalent Aptamer Nanoparticles with Potential CAR-Like Characteristics Could Activate T Cells and Inhibit Melanoma Growth. *Mol. Ther. Oncolytics* **2020**, *17*, 9−20.
(434) Woodruff, R. S.; Sullenger, B. A. Modulation of the Coagulation Cascade Using Aptamers. *Arterioscler., Thromb., Vasc. Biol.* **2015**, *35*, 2083−2091.
(435) Müller, J.; Wulffen, B.; Pötzsch, B.; Mayer, G. Multidomain Targeting Generates a High-Affinity Thrombin-Inhibiting Bivalent Aptamer. *ChemBioChem* **2007**, *8*, 2223−2226.
(436) Di Giusto, D. A.; King, G. C. Construction, Stability, and Activity of Multivalent Circular Anticoagulant Aptamers. *J. Biol. Chem.* **2004**, *279*, 46483−46489.
(437) Hansen, M. N.; Zhang, A. M.; Rangnekar, A.; Bompiani, K. M.; Carter, J. D.; Gothelf, K. V.; LaBean, T. H. Weave Tile Architecture Construction Strategy for DNA Nanotechnology. *J. Am. Chem. Soc.* **2010**, *132*, 14481−14486.
(438) Rangnekar, A.; Zhang, A. M.; Li, S. S.; Bompiani, K. M.; Hansen, M. N.; Gothelf, K. V.; Sullenger, B. A.; LaBean, T. H. Increased Anticoagulant Activity of Thrombin-Binding DNA Aptamers by Nanoscale Organization on DNA Nanostructures. *Nanomedicine* **2012**, *8*, 673−681.
(439) Rangnekar, A.; Nash, J. A.; Goodfred, B.; Yingling, Y. G.; LaBean, T. H. Design of Potent and Controllable Anticoagulants Using DNA Aptamers and Nanostructures. *Molecules* **2016**, *21*, 202.
(440) Peng, P.; Du, Y.; Zheng, J.; Wang, H.; Li, T. Reconfigurable Bioinspired Framework Nucleic Acid Nanoplatform Dynamically Manipulated in Living Cells for Subcellular Imaging. *Angew. Chem., Int. Ed.* **2019**, *58*, 1648−1653.
(441) Du, Y.; Peng, P.; Li, T. DNA Logic Operations in Living Cells Utilizing Lysosome-Recognizing Framework Nucleic Acid Nanodevices for Subcellular Imaging. *ACS Nano* **2019**, *13*, 5778−5784.
(442) Wang, H.; Peng, P.; Wang, Q.; Du, Y.; Tian, Z.; Li, T. Environment-Recognizing DNA-Computation Circuits for the Intracellular Transport of Molecular Payloads for mRNA Imaging. *Angew. Chem., Int. Ed.* **2020**, *59*, 6099−6107.
(443) Xing, X.; Li, J.; Qiu, L.; Tan, W. A Molecular Recognition-Activatable DNA Nanofirecracker Enables Signal-Enhanced Imaging in Living Cells. *Chem. Commun.* **2020**, *56*, 3131−3134.
(444) Ma, H.; Tu, L.-C.; Naseri, A.; Huisman, M.; Zhang, S.; Grunwald, D.; Pederson, T. Multiplexed Labeling of Genomic Loci with dCas9 and Engineered SgRNAs Using Crisprainbow. *Nat. Biotechnol.* **2016**, *34*, 528−530.
(445) Ma, H.; Tu, L.-C.; Naseri, A.; Chung, Y.-C.; Grunwald, D.; Zhang, S.; Pederson, T. CRISPR-Sirius: RNA Scaffolds for Signal Amplification in Genome Imaging. *Nat. Methods* **2018**, *15*, 928−931.
(446) Sun, Z.; Nguyen, T.; McAuliffe, K.; You, M. Intracellular Imaging with Genetically Encoded RNA-Based Molecular Sensors. *Nanomaterials* **2019**, *9*, 233.
(447) Paige, J. S.; Wu, K. Y.; Jaffrey, S. R. RNA Mimics of Green Fluorescent Protein. *Science* **2011**, *333*, 642−646.
(448) Höfer, K.; Langejürgen, L. V.; Jäschke, A. Universal Aptamer-Based Real-Time Monitoring of Enzymatic RNA Synthesis. *J. Am. Chem. Soc.* **2013**, *135*, 13692−13694.
(449) Pothoulakis, G.; Ceroni, F.; Reeve, B.; Ellis, T. The Spinach RNA Aptamer as a Characterization Tool for Synthetic Biology. *ACS Synth. Biol.* **2014**, *3*, 182−187.
(450) You, M.; Litke, J. L.; Jaffrey, S. R. Imaging Metabolite Dynamics in Living Cells Using a Spinach-Based Riboswitch. *Proc. Natl. Acad. Sci. U. S. A.* **2015**, *112*, E2756−E2765.
(451) Sando, S.; Narita, A.; Hayami, M.; Aoyama, Y. Transcription Monitoring Using Fused RNA with a Dye-Binding Light-up Aptamer as a Tag: A Blue Fluorescent RNA. *Chem. Commun.* **2008**, *33*, 3858−3860.
(452) Schwarz-Schilling, M.; Dupin, A.; Chizzolini, F.; Krishnan, S.; Mansy, S. S.; Simmel, F. C. Optimized Assembly of a Multifunctional RNA-Protein Nanostructure in a Cell-Free Gene Expression System. *Nano Lett.* **2018**, *18*, 2650−2657.

https://doi.org/10.1021/acs.chemrev.0c01332
Chem. Rev. XXXX, XXX, XXX−XXX

(453) Reif, R.; Haque, F.; Guo, P. Fluorogenic RNA Nanoparticles for Monitoring RNA Folding and Degradation in Real Time in Living Cells. *Nucleic Acid Ther.* **2012**, *22*, 428−437.
(454) Liu, P.; Mu, X.; Zhang, X.-D.; Ming, D. The Near-Infrared-II Fluorophores and Advanced Microscopy Technologies Development and Application in Bioimaging. *Bioconjugate Chem.* **2020**, *31*, 260−275.
(455) Li, J.; Jiang, D.; Bao, B.; He, Y.; Liu, L.; Wang, X. Radiolabeling of DNA Bipyramid and Preliminary Biological Evaluation in Mice. *Bioconjugate Chem.* **2016**, *27*, 905−910.
(456) Jiang, D.; Sun, Y.; Li, J.; Li, Q.; Lv, M.; Zhu, B.; Tian, T.; Cheng, D.; Xia, J.; Zhang, L.; et al. Multiple-Armed Tetrahedral DNA Nanostructures for Tumor-Targeting, Dual-Modality In Vivo Imaging. *ACS Appl. Mater. Interfaces* **2016**, *8*, 4378−4384.
(457) Song, L.; Wang, Z.; Liu, J.; Wang, T.; Jiang, Q.; Ding, B. Tumor-Targeted DNA Bipyramid for In Vivo Dual-Modality Imaging. *ACS Appl. Bio Mater.* **2020**, *3*, 2854−2860.
(458) Mammen, M.; Choi, S. K.; Whitesides, G. M. Polyvalent Interactions in Biological Systems: Implications for Design and Use of Multivalent Ligands and Inhibitors. *Angew. Chem., Int. Ed.* **1998**, *37*, 2754−2794.
(459) Gartner, Z. J.; Bertozzi, C. R. Programmed Assembly of 3-Dimensional Microtissues with Defined Cellular Connectivity. *Proc. Natl. Acad. Sci. U. S. A.* **2009**, *106*, 4606−4610.
(460) Liu, X.; Yan, H.; Liu, Y.; Chang, Y. Targeted Cell-Cell Interactions by DNA Nanoscaffold-Templated Multivalent Bispecific Aptamers. *Small* **2011**, *7*, 1673−1682.
(461) Zeng, Z.; Parekh, P.; Li, Z.; Shi, Z. Z.; Tung, C. H.; Zu, Y. Specific and Sensitive Tumor Imaging Using Biostable Oligonucleotide Aptamer Probes. *Theranostics* **2014**, *4*, 945−952.
(462) Dueber, J. E.; Wu, G. C.; Malmirchegini, G. R.; Moon, T. S.; Petzold, C. J.; Ullal, A. V.; Prather, K. L. J.; Keasling, J. D. Synthetic Protein Scaffolds Provide Modular Control over Metabolic Flux. *Nat. Biotechnol.* **2009**, *27*, 753−759.
(463) Agapakis, C. M.; Ducat, D. C.; Boyle, P. M.; Wintermute, E. H.; Way, J. C.; Silver, P. A. Insulation of a Synthetic Hydrogen Metabolism Circuit in Bacteria. *J. Biol. Eng.* **2010**, *4*, 3.
(464) Moon, T. S.; Dueber, J. E.; Shiue, E.; Prather, K. L. J. Use of Modular, Synthetic Scaffolds for Improved Production of Glucaric Acid in Engineered E. Coli. *Metab. Eng.* **2010**, *12*, 298−305.
(465) Conrado, R. J.; Wu, G. C.; Boock, J. T.; Xu, H.; Chen, S. Y.; Lebar, T.; Turnšek, J.; Tomšič, N.; Avbelj, M.; Gaber, R.; et al. DNA-Guided Assembly of Biosynthetic Pathways Promotes Improved Catalytic Efficiency. *Nucleic Acids Res.* **2012**, *40*, 1879−1889.
(466) Fu, J.; Liu, M.; Liu, Y.; Yan, H. Spatially-Interactive Biomolecular Networks Organized by Nucleic Acid Nanostructures. *Acc. Chem. Res.* **2012**, *45*, 1215−1226.
(467) Shin, S. W.; Yuk, J. S.; Chun, S. H.; Lim, Y. T.; Um, S. H. Hybrid Material of Structural DNA with Inorganic Compound: Synthesis, Applications, and Perspective. *Nano Converg.* **2020**, *7*, 2.
(468) Kim, J.; Kim, D.; Lee, J. B. DNA Aptamer-Based Carrier for Loading Proteins and Enhancing the Enzymatic Activity. *RSC Adv.* **2017**, *7*, 1643−1645.
(469) Cheglakov, Z.; Weizmann, Y.; Braunschweig, A. B.; Wilner, O. I.; Willner, I. Increasing the Complexity of Periodic Protein Nanostructures by the Rolling-Circle-Amplified Synthesis of Aptamers. *Angew. Chem., Int. Ed.* **2008**, *47*, 126−130.
(470) Wang, Z. G.; Wilner, O. I.; Willner, I. Self-Assembly of Aptamer-Circular DNA Nanostructures for Controlled Biocatalysis. *Nano Lett.* **2009**, *9*, 4098−4102.
(471) Delebecque, C. J.; Lindner, A. B.; Silver, P. A.; Aldaye, F. A. Organization of Intracellular Reactions with Rationally Designed RNA Assemblies. *Science* **2011**, *333*, 470−474.
(472) Sachdeva, G.; Garg, A.; Godding, D.; Way, J. C.; Silver, P. A. In Vivo Co-Localization of Enzymes on RNA Scaffolds Increases Metabolic Production in a Geometrically Dependent Manner. *Nucleic Acids Res.* **2014**, *42*, 9493−9503.
(473) Wang, S.; Shepard, J. R. E.; Shi, H. An RNA-Based Transcription Activator Derived from an Inhibitory Aptamer. *Nucleic Acids Res.* **2010**, *38*, 2378−2386.
(474) Konermann, S.; Brigham, M. D.; Trevino, A. E.; Joung, J.; Abudayyeh, O. O.; Barcena, C.; Hsu, P. D.; Habib, N.; Gootenberg, J. S.; Nishimasu, H.; et al. Genome-Scale Transcriptional Activation by an Engineered CRISPR-Cas9 Complex. *Nature* **2015**, *517*, 583−588.
(475) Qian, L.; Winfree, E.; Bruck, J. Neural Network Computation with DNA Strand Displacement Cascades. *Nature* **2011**, *475*, 368−372.
(476) You, M.; Peng, L.; Shao, N.; Zhang, L.; Qiu, L.; Cui, C.; Tan, W. DNA "Nano-Claw": Logic-Based Autonomous Cancer Targeting and Therapy. *J. Am. Chem. Soc.* **2014**, *136*, 1256−1259.
(477) Douglas, S. M.; Bachelet, I.; Church, G. M. A Logic-Gated Nanorobot for Targeted Transport of Molecular Payloads. *Science* **2012**, *335*, 831−834.
(478) Amir, Y.; Ben-Ishay, E.; Levner, D.; Ittah, S.; Abu-Horowitz, A.; Bachelet, I. Universal Computing by DNA Origami Robots in a Living Animal. *Nat. Nanotechnol.* **2014**, *9*, 353−357.
(479) Chang, X.; Zhang, C.; Lv, C.; Sun, Y.; Zhang, M.; Zhao, Y.; Yang, L.; Han, D.; Tan, W. Construction of a Multiple-Aptamer-Based DNA Logic Device on Live Cell Membranes via Associative Toehold Activation for Accurate Cancer Cell Identification. *J. Am. Chem. Soc.* **2019**, *141*, 12738−12743.
(480) Ouyang, C.; Zhang, S.; Xue, C.; Yu, X.; Xu, H.; Wang, Z.; Lu, Y.; Wu, Z.-S. Precision-Guided Missile-Like DNA Nanostructure Containing Warhead and Guidance Control for Aptamer-Based Targeted Drug Delivery into Cancer Cells In Vitro and In Vivo. *J. Am. Chem. Soc.* **2020**, *142*, 1265−1277.
(481) Kopecek, J. Hydrogel Biomaterials: A Smart Future? *Biomaterials* **2007**, *28*, 5185−5192.
(482) Yang, H.; Liu, H.; Kang, H.; Tan, W. Engineering Target-Responsive Hydrogels Based on Aptamer-Target Interactions. *J. Am. Chem. Soc.* **2008**, *130*, 6320−6321.
(483) Yin, B.-C.; Ye, B.-C.; Wang, H.; Zhu, Z.; Tan, W. Colorimetric Logic Gates Based on Aptamer-Crosslinked Hydrogels. *Chem. Commun.* **2012**, *48*, 1248−1250.
(484) Yan, L.; Zhu, Z.; Zou, Y.; Huang, Y.; Liu, D.; Jia, S.; Xu, D.; Wu, M.; Zhou, Y.; Zhou, S.; et al. Target-Responsive "Sweet" Hydrogel with Glucometer Readout for Portable and Quantitative Detection of Non-Glucose Targets. *J. Am. Chem. Soc.* **2013**, *135*, 3748−3751.
(485) Zhu, Z.; Wu, C.; Liu, H.; Zou, Y.; Zhang, X.; Kang, H.; Yang, C. J.; Tan, W. An Aptamer Cross-Linked Hydrogel as a Colorimetric Platform for Visual Detection. *Angew. Chem., Int. Ed.* **2010**, *49*, 1052−1056.
(486) Zhao, M.; Wang, P.; Guo, Y.; Wang, L.; Luo, F.; Qiu, B.; Guo, L.; Su, X.; Lin, Z.; Chen, G. Detection of Aflatoxin B(1) in Food Samples Based on Target-Responsive Aptamer-Cross-Linked Hydrogel Using a Handheld pH Meter as Readout. *Talanta* **2018**, *176*, 34−39.
(487) Khajouei, S.; Ravan, H.; Ebrahimi, A. DNA Hydrogel-Empowered Biosensing. *Adv. Colloid Interface Sci.* **2020**, *275*, 102060−102060.
(488) Um, S. H.; Lee, J. B.; Park, N.; Kwon, S. Y.; Umbach, C. C.; Luo, D. Enzyme-Catalysed Assembly of DNA Hydrogel. *Nat. Mater.* **2006**, *5*, 797−801.
(489) Shahbazi, M.-A.; Bauleth-Ramos, T.; Santos, H. A. DNA Hydrogel Assemblies: Bridging Synthesis Principles to Biomedical Applications. *Adv. Ther.* **2018**, *1*, 1800042.
(490) Oishi, M.; Nakatani, K. Dynamically Programmed Switchable DNA Hydrogels Based on a DNA Circuit Mechanism. *Small* **2019**, *15*, 1900490.
(491) Sun, Y.; Li, S.; Chen, R.; Wu, P.; Liang, J. Ultrasensitive and Rapid Detection of T-2 Toxin Using a Target-Responsive DNA Hydrogel. *Sens. Actuators, B* **2020**, *311*, 127912.
(492) Lee, J. B.; Peng, S.; Yang, D.; Roh, Y. H.; Funabashi, H.; Park, N.; Rice, E. J.; Chen, L.; Long, R.; Wu, M.; et al. A Mechanical Metamaterial Made from a DNA Hydrogel. *Nat. Nanotechnol.* **2012**, *7*, 816−820.
(493) Liu, H.; Cao, T.; Xu, Y.; Dong, Y.; Liu, D. Tuning the Mechanical Properties of a DNA Hydrogel in Three Phases Based on ATP Aptamer. *Int. J. Mol. Sci.* **2018**, *19*, 1633.

https://doi.org/10.1021/acs.chemrev.0c01332
Chem. Rev. XXXX, XXX, XXX−XXX

(494) Simon, A. J.; Walls-Smith, L. T.; Plaxco, K. W. Exploiting the Conformational-Selection Mechanism to Control the Response Kinetics of a "Smart" DNA Hydrogel. *Analyst* **2018**, *143*, 2531−2538.
(495) Nelson, C. E.; Wu, Y.; Gemberling, M. P.; Oliver, M. L.; Waller, M. A.; Bohning, J. D.; Robinson-Hamm, J. N.; Bulaklak, K.; Castellanos Rivera, R. M.; Collier, J. H.; et al. Long-Term Evaluation of Aav-Crispr Genome Editing for Duchenne Muscular Dystrophy. *Nat. Med.* **2019**, *25*, 427−432.
(496) Han, X.; Liu, K.; Sun, C. Plasmonics for Biosensing. *Materials* **2019**, *12*, 1411.
(497) Mauriz, E.; Dey, P.; Lechuga, L. M. Advances in Nanoplasmonic Biosensors for Clinical Applications. *Analyst* **2019**, *144*, 7105−7129.
(498) Dahlin, A. B.; Wittenberg, N. J.; Höök, F.; Oh, S.-H. Promises and Challenges of Nanoplasmonic Devices for Refractometric Biosensing. *Nanophotonics* **2013**, *2*, 83−101.
(499) Funck, T.; Nicoli, F.; Kuzyk, A.; Liedl, T. Sensing Picomolar Concentrations of RNA Using Switchable Plasmonic Chirality. *Angew. Chem., Int. Ed.* **2018**, *57*, 13495−13498.
(500) Huang, Y.; Nguyen, M.-K.; Natarajan, A. K.; Nguyen, V. H.; Kuzyk, A. A DNA Origami-Based Chiral Plasmonic Sensing Device. *ACS Appl. Mater. Interfaces* **2018**, *10*, 44221−44225.
(501) Jeong, H.-H.; Mark, A. G.; Lee, T.-C.; Alarcón-Correa, M.; Eslami, S.; Qiu, T.; Gibbs, J. G.; Fischer, P. Active Nanorheology with Plasmonics. *Nano Lett.* **2016**, *16*, 4887−4894.
(502) Ramakrishnan, S.; Ijäs, H.; Linko, V.; Keller, A. Structural Stability of DNA Origami Nanostructures under Application-Specific Conditions. *Comput. Struct. Biotechnol. J.* **2018**, *16*, 342−349.
(503) Chandrasekaran, A. R. Nuclease Resistance of DNA Nanostructures. *Nat. Rev. Chem.* **2021**, *5*, 225−239.
(504) Li, H.; Lee, T.; Dziubla, T.; Pi, F.; Guo, S.; Xu, J.; Li, C.; Haque, F.; Liang, X.-J.; Guo, P. RNA as a Stable Polymer to Build Controllable and Defined Nanostructures for Material and Biomedical Applications. *Nano Today* **2015**, *10*, 631−655.
(505) Ramezani, H.; Dietz, H. Building Machines with DNA Molecules. *Nat. Rev. Genet.* **2020**, *21*, 5−26.
(506) Feng, L.; Li, J.; Sun, J.; Wang, L.; Fan, C.; Shen, J. Recent Advances of DNA Nanostructure-Based Cell Membrane Engineering. *Adv. Healthcare Mater.* **2021**, *10*, 2001718.
(507) Kim, J.; Franco, E. RNA Nanotechnology in Synthetic Biology. *Curr. Opin. Biotechnol.* **2020**, *63*, 135−141.
(508) Jun, H.; Wang, X.; Bricker, W. P.; Bathe, M. Automated Sequence Design of 2D Wireframe DNA Origami with Honeycomb Edges. *Nat. Commun.* **2019**, *10*, 5419.
(509) Jun, H.; Shepherd, T. R.; Zhang, K.; Bricker, W. P.; Li, S.; Chiu, W.; Bathe, M. Automated Sequence Design of 3D Polyhedral Wireframe DNA Origami with Honeycomb Edges. *ACS Nano* **2019**, *13*, 2083−2093.
(510) Jun, H.; Zhang, F.; Shepherd, T.; Ratanalert, S.; Qi, X.; Yan, H.; Bathe, M. Autonomously Designed Free-Form 2D DNA Origami. *Sci. Adv.* **2019**, *5*, No. eaav0655.
(511) Sparvath, S. L.; Geary, C. W.; Andersen, E. S. In *3D DNA Nanostructure: Methods and Protocols*; Ke, Y., Wang, P., Eds.; Springer New York: New York, NY, 2017.
(512) Li, M.; Zheng, M.; Wu, S.; Tian, C.; Liu, D.; Weizmann, Y.; Jiang, W.; Wang, G.; Mao, C. In Vivo Production of RNA Nanostructures via Programmed Folding of Single-Stranded RNAs. *Nat. Commun.* **2018**, *9*, 2196.

https://doi.org/10.1021/acs.chemrev.0c01332
Chem. Rev. XXXX, XXX, XXX−XXX